

Spatiotemporal regulation of anti-remodelling signalling pathways in primary human lung fibroblasts

Maxine Roberts, BSc (Hons)

Thesis submitted to the University of Nottingham and Monash
University for the degree of Doctor of Philosophy

SEPTEMBER 2019

This thesis is entirely the candidate's own work. The candidate was enrolled in a joint PhD Programme with both University of Nottingham, at the Cell Signalling and Pharmacology Department, in Nottingham, UK, and with Monash University, at the Monash Institute of Pharmaceutical Sciences (MIPS) and the Drug Discovery Biology Department, Melbourne, Australia. The experiments described in this thesis were performed by the author between October 2015 and August 2019. Experiments performed between September 2017 and September 2018 were conducted at Monash University (MIPS). No part of the material has been submitted previously for a degree or any other qualification at any university.

Chapter 3 contains data that has been published in a peer reviewed journal acquired by Toby C Kent and Rebecca E Broome, researchers at Novartis Institute for Biomedical Research, and Elizabeth M Rosethorne, Senior Research Fellow at the University of Nottingham (more details in Chapter 3).

Publications arising from this thesis

- Roberts, M. J., et al. (2018). The inhibition of human lung fibroblast proliferation and differentiation by Gs-coupled receptors is not predicted by the magnitude of cAMP response. Respir Res **19**(1): 56.

Abstract

Idiopathic pulmonary fibrosis (IPF) is a devastating chronic lung disease caused by a dysregulated wound healing process that results in fibrosis and scarring of lung tissue rather than repair. Current approved IPF therapeutics target multiple known fibrotic mediators and pathways, however this multi target-kinase approach results in numerous severe adverse effects. Dysregulated lung fibroblasts are one of the key cell types involved in the progression of lung fibrosis. Increasing evidence has revealed the role of cAMP in inhibiting fibroblast pro-fibrotic phenotypic responses via crosstalk with the mitogen-activated protein kinase (MAPK)/extracellular regulated kinase (ERK) pathway. However, what makes cAMP elevating agonists efficacious at inhibiting pro-fibrotic process is unclear.

By activating G_s-coupled G protein-coupled receptor (GPCRs) that we showed to be expressed in human lung fibroblasts, we confirm that increasing cAMP inhibits fibroblast proliferation and differentiation. However, the efficacy of agonists to generate cAMP did not correlate to its ability to inhibit phenotypic responses. This disconnect was observed when targeting the prostacyclin receptor (IPR) with a partial agonist for generating cAMP (MRE-269) having more efficacy at inhibiting fibroblast proliferation in comparison to full agonists for generating cAMP (iloprost/treprostinil). We hypothesised that the location of cAMP accumulation and/or the temporal regulation of cAMP signalling may be important for the inhibition of fibroblast proliferation.

As such, targeted fluorescence resonance energy-transfer (FRET) biosensors were used to investigate cAMP and ERK signalling with high spatial and temporal resolution. A complex relationship was discovered between IPR cAMP elevating agents and the inhibition of ERK in different cellular compartments. We demonstrated that IPR

agonists that are efficacious at inhibiting fibroblast proliferation have sustained nuclear cAMP activity and can inhibit nuclear ERK. This suggests nuclear cAMP and the inhibition of nuclear ERK may be important for the inhibition of phenotypic responses. However, forskolin, which increases cAMP independent of receptor activation and is efficacious at inhibiting fibroblast proliferation, had a sustained nuclear cAMP response but was unable to inhibit nuclear ERK.

GloSensor™ cAMP assay was used to measure cAMP levels at a range of time points. We demonstrated that IPR agonists that are low efficacy agonists at acute time points, maintained efficacy at later time points, whereas high efficacy agonists had a reduction in efficacy. By comparing efficacy of IPR agonists to increase cAMP at acute time points vs later, more phenotypically relevant time points, we demonstrated that efficacy switched, with partial agonists switching to full agonists and full agonists switching to partial agonists.

The activation of IPR signalling, using select IPR agonists, represents a potential therapeutic approach for the treatment of IPF. This study demonstrated the importance of measuring cAMP spatially and temporally to understand agonist actions. Although spatial control of cAMP may have some role in phenotypic response more research needs to be conducted. The most significant result was the reversal of efficacy at phenotypically relevant readouts, demonstrating that sustained cAMP signalling may be important for IPF therapeutics.

Acknowledgements

First and foremost, I would like to thank my supervisors Professor Steven Charlton, Dr Elizabeth Rosethorne, and Dr Michelle Halls, for all their support, advice, and guidance throughout my PhD. A special thank you to Michelle at Monash University, who welcomed me into her group and helped make my time there a fantastic experience. Especially thank you for the amazing support and comfort when I only had a couple of weeks left and my cells were not behaving!

I would like to thank both the University of Nottingham and Monash University for the fantastic opportunity to undertake my PhD with these two excellent institutions. It was a fantastic opportunity to spend an entire year in Australia doing my PhD, and to explore Australia and New Zealand. I thank all the postdocs, PhD students, and members of staff from the Cell Signalling and COMPARE departments at the University of Nottingham for their friendship and incredible teamwork. A special thank you to Jackie Glenn for her support and friendship.

I would also like to thank Dr Lauren May for agreeing to “adopt” me during my time at Monash University so I could always have someone to discuss my experiments and results with. Thank you to all of Hall’s and May’s lab members at Monash University for their support and guidance during my time at the Monash Institute of Pharmacological Sciences (MIPS).

Finally, I would like to thank my husband, Jake, who moved to Nottingham with me when I started my PhD, and then was left in Nottingham when I moved to Australia for a year. Thank you for supporting me when I have struggled to get through this process, I couldn’t have done this without you.

Abbreviations

A _{2A}	Adenosine 2A
A _{2B}	Adenosine 2B
AC	Adenylyl cyclase
AEC	Alveolar epithelial cell
AKAP	A-kinase anchoring protein
AMP	Adenosine monophosphate
ASM	Airway smooth muscle
ATP	Adenosine triphosphate
AUC	Area under the curve
BAL	Bronchoalveolar lavage
BrdU	Bromodeoxyuridine
cAMP	cyclic adenosine monophosphate
CBD	cAMP-binding domain
CFP	Cyan fluorescent protein
COPD	Chronic obstructive pulmonary disease
EBFP	Enhanced blue fluorescent protein
ECM	Extracellular matrix
EGF	Epidermal growth factor
EMT	Epithelial-mesenchymal transition
EP ₂	PGE ₂ receptor 2
EP ₄	PGE ₂ receptor 4
Epac	Exchange protein directly activated by cAMP
EKAR	Extracellular signal-related kinases activity reporter

ERK	Extracellular regulated kinase
FBS	Foetal bovine serum
FGF	Fibroblast growth factor
FITC	Fluorescein isothiocyanate
FMT	Fibroblast –myofibroblast transition
FRET	Fluorescence resonance energy transfer
GDP	Guanosine-diphosphate
GEF	Guanine nucleotide exchange factor
GFP	Green fluorescent protein
GPCR	G protein-coupled receptor
GRK	G protein receptor kinases
GTP	Guanosine-5'-triphosphate
GTPase	Guanine triphosphatase
G α_s	G $_s$ protein
HCI	High content imaging
HLF	Human lung fibroblast
ICS	Inhaled corticosteroids
IPF	Idiopathic pulmonary fibrosis
IPR	Prostacyclin receptor
KSR	Kinase suppressor of Ras
LABA	Long acting β_2 adrenoceptor agonist
LDH	Lactate dehydrogenase
LPA	Lysophosphatidic acid
MAPK	Mitogen-activated protein kinase
MC1	Melanocortin-1

MEK	MAPK/ERK kinase
MOPr	μ -opioid receptor
MP1	MEK Partner 1
NLS	Nuclear localisation signal
PAH	Pulmonary arterial hypertension
PASMC	Pulmonary arterial smooth muscle cells
PDBu	Phorbol 12,13-dibutyrate
PDE	Phosphodiesterase
PDGF	Platelet-derived growth factor
PGE ₂	Prostaglandin E ₂
PGI ₂	Prostacyclin
PKA	Protein kinase A
PKC	Protein dependent kinase C
PPAR- γ	Peroxisome proliferator-activated receptor- γ
PTH	Parathyroid hormone
RFP	Red fluorescent protein
RTK	Receptor tyrosine kinase
S1P	Sphingosine 1 phosphate
SABA	Short acting β_2 adrenoceptor agonist
SOS	Son of sevenless
TGF- β	Transforming growth factor- β
TMP	Thrombin-mimicking peptide
TR-FRET	Time resolved-fluorescence resonance energy transfer
TSH	Thyroid-stimulating hormone
VEGF	Vascular endothelial growth factor

YFP	Yellow fluorescent protein
α -SMA	alpha-smooth muscle actin

Table of Contents

Chapter 1 – Introduction.....	1
1.1 Idiopathic pulmonary fibrosis	2
1.1.1 Pathophysiological features	5
1.1.2 Mediators of Fibrosis	9
1.1.3 Therapeutics for IPF.....	17
1.2 G protein-coupled receptors	21
1.2.1 GPCR activation and signalling.....	23
1.2.2 GPCR desensitisation and internalisation	26
1.3 cAMP as a target for the treatment of IPF	29
1.3.1 cAMP pathway	29
1.3.2 cAMP pathway crosstalk with MAPK/ERK pathway	32
1.3.3 cAMP elevating agents as novel IPF therapeutics	33
1.4 Prostacyclin receptor	37
1.4.1 IPR signalling	37
1.4.2 Therapeutic potential of the IPR.....	38
1.5 Spatiotemporal regulation of cAMP and MAPK/ERK pathway.....	42
1.5.1 Spatiotemporal regulation of the cAMP pathway	42
1.5.2 Spatiotemporal regulation of the MAPK/ERK pathway.....	48
1.5.3 Tools to measure spatiotemporal signalling.....	50
1.6 Aims	56
Chapter 2 – Materials and Methods	57
2.1 Materials.....	58
2.2 Cell culture	59
2.3 Receptor expression levels	59
2.4 ERK phosphorylation.....	60
2.4.1 Antibody detection	60
2.4.2 AlphaScreen SureFire.....	61
2.5 cAMP accumulation	61
2.6 Proliferation.....	62
2.6.1 Nuclei Count	62

2.6.2	BrdU incorporation	63
2.7	Fibroblast to myofibroblast transdifferentiation.....	63
2.8	Cell viability.....	64
2.8.1	Caspase-3/7 detection.....	64
2.8.2	LDH assay.....	65
2.9	Expression of FRET biosensors in HLFs	66
2.10	FRET imaging with widefield microscopy	67
2.10.1	Generation of pseudocolour ratiometric images	68
2.11	FRET imaging with confocal microscope and perfusion system.....	68
2.12	GloSensor™ assay	69
2.13	Data analysis	70
	Chapter 3 – The inhibition of human lung fibroblast proliferation and differentiation by Gs-coupled receptors is not predicted by the magnitude of cAMP response	72
3.1	Introduction.....	74
3.2	Results.....	76
3.2.1	Role of cAMP in the inhibition of ERK phosphorylation, and ERK phosphorylation in proliferation	76
3.2.2	GPCR mRNA expression in HLF	78
3.2.3	cAMP signalling in HLF.....	81
3.2.4	Proliferation of human lung fibroblasts.....	86
3.2.5	Cytotoxicity of ligands in human lung fibroblasts.....	95
3.2.6	Fibroblast to myofibroblast transdifferentiation.....	100
3.2.7	Correlation between cAMP and the inhibition of proliferation and differentiation.....	102
3.3	Discussion	105
	Chapter 4 – Compartmentalisation of cAMP and ERK in human lung fibroblasts	115
4.1	Introduction.....	116
4.2	Results.....	123
4.2.1	HLF donor variation in cAMP and inhibition of proliferation when targeting the IP receptor	123
4.2.2	Inhibition of ERK phosphorylation by IP receptor ligands.....	125
4.2.3	Compartmentalised cAMP signalling.....	128
4.2.4	Compartmentalised ERK signalling	140

4.2.5	The dependence of the inhibition of nuclear ERK on cAMP.....	149
4.3	Discussion	154
	Chapter 5 – cAMP kinetics in human lung fibroblasts.....	161
5.1	Introduction	162
5.2	Results.....	165
5.2.1	Measuring cAMP kinetics using targeted FRET biosensors	165
5.2.2	Kinetics of cAMP accumulation	171
5.2.3	Efficacy of IPR agonists to increase cAMP over time.....	179
5.3	Discussion	183
	Chapter 6 – General Discussion	189
	Chapter 7 – References.....	201

Chapter 1 – Introduction

1.1 Idiopathic pulmonary fibrosis

Lungs are designed to optimise exposure of blood to oxygen and for the rapid exchange of gas. The respiratory system is divided into airways and lung parenchyma (Figure 1:1). The airways consist of the bronchus which bifurcates off the trachea and divides into bronchioles and then further into alveoli. The parenchyma is responsible for gas exchange and includes the alveoli, alveolar ducts, and bronchioles. The alveoli are air sacs of the lungs that provide a large surface area and a thin diffusion barrier for rapid gas exchange between the air and blood. The barrier between air and blood consists of alveolar epithelium, capillary endothelium, and the connective tissue layer in between, termed the interstitium (Knudsen & Ochs, 2018). The structure of the alveoli is key for efficient diffusion of oxygen and carbon dioxide and any alterations can be damaging for the respiratory system.

Respiratory diseases encompass numerous pathological conditions that affect the airways and other structures of the lung. Hundreds of millions of people suffer and four million people die prematurely from respiratory diseases each year (WorldHealthOrganization, 2013). Acute respiratory disease is a sudden condition in which breathing is difficult and the oxygen levels in the blood drops lower than normal. Examples include acute lung injury and acute respiratory distress syndrome, where damage to the alveolar epithelium occurs from conditions such as pneumonia, aspiration, sepsis, or shock, and the resulting inflammatory response leads to impaired gas exchange (Ragaller & Richter, 2010). In contrast, chronic respiratory diseases result in progressive loss of lung function leading to the inability to breathe and subsequently death. Types of chronic lung disease include asthma, chronic obstructive pulmonary disease (COPD), and pulmonary fibrosis.

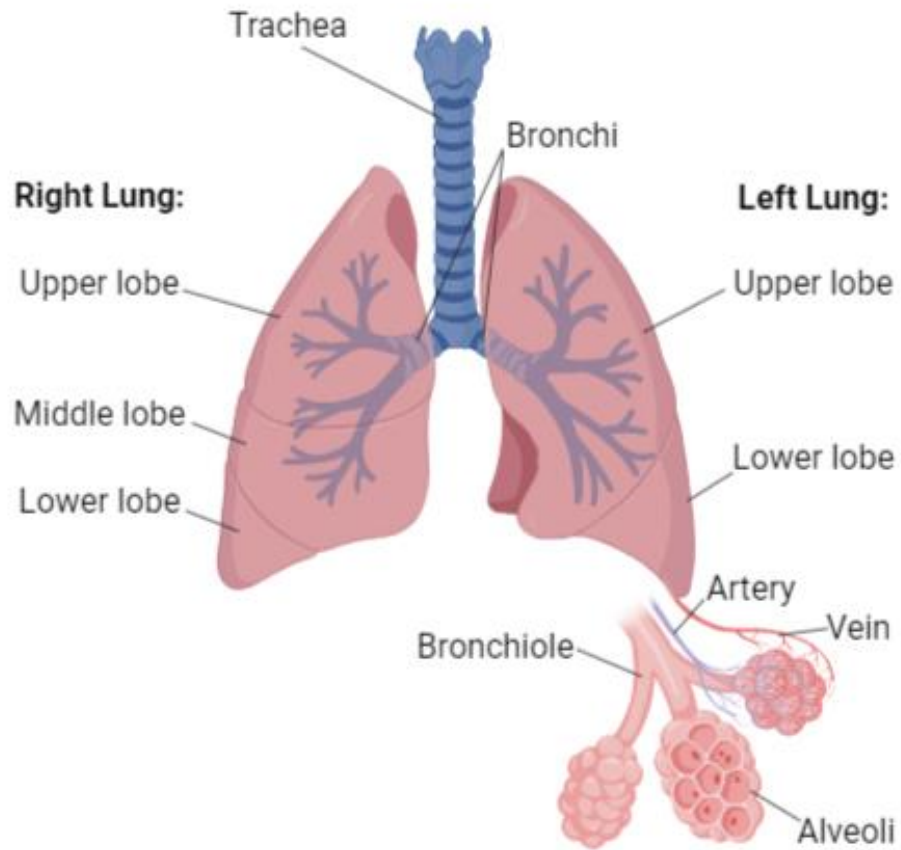


Figure 1:1 - Lung anatomy

Each lung is composed of units called lobes; the left lung consists of two lobes, the upper and the lower, whereas the right lung consists of three lobes, the upper, middle and lower. The lung is comprised of progressively smaller branches from the trachea to the bronchioles. The alveoli are the air sacs of the lung where rapid gas exchange between the air and blood occurs. Image created using BioRender.com

Pulmonary fibrosis is a term that covers many different lung diseases that cause lung damage and scar tissue/fibrosis to build up inside lungs. It is a type of interstitial lung disease, with “interstitial” meaning the disease affects the interstitium – the network of tissue between the epithelial and endothelial basement membrane that supports the alveoli. The family of interstitial lung diseases are characterised by cellular proliferation, interstitial inflammation, and fibrosis. The most common idiopathic interstitial disease is IPF, a chronic, progressive, irreversible, fibrotic interstitial pneumonia of unknown aetiology that occurs primarily in older adults (Raghu et al, 2011). In the UK, the annual incidence is 7.44 per 100,000 people, with a median survival of approximately 3 years from diagnosis (Navaratnam et al, 2011). IPF usually manifests with breathlessness on exertion, increasing cough and dyspnoea, bibasilar inspiratory crackles, worsening pulmonary function tests, as well as finger clubbing. Early recognition and accurate diagnosis are likely to improve outcomes through avoidance of potentially harmful therapies, such as glucocorticoids which increase rates of death in IPF patients (Raghu et al, 2012), and prompt initiation of therapies (Albera et al, 2016; Kolb et al, 2017).

As underlined in its name, the aetiology of IPF is unknown. Unsurprisingly, smoking has been shown to be a risk factor for IPF, although the exact relationship between smoking and survival is not clear as some studies have reported better survival for current smokers with IPF – known as the healthy smoker effect (Antoniou et al, 2008; Bellou et al, 2017). Additional risk factors identified include gastroesophageal reflux (Raghu et al, 2006; Savarino et al, 2013), and viral infections (Molyneaux & Maher, 2013). There is also a growing body of evidence suggesting genetic factors contribute to disease risk. Mutations in genes involved in the maintenance of telomere length (e.g. TERT, TERC, PARN, and RTEL1) are associated with an increased risk of IPF

(Armanios et al, 2007; Diaz de Leon et al, 2010). In addition, overexpression of genes that are responsible for cell adhesion, integrity, and mechanotransduction (i.e. DSP, CTNNA, and DPP9) also confer a predisposition to IPF (Allen et al, 2017; Fingerlin et al, 2013).

1.1.1 Pathophysiological features

Originally, IPF had been described as an inflammatory disease where chronic inflammation leads to lung injury and inflammatory modulated fibrogenesis. It was thought that inflammation precedes, and thus causes, derangements to the alveolar structures in the IPF lung (Keogh & Crystal, 1982). However, there was a shift away from this view as it was shown that (1) inflammation is not a prominent histopathological finding, with disconnect observed between clinical measurements of inflammation and stage or outcome in IPF (Selman et al, 2001), and (2) anti-inflammatory therapy, such as corticosteroids, do not improve disease outcome (Richeldi et al, 2003).

The current hypothesis is that IPF is a consequence of aberrant wound healing responses resulting in fibrosis rather than repair (Figure 1:2). Wound repair is an essential physiological process during which damaged or dead cells are replaced and tissue architecture is restored after injury. There has been a lot of research describing the pathogenesis of IPF, and the processes driving the development of disease are now fairly well known, with fibroblasts and alveolar epithelial cells (AECs) emerging as the principle players in IPF.

AECs form the alveolar epithelium of which there are two types with distinct functions. Type I AECs are highly specialised cells for the key lung function of gas exchange that cover around 95 % of the total alveolar surface (Williams, 2003). They are squamous,

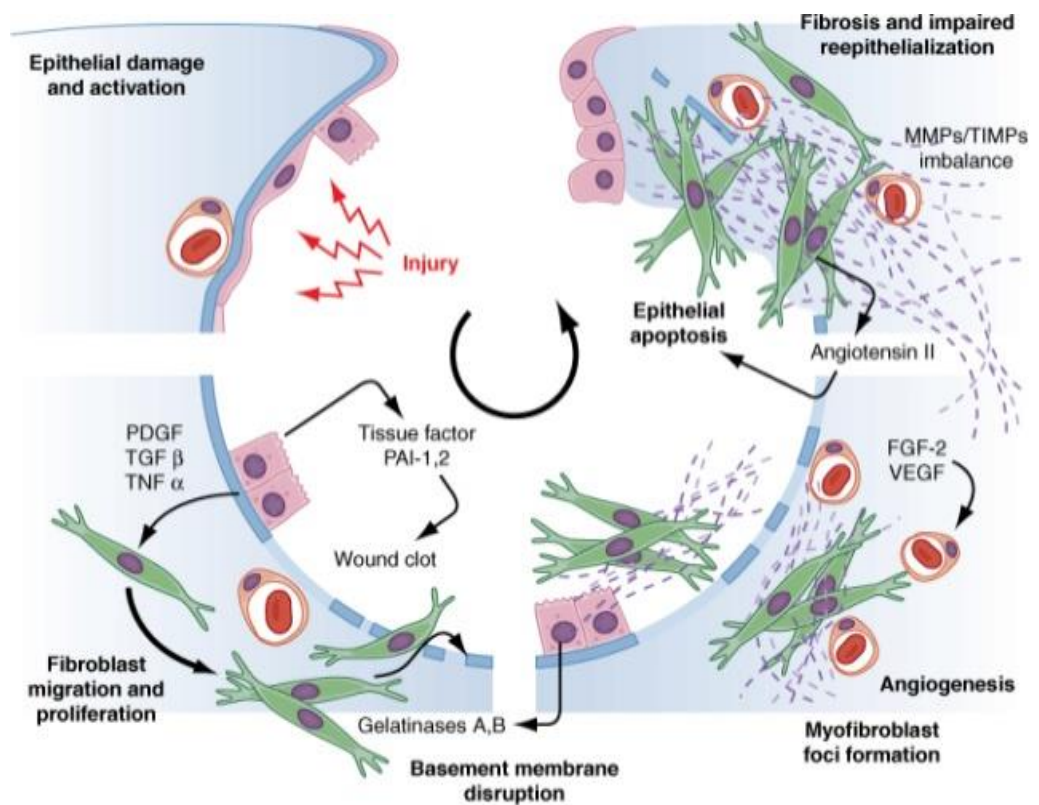


Figure 1:2 - Pathogenesis of IPF

Schematic representation of the dysregulated wound healing cascade in IPF pathogenesis. Injury to the alveolar epithelium results in the secretion of a variety of growth factors that enhance fibroblast migration, proliferation, and differentiation to myofibroblasts. This results in exaggerated extracellular matrix production, which increases lung stiffness and impairs gas exchange.

Image taken from (Macdonald, 2008).

large, thin cells, thus minimizing the diffusion distance between the alveolar air space and the pulmonary capillary blood. Type II AECs are cuboidal cells that are responsible for epithelium regeneration upon injury, serve as progenitor cells for type I AECs, and contribute to lung defence by secreting antimicrobial products such as lysozyme and surfactant proteins (Castranova et al, 1988; Fehrenbach, 2001).

Fibroblasts are the most abundant cells in the interstitium and are key cells in producing and maintaining the extracellular matrix (ECM) required for the structural framework of the lung. The ECM is a macromolecular structure comprised of fibrous proteins, glycoproteins, and proteoglycans that provides physical support to tissues and is essential for normal organ function (Hynes & Naba, 2012). Lung fibroblasts migrate and proliferate early after lung injury to aid wound closure. They have been shown to control proliferation and differentiation of AECs through direct contact as well as by secretion of mediators, such as hepatic growth factor (Myerburg et al, 2007). During wound healing fibroblasts can differentiate to myofibroblasts, spindle-shaped cells that are contractile and contain alpha-smooth muscle actin (α -SMA) stress fibres. Myofibroblasts are key in regulating the ECM remodelling after wound healing, and after facilitating wound closure they typically disappear via a de-differentiation mechanism (Kisseleva et al, 2012), or a clearance mechanism (Krizhanovsky et al, 2008).

Under normal conditions damaged lung epithelium is able to repair itself rapidly, with fibroblasts and myofibroblasts playing key roles in regulating re-epithelialisation of the lung and ECM remodelling, however in IPF wound healing is dysregulated. In IPF, injuries to AECs cause their destruction, revealing a denuded basal lamina. Reepithelialisation through epithelial cell migration, proliferation, and differentiation, is necessary to cover the denuded area and restore lung function (Gorissen et al, 2013;

Kheradmand et al, 1994). However in IPF this process is slow, and the capacity of type II AECs to restore damaged type I AECs is seriously altered. This destruction of the lung structure affects its ability to facilitate normal gas exchange, and the consequent decrease in gas exchange results in the clinical presentation of breathlessness in IPF patients. In IPF, recurrent and/or persistent injury to the lung epithelium leads to increased death of AECs and to the emergence of a surviving AEC population with altered phenotype, resulting in AECs overlying fibroblastic foci rather than forming a single layer suitable for gaseous exchange (Sakai & Tager, 2013). Altered AECs have been shown to predispose the lung to further AEC injury and abnormal repair, facilitating further development of fibrosis (Selman & Pardo, 2006; Tanjore et al, 2013).

Areas of active AECs and myofibroblasts colocalise in the lungs of IPF patients, making it possible for the two cell types to influence each other (Uhal et al, 1998). Altered AECs trigger the secretion of a range of cytokines/growth factors, such as transforming growth factor- β (TGF- β) and platelet-derived growth factor (PDGF), which promote the migration, proliferation, and differentiation of fibroblasts (Khalil et al, 1996; Pan et al, 2001).

It has been shown that IPF fibroblasts are more resistant to apoptosis in comparison to normal fibroblasts and therefore reside inappropriately in the lung after wound healing (Moodley et al, 2004). Fibroblast proliferation is enhanced in IPF through numerous mediators, including PDGF (Alexander et al, 2011). In the IPF lung, aggregates of proliferating fibroblasts and myofibroblasts, termed "fibroblast foci", are a key histopathological finding which indicates that fibrosis is actively ongoing (Katzenstein & Myers, 1998). Myofibroblasts are the mesenchymal cell type most associated with the development of IPF. There are several concepts as to their origin;

(1) resident interstitial fibroblasts differentiate into myofibroblasts, termed fibroblast-myofibroblast transdifferentiation (FMT), in response to growth factors including TGF- β (Wynn & Ramalingam, 2012); (2) alveolar epithelial cells undergo epithelial-mesenchymal transition (EMT) in response to TGF- β (Kim et al, 2006); (3) fibrocytes, which migrate into wounds to facilitate repair, differentiate into myofibroblasts (Hashimoto et al, 2004).

In IPF myofibroblasts persist inappropriately. Accumulation of myofibroblasts leads to excessive deposition of ECM material, increased tissue stiffness, and scarring, all of which contribute to the progressive loss of lung function. In addition, a positive feedback loop between matrix stiffness and myofibroblast differentiation may drive fibrosis progression; increased matrix stiffness increases fibroblast differentiation, and myofibroblasts are in turn able to increase matrix stiffness through collagen synthesis and cross-linking (Georges et al, 2007).

1.1.2 Mediators of Fibrosis

In IPF, increased levels of profibrotic mediators maintains an environment supportive of exaggerated fibroblast and myofibroblast activity resulting in chronic proliferation, differentiation, ECM deposition, and fibrosis. Many profibrotic mediators believed to play important roles in the pathogenesis of IPF are growth factors (Allen & Spiteri, 2002). Many growth factors, such as TGF- β 1, PDGF, vascular endothelial growth factor (VEGF), and fibroblast growth factor (FGF), are important in the wound healing process. However in IPF, growth factor signalling can be enhanced and therefore contribute to the development of fibrosis.

Growth factors activate receptor tyrosine kinases (RTKs), which regulate numerous cellular processes such as proliferation and differentiation, survival, and migration

(Lemmon & Schlessinger, 2010). Signalling by RTKs through the MAPK/ERK signalling cascade has been reported to be associated with many of the pro-fibrotic responses observed in IPF (Sun et al, 2015). Activation of this pathway is detected in lung samples from patients with fibrosis (Yoshida et al, 2002) and it has been shown that inhibition of the MAPK pathway, by the selective MAPK/ERK kinase (MEK) inhibitor ARRY-142886, prevents progression of established fibrosis in the TGF- α mouse model of fibrosis. Taken together, this highlights the importance of the MAPK pathway in fibrosis (Madala et al, 2012).

The MAPK/ERK pathway (Figure 1:3) is activated by growth factors binding to RTKs which results in receptor dimerization and autophosphorylation. The sequence homology 2 (SH2) domains of activated receptors are recognised by adaptor proteins such as Grb2, which in turn recruit guanine nucleotide exchange factors (GEFs) such as son of sevenless (SOS). SOS activates the small G protein Ras by promoting a conformational change that results in the displacement of guanosine-diphosphate (GDP) and subsequent binding of guanosine-5'-triphosphate (GTP). Subsequently, Raf, MEK, and ERK1/2 are activated in a cascade of phosphorylation events. ERK1/2 phosphorylates many substrates and plays an important role in diverse responses such as proliferation, differentiation, senescence, or survival. Two major growth factors that activate the MAPK/ERK pathway and have key roles in the development of IPF are PDGF and TGF- β .

1.1.2.1 Platelet-derived Growth Factor

PDGF was first isolated from platelets in the early 1970's and described as a growth factor for fibroblasts, smooth muscle cells, and glial cells (Kohler & Lipton, 1974; Ross et al, 1974; Westermark & Wasteson, 1976). The PDGF receptor (PDGFR) was

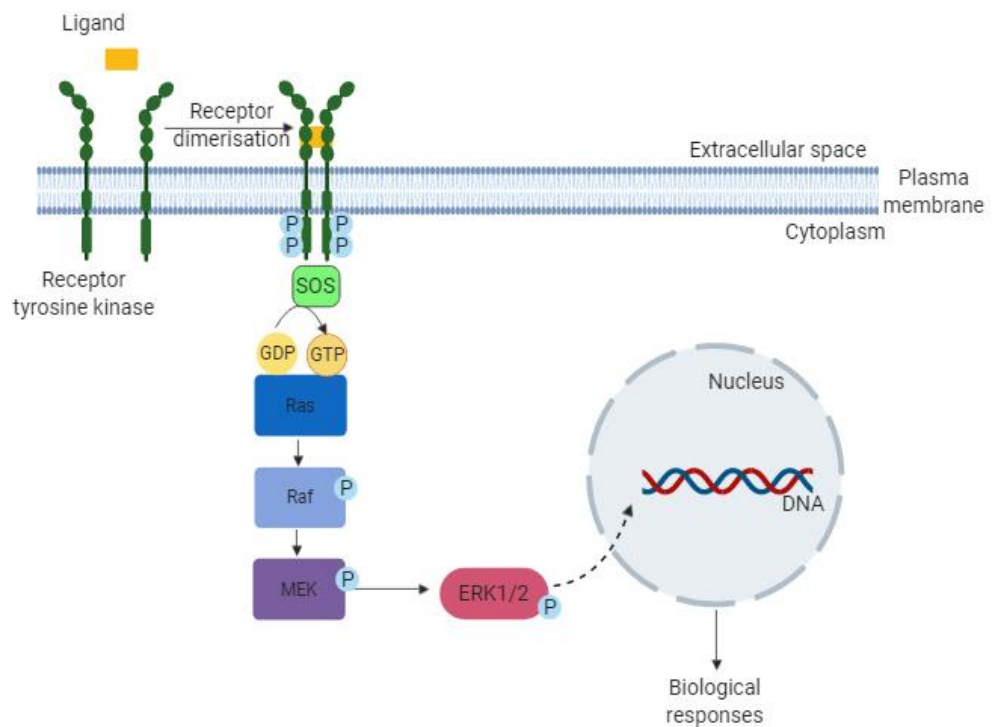


Figure 1:3 - Schematic representation of the MAPK/ERK signalling cascade

Ligand binding results in receptor tyrosine kinase dimerization and phosphorylation. Activated receptor induces displacement of GDP from Ras, subsequently allowing the binding of GTP. Activated Ras phosphorylates and subsequently activates the protein kinase Raf. Phosphorylated Raf then phosphorylates and activates MEK. The last step of the MAPK/ERK cascade results in phosphorylation of ERK1/2 leading to its translocation to the nucleus, gene transcription, and a range of biological responses. Image created using BioRender.com

identified as a RTK (Ek & Heldin, 1982). The PDGF family consists of four polypeptide growth factors denoted A, B, C and D, encoded by four different genes. PDGF-A and – B are highly expressed in human lung, whereas PDGF-C is expressed at lower levels and PDGF-D is not detected (Fredriksson et al, 2004). All four PDGF chains contain a highly conserved growth factor domain of approximately 100 amino acids. PDGF-C and –D are secreted as latent, inactive factors, with a protease required for their extracellular activation. PDGF isoforms function as homodimers with the exception of ligand “AB”, which acts as a heterodimer. These isoforms, PDGF-AA, PDGF-AB, PDGF-BB, PDGF-CC and PDGF-DD, act via two RTKs, PDGFRs α and β (Figure 1:4). Four of these dimeric isoforms, PDGF-AA, PDGF-AB, PDGF-BB, and PDGF-CC can bind to and activate PDGFR α , while PDGF-BB and PDGF-DD can specifically bind to and activate PDGFR β . PDGF-AB, PDGF-BB and PDGF-CC can also stimulate heterodimeric PDGFR α/β complexes.

Ligand-binding to receptors induces receptor dimerization, which leads to activation of the intrinsic tyrosine kinase domain and subsequent recruitment of SH2-domain-containing signalling proteins (Heldin et al, 1998). Examples of SH2-domain-containing molecules that bind to the PDGF receptors include phosphatidylinositol 3'-kinase (PI3-kinase), the adaptor molecule Grb2 which forms a complex with the nucleotide exchange molecule Sos1 that activates the small guanine triphosphatase (GTPase) Ras, and the tyrosine kinase Src (Heldin et al, 1998). Finally, activation of these pathways leads to cellular responses, such as proliferation and migration. PI3-kinase is important in particular for cell migration, actin reorganization, and prevention of cell death by apoptosis (Peng et al, 2008; Wennstrom et al, 1994a; Wennstrom et al, 1994b). Ras, which induces activation of the mitogen-activated protein kinase (MAPK) cascade, and

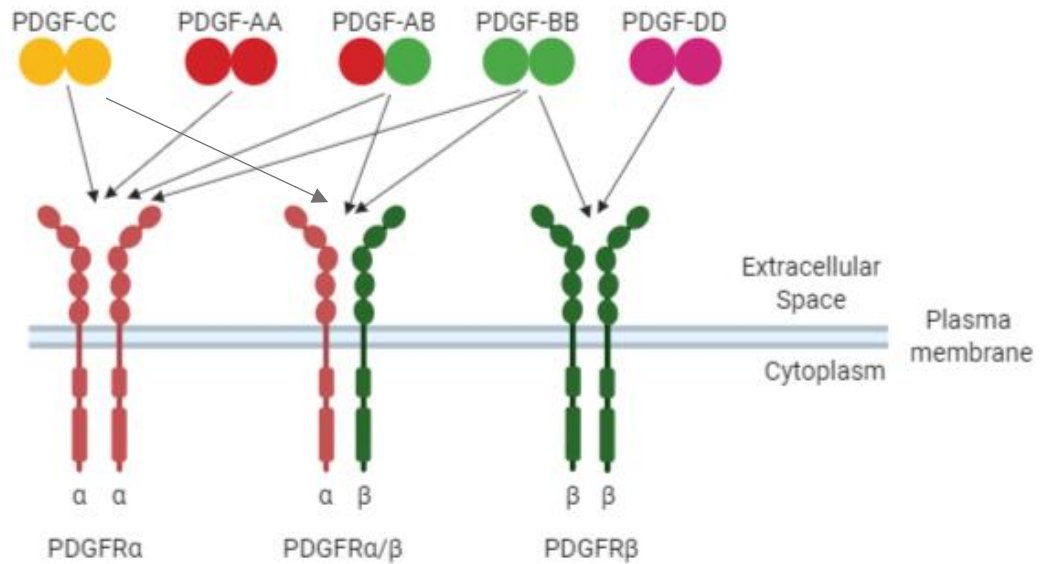


Figure 1:4 - Receptor-ligand interactions of the PDGF family members

The PDGF family consists of four polypeptide growth factors denoted: A, B, C and D, which form homodimers or heterodimers and act via two receptor tyrosine kinases, PDGFRs α and β . PDGF-AA, PDGFAB, PDGF-BB and PDGF-CC can bind to and activate PDGFR α . PDGF-BB and PDGF-DD can bind to and activate PDGFR β . PDGF-AB, PDGF-BB and PDGF-CC can also stimulate heterodimeric PDGFR α/β . Image created using BioRender.com.

the tyrosine kinase Src, which induces the transcription factor Myc, are particularly important for the mitogenic effect of PDGF (Heldin et al, 1998).

The PDGF family of growth factors are thought to play a critical role in lung fibrosis. PDGF is secreted by macrophages, epithelial cells, and fibroblasts in response to tissue injury to promote wound healing (Andrae et al, 2008; Beyer & Distler, 2013). PDGF, through its cognate receptor PDGFR, stimulates fibroblast and myofibroblast proliferation, migration, and survival (Hetzl et al, 2005; Wollin et al, 2014). Although PDGF is necessary for normal wound healing, elevated levels of PDGF have been found in bronchoalveolar lavage (BAL) fluid in animal models of disease (Walsh et al, 1993) as well as in epithelial cells from the lung of IPF patients (Antoniades et al, 1990), suggesting PDGF is an important contributing factor in the abnormal fibroblast proliferation observed in IPF.

1.1.2.2 Transforming Growth Factor- β 1

TGF- β belongs to a group of cytokines collectively known as the TGF- β superfamily, members of which regulate epithelial cell growth, differentiation, motility, organization, and apoptosis. In mammals, three isoforms of TGF- β are currently identified, TGF- β 1-3, each encoded by different genes. TGF- β is a homodimer and functions by interacting with serine/threonine kinase receptors, for which there are two types: type I and type II. Binding of the TGF- β ligand dimer to the type II TGF- β receptor promotes dimerization of the type II receptor with the type I receptor and subsequent phosphorylation of the type I receptor, leading to activation of downstream signals (Figure 1:5). SMADs comprise a family of structurally similar proteins that are one of the main signal transducers for TGF- β receptors. The activated type I TGF- β receptor activates SMAD2 and SMAD3 via phosphorylation. SMAD2 and

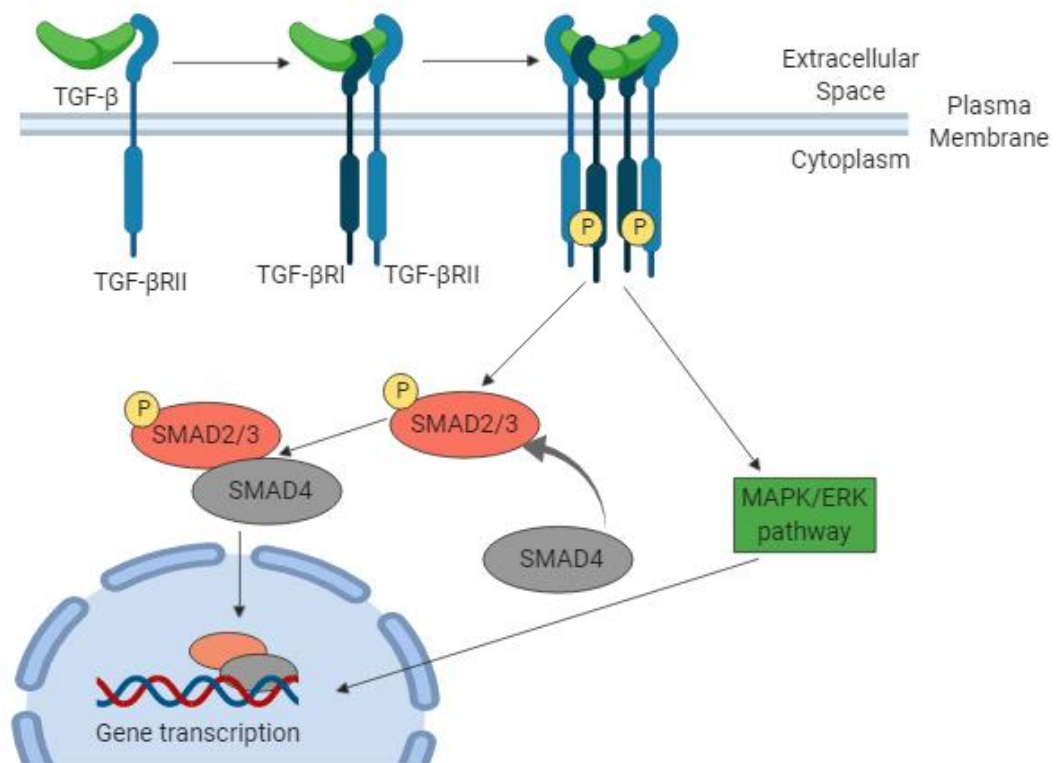


Figure 1:5 - Schematic representation of TGF- β signalling

Binding of TGF- β ligand dimer to the TGF- β receptor type II promotes dimerisation with TGF- β receptor type I, resulting in the transphosphorylation and activation of the receptor. The activated receptor phosphorylates SMAD2/3, which forms a trimeric complex with SMAD4. The SMAD trimer enters the nucleus to activate gene transcription. Activated TGF- β receptors also activate the MAPK/ERK pathway to activate gene transcription. Image created using BioRender.com

SMAD3 then form a trimer with SMAD4, which enters the nucleus to activate gene transcription (Hata & Chen, 2016). SMAD pathways are not the only means by which TGF- β regulates cellular functions. SMAD-independent pathways, including the MAPK/ERK pathway, are also activated by TGF- β signalling via activation of Ras (Mulder, 2000).

In response to TGF β stimulation, fibroblasts become activated and transform into contractile α -SMA expressing myofibroblasts that produce and secrete ECM proteins (Desmouliere et al, 1993; Roy et al, 2001). In addition, TGF- β indirectly stimulates fibroblast proliferation via induction of PDGF expression and by stimulating expression of pro-inflammatory and fibrogenic cytokines (Fernandez & Eickelberg, 2012). Alveolar macrophages express a large proportion of TGF- β , though it is also expressed by neutrophils, activated AECs, endothelial cells, fibroblasts, and myofibroblasts.

Excess or dysregulated TGF- β signalling is implicated in the pathogenesis of IPF. The specific deletion of type II TGF- β receptor in epithelial cells in a bleomycin-induced fibrosis mouse model provided protection against fibrosis, hypothesized to be due to improved epithelial cell survival and inhibition of EMT (Fernandez & Eickelberg, 2012; Li et al, 2011). TGF- β levels have been shown to be increased in IPF lungs, especially in alveolar epithelium and macrophages (Khalil et al, 1996; Khalil et al, 1991). However, anti-TGF- β therapy may not be ideal as TGF- β plays essential roles in regulating inflammation and acts as a tumour suppressor in certain contexts. It could lead to lung inflammation which would be counterproductive in the treatment of fibrosis as well as an increased risk to lung cancer (Lasky & Brody, 2000; Ozawa et al, 2009; Seoane & Gomis, 2017).

1.1.2.3 *Other profibrotic mediators*

Although growth factors play a key role in the development of fibrosis other mediators including integrins and phospholipids can contribute to the fibrotic environment.

Integrins are a large family of transmembrane proteins that constitute the main receptors for ECM components. They are primarily involved in the maintenance of cell adhesion and tissue integrity, although they have also been shown to influence cell survival, proliferation, differentiation, migration, shape, polarity and other biological processes (Teoh et al, 2015). Several integrins have been implicated in the development of fibrosis including, $\alpha 5\beta 1$ which plays a key role in the activation, proliferation, differentiation, and increased ECM synthesis of fibroblasts and myofibroblasts (Wu et al, 1999) and $\alpha v\beta 6$ which has been reported to activate the growth factor TGF- β (Agarwal, 2014).

Lysophosphatidic acid (LPA) is a phospholipid for which there are five cognate receptors (LPA₁-LPA₅), all of which are GPCRs. LPA induces fibroblast proliferation, survival and differentiation, cell migration, and cytoskeletal change (Choi et al, 2010; Tager et al, 2008). Tager and colleagues have shown that LPA levels are enhanced in BAL samples from patients with IPF, as well as in mice following lung injury in the bleomycin model of pulmonary fibrosis. In addition, mice lacking the LPA₁ receptor are protected from fibrosis and IPF-induced mortality in this model (Tager et al, 2008).

1.1.3 Therapeutics for IPF

IPF has an unpredictable and variable clinical course and is associated with extremely poor prognosis, therefore development of efficacious therapeutics is in high demand. A key therapeutic goal in the treatment of IPF is to slow or prevent progression of tissue fibrosis, which may be achieved by enhancing signals that counteract fibrotic

processes, and/or inhibiting signals and mediators that promote fibrosis. There are at present two drugs that are approved for use in the treatment of IPF; nintedanib and pirfenidone.

Nintedanib is an intracellular tyrosine kinase inhibitor that was originally developed as an anticancer drug. It has been shown to inhibit FGF, PDGF and VEGF receptors via binding to the adenosine triphosphate- (ATP) binding sites in the kinase domains (Hilberg et al, 2008). Hostettler and colleagues demonstrated that nintedanib shows an anti-fibrotic effect in IPF fibroblasts via inhibition of pro-proliferative effects of PDGF, FGF and VEGF (Hostettler et al, 2014). The efficacy of oral nintedanib in the treatment of IPF has been assessed in randomised, placebo controlled, double-blind trials; the TOMORROW, IMPULSIS-1, and IMPULSIS-2 trials (Richeldi et al, 2011; Richeldi et al, 2014). All trials concluded that treatment is associated with a reduction in the decline in lung function, which is consistent with a slowing of disease progression. In the TOMORROW trial a 68.4 % reduction in the rate of loss of forced vital capacity (FVC), the total volume of air that a person can exhale after full inspiration and a lower incidence of acute exacerbations, 2.4 vs. 15.7 per 100 patient-years, was observed for the nintedanib group, as compared with placebo (Richeldi et al, 2011). However, all three trials reported that 23-26 % of study participants discontinued the study medication prematurely due to adverse effects. The most frequent adverse event in the trials was diarrhoea, but other adverse events included nausea, dyspnoea, decreased appetite, vomiting, and weight loss. In addition, liver enzyme levels were reported to be increased to at least three times the upper limit of the normal range for aspartate aminotransferase or alanine aminotransferase, indicative of liver damage.

Pirfenidone is a pyridine derivative with broad anti-inflammatory/anti- TGF β activity (Iyer et al, 1999; Iyer et al, 2000). Much remains to be understood about the mechanism of action of pirfenidone. Pirfenidone's anti-fibrotic properties are mainly attributed to its effects on levels of various cytokines, growth factors, and chemokines (Kim & Keating, 2015). Bleomycin animal models have shown that pirfenidone suppresses FGF, TGF- β 1, and PDGF levels (Gurujeyalakshmi et al, 1999; Oku et al, 2008), as well as inflammatory cell levels, including neutrophils, macrophages, and lymphocytes (Iyer et al, 2000). Furthermore, Conte and colleagues demonstrated that pirfenidone reduced TGF- β -induced phosphorylation of Smad3, p38, and Akt, which are all mediators of the TGF- β pathway, and inhibited proliferation and TGF- β -induced differentiation of lung fibroblasts (Conte et al, 2014). CAPACITY and ASCEND phase III trials have shown that pirfenidone reduces the decline in lung function in patients with IPF (King et al, 2014; Noble et al, 2011). In the ASCEND trial the proportion of patients who had a decline of 10 percentage points or more in the percentage of the predicted FVC, or who had died, was reduced by 47.9 % in the pirfenidone group in comparison to the placebo group (King et al, 2014). However, higher incidences of adverse effects were seen in the pirfenidone groups in comparison with the placebo group in both trials, with 14.4 % and 15 % of participants discontinuing the study due to adverse effects in the ASCEND and CAPACITY trials, respectively. Nausea was the most common adverse effect, affecting over a third of participants taking pirfenidone. Other adverse effects included rash, dyspepsia, dizziness, vomiting, photosensitivity reaction, anorexia, insomnia, decreased appetite, weight reduction, and abdominal pain.

Nintedanib and pirfenidone are both examples of a multi kinase-targeted approach to the treatment of IPF, a standard approach that targets multiple known fibrotic

mediators and pathways. Although various trials have shown that these treatments have some benefits to patients, their non-specific action leads to severe adverse effects, therefore research to identify alternative approaches in IPF treatment is essential to enable the development of efficacious drugs that are safer and better tolerated.

1.2 G protein-coupled receptors

GPCRs are the largest family of cell surface receptors, with approximately 800 GPCRs identified in the human genome (Fredriksson et al, 2003). GPCRs mediate most of our physiological responses to hormones, neurotransmitters, and environmental stimulants, thus have been exploited as therapeutic targets for a broad spectrum of diseases, with over 30 % of current clinically available drugs targeting this receptor family (Hauser et al, 2017; Santos et al, 2017). Although GPCRs bind a wide variety of signalling molecules they share a common structure consisting of 7 transmembrane (TM) domain structural motifs, with three extracellular and three intracellular loops connecting the individual helices, and the carboxy terminus located intracellularly and the amino terminus extracellularly (Figure 1:6). GPCRs have been grouped according to sequence homology into five different classes, rhodopsin (also known as class A), secretin (class B), glutamate (class C), adhesion, and frizzled/taste2 receptors.

Class A GPCRs are the largest family, with approximately 700 receptors including the adrenergic, prostacyclin, and prostaglandin receptors. In addition to the usual 7TM domains, class A GPCRs often contain an additional 8th helix as part of the C terminus, which runs parallel to the membrane and is bounded by one or more sites for palmitoylation (Cherezov et al, 2007; Lee et al, 2015). Class B contains around 70 receptors which are characterised by an N terminal extracellular domain of approximately 120 amino acids, which forms an α -helix and four β -strands that are stabilised by conserved disulphide bridges. Peptides bind to this extracellular domain, which governs affinity and specificity, as well as to the 7TM domain to activate the receptor (Lee et al, 2015). Class C contains 22 GPCRs including the metabotropic glutamate family, GABA receptors, calcium-sensing receptors, and type 1 taste

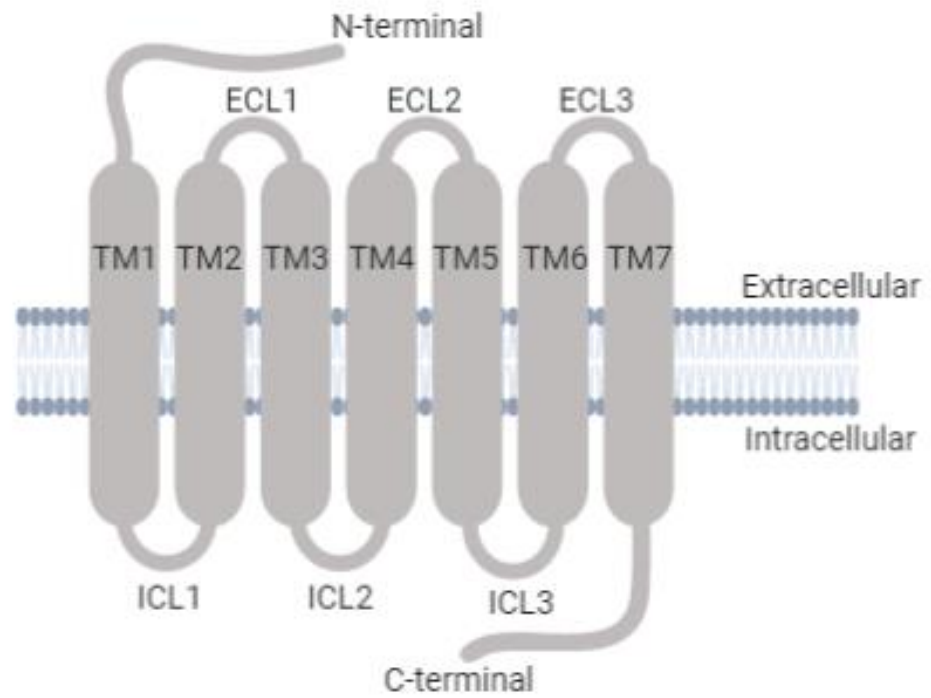


Figure 1:6 - General structure of G protein-coupled receptors

Seven transmembrane helices (TM1-7) span the membrane connected via intracellular (ICL1-3) and extracellular loops (ECL1-3), with extracellular N-terminal and intracellular C-terminal domains. Image created using BioRender.com

receptors. These receptors are characterized by seven TM helices and a large extracellular N-terminal domain with approximately 600 residues to which ligands bind (Bjarnadottir et al, 2005). Adhesion GPCRs are characterised by a long N-terminal region that contain a high percentage of serine and threonine residues that can create O- and N-glycosylation sites. There are 33 members of this group, with the majority being orphan receptors (Bjarnadottir et al, 2004). The frizzled/taste2 receptor group includes two distinct clusters, the frizzled receptors and the taste 2 receptors, which are grouped together due to consensus sequences that are not found in any of the other four families (Fredriksson et al, 2003). Little is known about the role and function of the taste 2 receptors except that they are expressed in the tongue and palate epithelium, and that they function as bitter taste receptors (Lu et al, 2017). The frizzled receptors mediate signals from glycoproteins termed Wnt, and are important in controlling cell fate, proliferation, and polarity (Fredriksson et al, 2003).

1.2.1 GPCR activation and signalling

The first step in signal transduction is ligand binding. GPCR ligands can be broadly categorised depending on where they bind and how they affect receptor signalling. Orthosteric ligands bind to the endogenous ligand binding site whereas allosteric ligands bind to a site separate to the orthosteric site. Ligands are then further described by two key parameters: affinity, the ability of the ligand to bind the receptor and efficacy, the ability of the ligand to activate (or inhibit) the receptor once bound (Kenakin & Williams, 2014).

Orthosteric ligands can be classified according to their efficacy as either agonists, antagonists, or inverse agonists. Agonists bind and activate receptors to modulate downstream signalling by promoting stabilisation of an active state of the receptor.

Full agonists induce a maximal signalling response whereas partial agonists induce a submaximal response at the receptor relative to a reference full agonist. Antagonists have no efficacy as they block or dampen a biological response by binding to and blocking a receptor rather than activating it like an agonist. Compounds possessing negative efficacy are termed inverse agonists. Inverse agonists block constitutive receptor activity by stabilising the inactive state of the receptor thus reversing the spontaneous elevated cellular response (Kenakin & Williams, 2014). Allosteric ligands modulate the activity of ligands bound to the orthosteric site. Positive allosteric modulators enhance orthosteric ligand binding and/or functional response, whereas negative allosteric modulators reduce binding and/or functional response of the orthosteric ligand. Allosteric modulators can also be neutral, where binding of the ligand to the allosteric site has no effect on orthosteric ligand binding or function. Allosteric ligands may also have efficacy in their own right, acting as either agonists or inverse agonists.

Agonist binding to GPCRs leads to a conformation change and rearrangement of the TM domains, which facilitates the binding of effector molecules such as G proteins (Schwartz et al, 2006). GPCR signalling requires heterotrimeric G proteins, intracellular partners that serve as canonical transducer proteins. G proteins are specialized proteins with the ability to bind the nucleotides GTP and GDP. They are heterotrimeric with three different subunits – alpha, beta, and gamma subunits- and in humans there are 21 $G\alpha$ subunits, 6 $G\beta$, and 12 $G\gamma$ subunits (Downes & Gautam, 1999). In the presence of inactivated receptor, GDP is bound tightly to the $G\alpha$ subunit, which is associated with the $\beta\gamma$ pair to form an inactive G protein. G protein coupling with the activated receptor induces a conformational change in the $G\alpha$ subunit reducing its affinity for GDP, facilitating its dissociation and replacement with GTP (Figure 1:7)

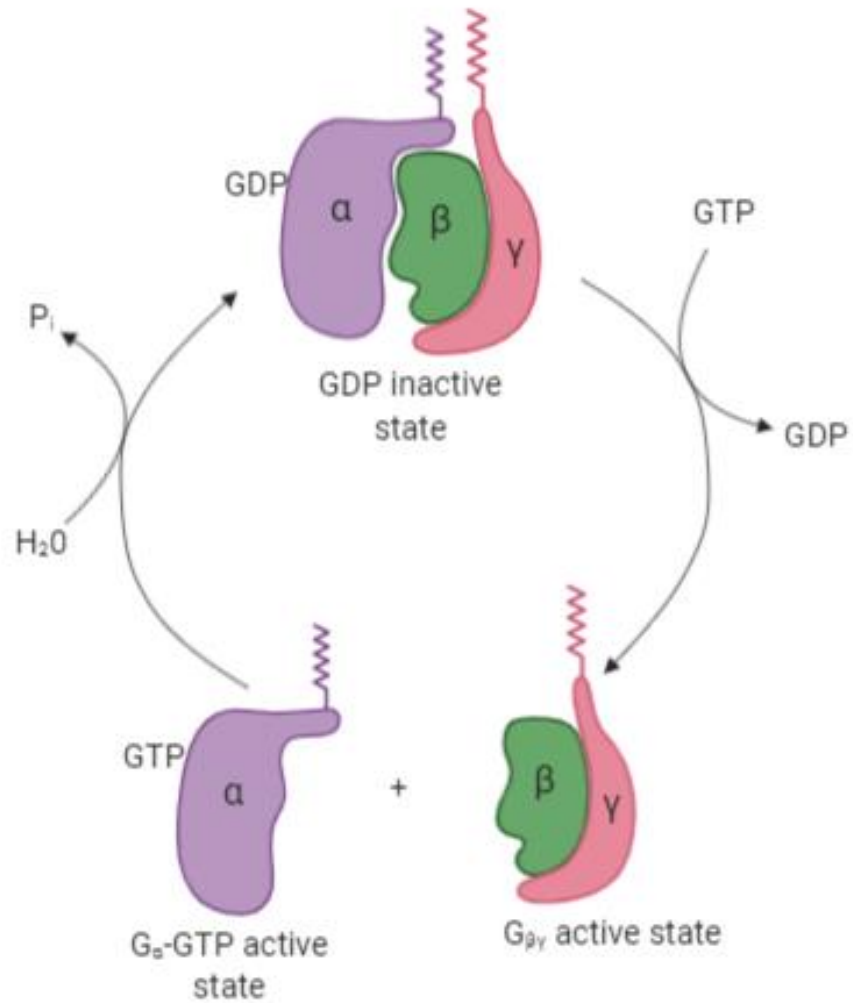


Figure 1:7 - Heterotrimeric G protein cycle

In the GDP-bound state G proteins exist as a $\alpha\beta\gamma$ trimer complex. Displacement of GDP with GTP dissociates the trimeric complex, generating a GTP-bound $G\alpha$ subunit and $G\beta\gamma$ subunit, which can interact with their effectors. Hydrolysis of GTP to GDP leads to the re-association of the $G\alpha\beta\gamma$ complex into the inactive state. Image created using BioRender.com.

(Dror et al, 2015). As a result, the G protein subunits dissociate into two parts: the GTP-bound $G\alpha$ subunit and a $G\beta\gamma$ dimer that remains anchored to the plasma membrane, but they are no longer bound to the GPCR, so they can now diffuse laterally to interact with other membrane proteins. The GTPase activity of the $G\alpha$ subunit results in the hydrolysis of GTP to GDP and the release of inorganic phosphate, with the cycle free to start again (Oldham & Hamm, 2008).

Depending on the type of G protein to which the receptor is coupled, a variety of downstream signalling pathways can be activated (Neves et al, 2002). On the basis of sequence similarity the $G\alpha$ subunits have been classified into four subfamilies, namely, $G\alpha_s$, $G\alpha_{i/o}$, $G\alpha_{q/11}$, and $G\alpha_{12/13}$. $G\alpha_s$ activates adenylyl cyclase (AC) to increase cellular cyclic adenosine monophosphate (cAMP) levels (discussed further in Section 1.3.1) and $G\alpha_{i/o}$ inhibits AC to decrease cellular cAMP. $G\alpha_{q/11}$ couples to phospholipase C β to increase inositol 1,4,5-trisphosphate (IP₃) production and subsequently intracellular calcium levels, and $G\alpha_{12/13}$ couples to Rho GTPase nucleotide exchange factors to modulate signalling of the Rho-ROCK pathway. Although initially described as a negative regulator of the $G\alpha$ subunit by reassociation, the $G\beta\gamma$ subunit has also been shown to modulate multiple kinase enzymes, including phospholipase C and ERK, as well as calcium ion channels (Currie, 2010; Khan et al, 2013).

1.2.2 GPCR desensitisation and internalisation

There are processes which are triggered by receptor activation that limit the extent of receptor signalling at the plasma membrane. These processes are termed receptor desensitisation and internalisation, and are mediated by two key protein families: G protein coupled receptor kinases (GRKs) and β -arrestins. GRKs are serine/threonine kinases that phosphorylate these residues on the carboxy terminus and intracellular

loop 3 of activated GPCRs (Black et al, 2016; Komolov & Benovic, 2018). This phosphorylation triggers the second step of signal termination, by marking activated receptors for binding of β -arrestin proteins to the phosphorylated receptor.

β -arrestins were first identified for their ability to desensitise agonist-induced β_2 adrenoceptor signalling (Lohse et al, 1990). They belong to the arrestin family which is composed of four members; arrestin-1 (also known as visual arrestin) and arrestin-4 (known as cone arrestin), which are expressed almost exclusively in the retina, and arrestin-2 (β -arrestin1) and arrestin-3 (β -arrestin 2), which are ubiquitously expressed (Attramadal et al, 1992; Luttrell & Lefkowitz, 2002). Binding of β -arrestins to phosphorylated receptor prohibits further G protein coupling via steric inhibition (Black et al, 2016). As well as playing a role in receptor desensitisation and internalisation, β -arrestins have also been shown to be signalling partners in their own right by acting as a scaffold for cellular signalling partners such as ERK1/2 and c-Jun N-terminal kinase (JNK) to modulate cellular signalling (Eichel et al, 2016; Smith & Rajagopal, 2016).

After GPCRs are desensitized, they are re-distributed away from the cell surface by internalisation. β -arrestins act as adaptor proteins, binding to AP-2 and clathrin to mediate receptor internalisation via clathrin-coated pits. These clathrin coated pits pinch off from the membrane in a process mediated by the GTPase dynamin, and intracellular vesicles are formed (Kang et al, 2013). Internalized GPCRs undergo one of two possible fates, involving either: 1) recycling back to the cell surface for another round of signalling or 2) degradation within lysosomes (Irannejad et al, 2015). Originally, internalisation of GPCRs was thought to terminate signalling by removal of the receptor from the cell surface, however there is now an accumulating amount of

evidence to suggest GPCRs can continue signalling from endocytic compartments
(discussed further in section 1.5.1.4).

1.3 cAMP as a target for the treatment of IPF

There is an evolving body of evidence demonstrating that the cAMP pathway is a potential target for the treatment of IPF. Strategies that activate the cAMP signalling pathway have been shown to be efficacious in inhibiting pro-fibrotic responses in fibroblasts by negatively impacting MAPK signalling, via inhibition of ERK phosphorylation (Nikam et al, 2011; Stork & Schmitt, 2002). This suggests that activation of the cAMP pathway could provide novel targets to treat IPF.

1.3.1 cAMP pathway

Substances that convert extracellular signals received by cell surface receptors to intracellular signals are known as second messengers. One of the most studied second messengers is cAMP. Intracellular levels of cAMP are tightly regulated by the balance between the activities of two enzymes, ACs and phosphodiesterases (PDEs). AC catalyses the cyclisation of ATP to cAMP, and its activity is regulated downstream from GPCRs, with $G\alpha_s$ proteins activating ACs and $G\alpha_{i/o}$ proteins inhibiting ACs (Figure 1:8). To date there are 10 identified AC isoforms, nine membrane associated and one cytosolic AC, that are differentially expressed in various cell types (Sunahara & Taussig, 2002). Membrane-bound ACs are classified into four different categories based on regulatory properties. Group I consists of Ca^{2+} -stimulated AC1, 3, and 8; group II consists of $G\beta\gamma$ -stimulated AC2, 4, and 7; group III is comprised of $G\alpha_i/Ca^{2+}$ -inhibited AC5 and 6, while group IV contains forskolin-insensitive AC (Sadana & Dessauer, 2009). Cytosolic, or soluble, AC (AC10) is an intracellular bicarbonate and calcium sensor and is most widely accepted to play a role in mammalian male fertility (Esposito et al, 2004; Hess et al, 2005; Tresguerres et al, 2011).

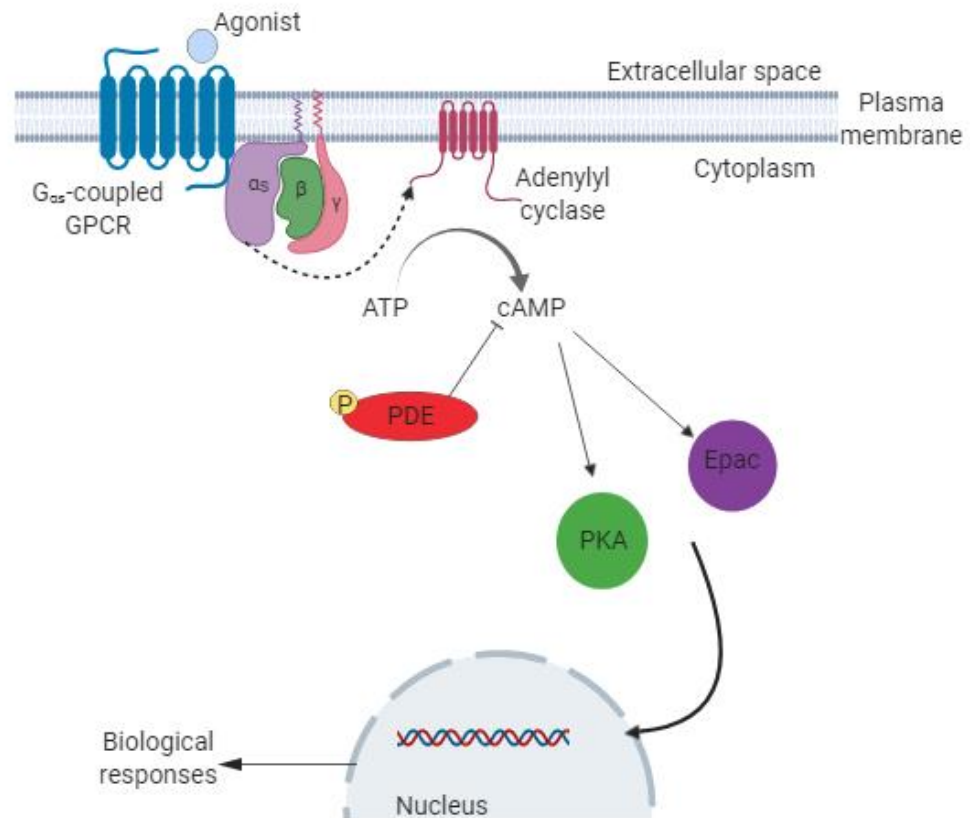


Figure 1:8 - Schematic representation of the cAMP signalling pathway

Upon agonist binding, G α_s -coupled GPCRs undergo a conformational change resulting in the exchange of GDP for GTP in the heterotrimeric G protein. The G α_s subunit dissociates from the G $\beta\gamma$ and then activates adenylyl cyclase, resulting in the production of cAMP from ATP. cAMP activates PKA or Epac, which have many downstream targets, resulting in gene transcription and a variety of biological responses. Phosphodiesterases (PDE) terminate cAMP signalling by hydrolysing cAMP.

Image created using BioRender.com.

One major target of cAMP is protein kinase A (PKA), a tetrameric serine/threonine kinase consisting of two catalytic and two regulatory subunits (Walsh et al, 1968). cAMP binds to the regulatory subunits, inducing a conformational change resulting in the dissociation of the catalytic subunits (Brostrom et al, 1971). The catalytic subunits then phosphorylate a multitude of proteins, influencing various cellular processes, such as cell growth, death, and differentiation, metabolism, and muscle contraction (Cheng et al, 2008). PKA can also regulate AC activity as it has been shown to phosphorylate and inactivate AC5 and AC6, which provides a negative feedback loop in the cAMP pathway (Iwami et al, 1995).

Another target of cAMP is exchange protein directly activated by cAMP (Epac), for which there are two isoforms, Epac1 and Epac2. Epac1 is most abundant in the heart, kidney, blood vessels, adipose tissue, central nervous system, ovary, and uterus, whereas Epac2 is mostly expressed in the central nervous system, adrenal gland, and pancreas (de Rooij et al, 1998; Kawasaki et al, 1998; Niimura et al, 2009). Epac1 and Epac2 possess one and two cAMP binding sites, respectively, and function as GEFs that activate small GTPases Rap1 and Rap2 (de Rooij et al, 1998; Kawasaki et al, 1998). Epac proteins regulate numerous cellular responses through their ability to promote the exchange of GDP for GTP on Raps, resulting in Rap activation (Breckler et al, 2011; Gloerich & Bos, 2010). Upon activation by GTP binding, Rap1 undergoes conformational changes, causing the recruitment of various effector proteins, including proteins involved in the MAPK/ERK signalling cascade (discussed in section 1.3.2). However a conflicting role of Rap1 in modulating ERK activity has been described, with Rap1 mediating the activation of ERK in PC12 cells (Vossler et al, 1997), and the inactivation of ERK in fibroblasts and HEK293 cells (Cook & McCormick, 1993; Schmitt & Stork, 2001). Studies using specific agonists for Epac, such as 8-pCPT-2'-O-

Me-cAMP, have shown that Epac participates in the regulation of various cellular functions including cellular adhesion of epithelial cells (Fukuhara et al, 2005), neurotransmitter release (Kaneko & Takahashi, 2004; Sakaba & Neher, 2003), and regulation of intracellular signalling by phospholipase C (Schmidt et al, 2001).

cAMP is inactivated by hydrolysis to adenosine monophosphate (AMP) by PDEs. There are 11 different PDE families (PDE1-PDE11) based on their amino acid sequences; sensitivity to different activators and inhibitors; and their ability to preferentially hydrolyse either cAMP, cGMP, or both (Bender & Beavo, 2006). Any single cell type can express several different PDEs, and the nature and localization of these PDEs are likely to be a major regulator of the local concentration of cAMP. PDE₄, PDE₅, and PDE₁ have been shown to be expressed in human lung fibroblasts (Dunkern et al, 2007; Obernolte et al, 1997).

1.3.2 cAMP pathway crosstalk with MAPK/ERK pathway

In addition to regulating many important cellular processes directly, cAMP is also implicated in crosstalk between intracellular signalling pathways. For example, cAMP exerts its inhibition of growth effects through interactions with the MAPK/ERK pathway (Stork & Schmitt, 2002). The MAPK/ERK signalling cascade (discussed in Section 1.1.2) is a major pathway controlling cellular processes associated with fibrogenesis, including cell growth, proliferation, and survival (Schaeffer & Weber, 1999).

Early studies showed that increasing concentrations of cAMP blocked growth factor stimulated Raf-1 and ERK activation in Rat1 and NIH3T3 fibroblasts (Cook & McCormick, 1993; Wu et al, 1993). Since then various studies have shown that cAMP inhibits the MAPK/ERK pathway (Graves et al, 1993; Nikam et al, 2011; Stork & Schmitt,

2002). The current model of cAMP and MAPK/ERK pathway crosstalk suggests that the target of cAMP is Raf. PKA has been shown to phosphorylate three sites within the Raf N-terminal domain, blocking Raf interaction with Ras, thus obstructing the MAPK/ERK signalling cascade (Dhillon et al, 2002; Dumaz et al, 2002; Sidovar et al, 2000). Obstruction of the Raf/Ras interaction is achieved by either steric hindrance or by the recruitment of 14-3-3 proteins that may directly compete with Ras binding, or induce a conformational change that disrupts Ras binding (Dumaz & Marais, 2003; Light et al, 2002).

1.3.3 cAMP elevating agents as novel IPF therapeutics

The crosstalk between the cAMP pathway and the MAPK/ERK pathway creates a new avenue for the inhibition of pro-fibrotic processes observed in IPF. In support of this, numerous studies have shown that activating GPCRs that increase cAMP formation and inhibiting PDEs that hydrolyse cAMP are effective in inhibiting pro-fibrotic processes both *in vitro* and *in vivo*.

PDE₄ inhibitors such as roflumilast are currently approved for the treatment of the chronic lung disease COPD and the inhibition of PDEs, which catalyse cAMP degradation, has also been described as a potential route for the inhibition of fibrotic pathways. The knockdown of PDE₄ isoforms have been shown to inhibit lung fibroblast proliferation and differentiation, highlighting an important role for PDEs for the development of lung fibrosis (Selige et al, 2011). The PDE₄ inhibitor piclamilast was found to attenuate TGF- β -mediated FMT (Dunkern et al, 2007). Furthermore, PDE₄ inhibitor, roflumilast, was shown to inhibit TGF- β stimulated fibroblast contraction and migration *in vitro* and to attenuate bleomycin-induced lung fibrosis in mice (Cortijo et al, 2009; Togo et al, 2009). Although PDE₄ inhibitors have been shown to have

promising anti-fibrotic properties in numerous *in vitro* and *in vivo* studies, negative results were obtained with the PDE₅ inhibitor sildenafil in clinical trials (Zisman et al, 2010). This may not be surprising as sildenafil was shown to have no inhibiting effects *in vitro* on fibroblast differentiation, which highlights the need to target the correct PDE isoform for developing therapeutics for IPF (Dunkern et al, 2007).

A range of G α_s -coupled GPCRs have been identified as potential targets for the treatment of IPF. Studies in patients with IPF indicated that prostaglandin E₂ (PGE₂) production and signalling can be diminished in lung fibrosis (Borok et al, 1991). Furthermore, more recent work in animal models and human tissues have identified epigenetic changes that show downregulation of PGE₂ production in fibrotic lung tissues (Coward et al, 2009; Huang et al, 2010), and have revealed PGE₂ signalling defects in fibrotic fibroblasts (Huang et al, 2008b). Combined these studies suggest PGE₂ plays an important role in modulating lung fibrosis. There are four PGE₂ receptors, designated EP₁, EP₂, EP₃, and EP₄, with stimulation of EP₂ and EP₄ increasing cAMP levels and stimulation of EP₁ and EP₃ inhibiting cAMP accumulation and increasing calcium. By signalling through EP₂ and EP₄ and elevating cAMP levels, PGE₂ has been shown to limit fibroblast differentiation and migration (Kolodsick et al, 2003; Thomas et al, 2007; White et al, 2005), as well as collagen expression and proliferation (Huang et al, 2007) of lung fibroblasts. The inhibition of fibroblast collagen expression has been shown to involve activation of PKA (Huang et al, 2007; Huang et al, 2008a), whereas inhibition of proliferation required Epac (Huang et al, 2008a). Although PGE₂ signalling via EP₂ and EP₄ has anti-fibrotic properties, PGE₂ is capable of promoting fibroblast proliferation by binding to EP₁ or EP₃ receptors which inhibit cAMP production and increase calcium (Watanabe et al, 1996; White et al, 2008). As well as being non-selective, PGE₂ has a short half-life *in vivo* due to its metabolism into

biologically inactive molecules by prostaglandin dehydrogenase, therefore the development of novel EP₂ and EP₄ selective agonists could increase the therapeutic potential of targeting these receptors for the treatment of IPF (Markovic et al, 2017; Sieber et al, 2018).

Another GPCR identified as having anti-fibrotic properties is the β_2 adrenoceptor. Inhaled β_2 adrenoceptor agonists are widely used for the treatment of lung diseases such as COPD and asthma, providing relief by inducing bronchodilation of airway smooth muscle (Fitzgerald & Fox, 2007; Sin et al, 2003; Walters et al, 2005). More recently, β_2 adrenoceptors have been shown to exert various inhibitory effects on profibrotic features in lung fibroblasts. β_2 adrenoceptors have been shown to be expressed on lung fibroblasts and β_2 adrenoceptor agonist-induced downregulation of proliferation, collagen synthesis, and differentiation in human lung fibroblasts has been demonstrated (Herrmann et al, 2017; Lamyel et al, 2011; Liu et al, 2004). In addition, the β_2 adrenoceptor agonist olodaterol has been shown to attenuate bleomycin-induced profibrotic mediator release, thus further demonstrating the potential of β_2 adrenoceptor agonists as anti-fibrotic therapeutics (Herrmann et al, 2017).

Another GPCR that has recently gained attention for its anti-fibrotic activity and potential as a novel therapeutic target for IPF is the IPR. More details of IPR signalling and therapeutic potential are outlined in the next section.

Overall, the literature shows that elevating cAMP in lung fibroblasts has the potential to inhibit fibrotic activity associated with the development of IPF. However, other cell types, such as alveolar epithelial cells, play a key role in the development of IPF. In IPF, alveolar epithelial cells are unable to regenerate after injury, and undergo EMT, in

which epithelial cells lose part of their characteristics and markers, while gaining mesenchymal ones (Salton et al, 2019). The cAMP pathway has been implicated in EMT, with evidence suggesting that cAMP acts as a potential novel pharmaceutical target. Inhibition of PDE4 has been demonstrated to restore epithelial markers, inhibit mesenchymal markers, and prevent EMT (Kolosionek et al, 2009; Milara et al, 2014). Furthermore, cAMP elevating agents including forskolin and PGE₂ have been demonstrated to inhibit EMT (Zhang et al, 2006). As fibroblasts and epithelial cells are the two main drivers of IPF, inhibiting the profibrotic activity of both cell types could be therapeutically beneficial. Thus, identifying a drug that can elevate cAMP and inhibit profibrotic processes in both cell types could result in greater efficacy in treating IPF.

1.4 Prostacyclin receptor

The IPR is a Class A rhodopsin-type GPCR that has been identified as having the potential to inhibit pro-fibrotic processes, and therefore is an interesting target for the development of novel therapeutics for IPF.

1.4.1 IPR signalling

The endogenous ligand for the IPR is prostacyclin (PGI_2), an arachidonic acid metabolite synthesized mainly through endothelial cells by cyclooxygenase enzymes in conjunction with PGI_2 synthase (Caughey et al, 2001; Weksler et al, 1978). Arachidonic acid is converted to prostaglandin H_2 by PGH_2 synthase, which is subsequently converted to PGI_2 by PGI_2 synthase. As a GPCR, ligand binding to the IPR activates heterotrimeric G proteins for signal transduction. Studies of the IPR have shown differences in coupling to G proteins depending upon cellular context. In heterologous over-expression systems IPR couples to both $\text{G}\alpha_s$ and $\text{G}\alpha_{q/11}$, therefore increasing cAMP levels and intracellular calcium concentrations, has been described (Smyth et al, 1996). In contrast, studies of endogenously expressed IPRs in cells, including neuroblastoma cells and vascular smooth muscle cells, show the IPR couples to $\text{G}\alpha_s$, not $\text{G}\alpha_{q/11}$ (Kam et al, 2001; Midgett et al, 2011).

Studies investigating the desensitisation of activated IPR in HEK-293 cells have shown that PKC-mediated phosphorylation is required for IPR desensitisation (Smyth et al, 1998). However, experiments using endogenously expressed IPR in human fibroblasts demonstrated that the receptor is not desensitised by PKC, as a PKC activator and inhibitor had no effect on cAMP responses (Nilius et al, 2000). After desensitisation the IPR has been shown to undergo agonist-dependent internalisation (Midgett et al, 2011). In pulmonary arterial smooth muscle cells (PASMC) limited β -arrestin

recruitment and lack of sustained IPR internalisation has been observed with the IPR agonist MRE-269, whereas larger β -arrestin recruitment and internalisation was observed with other agonists, including iloprost, beraprost, and treprostinil (Gatfield et al, 2017). Desensitisation and internalisation are key processes in controlling duration of signalling in cells, and considering the important role of IPR activity in long-term phenotypic changes in cells, further studies into how different agonists drive varying levels of receptor internalisation are essential.

1.4.2 Therapeutic potential of the IPR

The IPR is an important cardiovascular GPCR with PGI_2 having a cardioprotective role as a pulmonary vasodilator synthesised in the endothelium (Gryglewski, 2008; Gryglewski et al, 1978). Prostacyclin analogues, such as iloprost, are currently used in the treatment of pulmonary arterial hypertension (PAH) (Humbert & Ghofrani, 2016). PAH is caused by progressive remodelling of the pulmonary vasculature by cell proliferation and fibrosis, occluding the blood vessels, leading to heart failure and death (Voelkel et al, 2012). Targeting the IPR in vascular smooth muscle cells results in activation of the cAMP pathway, leading to downstream effects including relaxation and inhibition of proliferation (Kamio et al, 2007; Kothapalli et al, 2003). Similarities between PAH and IPF pathophysiology is evident, with both diseases resulting from tissue remodelling and fibrosis. Due to the similarities, drugs that are currently used for the treatment for PAH, such as iloprost, are being described as potential IPF therapeutics, suggesting the IPR as a novel target for the treatment of IPF (Zhu et al, 2010).

A decreased level of the endogenous IPR agonist PGI_2 was found in fibroblasts isolated from IPF patients, and PGI_2 has been shown to inhibit migration, proliferation, and

collagen synthesis of fibroblast *in vitro* (Cruz-Gervis et al, 2002; Kohyama et al, 2002). Numerous agonists that target the IPR have been developed, including prostacyclin analogues such as iloprost, cicaprost, beraprost, and treprostinil, and non-prostacyclin analogues such as MRE-269. Targeting the IPR with these agonists results in the inhibition of numerous pro-fibrotic processes, including fibroblast proliferation, differentiation, and collagen secretion (Table 1:1) (Ali et al, 2006; Kamio et al, 2007; Lambers et al, 2018; Larsson-Callerfelt et al, 2013; Liu et al, 2010; Zmajkovicova et al, 2018). Furthermore, iloprost and treprostinil have been shown to inhibit bleomycin induced pulmonary fibrosis (Corboz et al, 2018; Manitsopoulos et al, 2015; Zhu et al, 2010).

A common complication of IPF that is strongly linked to mortality is the presence of PAH (Klinger, 2016). The AEC injury sustained in IPF results in the release of mediators, such as VEGF and TGF- β , that not only contribute to the development of lung fibrosis but also result in endothelial cell apoptosis and remodelling of the arterial wall, leading to the development of PAH (Farkas et al, 2009; Farkas et al, 2011; Nathan et al, 2007). The production of less vasodilators and more vasoconstrictors such as endothelin-1, by injured endothelial cells results in augmented vasoconstriction of smooth muscle cells (Budhiraja et al, 2004; Giaid et al, 1993; Trakada & Spiropoulos, 2001). Patients with IPF that is also complicated by PAH have a worse prognosis than those without PAH, therefore drugs that target PAH as well as the progression of lung fibrosis could result in a better clinical outcome (Rivera-Lebron et al, 2013). A clinical trial (NCT02630316) is currently investigating the effect of IPR agonist treprostinil on lung function and heart morphology/function in patients with PAH associated with interstitial lung disease.

Overall, the IPR provides a potential novel therapeutic strategy for the treatment of IPF, and research to identify efficacious anti-fibrotic agonists that target this receptor is ongoing.

Table 1:1 - Anti-fibrotic properties of selected prostacyclin receptor agonists

	Anti-fibrotic properties	References
Prostacyclin analogues		
Iloprost	<ul style="list-style-type: none"> • Inhibits fibroblast contraction and fibronectin release • Protects from bleomycin-induced pulmonary fibrosis in mice • Reduces fibroblast collagen synthesis, proliferation and contraction 	<ul style="list-style-type: none"> • (Kamio et al, 2007) • (Zhu et al, 2010) • (Larsson-Callerfelt et al, 2013) • (Ali et al, 2006)
Cicaprost	<ul style="list-style-type: none"> • Inhibits fibroblast proliferation 	<ul style="list-style-type: none"> • (Ali et al, 2006)
Treprostinil	<ul style="list-style-type: none"> • Inhibits fibroblast proliferation, differentiation, and collagen secretion • In the bleomycin mouse model maintained respiratory function, reduced airspace inflammation, and attenuated collagen deposition • Inhibits bleomycin-induced pulmonary fibrosis in rats 	<ul style="list-style-type: none"> • (Lambers et al, 2018) • (Manitsopoulos et al, 2015) • (Corboz et al, 2018) • (Ali et al, 2006)
Beraprost	<ul style="list-style-type: none"> • Inhibits fibroblast contraction and fibronectin release • Inhibits fibroblast collagen synthesis and differentiation 	<ul style="list-style-type: none"> • (Kamio et al, 2007) • (Liu et al, 2010)
Non-prostacyclin analogues		
MRE-269	<ul style="list-style-type: none"> • Inhibits fibroblast proliferation, differentiation, ECM deposition, and contraction 	<ul style="list-style-type: none"> • (Zmajkovicova et al, 2018)

1.5 Spatiotemporal regulation of cAMP and MAPK/ERK pathway

Cells are exposed to a multitude of different stimuli, but intracellular signalling is limited to a number of second messengers, for example, cAMP. With cells being exposed to a host of signals at any one time it is important that the intracellular signals can be differentiated in order to result in specific cellular responses. In order to direct receptor-specific functions in cells, ubiquitous second messengers can be controlled spatially and temporally.

1.5.1 Spatiotemporal regulation of the cAMP pathway

cAMP is a ubiquitous second messenger that regulates a multitude of cellular processes, thus precise regulation is very important in ensuring specific biological responses. One of the ways in which this may occur is via compartmentalisation of cAMP into specific intracellular microdomains. Some of the earliest evidence suggesting that cAMP is compartmentalised came from studies using isolated perfused hearts. It was shown that isoprenaline and PGE₁, acting via the β_2 and EP receptors respectively, increased cAMP to comparable levels in addition to activating PKA to similar degrees, but had very different effects on the phosphorylation of PKA substrates. Isoprenaline activated the particulate fraction of PKA (PKA-type II), increased the activation state of phosphorylase kinase and glycogen phosphorylase, inducing positive inotropic effects. In contrast, PGE₁ led to activation of soluble PKA (PKA-type I) and did not produce any change in the contractive activity or in the activities of PKA substrates related to glycogen metabolism (Hayes et al, 1979; Hayes et al, 1980). The identification of the two PKA isoforms that differ in their regulatory subunit and subcellular distribution, and the finding that activation of PKA-type I or

PKA-type II result in distinct biological responses, fuelled the hypothesis that the compartmentalisation of cAMP is required to selectively activate the distinct subsets of PKA (Brunton et al, 1981; Corbin et al, 1977; Hayes et al, 1980). Since these early studies, compartmentalisation of the cAMP pathway has emerged as an important mechanism in ensuring intracellular signals can be differentiated in order to result in specific cellular responses.

1.5.1.1 Plasma membrane microdomains

The fluid mosaic model of the plasma membrane proposed that proteins diffuse freely and that signal transduction occurs through random protein interaction (Singer & Nicolson, 1972). However, it has been shown that the movement of membrane proteins is restricted through the establishment of membrane microdomains where different signalling proteins can be concentrated (Bethani et al, 2010). Plasma membrane microdomains can be established by the formation of lipid rafts, which contain cholesterol and sphingomyelin-rich areas (Jacobson et al, 2007). Compartmentalised signalling at lipid-rich versus non-lipid-rich domain of the plasma membrane has been directly demonstrated in both cardiomyocytes (Agarwal et al, 2018) and airway smooth muscle cells (Agarwal et al, 2017) using targeted cAMP biosensors (discussed in Section 1.5.3.1). In cardiomyocytes, β_1 adrenoceptors are localised to both lipid-rich and non-lipid-rich plasma membrane domains, whereas EP₃ receptors are found only in non-lipid-rich domains (Agarwal et al, 2011). Targeting β_1 adrenoceptors with isoproterenol resulted in cAMP production in lipid rafts as well as non-raft domains of the plasma membrane, whereas targeting EP₃ receptors with PGE₁ stimulated cAMP production in non-raft domains of the plasma membrane (Agarwal et al, 2018). In airway smooth muscle cells, β_2 adrenoceptors are found in lipid-rich domains, whereas EP₂ receptors are excluded from lipid-rich domains. Stimulation of

β_2 adrenoceptors with isoprenaline on airway smooth muscle cells produces cAMP that is detected in both lipid-rich and non-lipid-rich domains, however stimulation of EP₂ receptors with butaprost stimulated cAMP production only in non-lipid-rich domains (Agarwal et al, 2017).

Membrane microdomains are also known for concentrating other signalling molecules, such as G proteins (Allen et al, 2009; Oh & Schnitzer, 2001) and AC isoforms. For example AC1, AC3, AC5, AC6, and AC8 associate with lipid rafts whereas AC2, AC4, AC7, and AC9 are found within non-raft plasma membrane microdomains (Cooper & Tabbasum, 2014; Dessauer et al, 2017; Ostrom & Insel, 2004). AC localisation to specific membrane microdomains has been shown to be correlated with GPCR coupling to specific ACs. Specific GPCR/AC coupling has been elucidated using knockdown or overexpression of different AC isoforms (Johnstone et al, 2018). For example, AC6 overexpression enhances β_2 adrenoceptor and IPR signalling in cardiac fibroblasts (Liu et al, 2008) and enhances β_1 adrenoceptor signalling in cardiac myocytes (Ostrom et al, 2000). In contrast, overexpression of AC2 in human airway smooth muscles cells enhanced EP₂ receptor signalling (Bogard et al, 2012). Overexpression experiments do not necessarily confirm that these couplings occur endogenously in these cells, just that they can couple. The best way to determine endogenous coupling is using knockdown experiments. Coupling of the β_2 adrenoceptor to AC6 was shown when β_2 adrenoceptor agonist-stimulated relaxation of ASM cells from AC6 knock-out mice was abolished (Birrell et al, 2015).

The co-localization of various signalling components at the plasma membrane allows cells to shape cellular responses by spatially organizing components to allow specific and kinetically favourable GPCR signal transduction.

1.5.1.2 *A-Kinase Anchoring Proteins*

Another important factor in maintaining the fidelity of receptor-mediated responses is the formation of signalling complexes that organize effectors of cAMP, such as PKA, together with the target proteins they regulate. This often occurs through interactions with scaffolding proteins like A-kinase anchoring proteins (AKAPs). Over 50 AKAPs have been identified in mammals and lower organisms, and all AKAPs share common properties including a PKA-anchoring domain, localisation signals, and the ability to form complexes with other signalling molecules (Wong & Scott, 2004). AKAPs can be targeted to numerous subcellular locations, including to the plasma membrane through sequences that bind phospholipids (Dell'Acqua et al, 1998), mitochondria through mitochondrial-targeting sequences (Huang et al, 1999), and the centrosome through a protein-interaction module known as the pericentrin-AKAP350 centrosomal targeting domain – or PACT for short (Diviani et al, 2000). AKAPs were originally classified on the basis of their ability to compartmentalise PKA, however it is now recognised that AKAPs form signalling complexes that contain GPCRs, ACs, G proteins, and PDEs. An example of this includes AKAP15/18 δ which has been suggested to serve as a scaffold for β_2 -adrenergic receptor, G_s protein, AC, PKA and its target, the L-type calcium channel Cav1.2 (Davare et al, 2001; Hulme et al, 2003), which ensures highly specific regulation of the channel. Recently, an increased susceptibility to IPF has been associated with increased expression of AKAP13 in lung tissues from patients (Allen et al, 2017). AKAP13 is a scaffolding protein which functions as a PKA-targeting protein as well as a GEF for Ras homolog gene family member RhoA, which has been shown to be involved in pro-fibrotic signalling pathways (Diviani et al, 2001). Therefore, disruption of this scaffolding protein may provide a novel therapeutic strategy for the treatment of IPF.

1.5.1.3 Phosphodiesterases

Instead of being freely diffusible, movement of cAMP through the cell is thought to be restricted. Using monocytes and imaging approaches, Zaccolo and colleagues showed that cAMP diffusion is limited, with cAMP microdomain formation due to the presence of PDEs which degrade cAMP (Zaccolo & Pozzan, 2002). The mechanism which enables PDEs to sculpt cAMP microdomains by controlling intracellular diffusion of cAMP is thought to involve the localisation of PDEs to different subcellular locations. The localisation of PDEs is regulated through their N-terminal targeting domain, which is highly variable in the multiple PDE splice variants, leading to specific subcellular targeting sites (Houslay & Milligan, 1997). For example, PDE_{4D3} is targeted to the Golgi/centrosomal region through anchoring by myomegalin (Verde et al, 2001), whereas PDE₃ isoforms are targeted to the endoplasmic reticulum (Shakur et al, 2000). One study in rat neonatal ventriculocytes, using the specific PDE₂ inhibitor EHNA and cAMP sensors, showed PDE₂ was largely responsible for the degradation of cAMP generated by β adrenoceptor stimulation, even though the PDE₂ isoform represented only a small proportion of overall PDE activity (Mongillo et al, 2006). Using immunocytochemistry and confocal microscopy, Mongillo and colleagues suggested that PDE₂ was localised to specific subcellular sites coupled to the pool of ACs activated by β adrenoceptor stimulation in rat neonatal ventriculocytes (Mongillo et al, 2006), however further experiments are required to confirm PDE₂ localisation.

1.5.1.4 Signalling at intracellular locations

It has recently emerged that various GPCRs initiate signalling from more than one subcellular location. Receptor internalization into endosomes was originally considered to contribute to cessation of signalling by reducing the number of receptors present on the plasma membrane. However, evidence for GPCR-G protein

signalling from endosomes emerged from the study of sphingosine 1-phosphate (S1P) 1 (S1P₁) receptors. By studying signal transduction events, internalization, and intracellular trafficking, FTY720, a S1P₁ receptor agonist, was shown to elicit sustained G $\alpha_{i/o}$ mediated signalling, associated with persistent receptor internalisation, suggesting that FTY720-bound S1P₁ receptors remain persistently activated after endocytosis (Mullershausen et al, 2009).

Studies of G α_s -mediated signalling initiated by the thyroid-stimulating hormone (TSH) receptor strongly supported the concept of endosome-based GPCR-G protein signalling. Using a transgenic mouse expressing a cAMP biosensor, it was observed that cAMP accumulation by binding of TSH to the TSH receptor is prolonged and poorly reversible after agonist washout. The sustained signalling coincided with receptor-agonist internalisation to endosomes, with the inhibition of endocytosis rendering the TSH-induced cAMP signal reversible after agonist washout (Calebiro et al, 2009). Another G α_s -coupled GPCR that has been demonstrated to signal from endosomes is the β_2 adrenoceptor. Irannejad and colleagues used a nanobody (Nb80) fused to GFP, which selectively binds the agonist-occupied β_2 adrenoceptor and stabilises an activated receptor conformation, as a sensor of β_2 adrenoceptor activation (Irannejad et al, 2013). The use of Nb80 showed β_2 adrenoceptors stimulated with isoprenaline promotes receptor and G $_s$ protein activation from both the plasma membrane and from endosomes after receptor internalisation (Irannejad et al, 2013). To investigate if β_2 adrenoceptor signalling from endosomes impacts downstream gene transcription, Dyngo, an inhibitor of endocytosis, was used to block receptor internalisation (Tsvetanova & von Zastrow, 2014). Inhibition of receptor internalisation was shown to reduce cAMP accumulation and diminish changes in gene expression in response to β_2 adrenoceptor activation by isoproterenol, which suggest

the endosome-initiated cAMP signal is important for downstream transcriptional control (Tsvetanova & von Zastrow, 2014).

The use of targeted cAMP biosensors (discussed in detail in Section 1.5.3.1) have subsequently identified the Golgi apparatus and trans-Golgi network as additional locations of GPCR signalling. Activation of the β_1 adrenoceptor initiates a $G\alpha_s$ -cAMP signal from the Golgi using a pre-existing receptor pool rather than receptor delivered from the cell surface (Irannejad et al, 2017). The catecholamine agonist epinephrine can gain access to the Golgi-localised receptor pool by facilitated transmembrane transport involving the organic cation transport 3. However hydrophobic drugs, including the β_1 adrenoceptor agonist dobutamine, can access the Golgi pool by passive diffusion, bypassing the need for transporters, thus providing an interesting avenue for the design of drugs to target select pools of receptors (Irannejad et al, 2017).

Signalling from intracellular locations such as endosomes and the Golgi appear to support signalling over different time scales and may produce different effects compared to those generated at the plasma membrane.

1.5.2 Spatiotemporal regulation of the MAPK/ERK pathway

Like the cAMP pathway, the MAPK/ERK pathway requires strict regulation due to a large number of substrates that can activate the pathway and the variety of processes that the pathway regulates. Scaffold proteins compartmentalise and temporally control ERK signalling to regulate signal strength and duration, and ensure signal specificity. For example, the scaffolding protein kinase suppressor of Ras (KSR) recruits Raf to optimally position the enzyme in proximity to its target substrate MEK (Muller et al, 2001; Rajakulendran et al, 2009). Another scaffolding protein, MEK Partner 1

(MP1), promotes interaction of MEK1 and ERK and facilitates its activation by Ras (Schaeffer et al, 1998).

The duration, magnitude, and subcellular compartmentalisation of ERK activation results in different cellular outcomes such as proliferation, differentiation, migration, or survival (Ebisuya et al, 2005; Mor & Philips, 2006). Because cell cycle regulatory proteins that are activated by ERK1/2 are localized in the nucleus, access of the ERKs to their substrates is a potential point of regulation. In resting cells, ERK is anchored in the cytoplasm by its association with MEK (Fukuda et al, 1997) or the microtubule network (Reszka et al, 1995). Cytosolic retention of ERK1/2 denies access to an array of targets in the nucleus, including transcription factors and the mitogen- and stress-activated protein kinases, which are responsible for the mitogenic response (Deak et al, 1998). Activation of the MAPK signalling pathway, and subsequent phosphorylation of ERK, results in its translocation to the nucleus by passive diffusion involving direct interaction with nuclear pore complex proteins (Adachi et al, 1999; Khokhlatchev et al, 1998; Whitehurst et al, 2002). The importance of nuclear translocation of ERK is highlighted in studies of PEA-15, a protein that contains a nuclear export signal, which binds ERK1/2 and sequesters ERK in the cytoplasm (Formstecher et al, 2001). Genetic depletion of PEA-15 in breast tumour cells stimulates ERK-dependent gene transcription and cell invasion, whereas overexpression of PEA-15 blocks invasion of cells (Glading et al, 2007). Furthermore, skin fibroblasts cultured from transgenic mice overexpressing PEA-15 showed reduced migration and wound healing ability, whereas skin fibroblasts isolated from knockout mice lacking PEA-15 displayed increased migration and wound closure ability (Buonomo et al, 2012).

The duration of ERK signalling has been implicated as a critical factor for ensuring proliferation of cells. ERK activation must be sustained for successful entry into the cell

cycle, with continuous ERK activation downregulating anti-proliferative genes until the onset of cell cycle progression (Yamamoto et al, 2006). Several studies have demonstrated the necessity of sustained activation of MAPK/ERK for cell proliferation. For example, in CCL39 cells, a fibroblast-like cell line, serum and thrombin stimulated a sustained activation of MAPK signalling, which was shown to be essential for the expression of genes, such as cyclin D1, that are required for cell cycle progression (Balmanno & Cook, 1999). By contrast, thrombin-mimicking peptide (TMP) or epidermal growth factor (EGF) stimulates transient ERK activation and cannot induce the onset of S phase (Murphy et al, 2002; Vouret-Craviari et al, 1993).

1.5.3 Tools to measure spatiotemporal signalling

1.5.3.1 Measuring cAMP signalling

There are numerous high throughput assays to measure cAMP that employ a variety of radiometric, absorbent, fluorescent, and luminescent endpoints. One approach to measure cAMP generation is to follow its conversion from ATP using radiolabelled adenine (^3H -adenine) incorporation and use chromatography to separate ^3H -cAMP from other tritium-labelled adenine derivatives. Although this method provides a direct read-out of cAMP accumulation and can be used to study the kinetics of cAMP accumulation (Baker et al, 2004; McCrea & Hill, 1996), it is time consuming and requires safety precautions, special lab requirements, and radioactive waste disposal.

There are a range of technologies that measure cAMP accumulation via competition between cellular cAMP and labelled cAMP moieties for binding to an anti-cAMP antibody. Moving away from radiolabelled moieties, a number of fluorescent and luminescent technologies have emerged, including chemiluminescent proximity assays (AlphaScreen, Perkin Elmer), enzyme complementation assays (Hit Hunter,

DiscoverRx), and time resolved-fluorescence resonance energy transfer (TR-FRET) assays (HTRF®, Cis Bio & LANCE®, DELFIA®, Perkin Elmer). These assays have high signal-noise-ratio and have the ability to be high throughput, an advantage in the drug discovery industry.

A disadvantage of the majority of the population-based cAMP assays mentioned above is that they require cell lysis prior to cAMP detection, therefore have limited capabilities in measuring cAMP with high temporal resolution. One assay that has been developed for the measurement of cAMP over time is the GloSensor™ cAMP assay. This assay uses a firefly luciferase-based cAMP biosensor that is expressed in live cells, and changes in cAMP-mediated luminescence can be measured over time and does not require cell lysis. This assay is based on the oxidation of firefly luciferin by firefly luciferase, which emits light at 550-570 nm. Genetic manipulation of firefly luciferase involved the insertion of the cAMP binding domain B from the regulatory subunit type IIβ (Binkowski et al, 2009; Fan et al, 2008).

Many of the cAMP assays mentioned above are end-point reads that require cell lysis, and although the GloSensor™ assay can be used to measure cAMP signalling in live cells with greater temporal resolution, none of the assays mentioned provides information on the spatial control of cAMP. Fluorescence resonance energy transfer (FRET) biosensors represent a major advantage over traditional population-based assays by allowing the visualisation of the spatial and temporal dynamics of intracellular signalling in real time and in live cells. In FRET biosensors a peptide chain containing a second messenger binding site or target peptide for the messenger of interest is fused to a complementary pair of fluorophores with overlapping spectra. Energy transfer between the fluorescence donor and fluorescence acceptor molecules depends on their close proximity and alignment. A conformational change of the

sensor peptide is triggered by binding of a second messenger or modification of the target peptide, which alters the distance between the two fluorophores, thus changing the FRET signal.

The first FRET cAMP reporter, named FICRhr, was introduced by Roger Tsien in the early 1990s (Adams et al, 1991) and was based on the cAMP-induced dissociation of fluorescein-labelled catalytic and rhodamine-labelled regulatory subunits of PKA. Binding of cAMP on the regulatory subunits causes dissociation of PKA subunits, increasing donor-acceptor distance, thus resulting in a loss of FRET. Microinjection of FICRhr had been successful in single cells, for example, neurons (Bacskai et al, 1993; Liu et al, 1999) and osteoblastic cells (Civitelli et al, 1994) to analyse single cell cAMP responses. The development of genetically-encoded versions of FICRhr led to its wider use due to the easy expression via simple transfection. Zacco and colleagues established the first genetically-encoded reporter by tagging PKA regulatory and catalytic subunits with enhanced blue fluorescent protein (EBFP) and green fluorescent protein (GFP), respectively (Zacco et al, 2000). This genetically-encoded reporter was subsequently improved by utilizing the more efficient cyan fluorescent protein (CFP) and yellow fluorescent protein (YFP) FRET pair, with efficiency measured as the percent of energy transfer from the donor to acceptor fluorophore (Zacco & Pozzan, 2002).

However, a disadvantage when FRET donor and acceptor pairs are on two separate molecules includes the association of mixed complexes with labelled- and non-labelled endogenous molecules, resulting in a loss of functional FRET biosensors. This concern encouraged the advancement of the use a single gene to encode FRET-based reporters. In 2004, several groups introduced FRET biosensors based on Epac, which undergoes a conformational change upon cAMP-association (DiPilato et al, 2004;

Nikolaev et al, 2004; Ponsioen et al, 2004). Having both the FRET donor and acceptor fluorophore on the same molecule ensures an equal expression of both. Furthermore, Epac-based biosensors do not contain catalytic domains and revealed a faster speed of activation than PKA-based sensors, and are therefore more suitable for measuring cAMP with high temporal resolution (Nikolaev et al, 2004).

In order to study cAMP compartmentalisation, cAMP FRET biosensors have been designed to be targeted to different subcellular compartments. This enables the direct measurement of spatially defined sections within living cells in real time. FRET biosensors have been established which can detect cAMP at the plasma membrane, in the cytoplasm, and in the nucleus (DiPilato et al, 2004; Nikolaev et al, 2004; Wachten et al, 2010). The Epac biosensor is expressed throughout cells and is used to measure cAMP in the cytoplasmic compartment. Plasma membrane targeting can be achieved by N-terminally modifying the global Epac biosensor with the 'SH4' motif of Lyn kinase (Wachten et al, 2010) and targeting to the nucleus can be accomplished via addition of a nuclear localisation signal (NLS) (DiPilato et al, 2004).

Subcellular targeted cAMP FRET biosensors have proved extremely useful for the study of GPCR signalling. As discussed earlier, precise temporal and spatial regulation of second messengers is required to ensure specific biological responses. These biosensors have the ability to increase understanding of how the location of GPCRs and their signalling effectors can control biological responses. Understanding the spatiotemporal control of GPCR signalling has impacted current interpretation of GPCR pharmacology which could also impact the development of new therapeutic strategies. For example, recognition that GPCRs can signal from multiple intracellular locations could provide novel strategies to target a distinct subcellular population of receptors for a specific cellular response. Indeed, selective targeting of neurokinin 1

receptor antagonists to endosomes has been proven to effectively block pain transmission, proving the importance of targeting receptors in the right location (Jensen et al, 2017).

1.5.3.2 Measuring ERK activity

As discussed previously, the location and duration of ERK signalling are both important in the specificity of downstream effects. Traditional techniques to measure ERK phosphorylation include western blotting, immunostaining, and chemiluminescent proximity assays (AlphaScreen SureFire), however these have limited spatiotemporal resolution. Insights into the spatial and temporal distribution of the ERK can be gained through live cell imaging of ERK cascade components tagged with fluorescent proteins. ERK2 tagged with GFP was used to image localisation and mobility of ERK2 in NIH-3T3 cells and it was shown that stimulation with serum resulted in ERK2 localisation in the nucleus (Costa et al, 2006). However, when overexpressing ERK care needs to be taken to avoid an abundance of ERK compared with upstream and downstream elements.

Another approach to measure spatiotemporal ERK activity involves the use of genetically-encoded FRET-based biosensors (Harvey et al, 2008). As well as monitoring the location of ERK, FRET-based biosensors also give a readout of the phosphorylation status of ERK. The ERK FRET biosensor, named extracellular signal-regulated kinase activity reporter (EKAR), consists of fluorophores GFP and RFP as the FRET donor and acceptor pair, respectively. FRET biosensors that detect ERK activity have a different mechanism of action than those developed to detect cAMP, as the biosensor is considered a substrate for ERK. A conformational change of the biosensor is induced following phosphorylation of a target sequence by ERK, which facilitates an interaction between the phosphorylated target sequence and an attached binding protein that is sensitive to such phosphorylation (discussed in more detail in Section 4.1). Second

generation EKAR sensors that contain teal fluorescent protein and Venus, as the FRET donor and acceptor, respectively, have since been developed for their increased brightness and dynamic range (Fritz et al, 2013).

ERK FRET biosensors targeted to the cytoplasm and nucleus have proven to be beneficial in measuring ERK signalling with high spatial and temporal resolution. For example, ligand-dependent differences in ERK signalling have been identified for opioids. Targeting the μ -opioid receptor (MOPr) with morphine induces sustained cytoplasmic ERK signalling, whereas DAMGO results in transient increases in both cytoplasmic and nuclear ERK (Halls et al, 2016). The use of EKAR FRET sensors has also established differences in ERK activity in HEK cells expressing the neurokinin 1 receptor. Substance P stimulated neurokinin 1 receptors stimulate a transient cytoplasm ERK response and a sustained nuclear ERK response, with the nuclear ERK response dependent on receptor internalisation (Jensen et al, 2017).

1.6 Aims

Various GPCR agonists that increase cAMP have previously been shown to have anti-fibrotic properties. The primary aim of the work reported in this thesis was to identify cAMP elevating agents that have the potential to be novel therapeutic agents in IPF.

In Chapter 3 the aim was to determine which G_s-coupled GPCRs are expressed in human lung fibroblasts using TaqMan gene arrays, explore their functional activity in a range of second messenger and phenotypic assays, and determine if there was a relationship between the different responses. The correlation between cAMP accumulation and inhibition of phenotypic response was explored and a disconnect was observed.

This disconnect was further explored in Chapter 4, examining whether IPR agonists exhibit compartmentalisation of cAMP and ERK signalling in human lung fibroblasts. The aim was to investigate cAMP accumulation at the plasma membrane, in the cytoplasm, and in the nucleus after stimulation of the IPR agonists. Another objective was to investigate ERK compartmentalisation in HLFs and the role of cAMP in the inhibition of ERK phosphorylation.

Finally, in Chapter 5 the aim was to explore cAMP kinetics in human lung fibroblasts by using cAMP FRET biosensors in conjunction with a perfusion system, as well as the GloSensor™ cAMP assay. The efficacy of IPR agonists to increase cAMP at later, more phenotypically relevant time points, is explored in order to give better link to biological outcome.

Chapter 2 – Materials and Methods

2.1 Materials

Foetal bovine serum (FBS), trypsin-EDTA, Hoechst 33,342, RNAqueous kit, TURBO DNase and High Capacity RNA-to-cDNA kit were purchased from Life Technologies (Paisley, UK). CGS-21680, BMY-45778, BAY60-6583, iloprost, and NECA were purchased from Tocris (Abingdon, UK). Beraprost was bought from Cayman Chemical Company (Michigan, USA). PDGF-BB was purchased from R&D Systems (Minneapolis, USA). MRE-269 (CAS:475085-57-5) and AGN-205204 (CAS:802906-77-0) were synthesized in house at Novartis (Horsham, UK). Phospho-p44/42 ERK1/2 (Thr202/Tyr204) (D13.14.4E) XP[®] Rabbit mAb primary antibody was purchased from Cell Signalling Technology (Leiden, The Netherlands). CF[™]647-conjugated Affini-pure goat anti-rabbit IgG and CF[™]647-conjugated Affini-pure goat anti-mouse IgG were purchased from Biotium, Inc., (Fremont, California). Pierce[™] LDH Cytotoxicity Assay Kit and CellEvent[™] Pierce[™] LDH Cytotoxicity Assay Kit and Caspase-3/7 Red Detection Reagent were purchased from ThermoFisher (Hemel Hempstead, UK). Staurosporine was purchased from VWR International Ltd. (Lutterworth, UK). 96-well white ViewPlates, AlphaScreen cAMP, AlphaScreen SureFire, and DELFIA proliferations assay kits were purchased from Perkin Elmer Life Sciences (Massachusetts, USA), 96-well black ViewPlates were purchased from Corning (New York, USA), and 384-well black, μ -clear Viewplates were purchased from Greiner bio-one (Stonehouse, UK). HitHunter[™] cAMP assay kits were purchased from DiscoverX (Birmingham, UK). The cAMP FRET biosensors were provided by Martin Lohse (cytoEpac2 (Nikolaev et al, 2004)), Dermot Cooper (pmEpac2 (Wachten et al, 2010)), and Robert Harvey (nucEpac2 (DiPilato et al, 2004)). The cytoEKAR and nucEKAR FRET biosensors were from Addgene (plasmids 18680 and 18681, respectively). All other reagents were purchased from Sigma Aldrich (Poole, UK).

2.2 Cell culture

All studies were performed on normal HLFs (C-12361), which were purchased from Promocell (Heidelberg, Germany). HLF were maintained in DMEM supplemented with 4.5 g L⁻¹ D-glucose, L-glutamine, pyruvate, FBS (10 % v/v), and 25 mM HEPES at 37°C, 5 % CO₂, in a humidified atmosphere. For experiments cells were harvested using trypsin/EDTA and seeded in their sub-culture medium. Three HLF donors were used across experiments in this thesis: HLF d91019001.2 (Chapter 3 and 5), HLF d9017402.1 (Chapter 3), HLF d42105.2 (Chapter 4), all from healthy/non-smoker Caucasian donors.

2.3 Receptor expression levels

Expression of GPCR was determined in HLF using high density, 384-well GPCR TaqMan arrays as previously described (Groot-Kormelink et al, 2012). RNA from 4 fibroblast donors (all from healthy/non-smoker Caucasian donors) was isolated using the RNAqueous kit and treated with TURBO DNase to remove genomic DNA, using a High Capacity RNA-to-cDNA kit according to manufacturer's instructions to synthesize cDNA. The GPCR array contained validated primer/probe sets for 367 GPCR. 100 ng of cDNA was loaded per port and the array was run on an Applied Biosystems 7900HT fast real-time PCR instrument according to the manufacturer's instruction. 13 housekeeping genes were included as controls in the arrays for the purpose of quality control and data normalisation: (ACTB, β -actin; B2M, β -2-microglobin; GAPDH, glyceraldehyde-3-phosphate dehydrogenase; GUSB, β -Glucuronidase; HMBS, hydroxymethylbilane synthase; HPRT1, hypoxanthine phosphoribosyltransferase 1; IPO8, importin 8; PGK1, phosphoglycerate kinase 1; POLR2A, RNA polymerase II subunit A; PPIA, peptidylprolyl isomerase A; RPLPO, ribosomal protein lateral stalk subunit P0; TBP, TATA-Box binding protein; TFRC, Transferrin Receptor). Data was

analyzed using RQ manager version 1.2 and DataAssist version 2 (Applied Biosystems) with a Cycle Threshold (CT) set at 0.2 for all samples.

2.4 ERK phosphorylation

2.4.1 Antibody detection

HLFs were seeded overnight at 6000 cells/well in 96-well black clear bottom plates then starved for 6 hours in the growth medium devoid of all additives (+ 0.1 % w/v HSA, sterile filtered). To assess ERK phosphorylation (pERK), cells were treated for 30 minutes with a range of concentrations of forskolin. After this time, cells were stimulated with an EC₈₀ concentration of PDGF (3 ng/mL) for 10 minutes, at 37°C, 5 % CO₂. After stimulation, cells were fixed in 4 % paraformaldehyde, washed 3× in PBS (with Ca²⁺/Mg²⁺), and incubated with permeabilising blocking buffer (dPBS (with Ca²⁺/Mg²⁺), 10 % FBS (v/v), 0.1 % Triton X-100 (v/v)) for 1 hours at 37°C. Wells were then washed 3× in wash buffer (Tris Buffered Saline (TBS), 0.05 % (v/v) Tween-20) and incubated with rabbit anti-pERK1/2 antibody (1:1000 dilution) in blocking buffer overnight at 4°C. Following 3× wash in wash buffer, wells were incubated with blocking buffer containing Hoechst to stain for nuclear DNA (2 µM), and FITC-conjugated Affini-pure goat anti-rabbit IgG (1:1000 dilution) for 30 minutes at 37°C. Fluorescence was then quantified on a widefield ImageXpress Micro microscope, with a Plan Fluor 20X objective, DAPI filter cube (excitation 400–418 nm, emission 435–470 nm), 50 ms exposure time for nuclei, and FITC filter cube (excitation 467–498 nm, emission 513–556 nm), 200 ms exposure time for pERK.

To quantify levels of ERK phosphorylation fluorescence, a standard Multi-Wavelength Cell Scoring algorithm was used in MetaXpress 5.3 software (Molecular Devices, California, USA). To account for the inter-assay variation in levels of ERK

phosphorylation produced in each experiment, data were normalized to the EC₈₀ PDGF response.

2.4.2 AlphaScreen SureFire

ERK1/2 phosphorylation was detected with the AlphaScreen ERK1/2 SureFire protocol (PerkinElmer). Briefly, HLFs were seeded overnight in clear 96-well plates (15,000 cells/well) then starved for at least 6 hours in the growth media devoid of FBS. To monitor time-dependent increases in ERK phosphorylation, HLFs were treated with a high concentration of PDGF (30 ng/ml) or phorbol 12,13-dibutyrate (PDBu) as a positive control for up to 30 minutes. To assess ERK phosphorylation, HLFs were stimulated with a range of concentrations of PDGF for 20 minutes. For inhibition of ERK phosphorylation, HLFs were pre-incubated with a range of concentrations of IPR agonists or forskolin for 30 minutes. After this time, HLFs were stimulated with an EC₈₀ concentration of PDGF (5.3 ng/ml) for 20 minutes. Then the medium was replaced with lysis buffer and agitated at room temperature for 10 minutes. For detection, lysates were mixed with activation buffer, reaction buffer, AlphaScreen acceptor beads, and AlphaScreen donor beads at 200:50:250:1:1 (v/v/v/v/v) ratio in a 384-well white Proxiplate. Plates were incubated in the dark for 1 hour at 37°C followed by measurement on an EnVision plate reader (PerkinElmer) using AlphaScreen settings. To account for the inter-assay variation in levels of ERK phosphorylation produced in each experiment data were normalised to the maximal PDGF response.

2.5 cAMP accumulation

HLF were grown to confluency in 96-well white ViewPlates, before incubation with a range of agonist concentrations, or vehicle, for 2 hours at room temperature in HBSS with 5 mM HEPES, 0.1 % w/v HSA, and 5 µM rolipram. Rolipram was included in these

assays to inhibit PDE activity, which resulted in increased maximal responses of cAMP accumulation, without any effect on EC₅₀ values generated (data not shown). Rolipram was excluded when measuring cAMP levels in response to PDE inhibitors. cAMP levels were measured using either HitHunter cAMP assay or AlphaScreen competition assay following manufacturer protocol, and were assessed on either a BMG LABTEK ClarioStar or a Packard EnVision plate reader. cAMP concentrations in each well were determined using a standard curve. To account for the inter-assay variation in levels of cAMP produced in each experiment, data were normalized to the maximal forskolin response.

2.6 Proliferation

2.6.1 Nuclei Count

Proliferation of HLF was measured by nuclei count. HLF were seeded overnight at 4,000 cells/well in 96-well black ViewPlates, before being starved for 24 hours in culture medium devoid of FBS. Proliferation was measured after incubation with a range of concentrations of FBS or PDGF, in DMEM supplemented with 0.1 % w/v HSA, for 24, 48, 72, or 96 hours for nuclei count assay.

For anti-remodelling assays, cells were incubated for 48 hours with a range of concentrations of test compounds in the presence of an EC₈₀ concentration of FBS (1.8 % v/v). Following stimulation, cells were fixed with 4 % paraformaldehyde and nuclei stained with Hoechst 33342 (1 µM) for 15 minutes at room temperature. Cells were then washed three times with dPBS before the plate was read using the widefield ImageXpress Micro microscope, with a Plan Fluor 4X objective, DAPI filter cube (excitation 400-418nm, emission 435-470nm), and 50 ms exposure time. Images were analysed using a nuclear count algorithm within the MetaXpress 5.3 software

(Molecular Devices, California, USA). To account for the inter-assay variation in levels of proliferation in each experiment, data were normalized to the EC₈₀ FBS response.

2.6.2 BrdU incorporation

Proliferation of HLF was measured by incorporation of bromodeoxyuridine (BrdU). HLF were seeded overnight at 4000 cells/well in 96-well black ViewPlates, before being starved for 24 hours in culture medium devoid of FBS. Proliferation was measured after incubation with a range of concentrations of FBS or PDGF, in DMEM supplemented with 0.1 % w/v HSA, for 24 hours.

For anti-remodelling assays using BrdU incorporation, cells were incubated for 24 hours with a range of concentrations of test compounds in the presence of near maximal concentrations of FBS or PDGF in DMEM supplemented with 0.1 % w/v HSA. Proliferation was assessed using the DELFIA BrdU incorporation assay kit following manufacturer protocol. Fluorescence was measured using a Packard EnVision plate reader. To account for the inter-assay variation in levels of proliferation in each experiment, data were normalized to the PDGF or FBS response.

2.7 Fibroblast to myofibroblast transdifferentiation

To assess the differentiation of fibroblasts to the myofibroblast phenotype, immunofluorescence was used to monitor increases in α SMA. HLF were seeded overnight at 1500 cells/well in 384-well black μ Clear plates, before being starved for 24 hours growth medium devoid of FBS.

For anti-remodelling assays using FMT, cells were incubated for 48 hours with a range of concentrations of test compounds, at 37°C, 5 % CO₂ in the presence of a near maximal concentration of TGF- β (0.3 ng/mL), to promote differentiation, in DMEM

supplemented with 0.1 % w/v HSA (sterile filtered). Following stimulation, cells were fixed in 4 % paraformaldehyde, washed 3× in PBS (with Ca²⁺/Mg²⁺), and incubated with permeabilising blocking buffer (dPBS (with Ca²⁺/Mg²⁺), 10 % FBS (v/v), 0.1 % Triton X-100 (v/v)) for 1 hour at 37°C. Wells were then washed 3× in wash buffer (Tris Buffered Saline (TBS), 0.05 % (v/v) Tween-20) and incubated with mouse anti- α SMA (1:1000 dilution in permeabilising blocking buffer) for 1 hour at room temperature, with gentle shaking. Following 3× wash in wash buffer, wells were incubated with blocking buffer containing Hoechst to stain for nuclear DNA (2 μ M), and FITC-conjugated Affini-pure goat anti-rabbit IgG (1:1000 dilution in blocking buffer) for 30 minutes at 37°C. Fluorescence was then quantified on a widefield ImageXpress Micro microscope, with a Plan Fluor 20X objective, DAPI filter cube (excitation 400–418 nm, emission 435–470 nm), 50 ms exposure time for nuclei, and FITC filter cube (excitation 467–498 nm, emission 513–556 nm), 200 ms exposure time for α SMA.

To quantify increases in α SMA fluorescence, a standard Multi-Wavelength Cell Scoring algorithm was used in MetaXpress 5.3 software (Molecular Devices, California, USA). To account for the inter-assay variation in levels of α SMA expression produced in each experiment, data were normalized to the response to TGF β .

2.8 Cell viability

2.8.1 Caspase-3/7 detection

Cell viability was measured using caspase-3/7 expression as a marker of apoptosis after treatment for 24 hours with test compounds. HLF were seeded overnight at 6,000 cells/well in 96-well black ViewPlates, before being starved for 24 hours in culture medium devoid of FBS. Cells were incubated for 24 hours in the presence of

test compounds at the highest concentrations used in the proliferation assays, or in the presence of 100 nM staurosporine to induce apoptosis.

The presence of the apoptotic marker caspase-3/7 was detected by incubating cells with 8 μ M CellEvent™ Caspase-3/7 Red Detection Reagent in dPBS with 5 % FBS (v/v), for 30 minutes at 37°C. Following incubation, cells were fixed with 4 % paraformaldehyde and the nuclei stained with Hoechst 33342 (1 μ M) for 15 minutes at room temperature. Cells were then washed three times with dPBS before the plate was read using the widefield ImageXpress Micro microscope, with a Plan Fluor 4X objective, DAPI filter cube (excitation 400-418nm, emission 435-470nm) with 50 ms exposure time, and Cy5 filter cube (excitation 604-644nm, emission 672-712nm) with 1000 ms exposure time. Images were analyzed using a multi wavelength cell scoring algorithm within the MetaXpress 5.3 software, which measures cell number using stained nuclei, and percent of these cells positive for caspase-3/7 from Cy5 readouts. To account for the inter-assay variation in levels of caspase 3/7 detected in each experiment, data were normalized to the staurosporine response.

Statistical significance across treatment groups was determined by using the one-way ANOVA with Dunnett's multiple-comparison post hoc test.

2.8.2 LDH assay

Lactate dehydrogenase (LDH) is a cytosolic enzyme present in cells, and plasma membrane damage releases LDH into cell culture media. Extracellular LDH in the media can be quantified by an enzymatic reaction in which LDH catalyses the conversion of lactate to pyruvate via NAD⁺ reduction to NADH. Diaphorase then uses NADH to reduce tetrazolium salt to a red formazan product which absorbance can be measured at 490 nm (Figure 2:1). The level of formazan formation is directly

proportional to the amount of LDH released into the medium and indicative of cytotoxicity.

HLFs were seeded overnight at 6,000 cells/well in 96-well black ViewPlates, before being starved for 24 hours in culture medium devoid of FBS. Cells were incubated for 24 hours at 37°C in the presence of test compounds at the top concentrations used in the proliferation assays, or in the presence of 100 nM staurosporine to induce apoptosis. LDH released from treated cells, as well as cells lysed using 0.1 % Triton X-100 (v/v), was measured using the Pierce™ LDH Cytotoxicity Assay Kit and absorbance at 490 nm was measured on the BMG LABTEK ClarioStar.

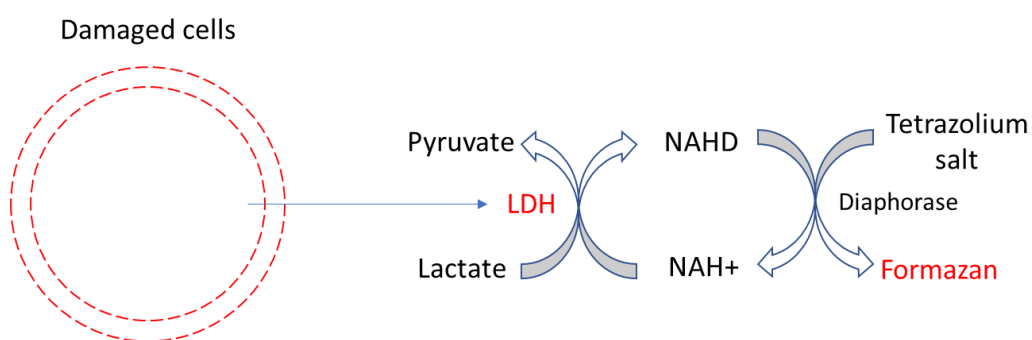


Figure 2:1 - Schematic of LDH cytotoxicity assay mechanism

2.9 Expression of FRET biosensors in HLFs

For all FRET biosensors, except nucEpac2, HLFs were transfected with the Nucleofector 4D protocol (Lonza). Briefly, 1×10^6 cells were suspended in Nucleofector Solution. Plasmid encoding cytoEpac2 (4 μ g), pmEpac2 (4 μ g), cytoEKAR (5 μ g), or nucEKAR (5 μ g) was added and the cell/DNA suspension was transferred to a Nucleocuvette vessel. Cells were transfected using programme EN150. HLFs were resuspended with 500 μ L culture media and cells plated.

For FRET experiments using the nucEpac2 biosensor, HLFs were transduced with adenovirus constructs containing nucEpac2-based cAMP biosensor for 24 - 48 hours in 96 wells plates prior to imaging.

2.10 FRET imaging with widefield microscopy

FRET was measured with a high-content GE Healthcare INCell 2000 Analyzer as described previously (Halls et al, 2015). Briefly, fluorescence imaging was performed with a Nikon Plan Fluor ELWD 10x (NA, 0.6) objective and FRET module. For CFP-YFP emission ratio analysis, cells were sequentially excited with a CFP filter (430/24) with emission measured with YFP (535/30) and CFP (470/24) filters and a polychroic mirror, optimized for the CFP-YFP filter pair (Quad3). For GFP-RFP emission ratio analysis, cells were sequentially excited with a fluorescein isothiocyanate (FITC) filter (490/20) with emission measured with dsRed (605/52) and FITC (525/36) filters and a polychroic mirror, optimised for the FITC-dsRed filter pair (Quad4). HLFs were imaged every 2 – 3 minutes with two fields of view per well. Prior to the addition of stimulus, 4 baseline images were obtained. At the end of every experiment, the same cells were stimulated for 10 minutes with the positive control (200 nM PDBu for ERK or 10 μ M forskolin/100 μ M IBMX for cAMP) to generate a maximal FRET change, and 4 positive emission ratio images were captured.

Data were analysed using FIJI distribution of ImageJ. The three emission ratio image stacks (baseline, stimulates, and positive) were collated and aligned with the StackCreator script (Halls et al, 2015). Cells were selected, and fluorescence intensity was measured. Background intensity was subtracted, and then FRET data were plotted as the change in FRET emission ratio normalized to baseline intensities for each cell

[FRET ratio/baseline FRET ratio (F/F₀)]. Cells that showed a response relative to baseline after stimulation with the positive control were considered for analysis.

2.10.1 Generation of pseudocolour ratiometric images

Ratiometric images of FRET biosensors were generated as previously described (Kardash et al, 2011). First, CFP and YFP, or GFP and RFP, images of the selected biosensor were opened and an ROI contained the cell to be analysed was selected and cropped. The cell selected was representative of the mean response observed with all the cells. Next, background was subtracted from both images, images were aligned, converted to 32-bit, and a smooth filter was applied to improve image quality by reducing the noise. Next a threshold was applied exclusive to the CFP or GFP image to eliminate artefacts from the background. Finally a CFP/YFP image was created and the Blue Green Red LUT was applied. After all images for the experiment were obtained the range between the active and inactive states was determined and set using the mean values obtained with images for the positive (forskolin for cAMP biosensor and PDBu for the ERK biosensor) and baseline controls.

2.11 FRET imaging with confocal microscope and perfusion system

HLFs transfected with either cytoEpac2 or pmEpac2 were plated on a 6-well plate with 32-mm coverslips at 250,000 cells/well and incubated for 24 hours. Imaging of the cAMP FRET biosensors was performed using Zeiss LSM710 Confocal Fluorescence Microscope with a Zeiss 40x1.3NA oil immersion objective. For excitation of CFP, the 458 argon laser was used at 30 % intensity, and to measure emission two band passes was set to measure between 463-499 nm and 520-560 nm, for CFP and YFP emission,

respectively. At all times during imaging cells were maintained at 37°C with 5 % CO₂. The pinhole diameter was set at 86 μm in all experiments using cytoEpac2 expressing cells. The pinhole was increased to maximum at 600 μm for HLFs expressing pmEpac2 and images were collected when focused on top of the cell instead of in a plane through the cell.

To deliver agonists with ease, a perfusion system was used to allow rapid changes between assay buffer (HBSS with HEPES (5mM) and HSA (0.1% w/v)) and agonists. A pressure pump was connected to a closed perfusion system with six reservoirs and a flow rate was set to 4 mL/minute. On the morning of experiment, the coverslip seeded with HLFs expressing cAMP FRET biosensors were placed in a specially designed closed imaging chamber, which was placed onto a microscope stage heated to 37°C, where tubes attached either side facilitated flow of fluid through the chamber. Initially, assay buffer is perfused over the cells in order to obtain baseline reads before investigation of addition of agonist on FRET levels.

All images taken on the Zeiss LSM710 microscope were captured using a 12bit greyscale, which allows 4096 different intensity levels of a given pixel. Using ZEN2010 software, regions of interests (ROIs) were selected from the background and around cells to measure intensity of both the CFP and YFP emission. First, background reads were subtracted away from intensity readings for each cell. Second, YFP/CFP ratios were calculated to find F, followed by the calculation of F/F₀, by division of F by the basal read.

2.12 GloSensor™ assay

For cAMP time-course experiments, HLFs were transiently transfected with the GloSensor™ cAMP plasmid using the Nucleofector protocol (Lonza). Briefly, 1×10^6

cells were suspended in Nucleofector Solution. GloSensor™ plasmid (4 µg) was added and the cell/DNA suspension was transferred to a Nucleocuvette vessel. Cells were transfected using programme EN150. HLFs were resuspended with 500 µL culture media and cells plated in a 384-well plate at 20,000 cells/well.

The GloSensor™ assay was carried out as per manufacturer's instructions (Promega, Madison, WI, USA). Briefly, media was aspirated and cells were incubated in CO₂-independent media containing 4 % GloSensor™ cAMP reagent and incubated for 2 hours at final experimental temperature of 37°C. Luminescence was measured on a BMG LABTEK ClarioStar plate reader continuously monitored over time, with 1 read per well every 3 minutes, following the addition of IPR agonists in the absence or presence of rolipram (5 µM).

2.13 Data analysis

All data were analysed using GraphPad Prism v7.00 (GraphPad software, San Diego CA, U.S.A) using pre-programmed equations and results expressed as mean ± standard error of mean (SEM), unless otherwise stated.

For functional responses, concentration-response data were fitted using a four-parameter logistic equation in GraphPad Prism. To measure correlation between responses the Pearson correlation coefficient (r) was determined using the standard correlation function in GraphPad prism, followed by a two-tailed T test to determine significance.

Rate of cAMP accumulation and decline for FRET biosensor responses were determined using plateau followed by one-phase association equation in GraphPad Prism, from time when response is observed until response plateau.

Association rates for cAMP accumulation in the GloSensor™ assay were determined using one-phase association equation from time point 0 until peak response in GraphPad Prism. Dissociation rates for cAMP decline in the GloSensor™ assay were determined using plateau followed by one-phase decay equations from time of peak response to the end of time course in GraphPad Prism.

Statistical Analysis

Where statistical analyses were required, the format of the data was taken into account in the selection of an appropriate test. For direct comparison of test values a two-tailed, unpaired Student's t-test was used. Statistical differences between multiple datasets were determined by one- or two-way analysis of variance (ANOVA) for multiple comparisons, followed by an appropriate post-hoc test using GraphPad Prism v7.00. All statistical tests used $P \leq 0.05$ as critical level of significance.

Chapter 3 – The inhibition of human lung fibroblast proliferation and differentiation by Gs-coupled receptors is not predicted by the magnitude of cAMP response

Chapter 3 includes data that has been published in peer reviewed journals. My contribution to the work involved the following:

Thesis Chapter	Publication Title	Status	Nature and % of student contribution	Co-author name(s) and % of Co-author's contribution
Chapter 3	The inhibition of human lung fibroblast proliferation and differentiation by Gs-coupled receptors is not predicted by the magnitude of cAMP response	Published	Designed and performed experiments, analysed and interpreted data, wrote and proofed the manuscript (80 %)	<p>1) TCK performed GPCR mRNA expression experiments (3 %)</p> <p>2) REB assisted in inhibition of proliferation experiments (3 %)</p> <p>3) EMR performed fibroblast to myofibroblast transdifferentiation experiments, assisted in inhibition of proliferation experiments, and conceived and/or supervised the study and co-written and edited the manuscript (9 %)</p> <p>4) SJC conceived and/or supervised the study and co-written and edited the manuscript (5 %)</p>

3.1 Introduction

IPF is a progressive and lethal lung disease characterised by the proliferation of fibroblasts and FMT, resulting in excess ECM deposition. A key therapeutic goal in the treatment of IPF is to prevent the progression of tissue fibrosis, which may be achieved by enhancing signals that counteract fibrotic processes and/or inhibiting signals and mediators that promote fibrosis. At present there are two drugs that are approved for use in the treatment of IPF, nintedanib and pirfenidone. Nintedanib inhibits multiple RTKs (Chaudhary et al, 2007) and pirfenidone has broad anti-inflammatory/anti-TGF β activity (Iyer et al, 1999; Iyer et al, 2000). Although various trials have shown that these treatments effectively reduce the rate of lung function decline up to 68.4 %, their non-specific action leads to severe adverse effects such as nausea and dyspnoea that are dose limiting, thereby restricting their use to the more severe patients and increasing patient non-compliance (Adams et al, 2016; Crestani et al, 2019; Inomata et al, 2015; Meyer & Decker, 2017; Richeldi et al, 2011). Research to identify alternative pathways in IPF treatment is essential to enable the development of safer, more efficacious, and better tolerated drugs.

Many profibrotic mediators signal through the MAPK signalling cascade, which is reported to be associated with many of the pro-fibrotic responses observed in IPF (Sun et al, 2015). Strategies that amplify cAMP signalling have been shown to be efficacious in inhibiting pro-fibrotic responses in fibroblasts by negatively impacting MAPK signalling via inhibition of ERK phosphorylation (Nikam et al, 2011; Stork & Schmitt, 2002). This suggests that activation of the cAMP pathway may provide novel targets for the treatment of IPF. In agreement, agonists that bind to G_s-coupled GPCRs to activate ACs and increase cAMP have already been shown to inhibit profibrotic processes. For example, PGE₂ binding to EP₂ and EP₄ receptors has been shown to limit

fibroblast differentiation, migration, and proliferation (Huang et al, 2007; Kolodsick et al, 2003). In addition, PGI₂ binding to the IPR has also been shown to inhibit fibroblast migration, proliferation, and collagen synthesis (Cruz-Gervis et al, 2002; Kohyama et al, 2002). Furthermore, directly activating AC using forskolin has been shown to promote an antifibrotic phenotype in pulmonary fibroblasts (Liu et al, 2004) and blocking cAMP degradation by inhibiting PDEs has been found to reduce TGFβ-mediated FMT (Dunkern et al, 2007).

The aim of this chapter was to investigate the antifibrotic capacity of a range of G_s-coupled GPCRs in order to identify potential new targets to treat IPF. GPCRs form a large group of over 800 receptor proteins, comprising approximately 4 % of the human genome (Alexander et al, 2015; Benovic & von Zastrow, 2014; Bjarnadottir et al, 2006), and therefore the first aim was to identify the G_s-coupled GPCRs endogenously expressed by HLF. The identification of G_s-coupled GPCRs on HLFs then enabled the selection of a range of ligands to investigate their ability to generate cAMP and inhibit pro-fibrotic processes.

3.2 Results

3.2.1 Role of cAMP in the inhibition of ERK phosphorylation, and ERK phosphorylation in proliferation

Increasing cAMP levels has been described to inhibit ERK phosphorylation (Nikam et al, 2011; Stork & Schmitt, 2002), which suggests cAMP elevating agents may have a role in inhibiting fibroblast proliferation. To determine if activation of the MAPK/ERK pathway, and therefore ERK phosphorylation, is important in proliferation of fibroblasts we investigated the effect of PD 0325901, a MEK inhibitor, on PDGF-driven proliferation in HLFs (Barrett et al, 2008). PD 0325901 inhibited PDGF-driven proliferation in a concentration-dependent manner, with maximal inhibition of $95.0 \pm 13.8 \%$ and pIC_{50} of 7.34 ± 0.16 (Figure 3:1). Our next aim was to determine if cAMP can inhibit ERK phosphorylation and thus play a role in inhibiting HLF proliferation. Forskolin, which increases cAMP through direct activation of AC, inhibited PDGF-driven ERK phosphorylation in a concentration dependent manner, with maximal inhibition of $93.4 \pm 4.55 \%$ and pIC_{50} of 7.56 ± 0.23 (Figure 3:1).

As elevating cAMP levels inhibited ERK phosphorylation and blocking ERK phosphorylation inhibited fibroblast proliferation, these results show that increasing cAMP has the potential to inhibit HLF proliferation. G_s -coupled GPCRs play a role in regulating cAMP levels through the activation of AC, therefore our next aim was to determine GPCR expression levels in HLF to identify potential targets to increase cAMP and hence inhibit HLF proliferation.

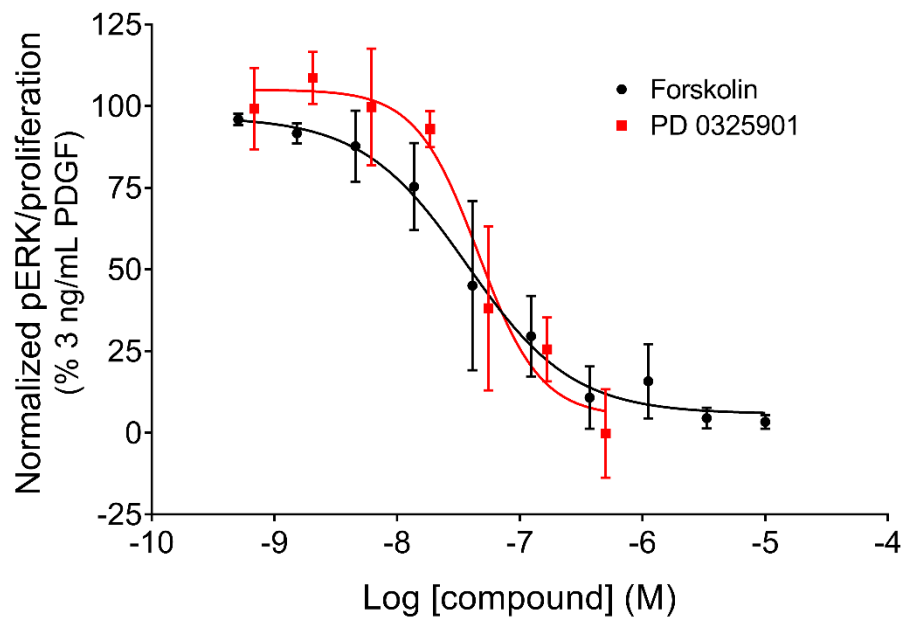


Figure 3:1 - Inhibition of ERK1/2 phosphorylation and proliferation

Concentration effect curves for forskolin-mediated inhibition of PDGF-driven ERK1/2 phosphorylation and PD 0325901-mediated inhibition of PDGF-driven HLF proliferation. For each individual experiment, data were normalised to the maximum amount of ERK phosphorylation or proliferation after addition of 3 ng/ml PDGF and are expressed as mean \pm SEM for 4 independent experiments.

3.2.2 GPCR mRNA expression in HLF

The expression profile of GPCR mRNA in HLFs was established to identify receptors to study further. In total, 91 GPCRs were identified to be expressed in HLFs at the mRNA level (Appendix A) and were classified according to the canonical G protein pathway they couple to (Alexander et al, 2011). Of these GPCRs, 8 were identified to be G_s-coupled receptors. These were, from high to low expression, IPR, PGE₂ receptor 2 (EP₂), melanocortin-1 (MC1) receptor, β₂ adrenoceptor, adenosine 2B (A_{2B}) receptor, PGE₂ receptor 4 (EP₄), dopamine-1 receptor, and adenosine 2A (A_{2A}) receptor (Table 3:1).

The IPR was highly expressed with 2TO-ΔCT value of 0.053 ± 0.016 , almost twice as much as the second highest expressing receptor EP₂, with a 2TO-ΔCT value of 0.029 ± 0.001 . The remaining 6 G_s-receptors had 2TO-ΔCT values ranging from 0.012 ± 0.002 to 0.002 ± 0.001 , for the MC1 and A_{2A} receptors, respectively. A range of ligands that target these receptors were selected, as well as non-receptor activators and inhibitors of the cAMP pathway, to use in subsequent experiments (Table 3:2).

Table 3:1 - Expression of endogenously expressed Gs-coupled receptors in HLF

Receptor	Expression (2 TO – ΔC _T)
IP	0.053 ± 0.016
EP₂	0.029 ± 0.001
MC1	0.012 ± 0.002
β₂	0.008 ± 0.004
A_{2B}	0.007 ± 0.003
EP₄	0.004 ± 0.002
Dopamine-1	0.004 ± 0.001
A_{2A}	0.002 ± 0.001

High density 384-well GPCR TaqMan arrays were run on HLFs to investigate the expression of G_s-coupled receptors. Expression is reported as 2 TO - ΔCT compared to the mean Cycle Threshold (CT) of the 13 housekeeping genes that were included as controls in the arrays (listed in Section 2.3), and each value is the mean ± SD of 4 biological replicates.

Table 3:2 - Ligands used in experiments, their molecular targets, and mechanism of action

Ligand	Target	Mechanism of action
Iloprost	IP = EP ₁ > EP ₃ > FP > EP ₄ > TP > EP ₂	Agonist
Treprostinil	IP > EP ₂ > EP ₃ > EP ₄ > EP ₁ > TP > FP	Agonist
MRE-269	IP	Agonist
BMY-45778	IP	Agonist
Beraprost	IP	Agonist
PGE₂	EP ₁₋₄	Agonist
Misoprostol	EP ₃ > EP ₄ > EP ₂ > EP ₁	Agonist
Butaprost	EP ₂ , EP ₄	Agonist
AGN-205204	EP ₄	Agonist
α-MSH	MC1, MC3, MC4, MC5	Agonist
Formoterol	β ₂	Agonist
Indacaterol	β ₂	Agonist
Salbutamol	β ₂	Agonist
Salmeterol	β ₂	Agonist
NECA	A ₃ , A ₁ , A _{2A} , A _{2B}	Agonist
CGS-21680	A _{2A}	Agonist
BAY60-6583	A _{2B}	Agonist
Dopamine	D ₁ = D ₅ > D ₃ > D ₂ > D ₄	Agonist
Forskolin	AC 1-8	Activator
IBMX	PDE ₄ , PDE ₃ , PDE ₁ , PDE ₅ , PDE ₂	Inhibitor
Rolipram	PDE ₄	Inhibitor

3.2.3 cAMP signalling in HLF

To determine if expression of the detected G_s -coupled receptors at mRNA level correlated to a functional receptor, cAMP accumulation was measured in HLFs in the presence of the selected ligands (Figure 3:2). cAMP was measured using a high throughput assay system, which measured global cAMP levels from the population of cells in each well. Out of the ligands tested 16 out of 21 increased cAMP levels in a concentration-dependent manner with a range of potencies and efficacies, relative to the forskolin response (Table 3:3).

Targeting the IPR with a range of ligands resulted in an increase of cAMP (Figure 3:2A). Treprostinil, iloprost, and beraprost were full agonists, whereas MRE-269 and BMY-45778 were partial agonists, with E_{max} of 52.9 ± 4.36 and 50.0 ± 4.59 % of forskolin response, respectively. All IPR ligands had similar potencies, with pEC_{50} values ranging from 6.75 ± 0.15 for MRE-269 to 7.25 ± 0.09 for BMY-45778. As treprostinil can target both the IPR and EP_2 receptor to increase cAMP (Table 3:2), IPR antagonist RO-1138452 was used to probe which receptor treprostinil cAMP accumulation is mediated through (Figure 3:3). RO-1138452 inhibited treprostinil cAMP accumulation 61.0 ± 4.00 %, demonstrating that some cAMP accumulation by treprostinil is mediated via the EP_2 receptor.

Non-selective or selective ligands targeting the EP_2 and/or EP_4 receptors also resulted in an increase of cAMP (Figure 3:2B). The endogenous EP_2/EP_4 receptor ligand PGE_2 was the most efficacious at increasing cAMP, with E_{max} of 85.5 ± 8.64 % of forskolin response. Misoprostol and butaprost, non-selective prostaglandin receptor agonists that also bind to and activate prostaglandin E_2 receptors, and AGN-205204, a selective EP_4 receptor agonist, were partial agonists with E_{max} of ranging between 8.76 ± 3.25 %

and 52.4 ± 6.23 % of forskolin response. In addition to being least efficacious butaprost was also the least potent, with pEC_{50} of 5.81 ± 0.16 .

Targeting the β_2 adrenoceptor with a range of ligands showed it was functionally active in HLFs (Figure 3:2C). Formoterol and indacaterol were most efficacious at increasing cAMP, with E_{max} of 103 ± 4.60 and 83.3 ± 4.47 % of forskolin response, respectively, whereas salbutamol and salmeterol were partial agonists, with E_{max} of 68.9 ± 1.40 and 45.8 ± 3.53 % of forskolin response, respectively. Formoterol and salmeterol had similar potencies with pEC_{50} values of 9.38 ± 0.20 and 9.91 ± 0.16 , respectively, whereas indacaterol and salbutamol were less potent, with pEC_{50} values of 8.58 ± 0.20 and 7.36 ± 0.34 , respectively.

Targeting the adenosine receptors non-selectively with NECA resulted in a partial cAMP response, E_{max} of 47.3 ± 3.40 , with low potency, pEC_{50} of 5.39 ± 0.13 . The A_{2B} selective agonist BAY 60-6583 resulted in a very small cAMP response, with E_{max} of 10.2 ± 2.89 , however, targeting the A_{2A} receptor selectively with CGS-21680 resulted in no detectable increase in cAMP (Figure 3:2D). Targeting the dopamine-1 receptor with endogenous ligand dopamine resulted in a partial cAMP response, with E_{max} of 41.2 ± 10.0 and pEC_{50} of 5.39 ± 0.07 (Figure 3:2D). Lastly, the MC1 receptor ligand α -MSH did not produce any detectable increase in cAMP (Figure 3:2D).

Directly activating AC with forskolin resulted in a concentration-dependent increase of cAMP, whereas inhibiting PDEs, enzymes that break down cAMP, with IBMX or rolipram, resulted in no detectable increase in cAMP (Figure 3:2E).

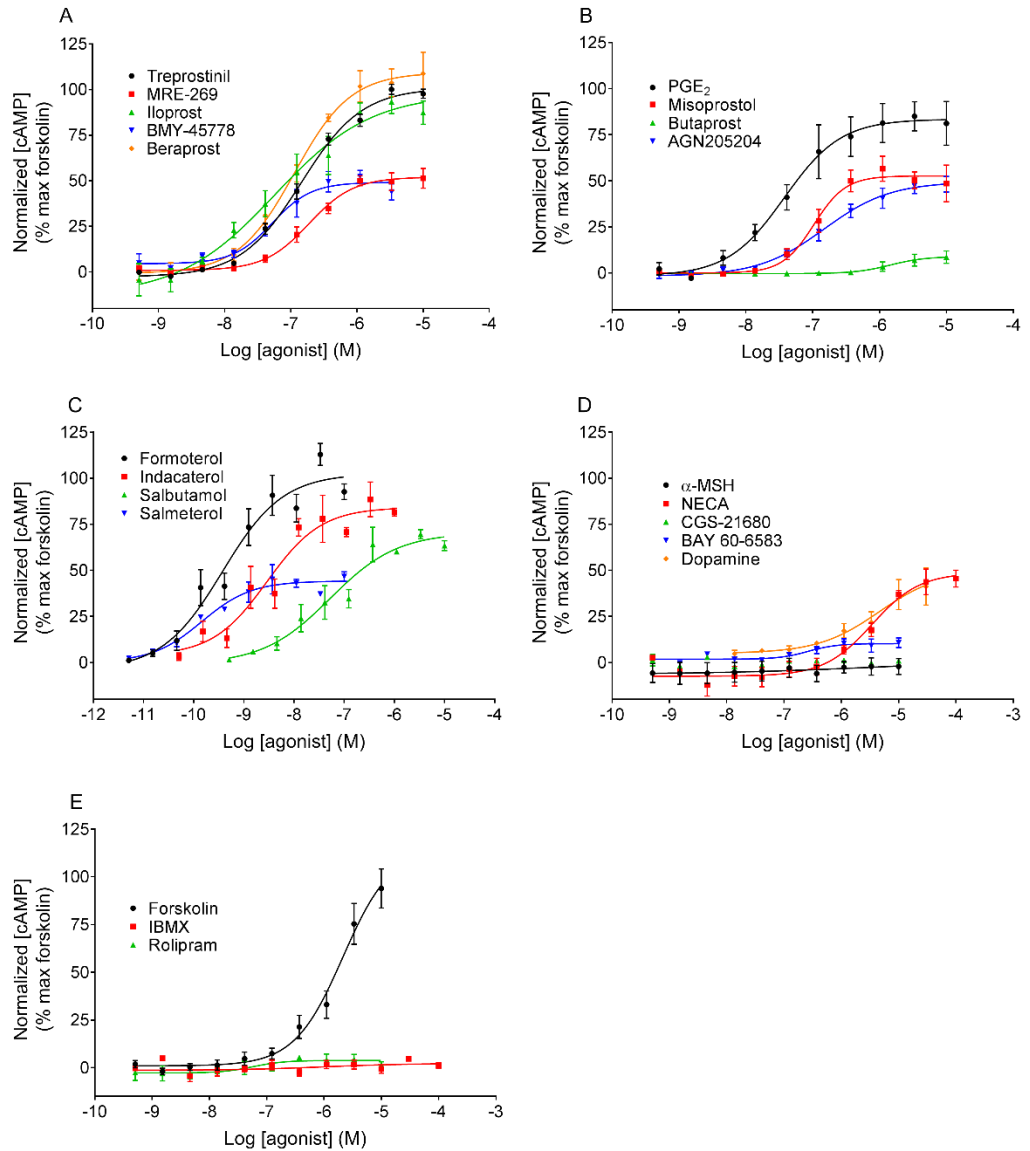


Figure 3:2 - Receptor mediated cAMP accumulation

Concentration effect curves for cAMP accumulation in HLF after treatment with a range of ligands targeting (A) IP receptor, (B) EP receptor, (C) β_2 adrenoceptor, (D) other GPCR, and (E) non-receptors. Data for each individual experiment were normalised to maximal cAMP accumulation observed with forskolin (10 μ M), and are expressed as mean \pm SEM for at least 3 independent experiments.

Table 3:3 - Potency and intrinsic activity of all ligands for cAMP accumulation in HLFs

Agonist	cAMP	
	pEC ₅₀	E _{max} (% max)
Treprostinil	6.82 ± 0.06	101 ± 0.58
MRE-269	6.75 ± 0.15	52.9 ± 4.36
Iloprost	7.11 ± 0.34	99.5 ± 7.22
BMY-45778	7.25 ± 0.09	50.0 ± 4.59
Beraprost	6.98 ± 0.08	107 ± 8.99
PGE ₂	7.34 ± 0.10	85.5 ± 8.64
Misoprostol	6.97 ± 0.06	52.4 ± 6.23
Butaprost	5.81 ± 0.16	8.76 ± 3.25
AGN-205204	6.62 ± 0.12	49.7 ± 3.84
Formoterol	9.38 ± 0.20	103 ± 4.60
Indacaterol	8.58 ± 0.20	83.3 ± 4.47
Salbutamol	7.36 ± 0.34	68.9 ± 1.40
Salmeterol	9.91 ± 0.16	45.8 ± 3.53
α-MSH	NC	NC
NECA	5.39 ± 0.13	47.3 ± 3.40
CGS-21680	NC	NC
BAY60-6583	6.57 ± 0.06	10.2 ± 2.89
Dopamine	5.39 ± 0.07	41.2 ± 10.0
Forskolin	NC	NC
IBMX	NC	NC
Rolipram	NC	NC

cAMP accumulation intrinsic activity was calculated as a percentage of the maximal forskolin response. Data were expressed as mean ± SEM for at least 3 independent experiments. NC – not calculated due to incomplete curve.

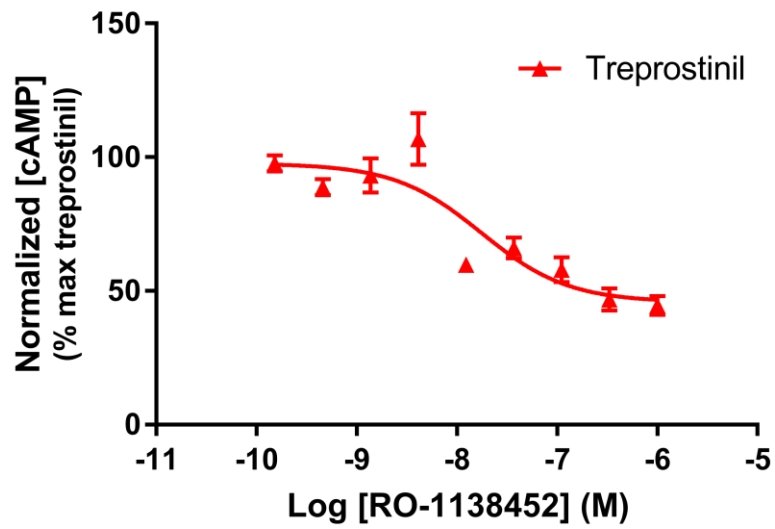


Figure 3:3 - IPR-mediated treprostnil cAMP accumulation

cAMP accumulation in HLF after treatment with an EC_{80} concentration of treprostnil (630 nM) in the presence of varying concentrations of IPR antagonist RO-1138452. Data for each individual experiment were normalised to maximal cAMP accumulation observed with treprostnil (630 nM), and are expressed as mean \pm SEM for at least 3 independent experiments.

3.2.4 Proliferation of human lung fibroblasts

3.2.4.1 *Nuclei count*

To determine if the cAMP responses from the ligands tested results in the inhibition of cellular processes associated with the development of IPF, the ability of ligands, PDE inhibitors, and AC activators to inhibit HLF proliferation was investigated.

One of the simplest ways to measure proliferation of cells is to directly count the number of cells after treatment with pro-proliferative stimuli. Hoechst 33,342 is a nucleic acid stain that emits blue fluorescence when bound to double-stranded deoxyribonucleic acid (dsDNA). By staining the nuclei with Hoechst 33,342 and taking images of the cells on a widefield microscope, cell number was monitored after treatment with a range of concentrations of serum or PDGF for 24, 48, 72, or 96 hours (Figure 3:4). Serum contains a multitude of growth factors that mediates cellular functions (Brunner et al, 2010) whereas PDGF is a single growth factor that has been described to promote fibroblast proliferation and is found elevated in IPF patients (Antoniades et al, 1990; Hetzel et al, 2005). Treatment with serum or PDGF for 24 hours resulted in no detectable increase in HLF proliferation. Serum stimulation for 48, 72, and 96 hours resulted in a concentration-dependent increase in HLF proliferation, with EC_{50} of 0.62 ± 0.08 % v/v at 48 hours, and estimated EC_{50} of 3.42 ± 0.77 % v/v and 4.97 ± 0.92 % v/v at 72 and 96 hours, respectively (Figure 3:4A). In contrast, proliferation after treatment with PDGF was only observed at 72 and 96 hours, with EC_{50} of 3.77 ± 0.13 ng/ml and 7.26 ± 3.23 ng/ml, respectively (Figure 3:4B). The PDGF response was partial compared to the serum response, with maximal proliferation of 29.2 ± 15.2 % of the maximal serum response observed after 96 hours treatment.

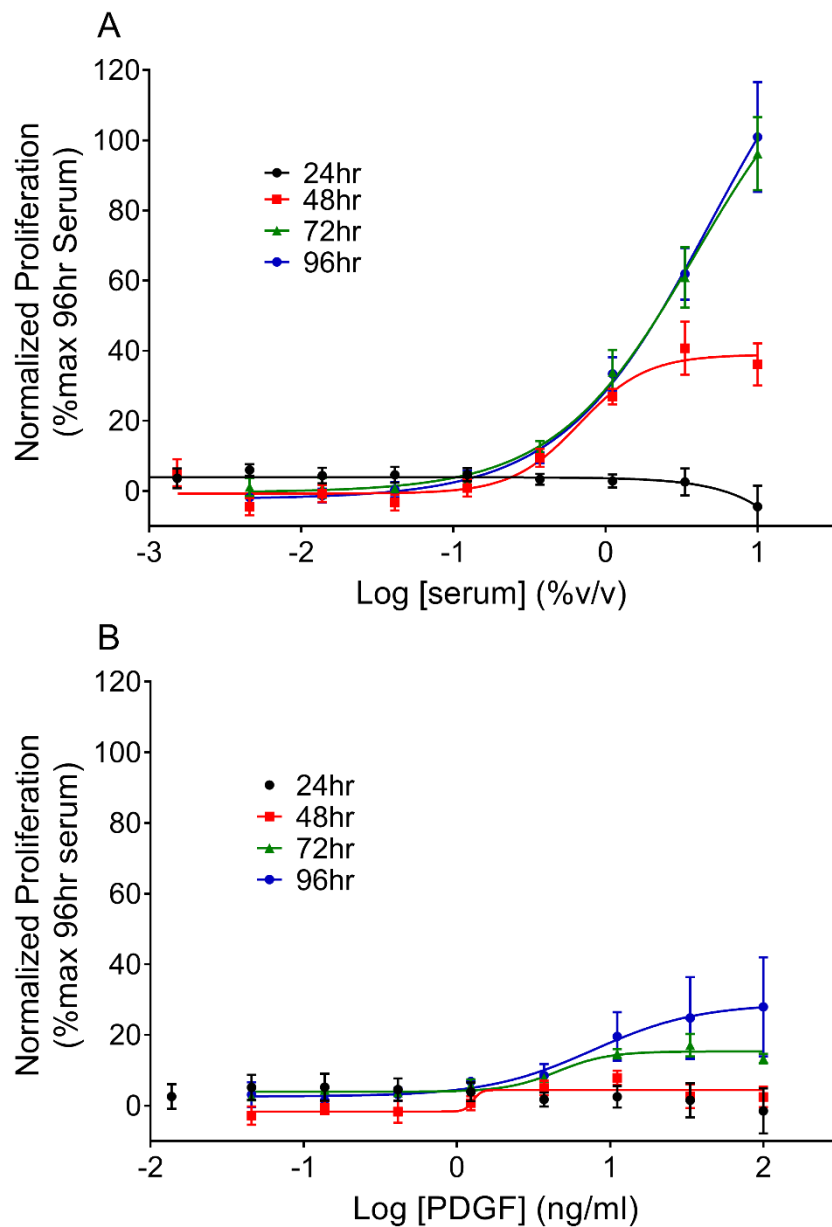


Figure 3:4 - HLF proliferation detected using nuclei count assay

Concentration-dependent increase in HLF proliferation following stimulation with (A) serum or (B) PDGF, for 24, 48, 72, or 96 hours, measured using nuclei count assay. Data were normalised to maximal proliferation observed with 10 % serum at 96 hours and expressed as mean \pm SEM for at least 3 independent experiments.

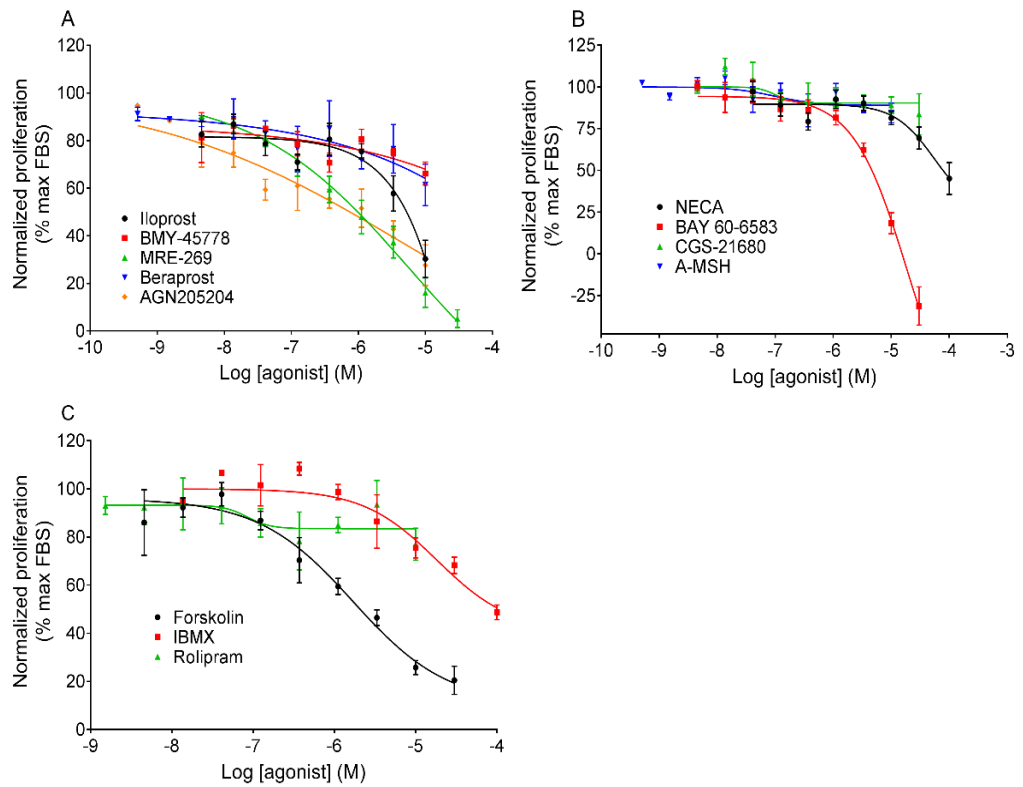


Figure 3:5 - Receptor-mediated inhibition of serum-driven proliferation, measured using nuclei count assay

Concentration-effect curves for the inhibition of HLF proliferation following treatment with a range of agonists targeting the (A) IP and EP receptor, (B) other GPCR, and (C) non-receptors, in the presence of an EC_{80} concentration of serum for 48 hours. Data for each individual experiment were normalised to the maximal response observed with serum and are expressed as mean \pm SEM for at least 3 independent experiments.

Various ligands were selected that targeted a range of receptors and had a range of efficacies for increasing cAMP. HLFs were treated with these ligands for 48 hours in the presence of an EC₈₀ concentration of serum (1.8 % v/v), calculated from Figure 3:4A. Agonists targeting the IP, EP, and adenosine receptors, inhibited HLF proliferation with varying efficacies and potencies (Figure 3:5). Furthermore, activating AC with forskolin and inhibiting PDEs with IBMX resulted in the inhibition of proliferation. However, full concentration response curves could not be established with most agonists, thus E_{max} and EC₅₀ values could not be calculated. Subsequently, the use of an alternate method for measuring HLF proliferation was investigated.

3.2.4.2 *BrdU incorporation assay*

BrdU is a synthetic nucleoside that is an analogue of thymidine. The BrdU assay measures the incorporation of BrdU into newly synthesized DNA of actively proliferating cells. Antibodies specific for BrdU can then be used to detect the incorporated chemical, thus indicating cells that were actively replicating their DNA. Treatment with a range of concentrations of serum or PDGF for 24 hours resulted in increased proliferation in a concentration dependent manner, with EC₅₀ values for serum and PDGF of 1.13 ± 0.24 % v/v and 1.50 ± 0.20 ng/ml, respectively. Comparable to the nuclei count assay, the PDGF response was partial compared to the serum response, with maximal proliferation of 41.0 ± 8.62 % for PDGF (Figure 3:6).

Various ligands were selected that targeted a range of receptors and had a range of efficacies for increasing cAMP. HLFs were then treated with ligands for 24 hours in the presence of a concentration of serum (1 % v/v) that correlates to near maximal proliferation (calculated from Figure 3:6). Agonists that targeted the IP, EP₂, EP₄, β_2 , and A_{2B} receptors, as well as forskolin and IBMX, were able to inhibit serum-driven proliferation (Figure 3:7). Targeting the IPR with treprostinil resulted in maximal

inhibition of 42.5 ± 5.36 %, with pEC_{50} of 6.99 ± 0.27 . MRE-269 was also able to inhibit serum-driven proliferation, however E_{max} and EC_{50} values could not be calculated due to the absence of a full concentration response curve. Furthermore, no inhibition of proliferation was observed when targeting the IPR with iloprost (Figure 3:7A).

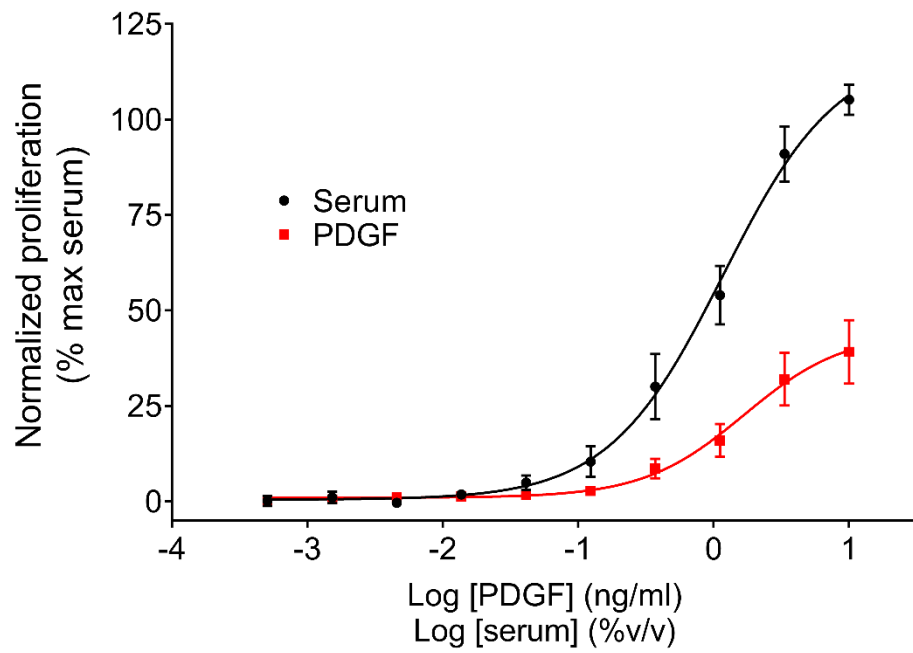


Figure 3:6 - Fibroblast proliferation detected using BrdU assay

Concentration-dependent increase in HLF proliferation following treatment with a range of concentrations of serum or PDGF for 24 hours, detected using BrdU incorporation. Data were normalised to maximal proliferation observed with 10 % serum and expressed as mean \pm SEM for 8 independent experiments.

Non-selective or selective ligands targeting the EP₂ and/or EP₄ receptors were only able to partially inhibit serum-driven proliferation with a range of potencies (Figure 3:7B). The endogenous ligand PGE₂ inhibited proliferation with E_{max} of 43.1 ± 6.14 % and pEC₅₀ of 7.04 ± 0.18. Non-selective prostaglandin receptor agonists misoprostol and butaprost inhibited proliferation with E_{max} of 34.7 ± 0.71 % and 29.1 ± 7.29 % respectively. Furthermore, the EP₄ selective agonist AGN205204 also inhibited proliferation with E_{max} of 51.3 ± 8.89 %.

Targeting the β₂ adrenoceptor with a range of agonists only resulted in partial inhibition of serum-driven proliferation (Figure 3:7C). Formoterol, indacaterol, salbutamol, and salmeterol had similar efficacies, with E_{max} values ranging between 32.4 ± 5.84 % for salbutamol and 47.9 ± 1.58 % for indacaterol. Formoterol and salmeterol had equal potencies, with pEC₅₀ values of 9.58 ± 0.29 and 9.58 ± 0.14, respectively. Indacaterol and salbutamol had potencies that were 10-fold different, with pEC₅₀ values of 7.96 ± 0.35 and 7.04 ± 0.57, respectively.

Investigating ligands that target the MC1, adenosine, and dopamine receptors, showed that only the A_{2B} selective agonist BAY 60-6583 inhibited serum-driven proliferation (Figure 3:7D). BAY 60-6583 fully inhibited proliferation, with pEC₅₀ value of 5.30 ± 0.16. No inhibition of proliferation was detected with α-MSH, NECA, CGS-21680, or dopamine. Lastly, directly activating AC with forskolin resulted in 74.0 ± 6.70 % inhibition, and inhibiting PDEs with either IBMX or rolipram led to a partial inhibition of serum-driven proliferation, however E_{max} and EC₅₀ values could not be calculated due to the absence of a full concentration response curve (Figure 3:7E).

Next, the ability of the same set of ligands to inhibit PDGF-driven proliferation was investigated. HLFs were treated with a range of ligands for 24 hours in the presence of

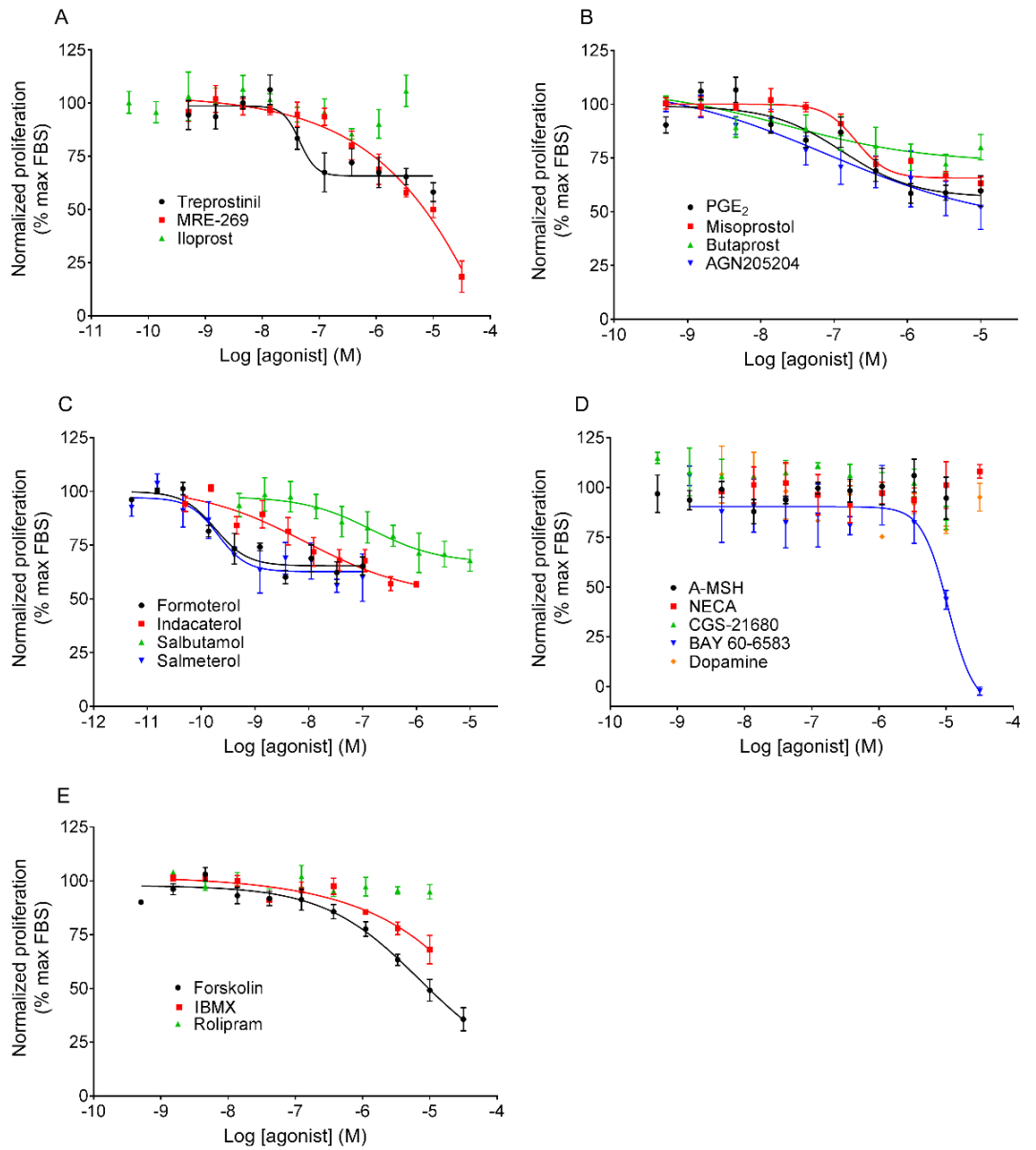


Figure 3:7 - Receptor-mediated inhibition of serum-driven proliferation

Concentration effect curves for the inhibition of proliferation of HLFs following treatment of a range of agonists targeting the (A) IP receptor, (B) EP receptor, (C) β_2 adrenoceptor, (D) other GPCR, and (E) non-receptor, in the presence of an EC₈₀ concentration of serum for 24 hours. Data for each individual experiment were normalised to the maximal proliferation observed with serum and are expressed as mean \pm SEM for at least 3 independent experiments.

a concentration of PDGF (3.9 ng/ml) that correlates to near maximal proliferation (calculated from Figure 3:6). Agonists that targeted the IP, EP₂, EP₄, β₂, adenosine, and dopamine receptors, as well as forskolin, were able to inhibit PDGF-driven proliferation (Figure 3:8). Targeting the IPR with MRE-269 or treprostinil resulted in 85.7 ± 7.65 % and 63.7 ± 6.39 % inhibition of proliferation, respectively. Furthermore, treprostinil was more potent at inhibiting proliferation in comparison to MRE-269. In contrast, iloprost showed little inhibition of proliferation, with E_{max} and EC₅₀ values not determined due to the absence of a full concentration response curve (Figure 3:8A).

As observed with serum-driven proliferation, ligands targeting the EP₂ and/or EP₄ receptor were found to inhibit PDGF-driven proliferation (Figure 3:8B). The endogenous ligand, PGE₂, partially inhibited proliferation by 71.0 ± 3.86 %, with pEC₅₀ value of 8.60 ± 0.08. Non-selective prostaglandin receptor agonist misoprostol and selective EP₄ receptor agonist AGN-205204 fully inhibited proliferation with E_{max} 94.1 ± 1.59 % and 101 ± 3.71 % respectively, however they were less potent in comparison to PGE₂. Butaprost was also observed to inhibit PDGF-driven proliferation, however E_{max} and EC₅₀ values could not be calculated due to the absence of a full concentration response curve.

All four β₂ adrenoceptor agonists were able to inhibit PDGF-driven proliferation (Figure 3:8C). Formoterol and salbutamol were least efficacious, with similar E_{max} values of 70.1 ± 2.96 % and 69.2 ± 5.53 % inhibition, respectively. Indacaterol and salmeterol were the most efficacious β₂ adrenoceptor agonists at inhibiting proliferation, with E_{max} values of 90.3 ± 5.25 % and 89.2 ± 0.27 %, respectively. β₂ adrenoceptor agonists potency for inhibiting proliferation were varied, with pEC₅₀ values ranging between 7.98 ± 0.17 for salbutamol and 10.5 ± 0.15 for salmeterol.

Targeting the adenosine receptors with non-selective agonist NECA resulting in partial inhibition of proliferation, with E_{\max} of 37.8 ± 14.7 % and pEC_{50} of 6.94 ± 0.43 . The selective A_{2A} agonist CGS-21680 had no detectable effect on proliferation of HLFs, however the selective A_{2B} agonist, BAY 60-6583, fully inhibited PDGF-driven proliferation, with E_{\max} of 100 ± 0.01 % and pEC_{50} of 5.30 ± 0.12 . Targeting the dopamine receptor with dopamine resulted in inhibition of proliferation with E_{\max} value of 73.5 ± 13.5 % and pEC_{50} of 4.78 ± 0.27 . Lastly, no inhibition of proliferation was observed with the MC1 receptor agonist α -MSH (Figure 3:8D). Directly activating AC with forskolin inhibited PDGF-driven proliferation 90.8 ± 9.12 %, however, inhibiting PDEs with IBMX or rolipram resulted in no detectable inhibition of proliferation (Figure 3:8E).

The efficacy and potency of all ligands tested in inhibiting either serum or PDGF-driven proliferation are summarised in Table 3:4. Overall, BAY 60-6583 was the only ligand that fully inhibited both serum and PDGF-driven proliferation. In addition, most ligands were more efficacious at inhibiting PDGF-driven proliferation than serum-driven proliferation.

3.2.5 Cytotoxicity of ligands in human lung fibroblasts

To ensure that any inhibitory effects on proliferation were not due to ligands promoting cell death, cell viability was measured using LDH release as a marker of cell membrane integrity and caspase-3/7 detection as a marker of apoptosis.

None of the compounds tested caused a significant increase in expression of caspase-3/7, whereas treatment with the toxic compound staurosporine resulted in statistically significant cell apoptosis ($P < 0.001$; Table 3:5). In addition, none of the compounds tested caused a statistically significant change in LDH release when

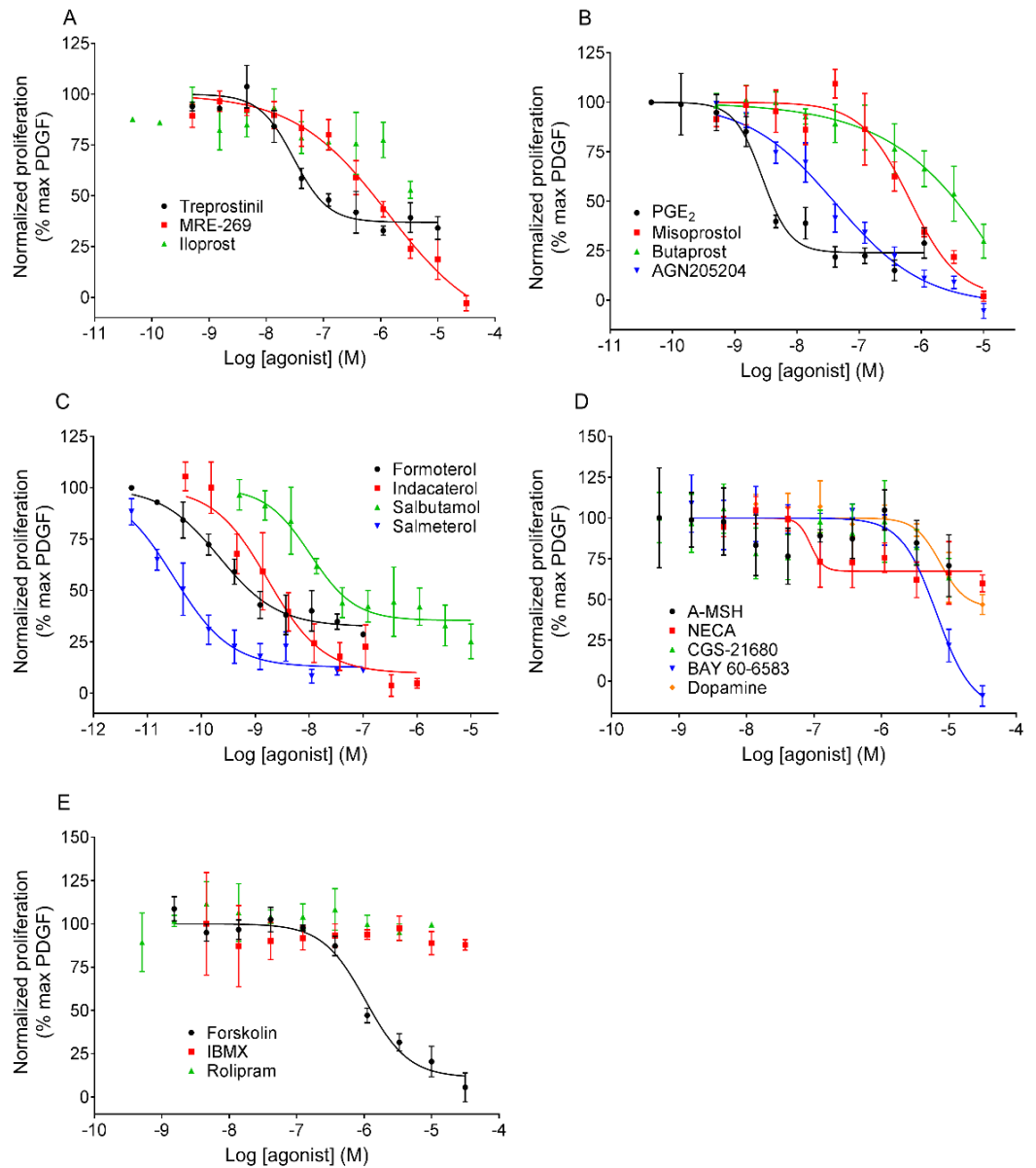


Figure 3:8 - Receptor-mediated inhibition of PDGF-driven proliferation

Concentration effect curves for the inhibition of proliferation of HLFs following treatment of a range of agonists targeting the (A) IP receptor, (B) EP receptor, (C) β_2 adrenoceptor, (D) other GPCR, and (E) non-receptor, in the presence of an EC_{80} concentration of PDGF for 24 hours. Data for each individual experiment were normalised to the maximal proliferation observed with PDGF and are expressed as mean \pm SEM for at least 3 independent experiments.

Table 3:4 - Potency and intrinsic activity of all ligands for inhibition of HLF proliferation

Agonist	Proliferation vs serum		Proliferation vs PDGF	
	pEC ₅₀	E _{max} (% max)	pEC ₅₀	E _{max} (% max)
Treprostinil	6.99 ± 0.27	42.5 ± 5.36	7.53 ± 0.12	63.7 ± 6.39
MRE-269	NC	NC	6.50 ± 0.23	85.7 ± 7.65
Iloprost	NC	NC	NC	NC
BMY-45778	ND	ND	ND	ND
Beraprost	ND	ND	ND	ND
PGE₂	7.04 ± 0.18	43.1 ± 6.14	8.60 ± 0.08	71.0 ± 3.86
Misoprostol	6.74 ± 0.10	34.7 ± 0.71	6.13 ± 0.04	94.1 ± 1.59
Butaprost	7.19 ± 0.38	29.1 ± 7.29	NC	NC
AGN-205204	6.91 ± 0.48	51.3 ± 8.89	7.45 ± 0.25	101 ± 3.71
Formoterol	9.58 ± 0.29	37.2 ± 2.64	9.08 ± 0.72	70.1 ± 2.96
Indacaterol	7.96 ± 0.35	47.9 ± 1.58	8.84 ± 0.28	90.3 ± 5.25
Salbutamol	7.04 ± 0.57	32.4 ± 5.84	7.98 ± 0.17	69.2 ± 5.53
Salmeterol	9.58 ± 0.14	37.7 ± 7.33	10.5 ± 0.15	89.2 ± 0.27
α-MSH	NC	NC	NC	NC
NECA	NC	NC	6.94 ± 0.43	37.8 ± 14.7
CGS-21680	NC	NC	NC	NC
BAY60-6583	5.30 ± 0.16	100 ± 0.01	5.30 ± 0.12	100 ± 0.01
Dopamine	ND	ND	4.78 ± 0.27	73.5 ± 13.5
Forskolin	5.28 ± 0.13	74.0 ± 6.70	5.98 ± 0.14	90.8 ± 9.12
IBMX	NC	NC	NC	NC
Rolipram	NC	NC	NC	NC

BrdU inhibition intrinsic activity was calculated as a percentage of maximal proliferation observed with serum or PDGF, as indicated. Data were expressed as mean ± SEM for at least 3 independent experiments. NC – not calculated due to incomplete curve; ND – not determined in this assay.

Table 3:5 - Cell viability measured by caspase-3/7 detection

	% cells positive for caspase-3/7	
	Top concentration	1:10 dilution
Negative Control + 1% FBS	4.27 ± 2.80	
Staurosporine (100 nM)	54.8 ± 13.6	
Treprostinil (10 µM)	0.76 ± 0.06	0.92 ± 0.25
Iloprost (3 µM)	0.88 ± 0.08	1.15 ± 0.29
MRE-269 (10 µM)	0.49 ± 0.21	0.49 ± 0.22
PGE₂ (10 µM)	0.68 ± 0.29	0.53 ± 0.04
Misoprostol (10 µM)	0.54 ± 0.18	0.55 ± 0.04
Butaprost (10 µM)	0.80 ± 0.29	0.90 ± 0.39
AGN-205204 (10 µM)	0.57 ± 0.09	0.56 ± 0.09
Formoterol (100 nM)	0.67 ± 0.22	0.88 ± 0.48
Indacaterol (1 µM)	0.62 ± 0.01	0.62 ± 0.15
Salbutamol (10 µM)	0.46 ± 0.09	0.53 ± 0.12
Salmeterol (100 nM)	0.40 ± 0.12	0.66 ± 0.24
NECA (30 µM)	1.04 ± 0.20	0.67 ± 0.09
BAY60-6583 (30 µM)	0.62 ± 0.14	1.04 ± 0.38
Dopamine (30 µM)	0.83 ± 0.14	1.21 ± 0.34
Forskolin (30 µM)	1.26 ± 0.35	0.61 ± 0.15
IBMX (10 µM)	0.98 ± 0.27	1.24 ± 0.59

Measurement of cell viability using caspase-3/7 expression as a marker for apoptosis, after treatment with ligands and staurosporine as a positive control. Data were normalised to the total number of cells in the field of view and are expressed as mean ± SEM for 3 independent experiments.

Table 3:6 - Cell viability measured by LDH release

	% LDH release	
	Top concentration	1:10 dilution
Treprostinil (10 μM)	-7.68 \pm 2.39	-9.62 \pm 3.70
Iloprost (3 μM)	-14.9 \pm 5.59	-11.4 \pm 4.56
MRE-269 (10 μM)	0.43 \pm 3.83	2.26 \pm 7.05
PGE₂ (10 μM)	-8.97 \pm 2.22	-14.0 \pm 4.73
Misoprostol (10 μM)	-3.60 \pm 8.72	3.45 \pm 5.45
Butaprost (10 μM)	-8.31 \pm 2.61	-6.69 \pm 2.29
AGN-205204 (10 μM)	4.65 \pm 11.5	-4.58 \pm 1.06
Formoterol (100 nM)	-5.96 \pm 3.72	-7.26 \pm 3.57
Indacaterol (1 μM)	-6.01 \pm 10.2	-1.24 \pm 7.88
Salbutamol (10 μM)	-5.37 \pm 7.86	-6.66 \pm 5.29
Salmeterol (100 nM)	-2.58 \pm 4.88	2.33 \pm 7.34
NECA (30 μM)	-11.9 \pm 6.35	-18.1 \pm 2.74
BAY60-6583 (30 μM)	0.87 \pm 4.62	-6.97 \pm 1.59
Dopamine (30 μM)	-14.4 \pm 4.35	-7.75 \pm 3.74
Forskolin (30 μM)	-11.2 \pm 6.22	2.00 \pm 7.91
IBMX (10 μM)	-2.15 \pm 2.71	-25.4 \pm 7.47

Measurement of cell viability using LDH release as a measure of membrane integrity after treatment with ligands and lysis of cells to measure total amount of cellular LDH. Data were expressed as a percentage of released LDH vs. total intracellular LDH and are expressed as mean \pm SEM for at least 3 independent experiments.

calculating the percentage of release LDH vs. the total amount of cellular LDH ($P < 0.001$; Table 3:6).

3.2.6 Fibroblast to myofibroblast transdifferentiation

Differentiation of fibroblasts to myofibroblasts is another pro-fibrotic process involved in IPF, therefore we wanted to determine if ligands were capable of inhibiting TGF β -induced FMT.

Treatment with a range of concentrations of TGF β for 48 hours resulted in robust FMT in HLF, with EC_{50} equal to 0.07 ± 0.01 ng/ml (data not shown). Various ligands were selected that targeted a range of receptors and had a range of efficacies for increasing cAMP. HLFs were then treated with a range of concentrations of ligands for 48 hours in the presence of a TGF β concentration (0.3 ng/ml) that relates to near maximal FMT. Agonists and PDE inhibitors inhibited TGF β -driven FMT with varying levels of efficacy and potency (Figure 3:9). Targeting the IPR with treprostinil and MRE-269 inhibited TGF β -driven FMT 63.8 ± 6.22 % and 97.6 ± 5.46 %, respectively (Figure 3:9A). Furthermore, targeting the EP $_2$ and/or EP $_4$ receptors with PGE $_2$, misoprostol, and AGN-205204 resulted in inhibition of FMT ranging from 53.2 ± 9.50 % to 71.4 ± 6.04 % (Figure 3:9A).

β_2 adrenoceptor agonists formoterol, indacaterol, salbutamol, and salmeterol, all inhibited TGF β -driven FMT partially, with E_{max} values ranging from 50.9 ± 6.68 % for salmeterol to 68.7 ± 11.8 % for indacaterol (Figure 3:9B). Selectively targeting the A $_{2B}$ receptor with BAY 60-6583 resulted in full inhibition of TGF β -driven FMT, however there was no detectable inhibition of FMT with non-selective adenosine receptor agonist NECA (Figure 3:9C). In addition, no inhibition of FMT was observed with

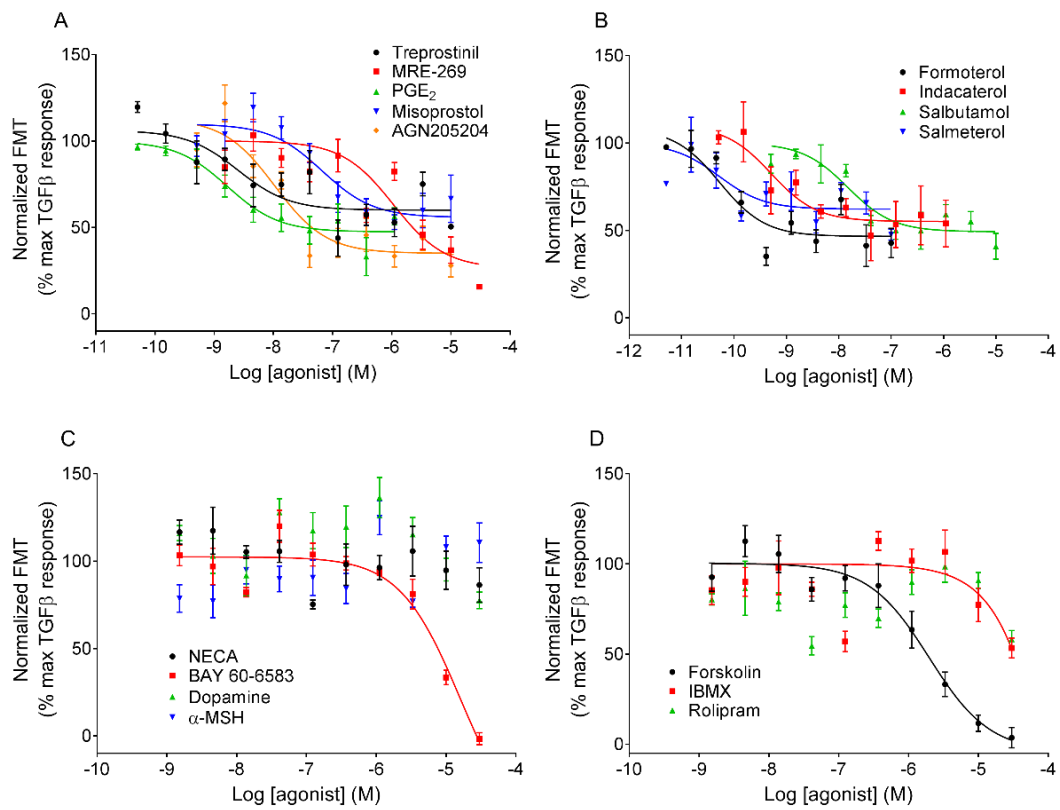


Figure 3:9 - Receptor-mediated inhibition of TGFβ-driven FMT

Concentration effect curves for the inhibition of FMT in HLFs following treatment of a range of agonists targeting (A) IP or EP receptors, (B) β₂ adrenoceptor, (C) other GPCR, and (D) non-receptors, in the presence of an EC₈₀ concentration of TGFβ for 48 hours. Data for each individual experiment were normalised to the maximal levels of FMT observed with TGFβ and are expressed as means ± SEM for 4 independent experiments.

dopamine or α -MSH, targeting the dopamine and MC1 receptors, respectively (Figure 3:9C).

Lastly, directly activating AC with forskolin and inhibiting PDEs with IBMX resulted in 103 ± 3.17 % and 49.3 ± 6.02 % inhibition of FMT, respectively. However, no inhibition of TGF β -driven FMT was detected with PDE₄ inhibitor rolipram (Figure 3:9D).

3.2.7 Correlation between cAMP and the inhibition of proliferation and differentiation

High throughput screening assays, like the cAMP assay, are vastly utilised in the drug discovery process over more relevant phenotypic assays due to the ability to quickly screen a large selection of ligands. Therefore the relevance of this method for predicting ligands that will be efficacious at inhibiting HLF proliferation and differentiation was explored. Correlation plots were generated between maximal cAMP accumulation and maximal inhibition of proliferation or FMT for the ligands investigated in this study (Figure 3:10). There was no significant correlation between the amount of cAMP accumulation and the degree of inhibition of PGDF-mediated proliferation ($r^2 = 0.06$, $p = 0.41$) (Figure 3:10A). Despite treprostinil and formoterol generating high levels of cAMP both ligands were relatively ineffective at inhibiting proliferation. In contrast, BAY 60-6583, AGN-205204, misoprostol, salmeterol, and MRE-269 were relatively strong inhibitors of proliferation despite generating lower levels of cAMP.

In addition, there was no significant correlation between the amount of cAMP accumulation and the degree of inhibition of TGF β -mediated FMT ($r^2 = 0.06$, $p = 0.46$) (Figure 3:10B). Again, treprostinil and formoterol were relatively ineffective at inhibiting FMT despite being highly efficacious at cAMP accumulation. In contrast,

both BAY 60-6583 and MRE-269 fully inhibited TGF β -driven FMT whilst being relatively ineffective at driving cAMP accumulation.

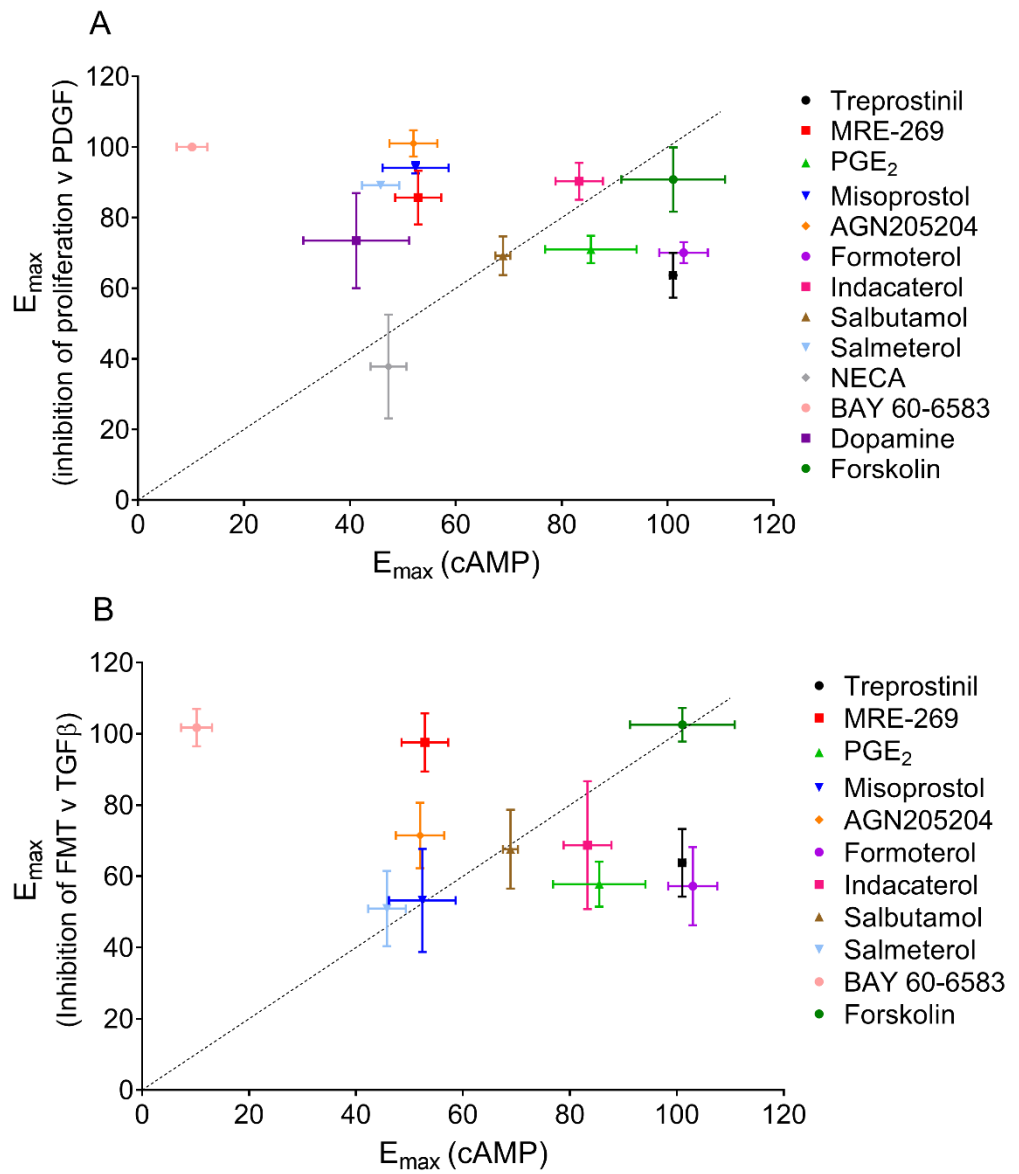


Figure 3:10 - Correlation plot

Correlation between global cAMP accumulation and maximal inhibition of PDGF-driven proliferation (A) or TGFβ-driven FMT (B). Pearson correlation, dashed line = line of unity.

3.3 Discussion

IPF is a devastating progressive disease with the two currently approved therapeutics only slowing disease progression with severe side effects. There is an evolving body of evidence demonstrating cAMP as a potential target for the treatment of IPF. Cross talk between the cAMP and MAPK pathway, with activation of the cAMP pathway able to inhibit proliferation in HLFs, has been previously described in literature (Gerits et al, 2008; Stork & Schmitt, 2002). Here, the rationale of investigating the cAMP pathway as a potential target for the inhibition of profibrotic processes was confirmed as it was shown that direct activation of AC with forskolin inhibits ERK phosphorylation. Subsequently, using an inhibitor of ERK1/2 phosphorylation, it was shown that proliferation is dependent on ERK activity. It has been reported in fibroblasts that the activation of Epac-1 and PKA in the cAMP pathway are responsible for PGE₂ inhibition of proliferation and collagen expression (Huang et al, 2008a). This provides a rationale to identify the expression of G_s-coupled GPCR in HLF, as well as their ability to increase cAMP and subsequently inhibit fibrotic processes, in order to identify new targets to treat IPF.

By determining the mRNA expression of GPCRs it was discovered that fibroblasts express several G_s-coupled receptors, including related receptor families, such as those for the prostaglandins (IP, EP₂, EP₄) and adenosine (A_{2A}, A_{2B}), as well as the MC1, β₂ adrenoceptor, and dopamine-1 receptors. Using the endogenous ligand α-MSH, the MC1 receptor could not be determined as functionally active in either the cAMP or phenotypic assays in these studies despite having the third highest expression levels. However, the novel α-MSH analogue STY39 has been shown to attenuate BLM-induced pulmonary fibrosis by lowering levels of ECM and reducing the production of TGFβ (Xu et al, 2011). Therefore, future work could investigate the ability of other MC1

receptor agonists to inhibit profibrotic processes in fibroblasts. In addition, this highlights the need to look at mRNA, protein expression, and a number of functional assays with a range of ligands to confirm active receptors.

HLFs are key mediators of fibrosis, and using primary cells that contain human receptors and signalling proteins at relevant levels, rather than recombinant cell systems, is likely more reflective of the *in vivo* environment. To model chronic aspects of IPF HLF proliferation and differentiation were investigated. Differentiation was monitored by using expression of α SMA as a marker for a myofibroblast phenotype. The monitoring of proliferation was performed using two complimentary methods, BrdU incorporation into newly synthesised DNA of actively proliferating cells, and direct cell counting using nuclear stain. Using BrdU incorporation it was identified that both PDGF and serum resulted in cell proliferation, with proliferation detectable at an earlier stage in comparison to the cell counting method. Furthermore, full concentration-response curves for the inhibition of cell counting could not be obtained for all ligands. This could be a result of the BrdU assay having greater sensitivity due to amplification of the signal through the incorporation of BrdU into multiple sites during each instance of DNA replication. In addition, ligands were typically more efficacious at inhibiting PDGF-driven proliferation over serum-driven proliferation. Serum contains multiple growth factors and proliferative stimuli (Brunner et al, 2010), thus inhibiting the effect of multiple mediators may be more difficult. Although the IPF lung is likely to have multiple pro-fibrotic mediators, which is mimicked by using serum, PDGF has been shown to be a critical growth factor in the development of IPF by stimulating the proliferation and migration of fibroblasts, therefore inhibiting proliferation mediated by PDGF could indicate potential therapeutics for IPF (Bonner, 2004; Nishioka et al, 2013).

Some of the receptors and agonists that inhibited serum- and/or PDGF-driven HLF proliferation are currently used in the treatment of other pulmonary diseases or have been highlighted as potential treatments for IPF, as discussed below.

A decreased production of PGE₂ has been found to be predictive of, and contribute to, fibrotic lung disease (Bozyk & Moore, 2011). *Ptger2*^{-/-} knock-out mice, lacking a functional copy of EP₂ receptor, exhibit a more severe fibrotic response to bleomycin instillation compared to wild-type mice (Moore et al, 2005). Furthermore, PGE₂ has previously been reported as an anti-fibrotic that activates the EP₂ and EP₄ receptors (Kolodsick et al, 2003; Thomas et al, 2007). In agreement, agonists in our study which target the EP receptors were able to inhibit HLF proliferation and differentiation. As well as abrogating FMT, targeting EP₂ and EP₄ receptors has also been found to reverse the phenotype (Garrison et al, 2013; Sieber et al, 2018). Targeting the EP receptors with PGE₂ or selectively targeting EP₂ with agonists ONO-18c/ONO-18k, reverted TGFβ1-induced differentiated myofibroblasts to fibroblasts (Sieber et al, 2018). This suggests EP₂/EP₄ receptor agonists are strong candidates for novel IPF treatments.

Recent studies have also identified the A_{2B} receptor as an important target in the regulation of acute lung injury, with extracellular signalling molecule adenosine and agonists signalling through the A_{2B} receptor having a key role in lung protection (Eckle et al, 2008; Hoegl et al, 2015). Whilst A_{2B} receptor signalling is implicated in lung protection in acute lung injury, several studies have suggested it may become detrimental in chronic forms of lung diseases, as A_{2B} receptor signalling can promote the production of inflammatory and fibrotic mediators in patients with chronic lung diseases (Sun et al, 2006; Zhou et al, 2010). A study examining the contribution of A_{2B} receptor signalling in acute versus chronic stages of bleomycin-induced lung injury showed genetic removal of the A_{2B} receptor enhanced loss of lung epithelial function

and increased pulmonary inflammation in acute lung injury, supporting an anti-inflammatory role for the A_{2B} receptor. However, in a chronic model genetic A_{2B} receptor removal was associated with reduction in pulmonary fibrosis, supporting a profibrotic role for this receptor during chronic lung injury (Zhou et al, 2011). In this thesis it was observed that the selective A_{2B} agonist BAY 60–6583, although not very potent, showed robust inhibition of HLF proliferation and FMT, indicating a protective role in fibrosis. BAY 60-6583 has high affinity for the human A_{2B} receptor (K_i 212 nM) and it has been reported to have an EC₅₀ of 98.7 nM for cAMP accumulation in CHO cells transfected with the human A_{2B} receptor (Hinz et al, 2014). Thus the effects of BAY 60-6583 observed in this study may not be a real effect at the A_{2B} receptor. Instead, at high concentrations, BAY 60-6583 could be having off-target effects at other receptors which effect cellular function. However, in Jurkat-T cells, a human leukaemia cell line endogenously expressing A_{2B} at low receptor expression levels, BAY 60-6583 had only a small effect on cAMP accumulation, suggesting receptor expression levels greatly affect BAY 60-658 efficacy and potency (Hinz et al, 2014). The A_{2B} receptor expression levels in Jurkat-T cells are likely to be similar to the expression levels observed in HLFs, than the high expression levels in CHO cells overexpressing A_{2B} receptors. With adenosine signalling in lung disease proving to be complex, future studies investigating the potential of targeting the A_{2B} receptor in the treatment of IPF is required.

β₂ adrenoceptor agonists have long been an important pharmacological approach to induce bronchodilation in patients suffering from COPD (Celli & MacNee, 2004; Vestbo et al, 2013) and asthma (NationalAsthmaEducationandPreventionProgram, 2007; Reddel et al, 2015). β₂ adrenoceptors on HLF have been demonstrated to inhibit fibroblast proliferation, differentiation, and collagen synthesis (Lamyel et al, 2011). β₂

adrenoceptors are classified as short or long-acting based on their duration of action after a single inhaled dose. In our studies it is observed that long acting β_2 adrenoceptor agonists (LABA) salmeterol and indacaterol robustly inhibited HLF proliferation and FMT, thus may act as potential anti-fibrotic agents in IPF. Furthermore, a recent small study investigating the potential of LABA in combination with inhaled corticosteroids (ICS) in IPF patients demonstrated the combination therapy had the potential to tackle various aspects of IPF (Wright et al, 2017). In our studies, the short acting β_2 adrenoceptor agonist (SABA) salbutamol was not as effective at inhibiting fibroblast proliferation and FMT. This suggests a temporal aspect of agonist signalling is required for long-term efficacy at inhibiting fibrotic processes.

Although the PDE inhibitor IBMX was not found to increase cAMP, it was shown to inhibit proliferation and FMT, albeit at higher concentrations. In fibroblasts, under basal conditions, there may not be sufficient turnover of cAMP for PDE inhibitors to increase levels of cAMP during the shorter time period of the cAMP assay, but with the extended incubation for phenotypic assays, IBMX may be able to increase cAMP enough to drive the inhibitory effect. In support of this, the anti-fibrotic potential of PDE₄ inhibitors has been investigated in several *in vitro* studies. Specifically, the PDE₄ inhibitor piclamilast abrogated TGF- β -induced FMT (Dunkern et al, 2007). Furthermore, roflumilast and rolipram inhibited both TGF- β induced fibroblast contraction and fibroblast chemotaxis towards fibronectin (Togo et al, 2009). PDE₄ inhibitors have also been found to reduce bleomycin-induced fibrosis *in vivo* (Cortijo et al, 2009; Milara et al, 2015). Promisingly, there have been several major clinical trials of roflumilast in COPD therapy (Fabbri et al, 2009; Martinez et al, 2015; Martinez et al, 2016) and roflumilast has been approved for treating COPD as an add-on to bronchodilators (NationalInstituteForHealthandCareExcellence, 2017). It would

therefore be interesting to investigate the effect of co-administrating PDE inhibitors with GPCR agonists in inhibiting fibroblast proliferation and FMT for the treatment of IPF. This approach may increase efficacy due to the dual effects of increasing cAMP levels by targeting G_s-coupled GPCRs and blocking cAMP degradation by inhibiting PDEs.

IPR PGI₂ analogues iloprost, treprostinil, and beraprost, are marketed vasodilators for the treatment of PAH (Olschewski et al, 2004). PAH occurs as a consequence of chronic obstruction of small pulmonary arteries caused by the dysfunction and proliferation of endothelial cells, vascular smooth muscle cells, and fibroblasts (Humbert et al, 2004). More recently, selexipag, for which MRE-269 is the activate metabolite of, was approved for the treatment of PAH (Asaki et al, 2015; Sitbon et al, 2015). Targeting the IPR with selexipag may also be useful in IPF treatment as it inhibited both fibroblast proliferation and FMT. MRE-269 (also known as ACT-333679) has high IPR selectivity, and although it was a partial agonist in the cAMP assay it was able to fully inhibit PDGF-driven proliferation and TGFβ-induced FMT. The anti-fibrotic properties of MRE-269 have previously been investigated where it was shown to prevent FMT, fibroblast proliferation, ECM synthesis, and exert relaxant effects in myofibroblast cell contraction assays (Zmajkovicova et al, 2018). Furthermore, MRE-269 treatment was also shown to revert an established myofibroblast phenotype (Zmajkovicova et al, 2018).

Traditional drug discovery relies on recombinant systems and simple second messenger assays to profile compounds prior to testing in models of disease. However, with the majority of compounds (52 %) failing in clinical trials due to lack of efficacy in humans (Harrison, 2016) there is a need to alter current practices. The use of second messenger assays in more disease relevant cells is more translational to

human disease, however these assays are acute, and diseases such as IPF are chronic diseases characterised by long-term changes. The assumption behind use of the simple, higher throughput second messenger assays is that the activity of a drug to generate or inhibit second messengers is directly related to its ability to generate or inhibit a phenotypic response. Based on this assumption partial agonists in second messenger assays may not be progressed to preclinical models on the assumption that they will not have the intrinsic activity required to generate efficacy in chronic disease models. The lack of correlation observed in this current study between the degree of cAMP accumulation and inhibition of proliferation suggests that this may not be the case. In agreement, of the 21 ligands tested in this study, BAY 60-6583, MRE-269, AGN-205204, misoprostol, salmeterol, indacaterol, and forskolin, fully inhibited serum- and/or PDGF-driven HLF proliferation, of which only forskolin was a full agonist in the cAMP assay.

The mechanism behind the disconnect observed between cAMP accumulation and inhibition of chronic phenotypic responses is not yet clear, however there are a few factors that need to be considered. One theory is that partial agonism reduces the degree of receptor phosphorylation and internalization, leading to a reduction in receptor desensitization, while still retaining efficacy in phenotypic relevant readouts due to signal amplification. Partial agonism of MRE-269 has been shown to result in limited β -arrestin recruitment and lack of sustained IPR internalisation (Gatfield et al, 2017). This partial agonism is in contrast to the full agonism displayed by other PGI₂ analogues iloprost, treprostinil, and beraprost (Gatfield et al, 2017). In line with *in vitro* studies, MRE-269 displayed sustained efficacy in *in vivo* models of pulmonary hypertension, whereas treprostinil did not (Gatfield et al, 2017). In contrast, it has been shown that desensitisation of the β_2 adrenoceptor is not dependent on agonist

efficacy (Rosethorne et al, 2015). In support of this, our data shows indacaterol produces an 80 % maximal cAMP response whereas salmeterol produces a 40 % maximal cAMP response. However both compounds were equally as efficacious at inhibiting proliferation. Interestingly both these compounds are LABA, which suggests a role for signalling kinetics in mediating chronic phenotypic responses.

In agreement, it has previously been demonstrated that for the regulation of gene transcription after GPCR activation it is not necessarily the magnitude of second messenger response, but rather the kinetics or duration of the response, that drives transcriptional activity (Baker et al, 2004; Rosethorne et al, 2008). Using CHO cells expressing the β_2 adrenoceptor it has been shown that short bursts of second messenger activation, regardless of the magnitude, are often incapable of initiating gene transcription, whereas a small second messenger response that is sustained over time is able to robustly activate transcription factors (Baker et al, 2004). This may explain why salmeterol, a long acting partial agonist, was more efficacious at inhibiting proliferation than might be predicted from its cAMP response, as it may result in a small but sustained increase in cAMP that over time results in significant changes in phenotypic responses.

GPCRs have the ability to signal through multiple G proteins or effector molecules, which may result in promiscuous signalling that could be contributing to the disconnect observed between cAMP and inhibition of proliferation and differentiation. β -arrestins have been shown to be important signalling scaffolds that facilitate the activation of the MAPK pathway (Smith & Rajagopal, 2016). However, increasing cAMP levels by directly activating AC without activating GPCRs results in inhibition of proliferation and FMT, supporting a direct role for the cAMP pathway in the inhibition of chronic phenotype. Furthermore, using the EP₂ receptor-selective

G α s-signalling biased agonist ONO-18k, which induces cAMP accumulation with less efficacy recruiting β -arrestin, FMT was still inhibited comparative to the unbiased agonist ONO-18c, which demonstrates that cAMP elevation is sufficient and β -arrestin does not play a key role (Sieber et al, 2018). However, the knockdown of β -arrestin2 in fibroblasts from patients with IPF has been shown to attenuate the invasive phenotype, implicating β -arrestins as mediators in the development of pulmonary fibrosis (Lovgren et al, 2011). This highlights the importance of further investigation into the role of β -arrestins in HLFs and IPF.

Another hypothesis for the observed disconnect is that the spatial control of signalling pathway components, rather than the magnitude of responses, may be important in regulating downstream effects. GPCRs are increasingly recognised to signal from intracellular membranes in addition to the plasma membrane. Irannejad and co-workers showed that targeting the β_2 adrenoceptor with isoprenaline promotes receptor and G protein activation in endosomes as well as the plasma membrane (Irannejad et al, 2013), with the endosome-initiated cAMP signal preferentially coupling to downstream transcriptional control (Tsvetanova & von Zastrow, 2014). Compartmentalised cAMP signalling has been demonstrated in primary ASM cells, with stimulation of β_2 adrenoceptors and EP $_2$ receptors resulting in the production of cAMP in distinctly different subcellular locations (Agarwal et al, 2017). Studies into the duration and location of cAMP signalling using HLFs are required to determine the importance for long-term phenotypic responses.

The current chapter has demonstrated that HLFs express a range of G $_s$ -coupled GPCRs and agonists that target some of these GPCRs increase cAMP levels and inhibit profibrotic processes such as HLF proliferation and differentiation, suggesting potential for the treatment of IPF. However, it appears that although cAMP is important in

driving the anti-fibrotic effects, the magnitude of acute global cAMP accumulation does not accurately predict the degree of inhibition of proliferation or differentiation. This suggests additional factors, such as the spatiotemporal control of cAMP, may be important and further research is required to understand this disconnect.

The remaining chapters in this thesis focus on investigating spatiotemporal cAMP signalling associated with three IPR agonists MRE-269, iloprost, and treprostinil. These IPR receptor agonists were selected to use in the following experiments as they demonstrate well the disconnect between cAMP accumulation and inhibition of proliferation. Iloprost and treprostinil were full agonists at generating cAMP and showed little inhibition of proliferation, whereas MRE-269 was a partial agonist at generating cAMP and fully inhibited fibroblast proliferation. Other agonists also demonstrated this disconnect, including the A_{2B} receptor agonist BAY60-6583, which was very partial in generating cAMP however could inhibit proliferation fully. Although it would be interesting to investigate the spatiotemporal properties of cAMP with BAY60-6583, we lack an A_{2B} receptor agonist to compare results to. Ideally, this would be an agonist that is fully efficacious at cAMP accumulation and has little effect on proliferation.

Chapter 4 – Compartmentalisation of cAMP and ERK in human lung fibroblasts

4.1 Introduction

Stimulation of cAMP production has anti-fibrotic effects in HLFs, suggests that activators of this pathway could be novel targets to fibrotic lung diseases such as IPF (Roberts et al, 2018). However, the magnitude of cAMP response is not a good predictor of antifibrotic effects. For example, targeting the IPR with the agonist MRE-269 results in a partial cAMP response that leads to full inhibition of proliferation and differentiation of HLFs. In contrast, targeting the IPR with iloprost or treprostinil results in a full cAMP response that leads to minimal/no inhibition of fibrotic processes (Roberts et al, 2018). This raises the question as to how a cell can discriminate between cAMP signals that are produced by different agonists at the same receptor. One hypothesis is that the spatial and/or temporal control of signalling pathway components, rather than the magnitude of responses, may be important in regulating downstream effects.

The diverse effects of cAMP require complex targeting and regulation of intracellular cAMP pools. Selective activation of cAMP pools can occur when receptors are compartmentalised in specific membrane microdomains. One example are EP₂ receptors, which are excluded from lipid raft fractions of the plasma membrane, and whose activation leads to cAMP production in non-raft regions of the plasma membrane in ASM cells. The activation of a distinct pool of cAMP is thought to be important in driving different physiological outcomes not observed with receptors that activate other pools of cAMP (Agarwal et al, 2017). In addition, the formation of scaffolds by AKAPs bring together proteins, such as receptors, PKA, ACs and PDEs, can create local signalling hubs for strict regulation of the cAMP pathway (Dema et al, 2015). Scaffolds ensure that the anchored enzymes are optimally positioned to receive signals and are placed in close proximity to their substrates, thereby controlling the

specificity, magnitude, and duration of signalling, as well as limiting the diffusion of cAMP in the cell.

GPCRs are increasingly recognised to signal from intracellular membranes in addition to the plasma membrane. Irannejad and co-workers showed that targeting the β_2 adrenoceptor with isoprenaline promoted receptor and G protein activation in endosomes as well as the plasma membrane, and internalised receptors contributed to the cAMP response (Irannejad et al, 2013). Furthermore, the β_1 adrenoceptor has been shown to initiate a cAMP signal from the Golgi apparatus (Irannejad et al, 2017). Golgi signalling was shown to use a pre-existing pool of receptors, rather than receptors delivered from the cell surface, thus requiring ligands to cross the plasma membrane to activate receptors. Hydrophobicity of ligands dictated the method of transport to the Golgi receptor pool, with lipophilic ligands able to passively diffuse across the plasma membrane to access the Golgi, whereas facilitated transmembrane transport is required for more hydrophilic drugs. Furthermore, the ability of β -blockers currently used in the clinic to antagonise the Golgi signal varied. Lipophilic β_1 adrenoceptor antagonist metoprolol blocked dobutamine-stimulated signalling at the plasma membrane and Golgi, whereas the less lipophilic β_1 adrenoceptor antagonist sotalol only blocked dobutamine-stimulated signalling from the plasma membrane (Irannejad et al, 2017). This highlights the need to investigate compartmentalised cAMP in drug discovery.

An increasing amount of evidence shows that the anti-fibrotic effects of the cAMP pathway are driven by negatively impacting MAPK signalling, via inhibition of ERK phosphorylation (Nikam et al, 2011; Stork & Schmitt, 2002). The large number of substrates, and the variety of distinct and even opposing processes that the ERK pathway regulates, raises the question of how signalling specificity is maintained. Not

only is the cAMP pathway tightly regulated, strict regulation of the ERK signalling cascade is also important to control cell outcomes. The ERK1/2 cascade is a signalling pathway activated by a wide variety of extracellular agents that transmit the messages of both GPCRs and RTKs. Accumulating evidence has demonstrated that differences in the duration, magnitude, and subcellular compartmentalisation of ERK activity determines signalling specificity, with the identification of several intracellular proteins, including scaffolding proteins KSR and MP1, that control the duration, localisation, or magnitude of ERK activity (Casar & Crespo, 2016; Ebisuya et al, 2005).

Sustained, but not transient, activation of ERK has been shown to be required for fibroblasts to proliferate (Balmano & Cook, 1999; Dobrowolski et al, 1994), with only sustained ERK activation causing phosphorylation and stabilisation of proteins encoded by immediate early genes, such as *Fos*, *Jun*, and *Myc*, that are required for cell cycle progression (Murphy et al, 2004). ERK1/2 can be localised to either the cytoplasm or the nucleus. In resting cells, ERK1/2 are localised in the cytosol due to their interactions with different anchoring proteins (Berti & Seger, 2017; Rubinfeld et al, 1999). ERK cytoplasmic retention sequences have been identified on MEK itself (Fukuda et al, 1997), PEA-15 which binds ERK1/2 and sequesters ERK in the cytoplasm (Formstecher et al, 2001), and β -arrestin (Ahn et al, 2004). After stimulation of cells, phosphorylation of ERK1/2 at threonine and tyrosine residues occurs, which permits their detachment from the anchoring proteins. This is followed by an additional phosphorylation at threonine and tyrosine residues, which consequently promotes their translocation to the nucleus (Berti & Seger, 2017). Nuclear ERK1/2 is thought to be important mainly for the induction of proliferation, with cytoplasmic sequestration of ERK correlating with senescence in fibroblasts (Brunet et al, 1999).

The aim of this chapter was to investigate if the spatiotemporal control of cAMP following activation of the IPR and/or ERK1/2 is important in regulating cellular activity in primary HLFs. The IPR was chosen because in Chapter 3 a disconnect between cAMP accumulation and inhibition of proliferation was observed with the IPR agonists MRE-269, treprostinil, and iloprost. MRE-269 inhibited HLF proliferation fully whilst generating a partial cAMP response, whereas iloprost and treprostinil were less efficacious at inhibiting proliferation of HLFs even though they were fully efficacious at generating a cAMP response. This disconnect was observed with other receptors, such as the β_2 adrenoceptor, however at this point there is no research on compartmentalised signalling from the IPR, so it would be interesting to establish the role it may or may not have on phenotypic responses. To measure cAMP and ERK spatially we used genetically encoded FRET-based cAMP and ERK biosensors targeted to different subcellular locations. FRET is the transfer of excited-state energy from an excited donor fluorophore to an acceptor, and it is dependent on the correct spectral overlap of the donor and acceptor and their distance from each other. The distance between the donor and acceptor must be sufficiently close for molecular interactions to occur.

The cAMP FRET biosensor Epac2 consists of a cAMP-binding domain (CBD) from Epac (Figure 4:1A). Epac2 is expressed throughout cells and is used to measure cAMP in the cytoplasmic compartment, termed cytoEpac2 (Nikolaev et al, 2004). CFP is fused to the C-terminus of Epac2 CBD which acts as the donor molecule and YFP has been added to the N-terminus and of the Epac2 CBD, acting as the acceptor. The fluorescent spectra shows the overlap between the CFP emission and YFP excitation spectra, making this fluorescent protein pair suitable for FRET experiments (Figure 4:1B). Binding of cAMP to the CBD results in a conformational change that leads to an increased distance between the fluorophores, resulting in a loss of FRET (Figure 4:1C).

N-terminally modifying cytoEpac2 with the 'SH4' motif (GCINSKRKD) of Lyn kinase, which is post-translationally modified with myristate and palmitate, results in a biosensor targeted to the plasma membrane, pmEpac2 (Wachten et al, 2010). For nuclear targeting, a NLS, PKKKRKVEDA, was added to the N-terminus of the cytoEpac2 biosensor, nucEpac2 (DiPilato et al, 2004) (Figure 4:1A).

The FRET-based biosensor of ERK activity, EKAR, can selectively and reversibly report ERK activity in living cells. EKAR consists of a GFP/RFP FRET pair, substrate phosphorylation peptide from Cdc25C containing the consensus MAPK target sequence (PRTP), and the proline-directed WW phospho-binding domain (Figure 4:2A) (Harvey et al, 2008). The fluorescent spectra show the overlap between the GFP emission and RFP excitation spectra, making this fluorescent protein pair suitable for FRET experiments (Figure 4:2B). Upon stimulation, activated ERK phosphorylates the substrate sequence in EKAR, and subsequent binding by the phospho-binding domain results in a conformational change leading to an increase in FRET between the two fluorophores (Figure 4:2C). The EKAR biosensor on its own is restricted to the nucleus (nucEKAR), and addition of a C-terminal nuclear export sequence results in cytoplasmic expression (cytoEKAR).

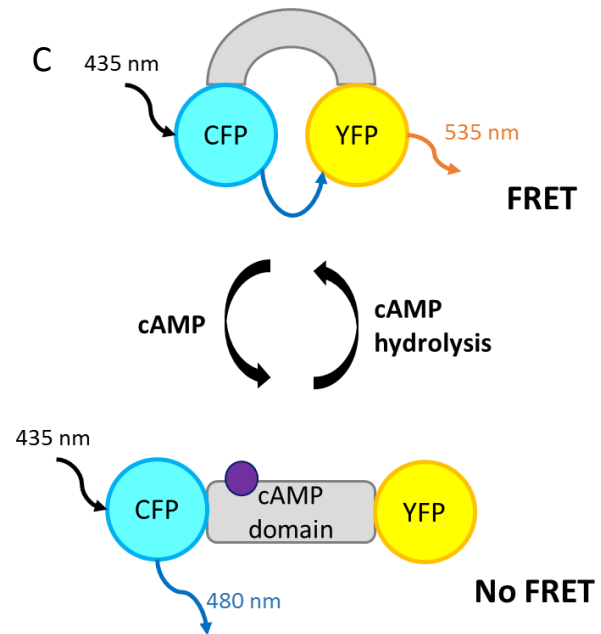
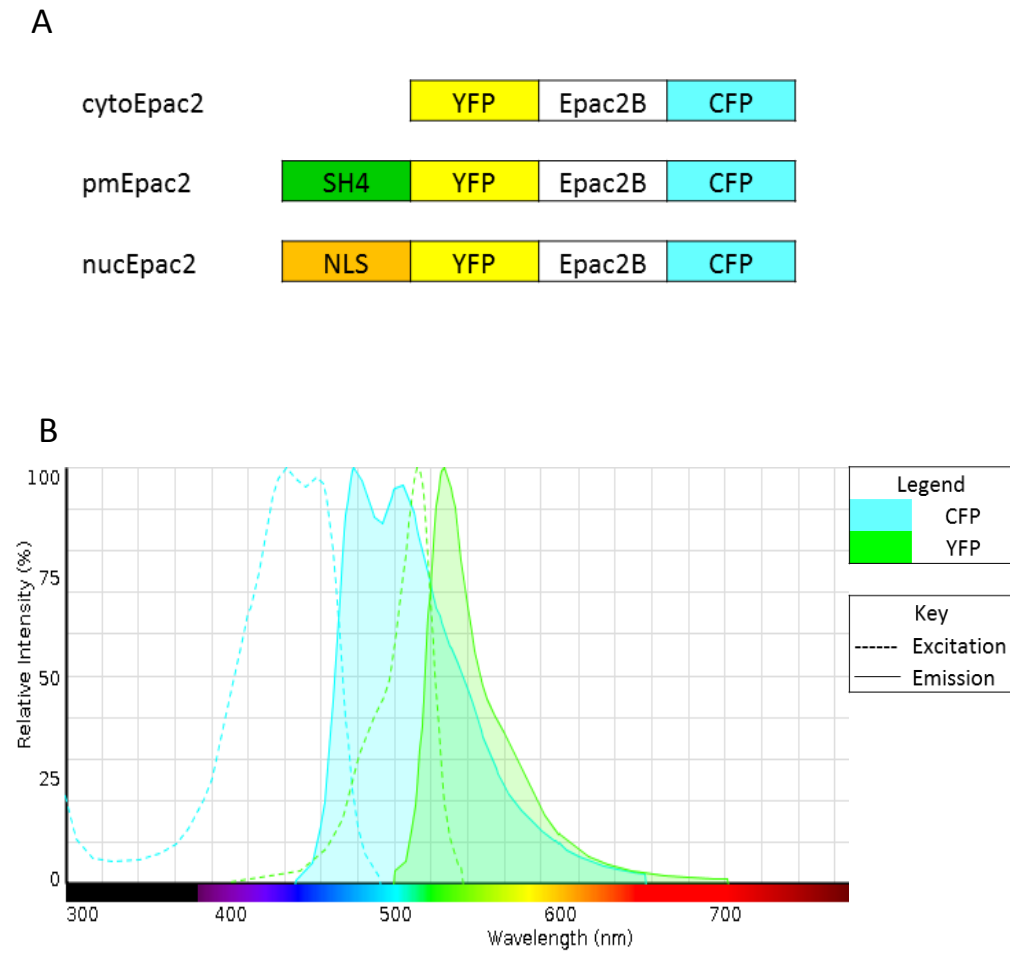


Figure 4:1 - cAMP FRET biosensors

(A) Structure of cAMP FRET biosensors targeted to the cytoplasm, plasma membrane, or nucleus. (B) Fluorescent emission spectra of CFP and YFP fluorophores. (C) Schematic showing intramolecular FRET changes in response to cAMP.

4.2 Results

4.2.1 HLF donor variation in cAMP and inhibition of proliferation when targeting the IP receptor

In Chapter 3 it was observed that cAMP accumulation is not a good predictor of inhibition of proliferation. This disconnect was observed when targeting the IPR, with MRE-269 fully inhibiting proliferation whilst only generating a partial cAMP response and iloprost having little effect on proliferation when generating a full cAMP response (Figure 3:10). To investigate if this disconnect was consistent across HLF donors, cAMP accumulation and inhibition of PDGF-driven proliferation by IPR agonists was measured in a second donor, HLFd.42105.2 (Figure 4:3). MRE-269 generated a partial cAMP response, E_{\max} 36.9 ± 3.01 % of forskolin response, and treprostinil and iloprost were more efficacious at cAMP accumulation with E_{\max} values of 86.6 ± 17.0 % and 76.0 ± 12.7 % of the forskolin response, respectively (Figure 4:3A).

Next, we determined if the IPR ligands could inhibit PDGF-driven HLF proliferation. Treatment with a range of concentrations of serum or PDGF for 24 hours resulted in increased proliferation in a concentration dependent manner, with EC_{50} values for serum and PDGF of 0.33 ± 0.07 % v/v and 2.58 ± 0.15 ng/ml, respectively. The PDGF response was comparable to the serum response, with maximal proliferation of 91.7 ± 5.11 % and 118 ± 1.90 %, respectively (Figure 4:3B). HLFs were then treated with the IPR ligands in the presence of a concentration of PDGF that correlated to near maximal proliferation (3.5 ng/ml; calculated from Figure 4:3B). MRE-269 and treprostinil fully inhibited proliferation, however treprostinil was more potent than MRE-269, with pEC_{50} of 7.45 ± 0.10 and 6.52 ± 0.37 for treprostinil and MRE-269, respectively. Iloprost showed partial inhibition of proliferation with pEC_{50} of 8.65 ± 0.17 (Figure 4:3C).

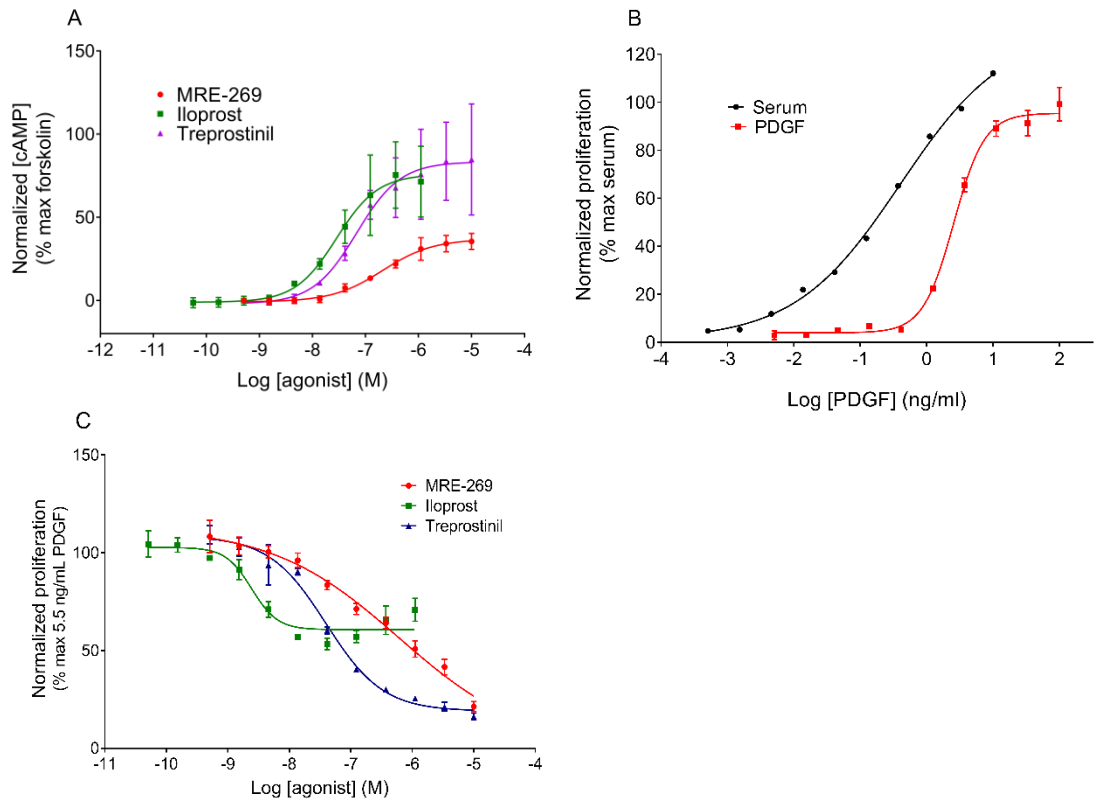


Figure 4:3 - cAMP accumulation and proliferation of HLFd42105.2

(A) Concentration effect curves for cAMP accumulation in HLF after treatment with ligands targeting the IPR. Data for each individual experiment were normalised to maximal cAMP accumulation observed with forskolin (10 μ M) and are expressed as mean \pm SEM for 3 independent experiments. (B) Concentration-dependent increase in HLF proliferation following treatment with a range of concentrations of serum or PDGF for 24 hours, detected using BrdU incorporation. Data were normalised to maximal proliferation observed with 10 % serum and expressed as mean \pm SEM for 3 independent experiments. (C) Concentration effect curves for the inhibition of proliferation of HLFs following treatment with ligands targeting the IPR in the presence of an EC_{80} concentration of PDGF (5.5 ng/ml) for 24 hours. Data for each individual experiment were normalised to the maximal proliferation observed with PDGF (5.5 ng/ml) and are expressed as mean \pm SEM for 4 independent experiments.

The efficacy and potency of IPR ligands to increase cAMP and inhibit PDGF-driven proliferation are summarised in Table 4:1. Overall, there was a disconnect between cAMP accumulation and degree of inhibition of proliferation. MRE-269 fully inhibited proliferation whilst only generating a partial cAMP response, whereas iloprost showed only partial inhibition of proliferation whilst being fully efficacious at cAMP accumulation.

4.2.2 Inhibition of ERK phosphorylation by IP receptor ligands

Fibroblast proliferation is dependent on ERK phosphorylation (Figure 3:1), therefore next we wanted to determine if the disconnect between cAMP accumulation and inhibition of proliferation could be observed at the level of ERK. ERK1/2 phosphorylation was monitored using a commonly used, high throughput, homogenous sandwich immunoassay that allows quantification of ERK phosphorylation in cellular lysates.

Initially a time course of ERK1/2 phosphorylation was assessed in HLFs after treatment with a high concentration of PDGF (30 ng/ml) or 200 nM PDBu, a PKC activator which increases ERK phosphorylation independent of growth factors and receptor activation. Peak ERK1/2 phosphorylation was observed within 10 minutes after stimulation with PDBu and was sustained for up to 30 minutes. Similarly, peak ERK1/2 phosphorylation was observed at 167.8 ± 14.0 % of the PDBu response after 10 minutes exposure of HLFs with PDGF, after which ERK1/2 phosphorylation levels slightly declined to 113.8 ± 10.6 % (Figure 4:4). A PDGF stimulation period of 20 minutes for HLFs was chosen for further experiments as this time point correlates to high levels of PDGF-driven ERK1/2 phosphorylation and a plateaued PDBu ERK1/2 phosphorylation response.

Table 4:1 - Potency and intrinsic activity of IP receptor ligands for cAMP accumulation and inhibition of HLF proliferation

Agonist	cAMP		Inhibition of PDGF-mediated proliferation	
	pEC ₅₀	E _{max} (% max)	pEC ₅₀	E _{max} (% max)
MRE-269	6.67 ± 0.01	36.9 ± 3.01	6.52 ± 0.37	108 ± 17.0
Iloprost	7.54 ± 0.06	76.0 ± 12.7	8.65 ± 0.17	43.7 ± 4.09
Treprostinil	7.11 ± 0.14	86.6 ± 17.0	7.46 ± 0.10	96.1 ± 11.1

Intrinsic activity for cAMP accumulation was calculated as a percentage of the response observed with forskolin (10 µM). Data are expressed as mean ± SEM for 4 independent experiments. Intrinsic activity for inhibition of proliferation measured using BrdU incorporation was calculated as a percentage of maximal proliferation observed with PDGF. Data are expressed as mean ± SEM for 3 independent experiments.

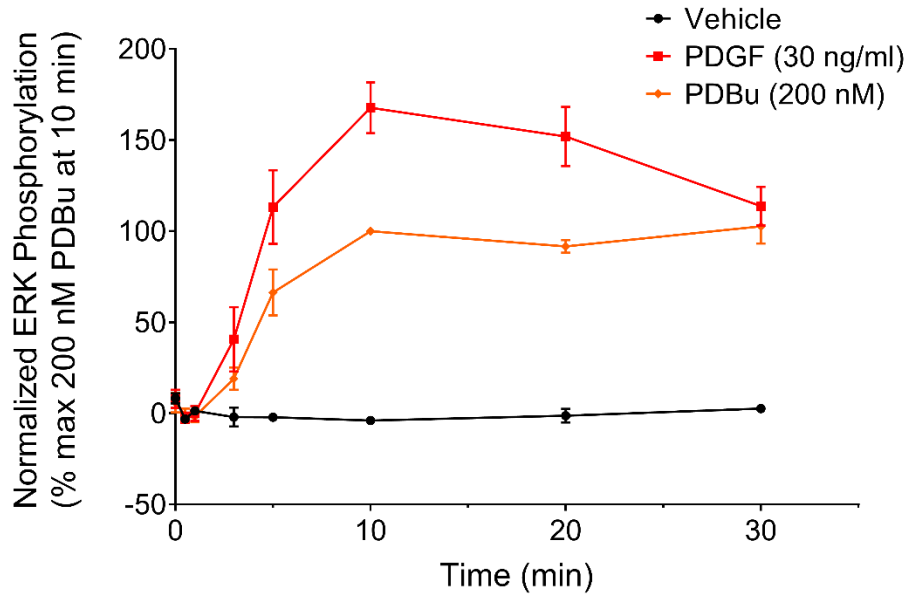


Figure 4:4 - Time course of ERK1/2 phosphorylation in HLFs

Time course of ERK1/2 phosphorylation in response to PDGF (30 ng/ml) or PDBu (200 nM) in HLFs. For each individual experiment, data were normalised to amount of ERK1/2 phosphorylation observed with 200 nM PDBu at 10 minutes. Data are expressed as mean \pm SEM for at least 3 independent experiments.

Next, HLFs were stimulated with a range of concentrations of PDGF and ERK1/2 phosphorylation was measured after 20 minutes (Figure 4:5A). PDGF elicited an increase in ERK1/2 phosphorylation in a concentration-dependent manner, with pEC_{50} value of 2.05 ± 0.12 ng/ml. To investigate the ability of IPR ligands to inhibit PDGF-driven ERK1/2 phosphorylation, HLFs were pre-treated with MRE-269, iloprost, or treprostinil for 30 minutes and then stimulated with 5.2 ng/ml of PDGF – an EC_{80} concentration calculated from Figure 4:5A. All ligands inhibited PDGF-driven ERK phosphorylation, and there was no significant differences in the efficacies and potencies between compounds (Figure 4:5B; Table 4:2). This indicates that the disconnect between cAMP accumulation and inhibition of proliferation observed with IPR agonists may not be due to differences in the ability of the ligands to inhibit ERK1/2 phosphorylation, and therefore it must be driven by another factor. Whether the inhibition of ERK occurs in the same cellular location for all ligands is one factor that could drive efficacy of the inhibition of phenotypic responses.

4.2.3 Compartmentalised cAMP signalling

One hypothesis for the ability of ligands to generate a different functional response at the same receptor is that the spatial control of signalling pathway components, rather than the magnitude of responses, may be important in regulating downstream effects. The majority of conventional biochemical tools for measuring cAMP require cell disruption and therefore can measure only the bulk of cAMP levels in cellular populations. In addition, they also have no spatial resolution resulting in the inability to obtain information of cAMP spatial distribution at subcellular levels.

To monitor cAMP with high spatial resolution, a range of genetically encoded FRET-based biosensors have been developed that can be targeted to distinct intracellular

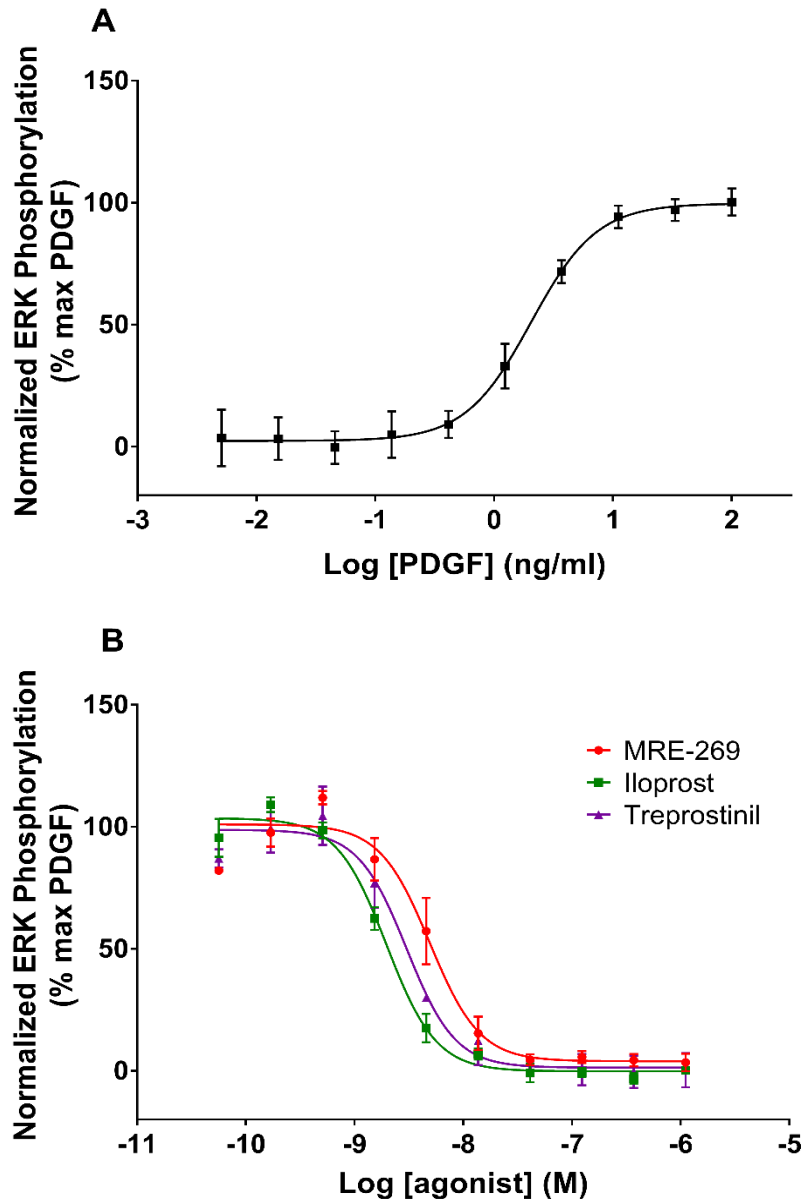


Figure 4:5 - Population ERK response in HLFs

(A) Concentration-dependent increase in ERK phosphorylation in HLFs following treatment with PDGF for 20 minutes. Data for each individual experiment were normalised to maximal ERK phosphorylation observed with 100 ng/ml PDGF. (B) Concentration effect curves for the inhibition of PDGF-driven ERK phosphorylation in HLFs following exposure to IPR agonists, in the presence of an EC_{80} concentration of PDGF (5.2 ng/ml) for 20 minutes. Data for each individual experiment were normalised to maximal ERK phosphorylation observed with 5.2 ng/ml PDGF.

Data sets are expressed as mean \pm SEM for 3 independent experiments.

Table 4:2 - Potency and intrinsic activity of inhibition of ERK phosphorylation

	pIC_{50}	% inhibition
MRE-269	8.34 ± 0.11	97.8 ± 1.63
Iloprost	8.70 ± 0.06	105 ± 5.84
Treprostinil	8.61 ± 0.12	99.4 ± 5.63

Intrinsic activity for the inhibition of ERK phosphorylation was calculated as a percentage of the maximal PDGF (5.2 ng/ml) response. Data are expressed as mean \pm SEM for 3 independent experiments.

domains to allow the monitoring of cAMP in living cells. In order to monitor changes in cAMP levels associated with specific subcellular locations in HLFs, we used a cAMP FRET biosensor targeted to different intracellular locations. HLFs were transiently transfected with Epac2-based biosensors targeted to the plasma membrane (pmEpac2), cytoplasm (cytoEpac2), or nucleus (nucEpac2) as described in Method Section 2.9.

We investigated the ability of IPR agonists to increase cAMP at the plasma membrane over 30 minutes. Stimulation of the IPR with EC₅₀ concentrations of MRE-269 (200 nM), iloprost (25 nM), or treprostinil (64 nM) (calculated from Figure 4:3A) in HLFs expressing pmEpac2, resulted in an immediate increase in cAMP which was sustained up to 30 minutes (Figure 4:6A). Calculating the area under the curve (AUC) of the cAMP response for the EC₅₀ concentrations and a high concentration of agonist (iloprost 300 nM, MRE-269 1 µM, and treprostinil 1 µM), showed a statistically significant increase in cAMP levels compared to vehicle that were concentration dependent (Figure 4:6B). Representative pseudocolour images before and after stimulation of cAMP production by exposure to IPR agonists at 5 and 20 minutes, followed by exposure to positive control (10 µM forskolin, 100 µM IBMX) depict changes in CFP/YFP fluorescence intensity ratio (Figure 4:7).

Sustained cAMP signalling up to 30 minutes was also observed in the cytoplasm upon stimulation of the IPR with MRE-269 (200 nM), iloprost (25 nM), or treprostinil (64 nM) (Figure 4:8A). Calculating the AUC of the cAMP response for the EC₅₀ concentration and high concentration of agonists (iloprost 300 nM, MRE-269 1 µM, and treprostinil 1 µM) showed a statistically significant increase in cAMP levels compared to vehicle (Figure 4:8B). Although the cAMP response was concentration dependent for iloprost and treprostinil, 1 µM MRE-269 resulted in the same magnitude of cAMP as 200 nM

MRE-269, which could indicate MRE-269 has a higher potency when using cytoplasm-targeted FRET biosensor in comparison to global measurements of cAMP. Representative pseudocolour images before and after stimulation of cAMP production by exposure to IPR agonists at 5 and 20 minutes, followed by exposure to positive control (10 μ M forskolin, 100 μ M IBMX) depict changes in CFP/YFP fluorescence intensity ratio (Figure 4:9).

Targeting the IPR of HLFs expressing nucEpac2 showed MRE-269 (200 nM), iloprost (25 nM), or treprostinil (64 nM) increased cAMP in the nucleus (Figure 4:10A). MRE-269 and treprostinil cAMP responses were sustained for 30 minutes, whereas iloprost produced a transient cAMP response, with cAMP returning to baseline levels within 30 minutes. Calculating the AUC of these responses, along with responses of a high concentration of agonists, showed a statistically significant increase in cAMP levels compared to vehicle (Figure 4:10B). High concentrations of iloprost (300 nM) resulted in a larger cAMP response in comparison to the EC₅₀ response, however, the magnitude of cAMP response was similar between 64 nM treprostinil and 1 μ M treprostinil, and 200 nM MRE-269 and 1 μ M MRE-269. This could indicate treprostinil and MRE-269 have higher potencies in the nucleus. Representative pseudocolour images before and after stimulation of cAMP production by exposure to IPR agonists at 6 and 20 minutes, followed by exposure to positive control (10 μ M forskolin, 100 μ M IBMX) depict change in CFP/YFP fluorescence intensity ratio (Figure 4:11).

Overall, all IPR agonists were able to increase cAMP in all locations investigated (Table 4:3). cAMP signalling at the plasma membrane and in the cytosol was sustained up to 30 minutes for all ligands. In contrast, signalling in the nucleus was transient with iloprost, and sustained for MRE-269 and treprostinil.

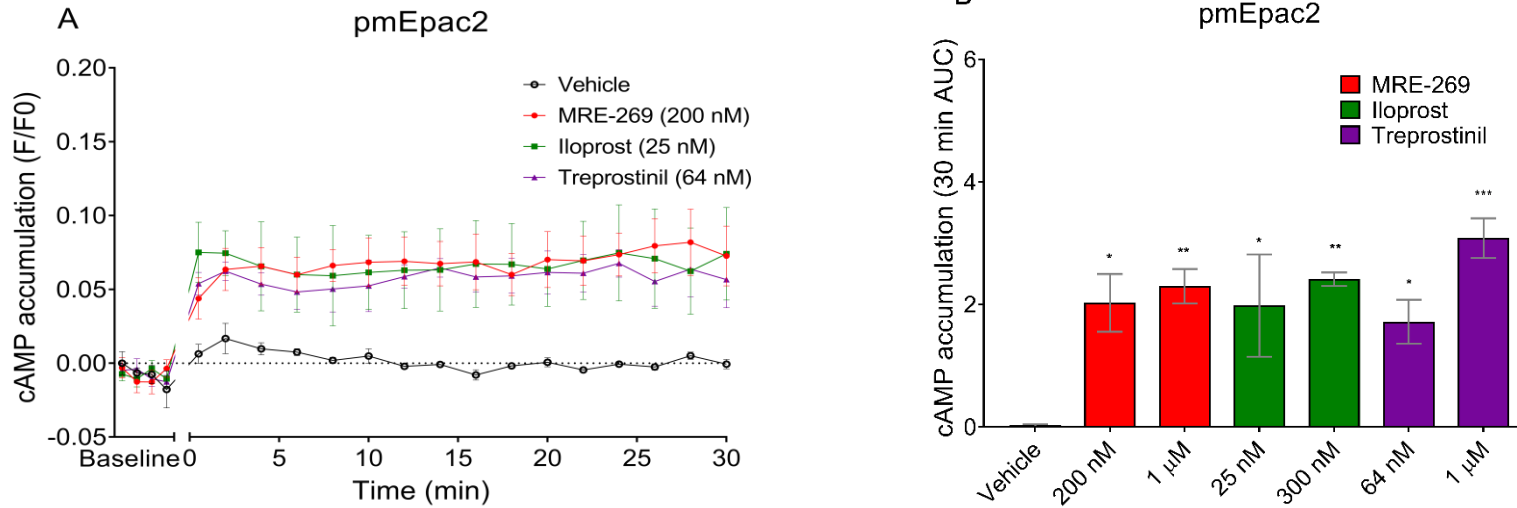


Figure 4:6 - Plasma membrane cAMP signalling

(A) Time course of cAMP accumulation at the plasma membrane upon stimulation of IPR with agonists MRE-269, iloprost, or treprostinil, measured by FRET biosensor pmEpac2 in HLFs. Data are expressed as change in CFP/YFP ratio relative to the donor intensity and baseline read for each cell, and baseline corrected to the vehicle response. (B) Corresponding AUC for plasma membrane cAMP response to IPR ligands. Data are expressed as mean \pm SEM for 3 independent experiments, with at least 36 individual cells per condition in each individual *n*. * p <0.05, ** p <0.01, *** p <0.001 versus vehicle control. Data were analysed by one-way ANOVA with Dunnett's multiple comparison test. AUC, area under the curve.

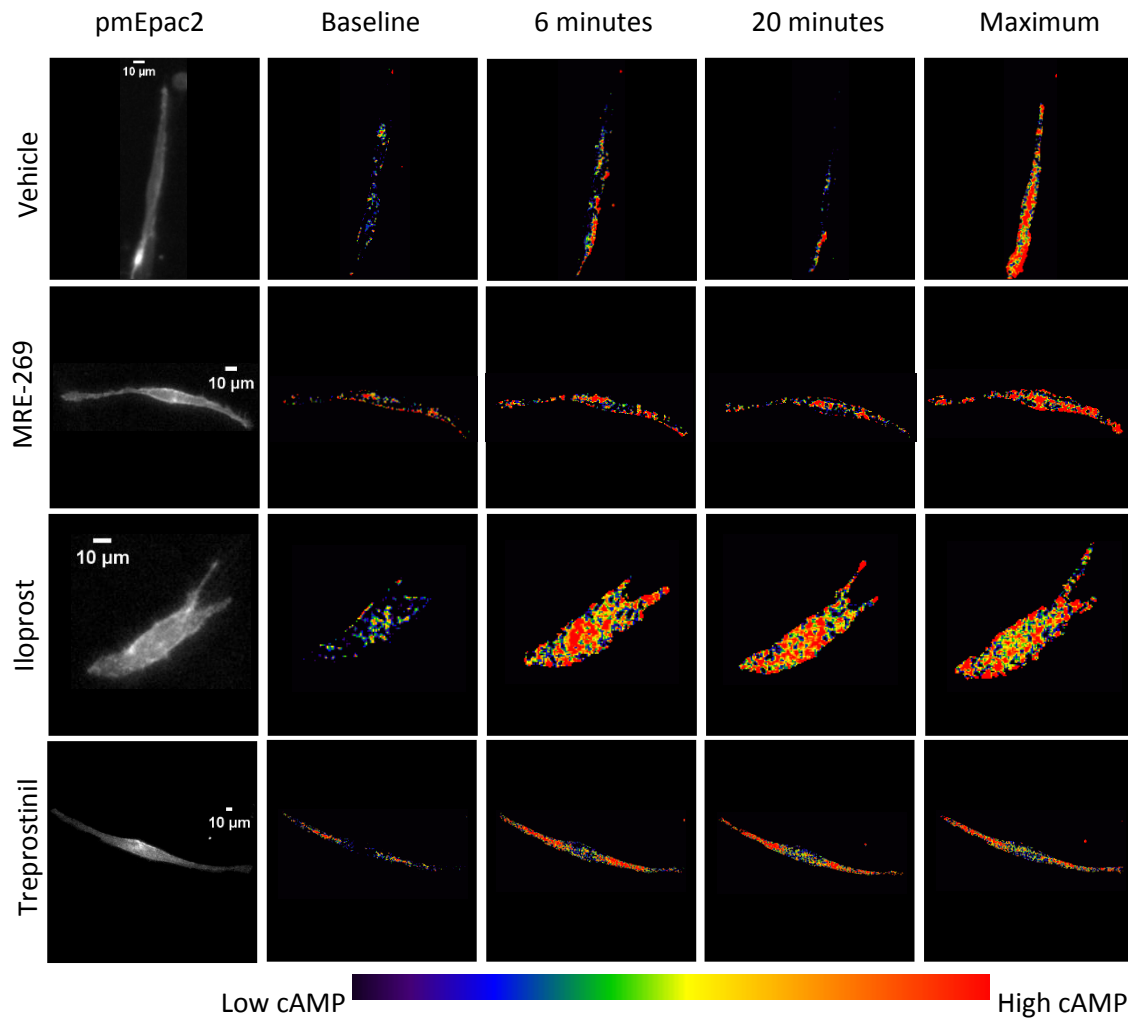


Figure 4:7 - Representative ratiometric images and biosensor localisation for pmEpac2

Widefield images show the localisation of pmEpac2 sensor to the plasma membrane. HLFs were transiently transfected with pmEpac2 and stimulated with either vehicle, MRE-269 (200 nM), iloprost (25 nM), or treprostinil (64 nM). Maximum is the response to positive control forskolin (10 μ M) plus IBMX (100 μ M).

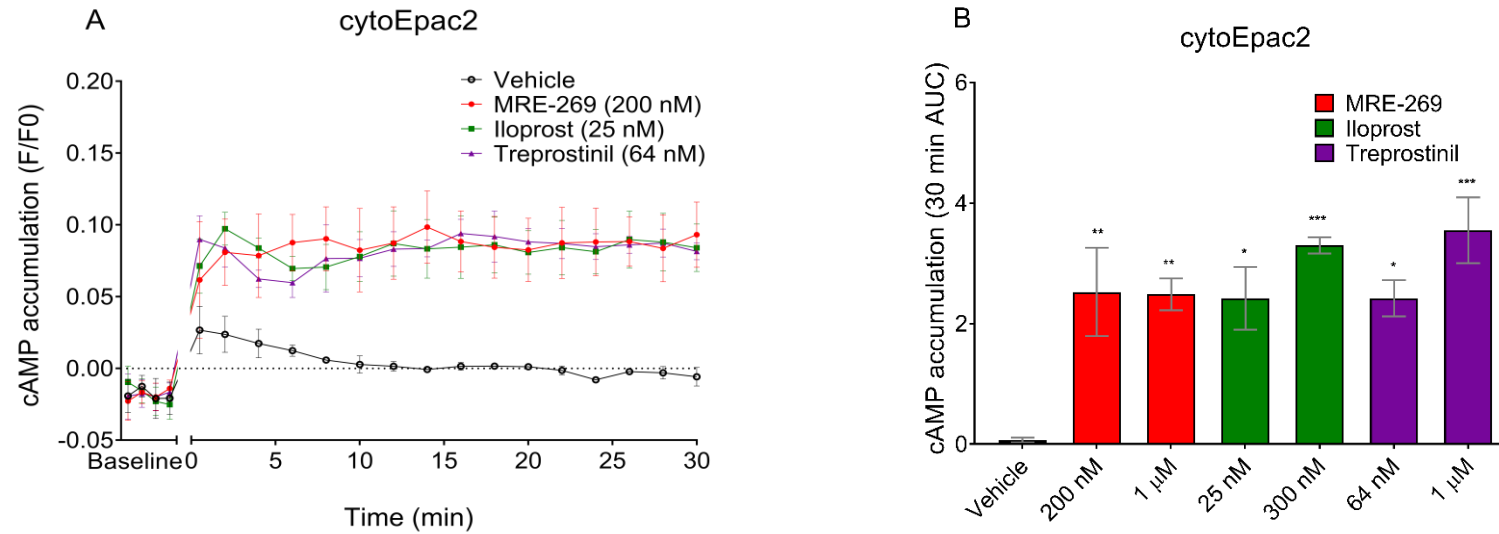


Figure 4:8 - Cytoplasm cAMP signalling in HLFs

(A) Time course of cAMP accumulation in the cytoplasm upon stimulation of IPR with agonists MRE-269, iloprost, or treprostinil, measured by FRET biosensor cytoEpac2 in HLFs. Data are expressed as change in CFP/YFP ratio relative to the donor intensity and baseline read for each cell, and baseline corrected to the vehicle response. (B) Corresponding AUC for cytoplasm cAMP response to IPR ligands. Data are expressed as mean \pm SEM for 3 independent experiments, with at least 18 individual cells per condition in each individual *n*. * $p < 0.05$, ** $p < 0.01$, *** $p < 0.001$ versus vehicle control. Data were analysed by one-way ANOVA with Dunnett's multiple comparison test. AUC, area under the curve.

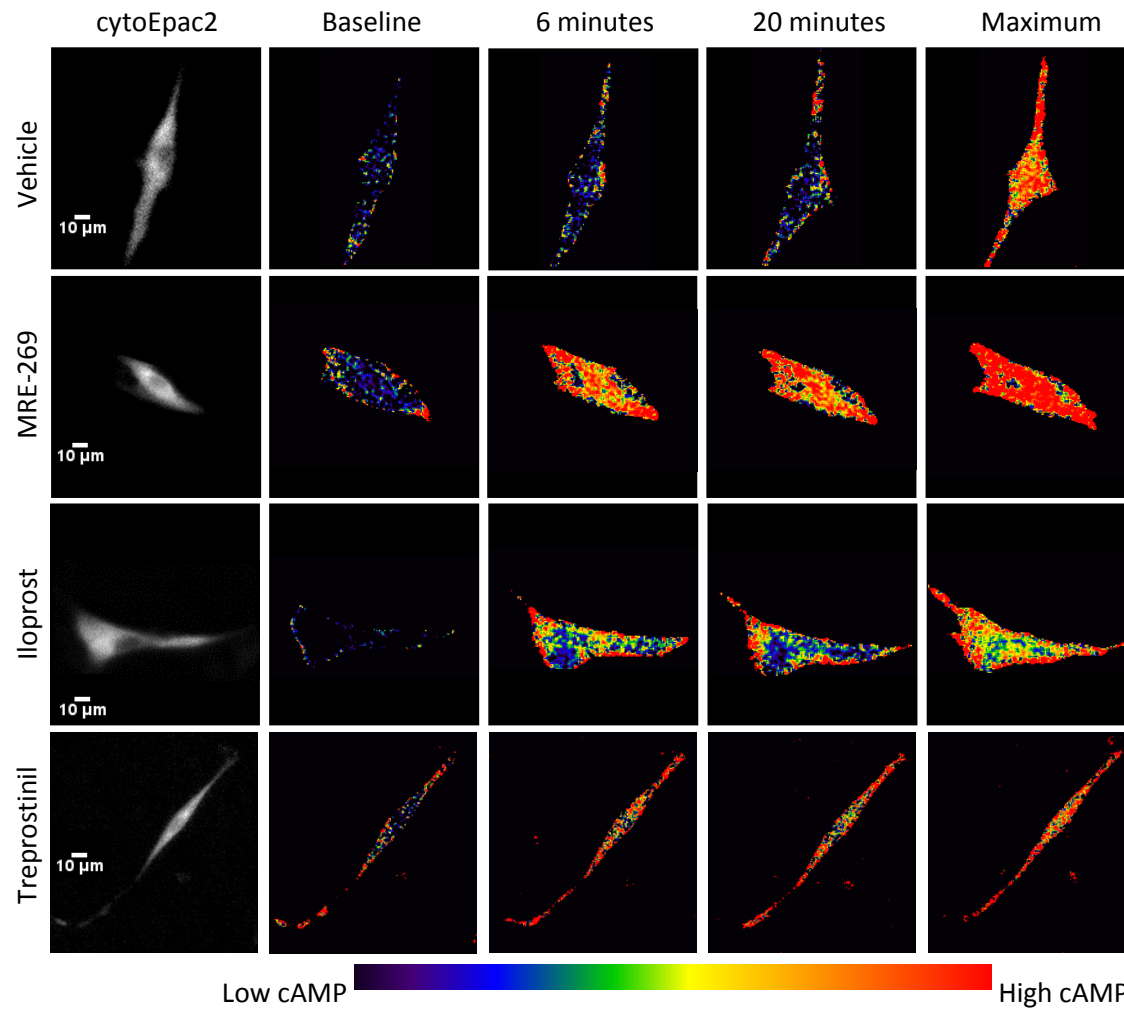


Figure 4:9 - Representative ratiometric images and biosensor localisation for cytoEpac2

Widefield images show the localisation of cytoEpac2 sensor to the cytoplasm. HLFs were transiently transfected with cytoEpac2 and stimulated with either vehicle, MRE-269 (200 nM), iloprost (25 nM), or treprostinil (64 nM). Maximum is the response to positive control forskolin (10 μ M) plus IBMX (100 μ M).

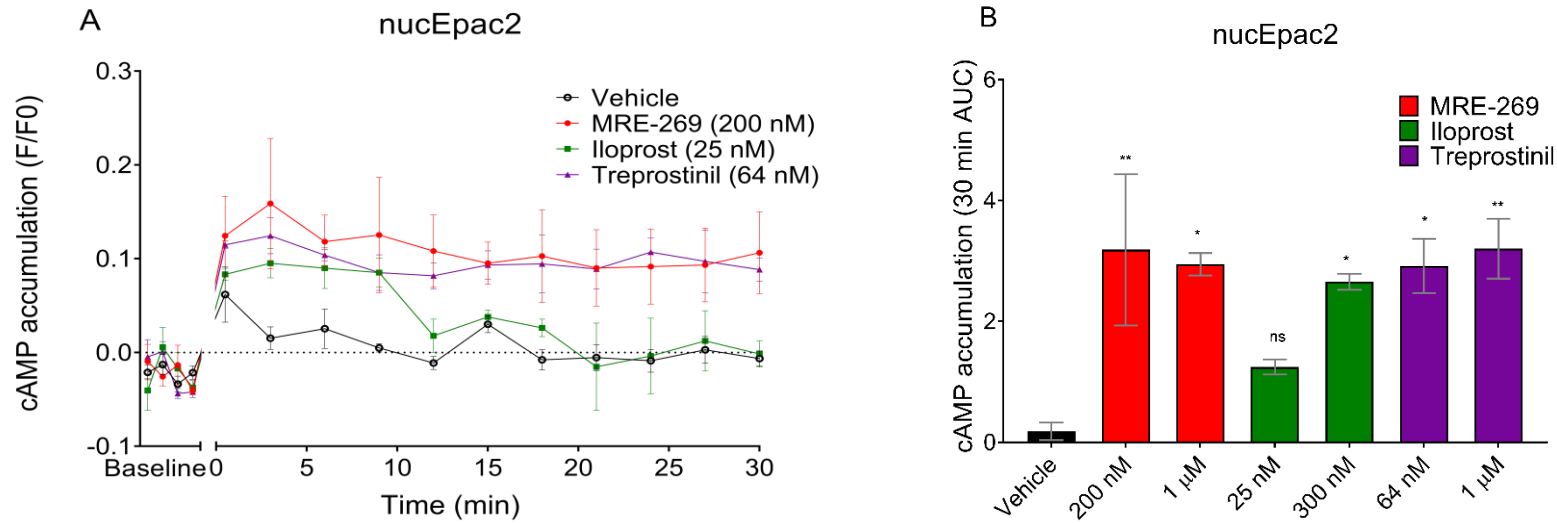


Figure 4:10 - Nuclear cAMP accumulation in HLFs

(A) Time course of cAMP accumulation in the nucleus upon stimulation of IPR with agonists MRE-269, iloprost, or treprostinil, measured by FRET biosensor nucEpac2 in HLFs. Data are expressed as change in CFP/YFP ratio relative to the donor intensity and baseline read for each cell, and baseline corrected to the vehicle response. (B) Corresponding AUC for nuclear cAMP response to IPR ligands. Data are expressed as mean \pm SEM for 3 independent experiments, with at least 4 individual cells per condition in each individual n . * p <0.05, ** p <0.01 versus vehicle control. Data were analysed by one-way ANOVA with Dunnett's multiple comparison test. AUC, area under the curve; ns, not significant.

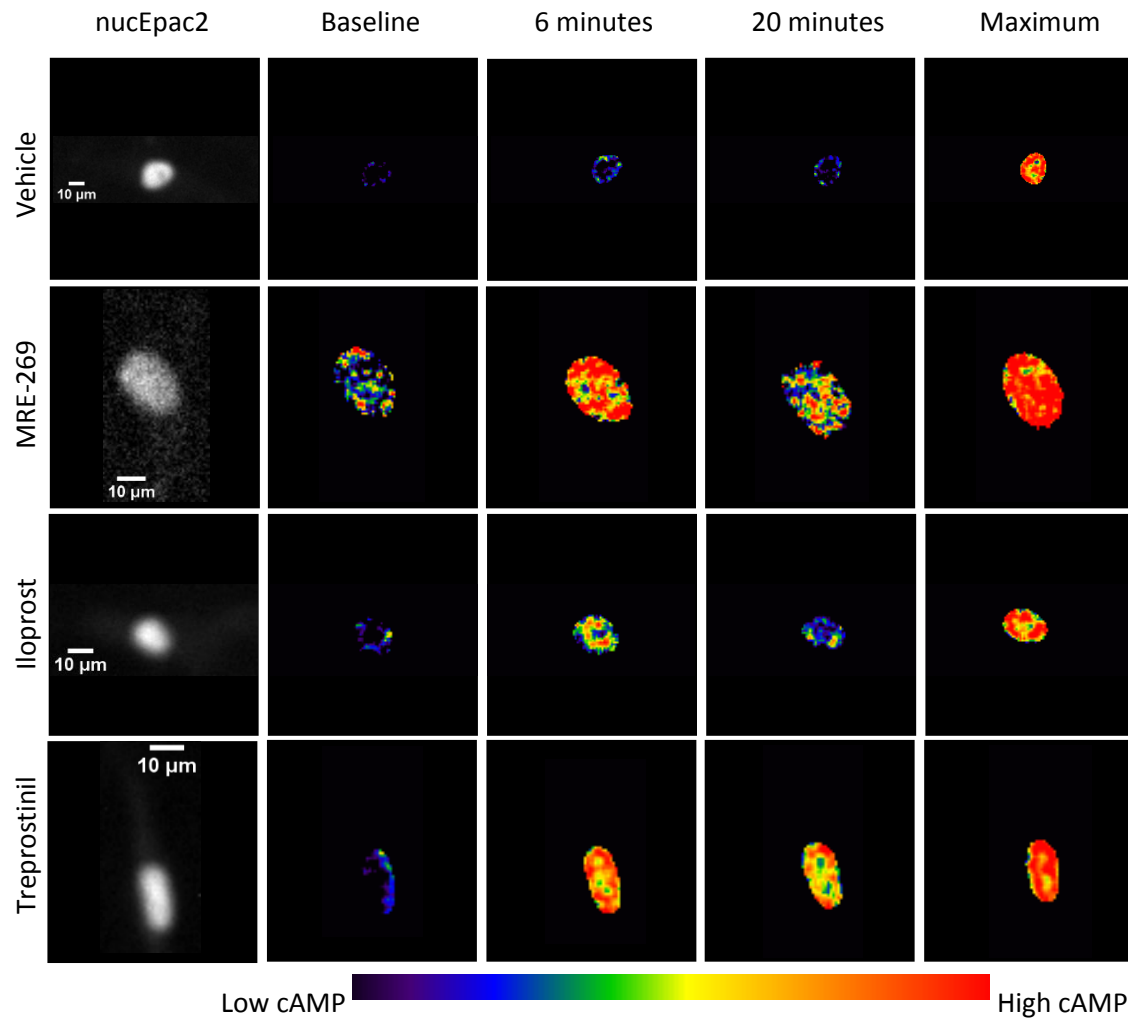


Figure 4:11 - Representative ratiometric images and biosensor localisation for nucEpac2

Widefield images show the localisation of nucEpac2 sensor to the nucleus. HLFs were transiently transfected with nucEpac2 and stimulated with either vehicle, MRE-269 (200 nM), iloprost (25 nM), or treprostinil (64 nM). Maximum is the response to positive control forskolin (10 μ M) plus IBMX (100 μ M).

Table 4:3 - cAMP response in subcellular locations in HLFs

	Plasma Membrane	Cytoplasm	Nucleus
MRE-269 (1 μ M)	2.30 \pm 0.279	2.49 \pm 0.263	2.95 \pm 0.182
MRE-269 (200 nM)	2.03 \pm 0.471	2.53 \pm 0.731	3.18 \pm 1.25
Iloprost (300 nM)	2.41 \pm 0.111	3.30 \pm 0.133	2.66 \pm 0.135
Iloprost (25 nM)	1.98 \pm 0.833	2.42 \pm 0.520	1.25 \pm 0.123
Treprostinil (1 μ M)	3.09 \pm 0.324	3.55 \pm 0.546	3.20 \pm 0.495
Treprostinil (64 nM)	1.72 \pm 0.359	2.42 \pm 0.301	2.92 \pm 0.452

Data are expressed as AUC for cAMP response in HLFs at the plasma membrane, in the cytoplasm, and in the nucleus. Data are expressed as mean \pm SEM for at least 3 independent experiments.

4.2.4 Compartmentalised ERK signalling

Spatiotemporal control of ERK pathway components has also been described, with ERK1/2 being localised to either the cytoplasm or the nucleus. We have shown that IPR agonists block PDGF-driven ERK1/2 phosphorylation with similar efficacy and potency (Figure 4:5), however this was measured using a method that detects global ERK1/2 phosphorylation levels from a population of cells with no spatial resolution. Genetically encoded FRET biosensors have been developed that can be targeted to different subcellular locations to measure ERK activity with higher spatial resolution. Compartmentalised ERK activity was investigated using HLFs transiently transfected with ERK FRET biosensors targeted to the cytoplasm (cytoEKAR) and the nucleus (nucEKAR).

4.2.4.1 Cytoplasmic ERK signalling

In HLFs, PDGF drives proliferation through activation of the MAPK/ERK pathway which results in phosphorylation of ERK. The ability of PDGF to drive ERK activity in the cytoplasm was investigated by transiently transfecting HLFs with cytoEKAR. HLFs were treated with a range of concentrations of PDGF and ERK activity was measured over time (Figure 4:12A). PDGF triggered a small transient concentration-dependent increase in ERK activity in the cytoplasm that peaked within 10 minutes. Plotting a concentration response curve of the AUC of the PDGF response in the cytoplasm, showed PDGF had an EC_{50} of 0.38 ± 0.09 ng/ml and E_{max} of 2.47 ± 0.35 (Figure 4:12B).

To investigate the efficacy of IPR agonists to inhibit PDGF-driven ERK activity in the cytoplasm, HLFs transfected with cytoEKAR were pre-treated for 30 minutes with a range of concentrations of agonist and then stimulated with a concentration of PDGF resulting in near maximal ERK activation (10 ng/ml) and ERK activity was measured over 60 minutes. Treprostinil (1 μ M) and iloprost (1 μ M) inhibited PDGF-driven ERK

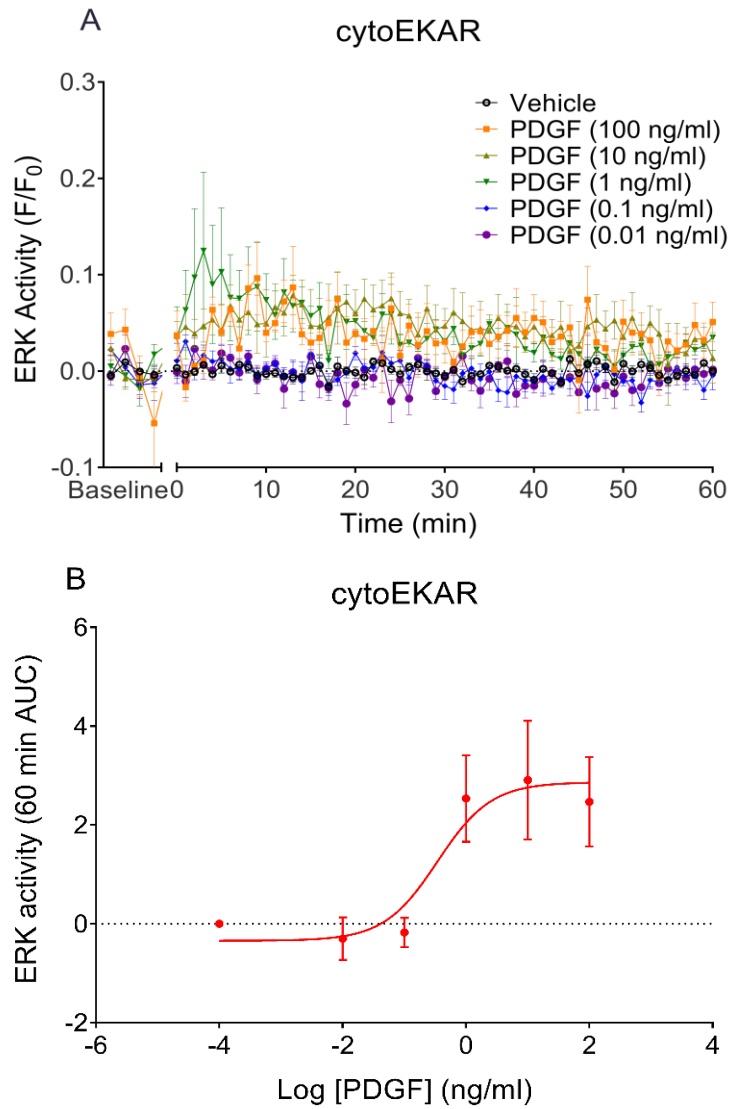


Figure 4:12 - Cytoplasm ERK activity in HLFs

PDGF-driven cytoplasmic ERK activity in HLFs was measured by transiently transfecting cytoEKAR FRET biosensor. (A) Time course of ERK activity in the cytoplasm of HLFs upon stimulation with a range of concentrations of PDGF for 60 minutes. Data are expressed as change in GFP/RFP ratio relative to the donor intensity and baseline read for each cell, and baseline corrected to the vehicle response. (B) Corresponding concentration response curve of PDGF-driven cytoplasmic ERK activity calculated using AUC. Data are expressed as mean \pm SEM for 4 independent experiments, with at least 3 individual cells per condition in each individual *n*. AUC, area under the curve.

activity to basal levels in the cytoplasm over a time course of 60 minutes (Figure 4:13A; Figure 4:13B). MRE-269 (1 μ M) also inhibited PDGF-driven cytoplasmic ERK activity over a time course of 60 minutes, however inhibition of ERK activity was also observed with a nanomolar concentration of MRE-269 (1 nM) (Figure 4:13:C). Corresponding concentration response curves calculated using the AUC of time courses showed MRE-269 inhibition of PDGF-driven cytoplasmic ERK activity was “bell-shaped”, with inhibition at 1 μ M and 1 nM MRE-269. In contrast, treprostinil and iloprost inhibited PDGF-driven cytoplasmic ERK activity in a concentration dependent manner (Figure 4:13D).

Representative pseudocolour images showed inhibition of PDGF-driven cytoplasmic ERK activity at 30 minutes for all IPR agonists at 1 μ M concentrations (Figure 4:14). Addition of positive control PDBu (200 nM) showed that although PDGF-driven cytoplasmic ERK activity was inhibited by IPR agonists, ERK activity could still be increased using the PKC activator.

4.2.4.2 Nuclear ERK signalling

Next, we wanted to examine ERK activity in the nucleus of HLFs. HLFs were transiently transfected with nucEKAR and stimulated with a range of concentrations of PDGF. PDGF was observed to drive a concentration dependent increase in nuclear ERK activity which was sustained for 60 minutes (Figure 4:15A). The corresponding concentration response curve, using the AUC calculated from the time course, showed PDGF had EC_{50} of 1.53 ± 0.20 ng/ml and E_{max} of 6.91 ± 0.67 (Figure 4:15B).

To investigate the efficacy of IPR agonists for the inhibition of PDGF-driven ERK activity in the nucleus, HLFs transfected with nucEKAR were pre-treated for 30 minutes with a range of concentrations of agonists and then stimulated with a near maximal concentration of PDGF (10 ng/ml) over a time period of 60 period. High concentrations

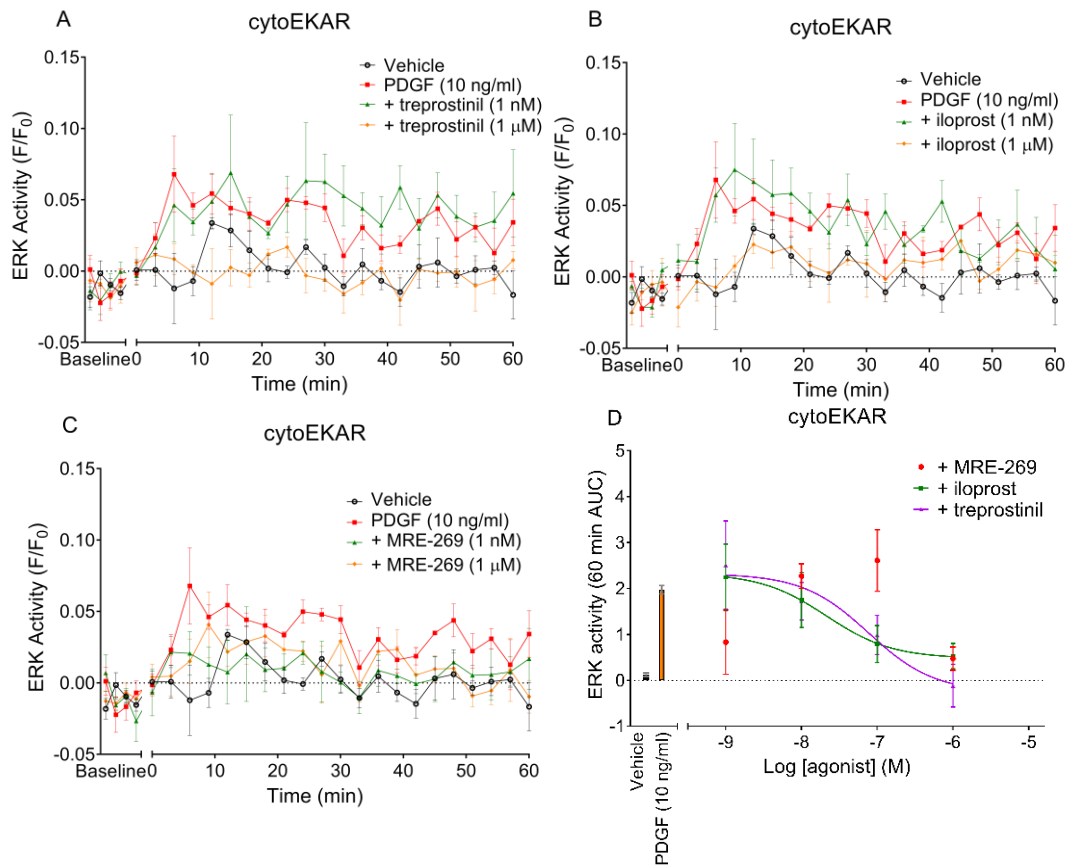


Figure 4:13 - IP receptor agonist inhibition of cytoplasm ERK activity

Inhibition of PDGF-driven cytoplasmic ERK activity by IPR agonists treprostinil (A), iloprost (B), and MRE-269 (C) measured by FRET biosensor cytoEKAR transiently transfected in HLFs. Data are expressed as change in GFP/RFP ratio relative to the donor intensity and baseline read for each cell, and baseline corrected to the vehicle response. (D) Corresponding concentration response curves calculated using AUC for inhibition of cytoplasm ERK activity by IPR agonists. Data are expressed as mean \pm SEM for 4 independent experiments, with at least 14 individual cells per condition in each individual *n*. AUC, area under the curve.

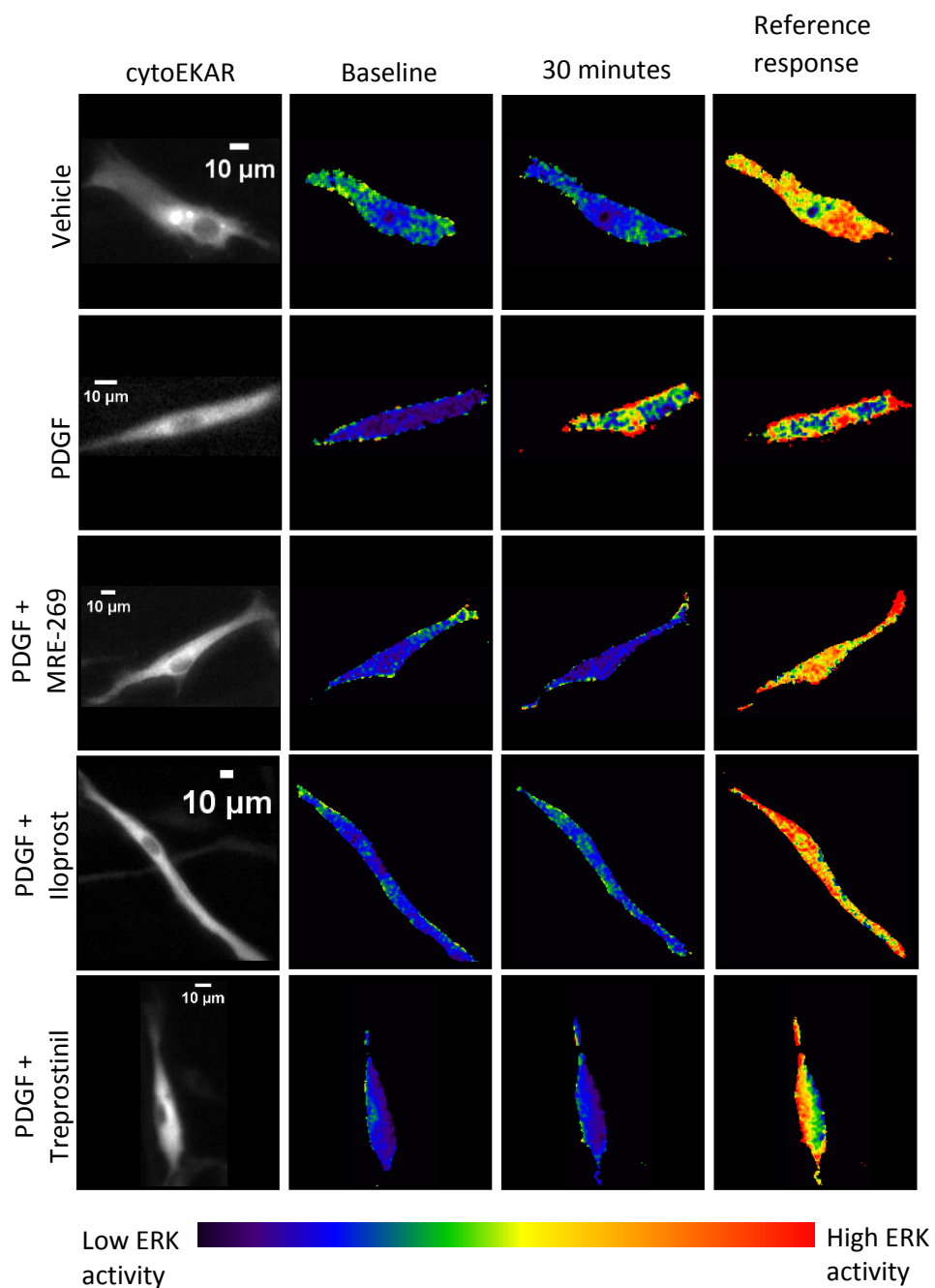


Figure 4:14 - Representative ratiometric images and biosensor localisation for cytoEKAR

Widefield images show the localisation of cytoEKAR sensor to the cytoplasm. HLFs were transiently transfected with cytoEKAR and stimulated with either vehicle or PDGF (10 ng/ml). Inhibition of the PDGF was investigated following treatment with IPR agonists, MRE-269 (1 μM), iloprost (1 μM), or treprostinil (1 μM). Reference response is the response to positive control PDBu (200 nM).

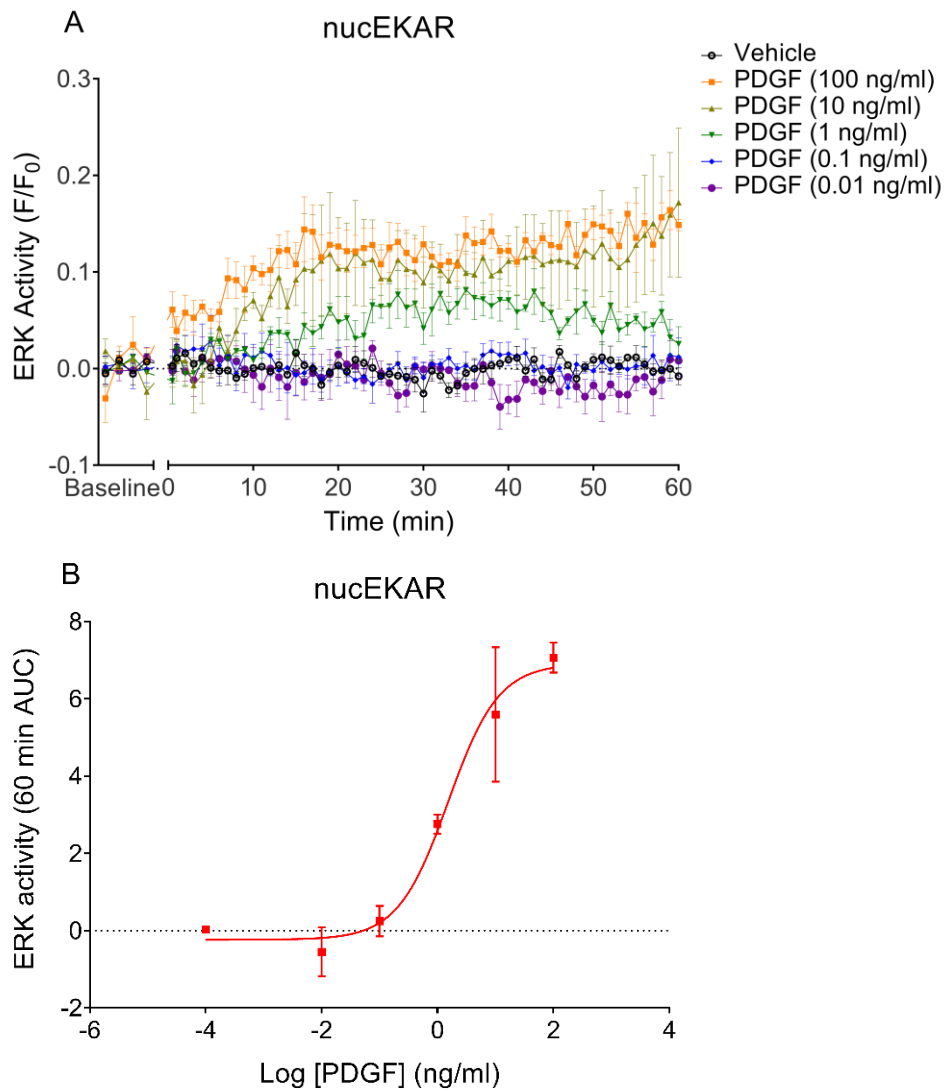


Figure 4:15 - Nuclear ERK activity in HLFs

PDGF-driven nuclear ERK activity in HLFs was measured by transiently transfecting nucEKAR FRET biosensor. (A) Time course of ERK activity in the nucleus of HLFs upon stimulation with a range of concentrations of PDGF for 60 minutes. Data are expressed as change in GFP/RFP ratio relative to the donor intensity and baseline read for each cell, and baseline corrected to the vehicle response. (B) Corresponding concentration response curve of PDGF-driven nuclear ERK activity calculated using AUC. Data are expressed as mean \pm SEM for 4 independent experiments, with at least 4 individual cells per condition in each individual n . AUC, area under the curve.

of treprostinil (1 μ M) and MRE-269 (1 μ M) inhibited PDGF-driven ERK activity (Figure 4:16A and Figure 4:16C). However, no inhibition of ERK activity was detected with iloprost (1 μ M) (Figure 4:16B). Corresponding concentration response curves calculated from the AUC of the time courses showed MRE-269 inhibited PDGF-driven nuclear ERK activity with a pIC_{50} of 6.51 ± 0.73 (Figure 4:16D). Potency values could not be calculated for treprostinil due to an incomplete curve, however it can be observed that treprostinil has lower potency in comparison to MRE-269 for inhibiting PDGF-driven nuclear ERK activity (Figure 4:16D). Furthermore, in agreement with observations from the time course data, no inhibition of PDGF-driven nuclear ERK activity was observed for iloprost (Figure 4:16D).

Representative pseudocolour images showed inhibition of PDGF-driven nuclear ERK activity at 30 minutes for treprostinil and MRE-269 at 1 μ M, whereas no inhibition was observed with iloprost (Figure 4:17). Addition of positive control PDBu (200 nM) showed that although PDGF-driven nuclear ERK activity was inhibited by IPR agonists, ERK activity could still be increased using a PKC activator.

4.2.4.2 *Non-receptor mediated inhibition of ERK activity*

Inhibition of ERK1/2 phosphorylation by cAMP has been shown to be due to the cross talk between the MAPK/ERK pathway and cAMP pathway (Stork & Schmitt, 2002). We have shown that directly activating AC using forskolin inhibits PDGF-driven ERK phosphorylation when using a population-based assay (Figure 3:1). Next, we wanted to investigate if forskolin can inhibit ERK activity in the nucleus and cytoplasm of HLFs to probe the role of cAMP in the inhibition of ERK activity.

Firstly, HLFs transiently transfected with cytoEKAR were pre-treated for 30 minutes with a range of concentrations of forskolin and then stimulated with 10 ng/ml PDGF. The maximal concentration of forskolin (10 μ M) inhibited PDGF-driven cytoplasmic

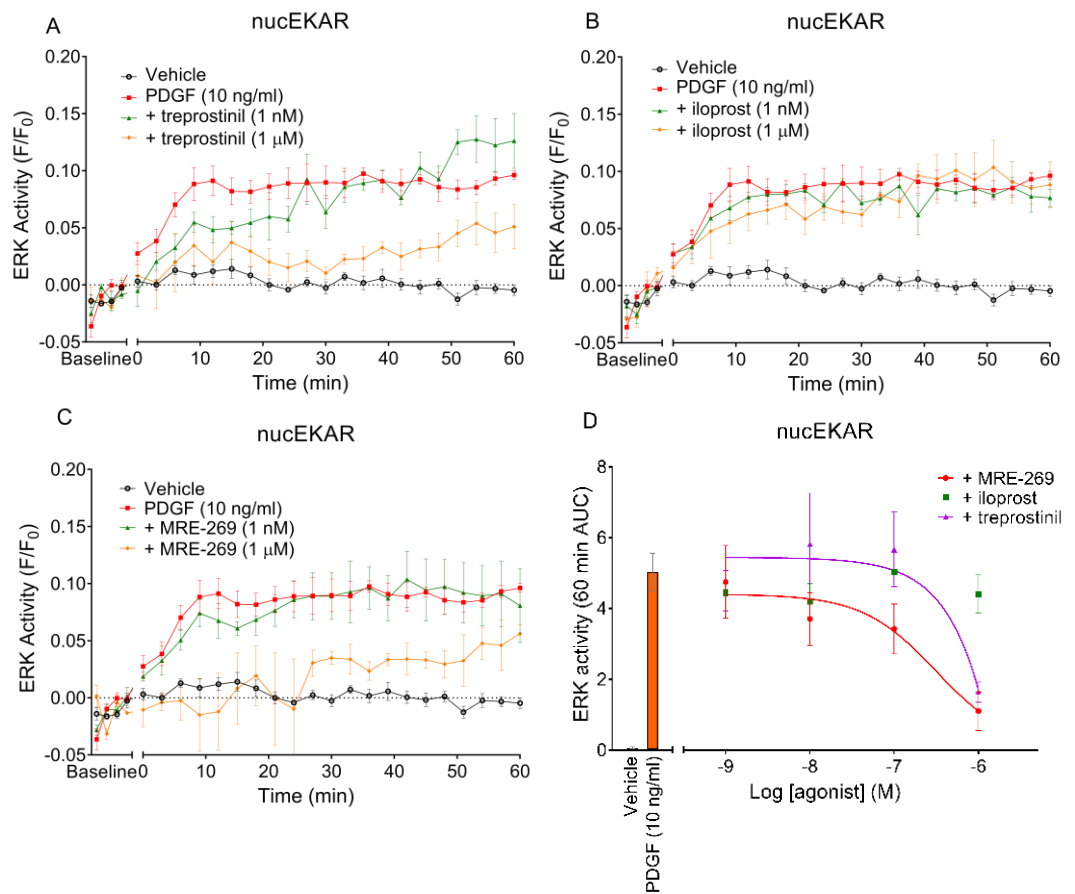


Figure 4:16 - IP receptor agonist inhibition of nuclear ERK activity

Inhibition of PDGF-driven nuclear ERK activity by IPR agonists treprostiril (A), iloprost (B), and MRE-269 (C) measured by FRET biosensor nucEKAR transiently transfected in HLFs. Data are expressed as change in GFP/RFP ratio relative to the donor intensity and baseline read for each cell, and baseline corrected to the vehicle response. (D) Corresponding concentration response curves calculated using AUC for inhibition of nuclear ERK activity by IPR agonists. Data are expressed as mean \pm SEM for 4 independent experiments, with at least 14 individual cells per condition in each individual *n*. AUC, area under the curve.

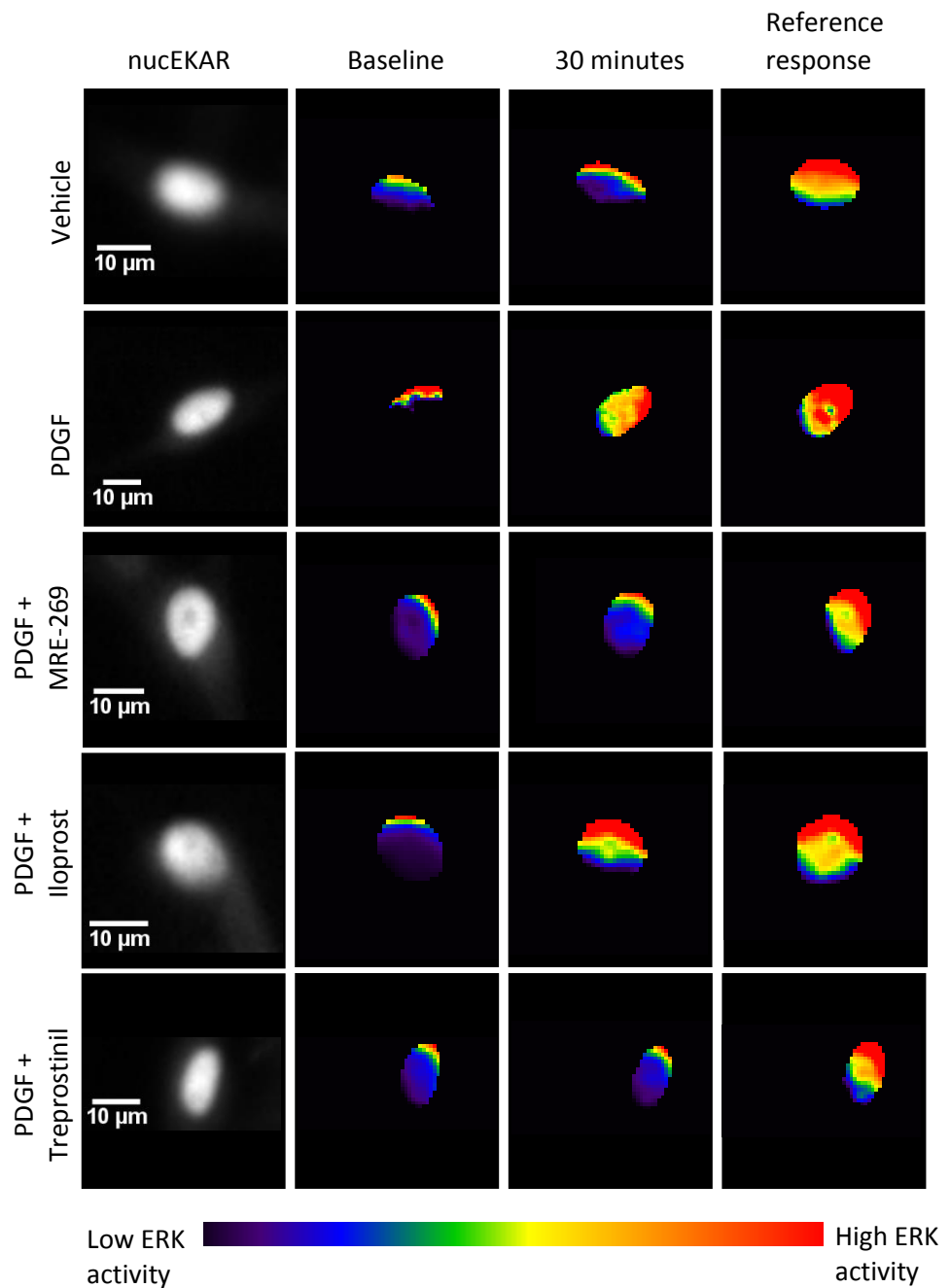


Figure 4:17 - Representative ratiometric images and biosensor localisation for nucEKAR

Widefield images show the localisation of nucEKAR sensor to the nucleus. HLFs were transiently transfected with nucEKAR and stimulated with either vehicle or PDGF (10 ng/ml). Inhibition of the PDGF was investigated following treatment with IPR agonists, MRE-269 (1 μ M), iloprost (1 μ M), or treprostiniil (1 μ M). Reference response is the response to positive control PDBu (200 nM).

ERK activity over a time course of 60 minutes (Figure 4:18A). Secondly, the same experiment was performed using HLFs transiently transfected with nucEKAR. In contrast to cytoplasmic ERK activity, forskolin (10 μ M) was unable to inhibit PDGF-driven nuclear ERK activity (Figure 4:18B). Corresponding concentration response curves calculated using the AUC of time courses showed forskolin inhibited PDGF-driven cytoplasmic ERK activity with a pIC₅₀ of 7.44 ± 0.47 , however no inhibition of nuclear ERK activity was observed (Figure 4:18C). This could suggest the inhibition of ERK1/2 phosphorylation in the nucleus is not dependent on cAMP or that forskolin does not increase nuclear cAMP.

We have previously suggested that iloprost could not inhibit ERK activity due to its ability to only increase cAMP in the nucleus in a transient manner. To investigate if this was the case with forskolin, HLFs transiently transfected with nucEpac2 were treated with a range of concentrations of forskolin to measure nuclear cAMP. Sustained cAMP signalling up to 30 minutes was observed in the nucleus after treatment with forskolin (10 μ M) (Figure 4:19A). Concentration response curve of forskolin-mediated nuclear cAMP response showed forskolin increased nuclear cAMP in a concentration dependent manner (Figure 4:19B).

4.2.5 The dependence of the inhibition of nuclear ERK on cAMP

To investigate if the inhibition of nuclear ERK is dependent on cAMP, AC inhibitors ddA and SQ22536 were utilised to block accumulation of cAMP by the IPR agonist MRE-269 when investigating its ability to inhibit PDGF-driven nuclear ERK activity. HLFs transiently transfected with nucEKAR were treated with either ddA (30 μ M) or SQ22536 (30 μ M) for 30 minutes prior to the addition of an IC₈₀ concentration of MRE-269 for 30 minutes, calculated from Figure 4:16D. PDGF-driven nuclear ERK activity

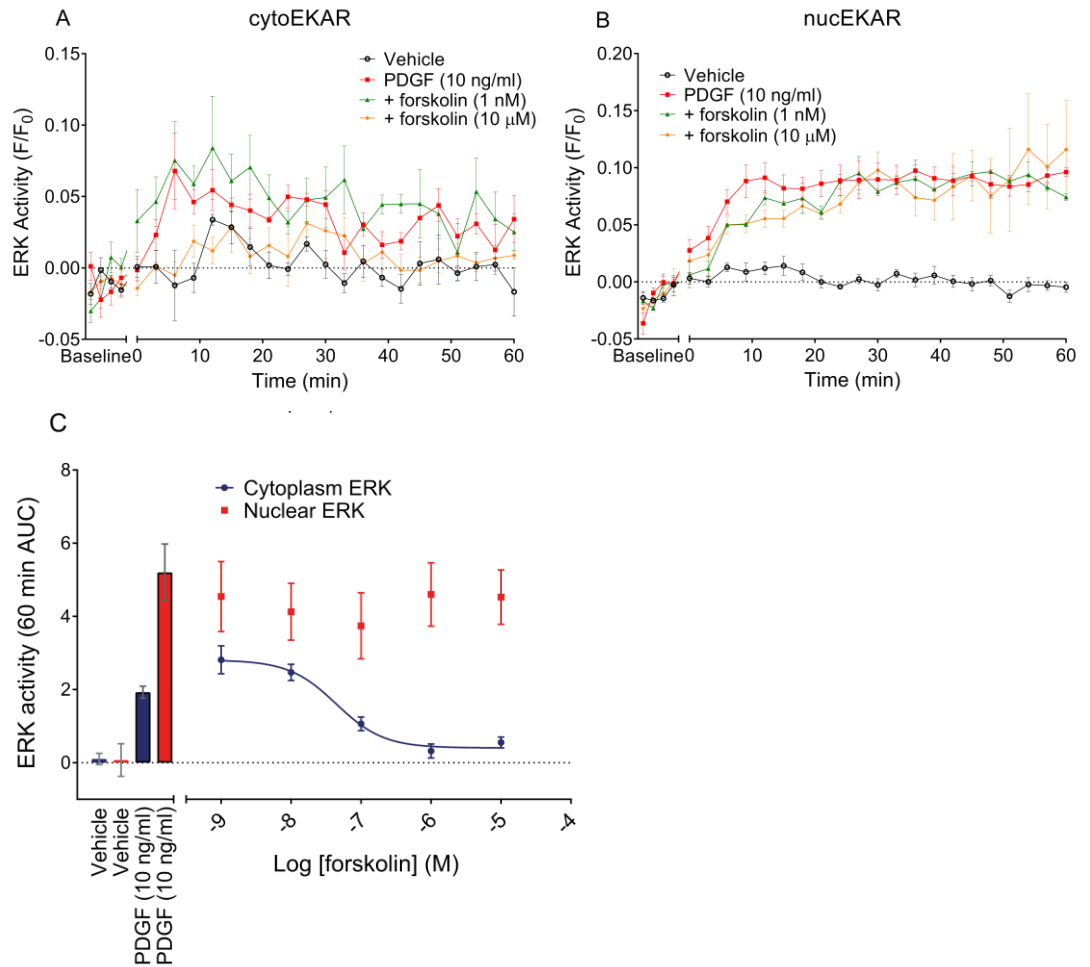


Figure 4:18 - Non-receptor mediated inhibition of compartmentalised ERK activity

Inhibition of ERK activity in the cytoplasm (A) and nucleus (B) of HLFs by directly activating AC using forskolin measured by FRET biosensors cytoE KAR or nucE KAR transiently transfected in HLFs. Data are expressed as change in GFP/RFP ratio relative to the donor intensity and baseline read for each cell, and baseline corrected to the vehicle response. (C) Corresponding concentration response curves calculated using AUC for inhibition of cytoplasm or nuclear ERK activity by forskolin. Data are expressed as mean \pm SEM for 4 independent experiments, with at least 14 individual cells per condition in each individual n. AUC, area under the curve.

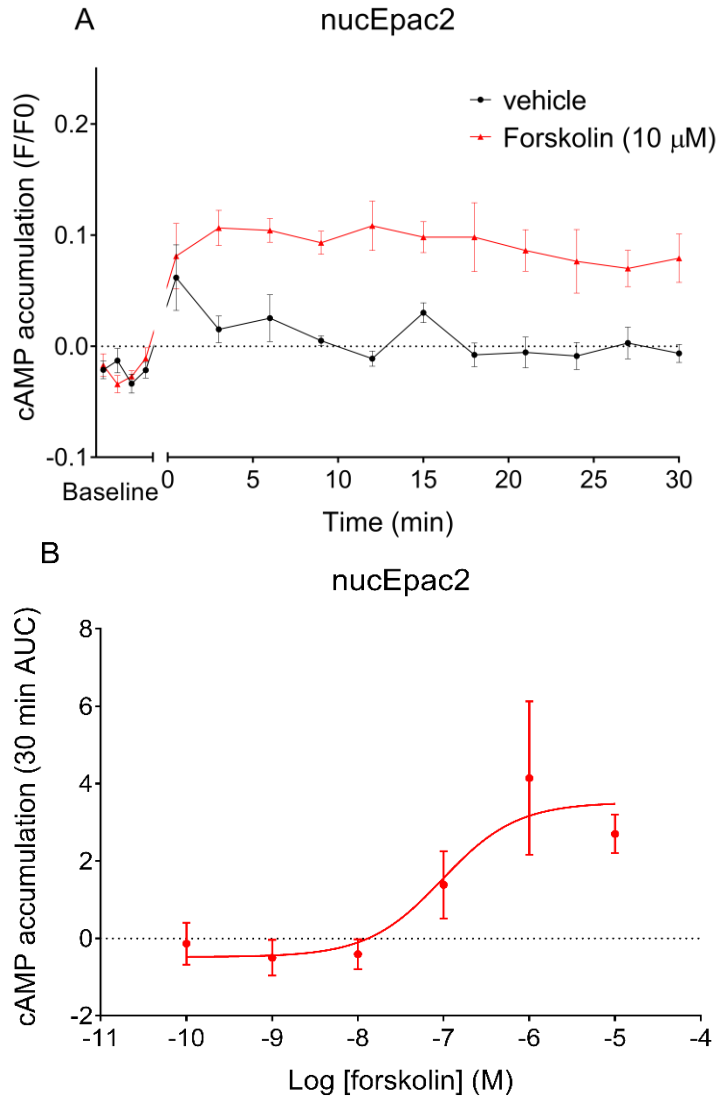


Figure 4:19 - Forskolin-mediated nuclear cAMP accumulation in HLFs

(A) Time course of cAMP accumulation in the nucleus upon stimulation of HLFs with forskolin (10 μM), measured by FRET biosensor nucEpac2. Data are expressed as change in CFP/YFP ratio relative to the donor intensity and baseline read for each cell, and baseline corrected to the vehicle response. (B) Corresponding concentration response curve using AUC for the nuclear cAMP response to forskolin. Data are expressed as mean ± SEM for 3 independent experiments, with at least 11 individual cells per condition in each individual n. AUC, area under the curve.

was then monitored for 60 minutes to investigate whether the cAMP generated by MRE-269 is important for the inhibition of nuclear ERK activity.

The presence of ddA on its own resulted in an increase in nuclear ERK activity, and PDGF-driven nuclear ERK activity was enhanced in the presence of ddA over the 60 minute time course (Figure 4:20A). This suggests there is a high level of basal cAMP in HLFs that is able to inhibit ERK activity, and the inhibition of AC lowers basal levels of cAMP thus reversing any basal inhibition of ERK. Furthermore, the inhibition of PDGF-driven ERK activity by MRE-269 was reversed in the presence of ddA (Figure 4:20A). Corresponding AUC bar charts show the effect of ddA on nuclear ERK activity (Figure 4:20B). Not only did ddA reverse MRE-269 inhibition of PDGF-driven nuclear ERK activity, PDGF-driven ERK activity was enhanced when HLFs were treated with both ddA and MRE-269 in comparison to just ddA.

To confirm the results observed with ddA a second AC inhibitor, SQ22536 was used. As observed following treatment with ddA, the presence of AC inhibitor SQ22536 on its own resulted in an increase in nuclear ERK activity over 60 minutes (Figure 4:20C). In addition, PDGF-driven nuclear ERK activity was enhanced in the presence of SQ22536. Furthermore, the inhibition of PDGF-driven ERK activity by MRE-269 was reversed in the presence of SQ22536 (Figure 4:20C). Corresponding AUC bar charts show the effect of SQ22536 on nuclear ERK activity, with SQ22536 blocking MRE-269 inhibition of PDGF-driven ERK activity (Figure 4:20D).

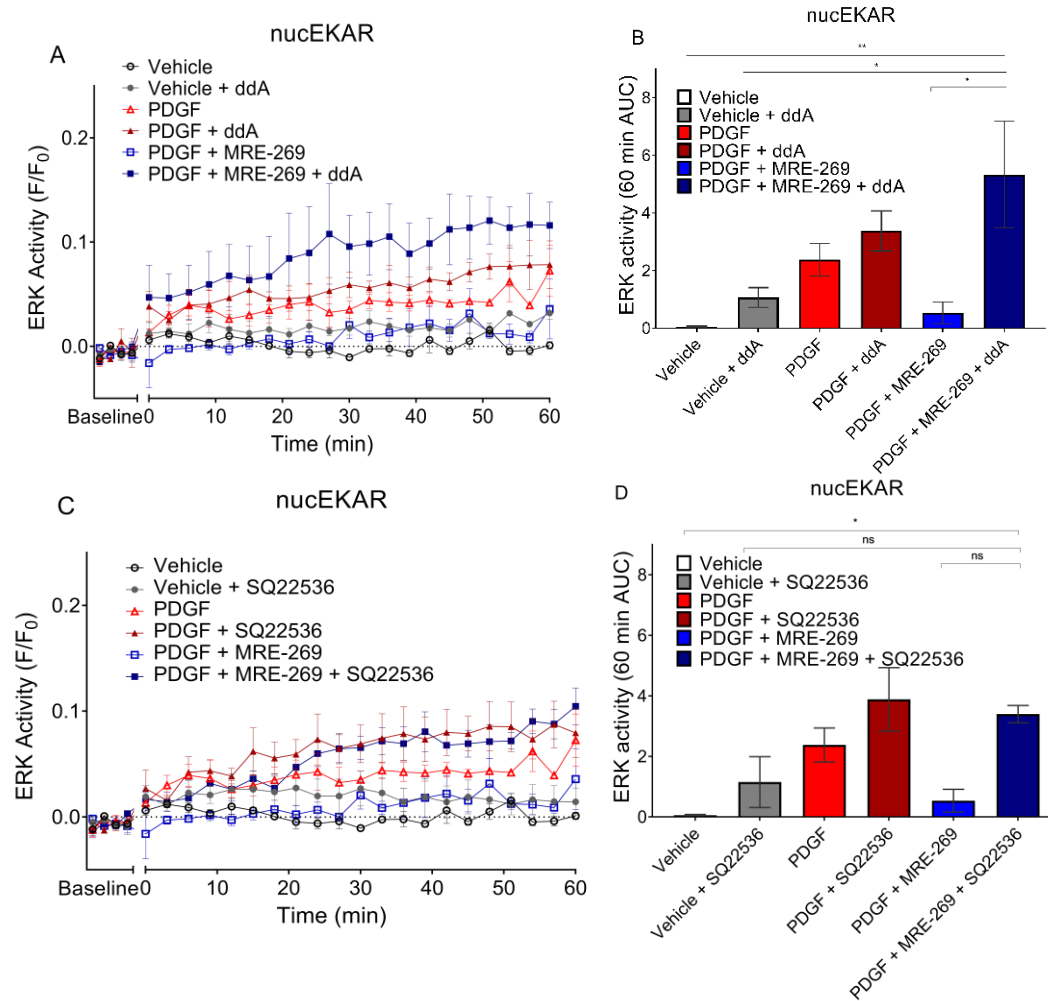


Figure 4:20 - Effect of adenylyl cyclase inhibitors on MRE-269 inhibition of PDGF-driven nuclear ERK activity

Time course (A) and corresponding AUC plot (B) of the effect of AC inhibitor 2'5'-dideoxyadenosine on nuclear ERK activity measured in HLFs expressing nucEKAR. Time course (C) and corresponding AUC plot (D) of the effect of AC inhibitor SQ22536 on nuclear ERK activity measured in HLFs expressing nucEKAR. Data are expressed as change in GFP/RFP ratio relative to the donor intensity and baseline read for each cell, and baseline corrected to the vehicle response. Data are expressed as mean \pm SEM for 4 independent experiments, with at least 14 individual cells per condition in each individual n. * $p < 0.05$, ** $p < 0.01$, data were analysed by one-way ANOVA with Dunnett's multiple comparison test. AUC, area under the curve; ns, not significant.

4.3 Discussion

Understanding what drives the disconnect between cAMP accumulation and the inhibition of proliferation of HLFs when targeting the IPR may help the development of more efficacious agonists for inhibiting biological responses, such as proliferation. cAMP and ERK signalling pathways are tightly controlled to ensure signals are relayed correctly in the cell. Using FRET biosensors to measure cAMP accumulation and ERK activity in different subcellular locations may help unravel why agonists that generate a high magnitude of cAMP may not be efficacious in inhibiting phenotypic changes, such as proliferation.

Although we have observed the disconnect in one HLF donor, we wanted to investigate if this disconnect can be observed in a different donor. In general, cAMP responses were comparable between HLF donors, however efficacy for inhibiting proliferation was enhanced for iloprost and treprostinil in HLFd.42105.2. Importantly, the disconnect between cAMP levels and ability to inhibit proliferation was maintained between donors. Differences in responses could be due to differences in donor age/sex, with the donor used in this chapter being slightly younger and female. Even slight changes in receptor number and cAMP/ERK pathway protein levels can result in variance, thus for all studies experiments should be performed with cells from a single donor, and then repeated with other donors.

To investigate if the spatial control of cAMP differs between IPR agonists we transiently transfected HLFs with cAMP FRET biosensors targeted to different subcellular locations. Utilising targeted cAMP FRET biosensors to measure cAMP have some advantages over previous methods, such as radioimmunoassay or enzyme immunoassay. FRET biosensors are highly sensitive and can detect smaller responses than population-based signalling, and they also provide greater temporal and spatial

resolution. However, increased sensitivity results in limitations in dynamic range, which results in biosensor saturation at sub-maximal concentrations of agonists, thus making it difficult to identify partial agonists and correctly calculate agonist efficacy. The introduction of targeting sequences can alter this range making the comparison of responses between biosensors difficult. For example, the original Epac2-camps expressed in the cytoplasm has an EC_{50} for cAMP of 0.4 μ M, which is decreased following targeting to the plasma membrane (EC_{50} of 1.7 μ M) (Nikolaev et al, 2004; Wachten et al, 2010). Therefore, caution should be taken when interpreting data from biosensors targeted to different locations.

Evidence for differences in the subcellular pattern of cAMP produced by different IPR agonists was not observed in these experiments because cAMP produced following treatment with sub-maximal concentrations of agonists resulted in saturation of all three biosensors used. This was demonstrated by the subsequent addition of forskolin and non-specific PDE inhibitor IBMX not causing any further increase in the FRET response observed (data not shown). This highlights the need to use an alternate biosensor which has a higher dynamic range than Epac2. Saturation of the cAMP FRET biosensor could explain why a lower concentration of MRE-269 did not cause a partial cAMP response in the different locations. Although maximal responses are hard to interpret, one key result from measuring subcellular localisation of cAMP is the difference in temporal profiles at the nucleus. Iloprost resulted in a transient cAMP response in the nucleus whereas MRE-299 and treprostinil caused a sustained cAMP response. This suggests that cAMP generated in the nucleus by iloprost either diffuses out or is degraded more quickly, and it could start to help explain why iloprost is not as efficacious at inhibiting proliferation as treprostinil and MRE-269.

From our data and from literature it has been shown that cAMP inhibits proliferation of HLFs through inhibiting the MAPK/ERK pathway, therefore we wanted to establish if the disconnect is observed at the level of ERK phosphorylation (Nikam et al, 2011; Stork & Schmitt, 2002). All IPR agonists inhibited global PDGF-driven ERK activity to similar efficacies and potencies. However, many studies have shown that ERK is compartmentalised to either the cytoplasm or the nucleus, therefore the use of FRET biosensors that can detect ERK in different compartments was important in providing more accurate insight into ERK activity within cells. The high throughput cellular lysate ERK assay may only be measuring ERK phosphorylation in the cytoplasm of HLFs, due to the inability of the lysate buffer to lyse the nuclear compartment of cells, as the PDGF response was transient in both the high throughput assay and when measuring cytoplasmic ERK activity, whereas PDGF-driven nuclear ERK activity was sustained. In addition, all agonists could inhibit PDGF-driven ERK activity in the high throughput assay and in the cytoplasmic compartment of HLFs, whereas variation in efficacy of IPR agonists in the nuclear compartment was observed. As the nuclear ERK compartment is key for driving proliferation of fibroblasts (Brunet et al, 1999) it is important to ensure the assay used to quantify ERK activity can measure nuclear ERK activity.

PDGF drove a small and transient increase in ERK activity in the cytoplasm, whereas it drove a larger and sustained increase in ERK activity in the nucleus. The observation that cytoplasmic ERK activity is transient upon stimulation of HLFs with PDGF is not surprising. In resting cells, ERK is localised to the cytoplasm due to interactions with anchoring proteins. After stimulation, ERK1/2 becomes phosphorylated which permits their detachment from the anchoring proteins and subsequent phosphorylation promotes translocation to the nucleus. This translocation to the nucleus will be measured as a decrease in cytoplasmic ERK activity. If this was the case in HLFs the

increase in nuclear ERK would be slightly delayed, and correspond with a decrease in cytoplasmic ERK. As this is not what is observed, the other possibility is that there are distinct pools of ERK that either remain in the cytosol or move to the nucleus.

All IPR agonists could inhibit PDGF-driven cytoplasmic ERK activity, however MRE-269 had a “bell-shaped” curve for inhibition (Figure 4:13). There are no clear reasons currently why this was observed, and further studies into why MRE-269 shows a different profile will be interesting. Due to MRE-269 being highly lipophilic, one hypothesis that can be investigated is that treatment of HLFs with high concentrations of MRE-269 results in passive diffusion of the ligand across the plasma membrane, resulting in activation of a different pool of IPRs. This pool of IPRs may not be able to inhibit cytosolic ERK but can inhibit nuclear ERK activity. Additional studies could involve investigating cAMP signalling and receptor activation at the Golgi (Irannejad et al, 2017) or from endosomes (Irannejad et al, 2013), along with the investigation of internalisation of the IPR, to further probe IPR signalling.

Iloprost was the only IPR agonist that did not inhibit PDGF-driven nuclear ERK activity. This raises the question of whether a sustained nuclear cAMP response is important for the inhibition of nuclear ERK activity. To investigate this, methodology to disrupt just the nuclear cAMP signal with MRE-269 or treprostinil could show if it is required to inhibit nuclear ERK. However, with the current tools available it may not be possible to disrupt just the nuclear cAMP compartment in cells. Other tools that could be utilized to investigate if certain subcellular pools of cAMP are important for inhibiting nuclear ERK are fluorescently tagged AC inhibitors that are targeted to inhibit AC in distinct locations. This would allow cAMP to be inhibited in targeted subcellular locations and could help distinguish the pool of cAMP that is important for inhibiting nuclear ERK. Although no inhibition of nuclear ERK was observed with iloprost, it did

inhibit proliferation, albeit only partially, which suggests that inhibition of nuclear ERK activity is important but not necessary for the inhibition of proliferation. In agreement, forskolin, a direct activator of AC, did not inhibit nuclear ERK activity but did strongly inhibit proliferation (Figure 4:18), which suggests that the inhibition of nuclear ERK activity is not dependent on cAMP or that forskolin activates different pools of ACs compared to IPR agonists, or that the diffusion of cAMP stimulated by forskolin is more restricted. However, the use of AC inhibitors with MRE-269 showed that this was not the case, as MRE-269-mediated inhibition of nuclear ERK was reversed when cAMP production was blocked. To complicate matters further, forskolin was able to drive nuclear cAMP accumulation, which again suggests other factors other than the location of cAMP are important for the inhibition of nuclear ERK activity. Another point to consider is that although cAMP is being measured in bulk compartments, there may be compartmentalisation within the nucleus itself.

PGI₂ analogues signal through the IPR, although the potential of IPR agonists to signal through peroxisome proliferator-activated receptor- γ (PPAR- γ) and effect proliferation of fibroblasts has been shown in studies PAH (Falcetti et al, 2007; Falcetti et al, 2010). Therefore studies into the ability of IPR agonists to signal through this alternate pathway and how this pathway regulates phenotypic changes in HLFs may help in the understanding of the different activities of IPR agonists.

Utilising AC inhibitors showed that the inhibition of PDGF-driven nuclear activity by MRE-269 was dependent on cAMP (Figure 4:20). However, evidence confirming AC inhibitors actually block cAMP production by MRE-269 could not be generated due to compounds interfering with the assay. AC inhibitors ddA and SQ22536 have similar structures to cAMP, thus they can bind to enzymes, antibodies, and sensors that detect cAMP and result in a false positive cAMP read. It is promising that both AC

inhibitors utilised here generated the same results, however future experiments using reporter gene assays such as CRE-SPAP as a readout that may not be interfered with by AC inhibitors to monitor cAMP changes by IPR agonists will be ideal to confirm inhibition of nuclear ERK activity is dependent on cAMP. An alternate route to confirm nuclear ERK activity is dependent on cAMP could involve using membrane-permeable cAMP analogues, such as 8-Br-2'-O-Me-cAMP-AM, to see if they affect nuclear ERK activity. However the actual permeability and kinetics of membrane-permeable cAMP analogues are poorly characterized (Borner et al, 2011).

As with all biosensors, Epac and EKAR expression may perturb endogenous signalling. The introduction of excessive amounts of any indicator for cellular activity into cells can cause problems. The Epac biosensor requires cAMP binding to undergo a conformational change therefore a buffering effect on cAMP is likely to occur. As the EKAR biosensor acts solely as a substrate, it may disturb the observed system to a lesser degree, however, the competition with endogenous substrates could still dampen ERK signalling. All this needs to be considered when performing experiments using FRET biosensors.

In this chapter it has been demonstrated that the spatial and temporal regulation of cAMP and ERK can be investigated in primary HLFs using genetically encoded FRET biosensors. Although these are useful tools, a lot more work needs to be done to fully characterise these biosensors in HLFs, especially when looking at the dynamic range. Iloprost, the least efficacious agonist at inhibiting proliferation, showed different profiles in generating nuclear cAMP and inhibiting nuclear ERK in comparison to MRE-269/treprostinil. Driving nuclear cAMP and inhibiting nuclear ERK may be important in inhibiting phenotypic processes in HLFs. However, directly activating AC with forskolin results in nuclear cAMP accumulation with no inhibition of nuclear ERK. This suggests

a more complex mechanism of the inhibition of nuclear activity other than whether or not cAMP is increased within bulk compartments.

Chapter 5 – cAMP kinetics in human lung fibroblasts

5.1 Introduction

In Chapter 4 targeted cAMP and ERK FRET biosensors were used to investigate the hypothesis that efficacy of IPR agonists to inhibit HLF phenotypic responses is related to the compartmentalisation of signalling molecules. Key differences between IPR agonists were observed, and a complex mechanism between the inhibition of nuclear ERK activity and localised cAMP was identified, with future experiments required to investigate spatial signalling in HLFs further. However, another factor that could play a role in the efficacy of IPR agonists to inhibit phenotypic responses is the kinetics of cAMP.

Traditionally, the pharmacology of many GPCR agonists has been determined by monitoring their activity using short-term cellular responses, such as cAMP accumulation and ERK phosphorylation, due to quick and easy high throughput assays. However, it is becoming clear that the long-term biological output of a signalling process depends not only on the magnitude of the response but also on how long the signal is emitted. Previous studies have established a correlation between the time-course of cAMP signalling and the corresponding cellular responses. In U-937 cells, cAMP elevating agents PGE₂ and forskolin, maintained a residual response of cAMP at later time points and had greater efficacy in inhibiting cell proliferation (Shayo et al, 2004). In this study, the initial maximal cAMP response was not representative of the phenotypic outcome.

Furthermore, the temporal characteristics of β_2 adrenoceptor agonist-mediated cAMP responses and related CRE-gene transcription responses were investigated in CHO cells (Baker et al, 2004). It was shown that small second messenger responses that are sustained over time can robustly activate transcription factors, whereas short bursts

of cAMP, regardless of magnitude, are often incapable of initiating gene transcription (Baker et al, 2004).

The duration of receptor signalling can be greatly altered by desensitisation of the receptor by phosphorylation/internalisation, and desensitisation of the signalling pathway (Midgett et al, 2011). Receptor desensitization refers to the decreased responsiveness that occurs with repeated or chronic exposure to agonist and is a general feature of most signalling membrane receptors. After two hour exposure of platelets to the IPR agonist iloprost, the number of iloprost binding sites was found to be reduced due to receptor internalisation, and the platelets were found to be desensitised to further treatments with iloprost (Fisch et al, 1997). Furthermore, it has been shown that continued stimulation of IPRs expressed in HEK293 cells with iloprost led to a decrease in the ability of forskolin to stimulate cAMP production, indicating desensitisation of the AC-cAMP signalling pathway (Smyth et al, 1998).

It has been a long held view that GPCR signalling occurs on the plasma membrane only, with initial agonist-receptor stimulation often being rapid and short lived, mainly due to desensitisation of the receptor through internalisation and degradation. The development of novel methods for visualising GPCR cAMP signalling in living cells has been instrumental for the recent finding that some GPCRs, such as the TSH receptor, parathyroid hormone (PTH) receptor, and β_1/β_2 adrenoceptors, continue signalling through cAMP after internalisation (Calebiro et al, 2009; Ferrandon et al, 2009; Irannejad et al, 2017; Irannejad et al, 2013). The resulting increase in the duration of second messenger signalling has been described to play a key role in biological outcome.

It remains to be established if, in HLFs, the inhibition of proliferation is driven by the initial cAMP response or whether a prolonged cAMP signal is required. In this chapter, the targeted cAMP FRET biosensors used in Chapter 4 were used in conjunction with a perfusion system to investigate duration of cAMP signalling on a short time scale in different compartments after washing off agonists. In addition, real-time kinetic changes in cAMP levels using the GloSensor™ biosensor were studied in intact living HLFs. This method allows monitoring of cAMP over longer time courses in a population of cells. The GloSensor™ technology is based on an engineered form of firefly luciferase encompassing a CBD (Fan et al, 2008). The GloSensor™ assay allows the study of cAMP signalling at later, more phenotypically relevant, time points. Using this methodology, the aim is to investigate the efficacy of IPR agonists at generating cAMP at later time points in order to give better link to biological outcome in HLFs.

5.2 Results

5.2.1 Measuring cAMP kinetics using targeted FRET biosensors

In Chapter 4 targeted FRET biosensors were used to measure cAMP accumulation at distinct locations in HLFs. Changes in FRET following addition of an IPR agonist were measured using a widefield high content imaging (HCI) platform and levels were monitored for 60 minutes. Although this method is suitable for investigating the magnitude of cAMP in distinct compartments, the early kinetics of cAMP accumulation were missed using this set up due to the time taken for manual addition of agonists and transfer of plate to the HCI platform. In order to measure the kinetics of cAMP accumulation in greater detail a confocal microscope with a perfusion system was used for quick change between assay buffer and agonists to enable the continuous uninterrupted measurement of FRET changes. HLFs transiently transfected with either pmEpac2 or cytoEpac2 were placed in the perfusion chamber with assay buffer to obtain a basal read and then stimulated with agonist for 5 minutes to monitor changes in cAMP levels. To investigate rates of decline of cAMP in HLFs after removal of agonists, HLFs were washed with assay buffer for 6 minutes. Finally, HLFs were treated with forskolin (10 μ M) for 6 minutes to generate a maximal cAMP response.

Stimulation of HLFs expressing pmEpac2 with IPR agonists resulted in an increase in cAMP levels at the plasma membrane which peaked within 5 minutes (Figure 5:1A). Treatment with maximal concentrations of treprostinil (1 μ M) and iloprost (300 nM) resulted in greater levels of cAMP accumulation in comparison to MRE-269 (1 μ M). In addition, the rate of accumulation of cAMP was slower with MRE-269 stimulation in comparison to iloprost and treprostinil (Table 5:1). MRE-269 had a rate of cAMP accumulation ($t_{1/2}$ on) of 37.9 ± 7.12 seconds, whereas treprostinil and iloprost had

rates of 24.3 ± 3.97 seconds and 19.1 ± 4.97 seconds, respectively. Removal of agonists by washing HLFs with assay buffer for 6 minutes returned the cAMP levels to basal levels for all conditions, with the rate of decline being slower at 193 ± 32.6 seconds with MRE-269 in comparison to the rates of decline of 119 ± 11.5 seconds and 117 ± 24.8 seconds for treprostinil and iloprost, respectively (Table 5:1).

Treatment of HLFs expressing cytoEpac2 with IPR agonists caused an increase in cAMP levels in the cytoplasm that peaked within 5 minutes (Figure 5:1B). Treprostinil stimulation resulted in higher levels of cAMP in comparison to MRE-269 and iloprost, with a F/F_0 value of 1.13 ± 0.01 for treprostinil, and F/F_0 values of 1.10 ± 0.01 and 1.09 ± 0.02 for iloprost and MRE-269, respectively. Similar to the plasma membrane, cAMP levels in the cytoplasm took longer to peak with MRE-269, with the rate of cAMP accumulation at the cytoplasm for MRE-269 calculated at 49.0 ± 15.0 seconds, over twice that of iloprost and treprostinil (Table 5:1). Removing agonists by washing HLFs with assay buffer resulted in a decline in cAMP levels, indicated by a decrease in F/F_0 . The rate of decline of cAMP levels was almost twice as fast when washing away iloprost, in comparison to MRE-269 and treprostinil (Table 5:1). After the 6 minute wash with assay buffer, cAMP levels had not returned to baseline after MRE-269 treatment, with approximately 33 % of the MRE-269 response remaining after a 6 minute wash period. Although the cAMP response at the plasma membrane had returned to basal levels after washing MRE-269 off for 6 minutes, cAMP was still present in the cytoplasm.

To investigate how long the cAMP remains sustained in the cytoplasm after treatment with MRE-269, cytoplasm cAMP levels were monitored in HLFs after 6 minutes stimulation with MRE-269 and an extended wash period of 25 minutes with assay

buffer (Figure 5:2). The extended wash period resulted in cAMP levels reaching a new plateau, with F/F_0 value at 1.01 ± 0.01 (Table 5:1).

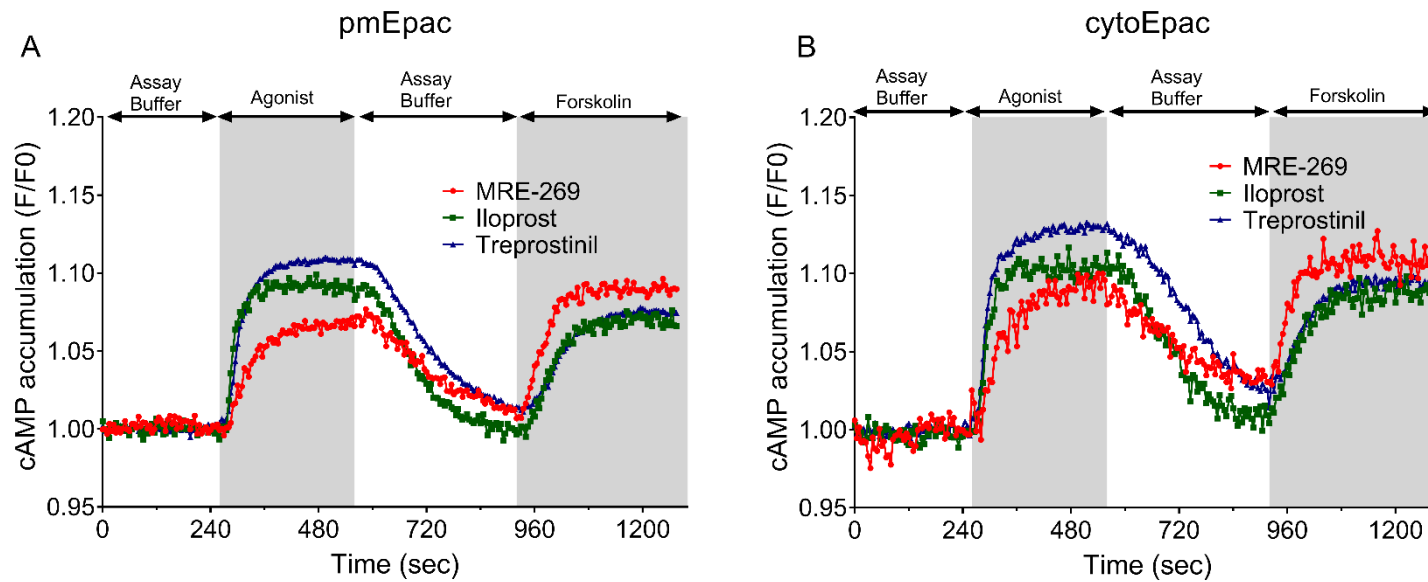


Figure 5:1 - cAMP kinetics in the cytoplasm and at the plasma membrane in HLFs

cAMP kinetics in the plasma membrane (A) and cytoplasm (B) measured using HLFs transiently transfected with cytoEpac2 and pmEpac2, respectively. HLFs were treated with agonists MRE-269 (1 μ M), iloprost (300 nM), or treprostinil (1 μ M) for 5 minutes, after which time agonists were washed away for 6 minutes with assay buffer. Forskolin (3 μ M) was added for 6 minutes as a positive control. Data are expressed as F/F_0 , which represents the change in CFP/YFP ratio relative to the baseline read for each cell. Data are expressed as mean \pm SEM for 10 separate runs, with a single cell analysed per run.

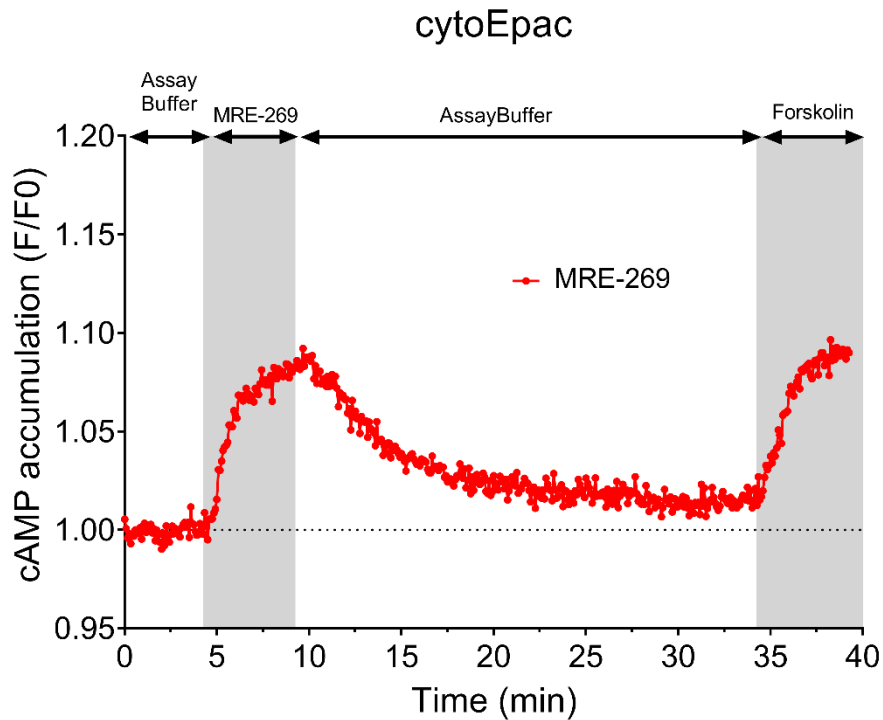


Figure 5:2 - cAMP kinetics in the cytoplasm after extended wash period following MRE-269 stimulation

cAMP kinetics in the cytoplasm measured using HLFs transiently transfected with cytoEpac2. HLFs were treated with MRE-269 (1 μ M) for 5 minutes, after which agonist was washed away for 25 minutes with assay buffer. Forskolin (3 μ M) was added for 6 minutes as a positive control. Data are expressed as F/F₀, which represents the change in CFP/YFP ratio relative to the baseline read for each cell. Data are expressed as mean \pm SEM for 10 separate runs, with a single cell analysed per run.

Table 5:1-Calculated cAMP response and rates in subcellular compartments of HLFs

	Cytoplasm cAMP			Plasma membrane cAMP		
	Iloprost (300 nM)	Treprostinil (1 μ M)	MRE-269 (1 μ M)	Iloprost (300 nM)	Treprostinil (1 μ M)	MRE-269 (1 μ M)
Rate of accumulation ($t_{1/2}$ on, seconds)	16.4 \pm 2.98	22.4 \pm 7.28	49.0 \pm 15.0	19.1 \pm 4.97	24.3 \pm 3.97	37.6 \pm 7.12
Peak response (F/F₀)	1.10 \pm 0.01	1.13 \pm 0.01	1.09 \pm 0.02	1.09 \pm 0.01	1.11 \pm 0.01	1.07 \pm 0.01
Rate of decline ($t_{1/2}$ off, seconds)	78.1 \pm 5.64	154 \pm 35.0	164 \pm 24.7	117 \pm 24.8	119 \pm 11.5	193 \pm 32.6
Plateau after 6 minute wash (F/F₀)	1.00 \pm 0.004	1.01 \pm 0.01	1.03 \pm 0.01	0.98 \pm 0.01	1.00 \pm 0.01	1.00 \pm 0.01
Plateau after 25 minute wash (F/F₀)	ND	ND	1.01 \pm 0.01	ND	ND	ND

Kinetics and magnitude of cAMP accumulation after stimulation with IPR agonists iloprost (300 nM), treprostinil (1 μ M), or MRE-269 (1 μ M) measured using targeted FRET biosensors in HLFs. Data are expressed as mean \pm SEM for 10 separate runs, with a single cell analysed per run. ND, not determined.

5.2.2 Kinetics of cAMP accumulation

Using genetically encoded FRET sensors alongside a perfusion system enabled the monitoring of cAMP kinetics in HLFs, however using this set up it is only possible to measure cAMP for a short time due to limited reservoir volumes in the perfusion system, as well as the potential to bleach the fluorophores from repeated excitation. Another assay that has been developed to measure cAMP kinetics in live cells is the GloSensor™ cAMP assay. Utilising this assay we wanted to investigate kinetics of cAMP accumulation in HLFs over longer time courses. The cAMP response was investigated after treating HLFs with a range of concentrations of IPR agonists or with forskolin (10 μ M) over 4 hours in the presence or absence of rolipram, to prevent the degradation of cAMP. Directly activating AC with forskolin (10 μ M) stimulated an increase in luminescence, that was larger in the presence of rolipram, which was followed by a slow decline in the luminescence signal over 4 hours that plateaued above baseline at 59.4 ± 6.92 % of peak forskolin response (Figure 5:3; Figure 5:4; Figure 5:5).

Stimulation of the IPR with iloprost in the presence of rolipram caused a concentration-dependent increase in the luminescence signal, with a large peak detected at 30 minutes (Figure 5:3A). The signal of the two highest concentrations of iloprost tested (3 μ M and 1 μ M) peaked above the forskolin response at 174 ± 10.6 % and 148 ± 9.56 % of peak forskolin response, respectively. After the peak response the luminescent signal declined and plateaued above baseline in a concentration dependent manner between 20.2 ± 2.56 % and 40.5 ± 6.58 % of peak forskolin response (Figure 5:3A). In the absence of rolipram, the luminescent signal after treatment with iloprost was smaller, with a peak at 30 minutes of 94.0 ± 20.5 % and 66.0 ± 11.7 % of peak forskolin response for 3 μ M and 1 μ M of iloprost, respectively (Figure 5:3B). After peaking, the luminescent signal declined to near to, but still above

basal levels, with a plateau of 16.0 ± 3.50 % of peak forskolin response after stimulation with $3 \mu\text{M}$ iloprost (Figure 5:3B). Concentration-response curves of the peak iloprost response showed the presence of rolipram increased the magnitude of cAMP accumulation (Figure 5:3C). Furthermore, potency was increased in the presence of rolipram, with pEC_{50} values of 6.71 ± 0.17 and 5.97 ± 0.44 in the presence and absence of rolipram, respectively.

Treprostinil, in the presence of rolipram, also resulted in a concentration-dependent increase in luminescence signal with a large peak detected at 30 minutes (Figure 5:4A). The highest concentration of treprostinil ($3 \mu\text{M}$) increased luminescent signal above that of forskolin, with a peak of 134 ± 8.95 % of peak forskolin response. After peaking, the luminescent signal declined and plateaued above baseline, with a plateau of 32.2 ± 5.00 % of peak forskolin response after stimulation with $3 \mu\text{M}$ treprostinil (Figure 5:4A). In the absence of rolipram, treprostinil resulted in a smaller luminescence signal which peaked at 30 minutes, with a peak of 38.2 ± 3.32 % of peak forskolin response for $3 \mu\text{M}$ treprostinil (Figure 5:4B). After peaking, the luminescence signal declined and plateaued nearer to, but still above, basal levels, with a plateau of 10.6 ± 2.45 % of peak forskolin response after stimulation with $3 \mu\text{M}$ treprostinil. Concentration-response curves of the peak treprostinil response showed the presence of rolipram increased the maximal levels of cAMP (Figure 5:4C). Potency of treprostinil in the presence of rolipram was calculated as pEC_{50} value of 6.04 ± 0.21 , however due to an incomplete curve potency could not be calculated for treprostinil in the absence of rolipram.

MRE-269 caused a concentration-dependent increase in luminescence signal, however, higher concentrations than that used with iloprost and treprostinil were required to detect cAMP accumulation. In the presence of rolipram, MRE-269 resulted

in an increase in luminescent signal that peaked at 30 minutes (Figure 5:5A). Peak response was $114 \pm 10.6 \%$ and $99.4 \pm 6.90 \%$ of peak forskolin response for $30 \mu\text{M}$ and $10 \mu\text{M}$ MRE-269, respectively. After peaking, the luminescent signal declined and plateaued above baseline, with a plateau of $52.0 \pm 3.76 \%$ of peak forskolin response after stimulation with $30 \mu\text{M}$ MRE-269. (Figure 5:5A). In the absence of rolipram, the luminescence signal caused by MRE-269 did not result in a large peak as observed with the other IPR agonists, but a small subtle peak at $42.8 \pm 8.66 \%$ of peak forskolin response for $30 \mu\text{M}$ MRE-269 (Figure 5:5B). After the less pronounced peak, luminescence signal declined slowly and plateaued below forskolin but above baseline levels at $15.1 \pm 2.53 \%$ following treatment with $30 \mu\text{M}$ MRE-269 (Figure 5:5B). Concentration-response curves of the peak MRE-269 response showed the presence of rolipram increased the maximal levels of cAMP (Figure 5:5C). Potency of MRE-269 in the presence of rolipram was calculated as pEC_{50} value of 5.34 ± 00.12 , however due to an incomplete curve potency could not be calculated for MRE-269 in the absence of rolipram.

To investigate the role of PDEs in desensitisation of the cAMP pathway the rate of increase and decline of the luminescence response was calculated for forskolin ($10 \mu\text{M}$) and the highest concentrations of IPR agonists in the presence and absence of rolipram.

It can be observed from the time course of cAMP accumulation that the presence of rolipram, a PDE inhibitor, increases the maximal amount of cAMP detected. Rolipram did not significantly change the rate of increase or decline of the luminescence signal with forskolin or the IPR agonists' treprostinil or iloprost (Table 5:2). However, the presence of rolipram did significantly decrease the rate of cAMP accumulation following treatment with MRE-269 ($30 \mu\text{M}$). Interestingly, in comparison to iloprost

and treprostinil, the rate of decline of the luminescence signal was slower for MRE-269 independent of the presence of PDE inhibitor. Statistical significance was observed in the presence of rolipram, with the rate of decline being statistically significantly slower for MRE-269 in comparison to iloprost and treprostinil. The rate of luminescent decay was markedly slower with MRE-269 in comparison with iloprost and treprostinil, which suggests less receptor desensitisation after treatment with MRE-269.

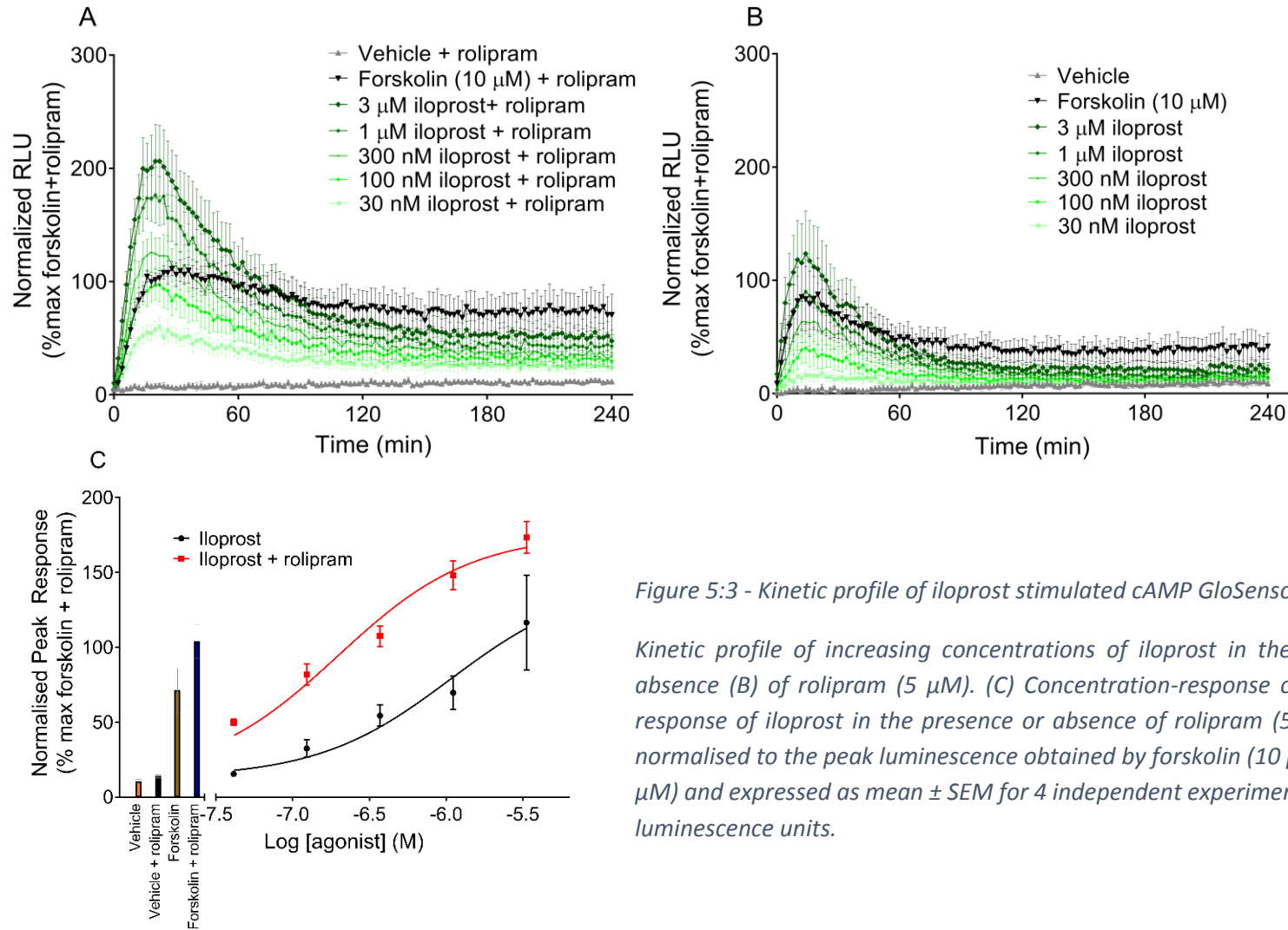


Figure 5:3 - Kinetic profile of iloprost stimulated cAMP GloSensor™ luminescence

Kinetic profile of increasing concentrations of iloprost in the presence (A) or absence (B) of rolipram (5 μ M). (C) Concentration-response curve of the peak response of iloprost in the presence or absence of rolipram (5 μ M). Data were normalised to the peak luminescence obtained by forskolin (10 μ M) + rolipram (5 μ M) and expressed as mean \pm SEM for 4 independent experiments. RLU – relative luminescence units.

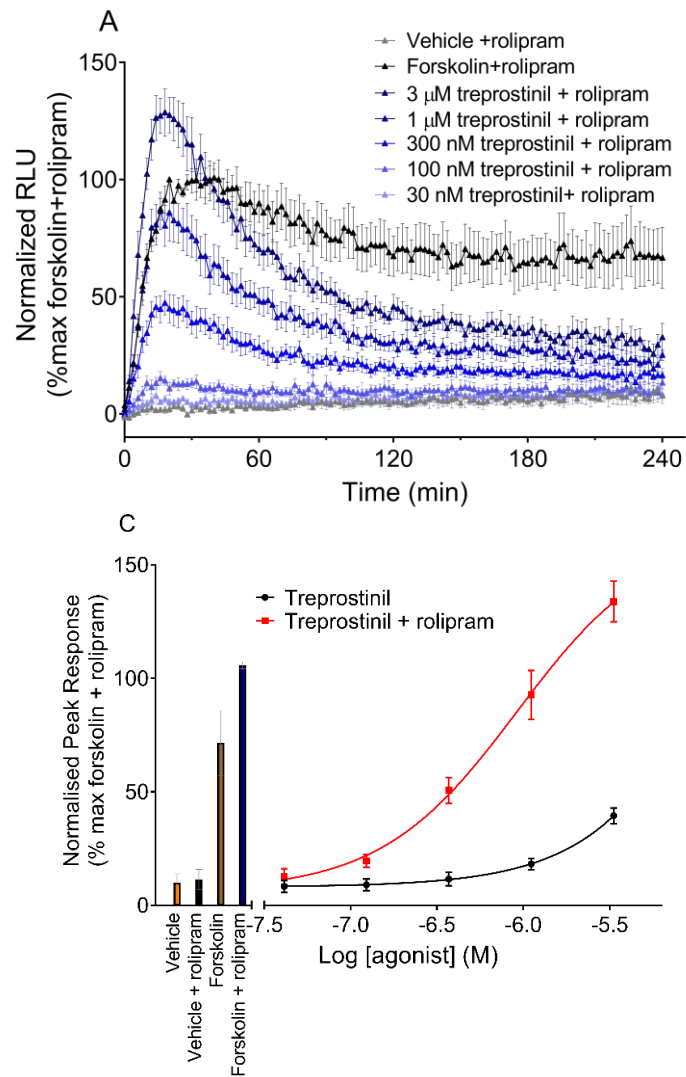


Figure 5:4 - Kinetic profile of treprostinil stimulated cAMP GloSensor™ luminescence

Kinetic profile of increasing concentrations of treprostinil in the presence (A) or absence (B) of rolipram (5 μM). (C) Concentration-response curve of the peak response of treprostinil in the presence or absence of rolipram (5 μM). Data were normalised to the peak luminescence obtained by forskolin (10 μM) + rolipram (5 μM) and expressed as mean \pm SEM for 4 independent experiments. RLU – relative luminescence units.

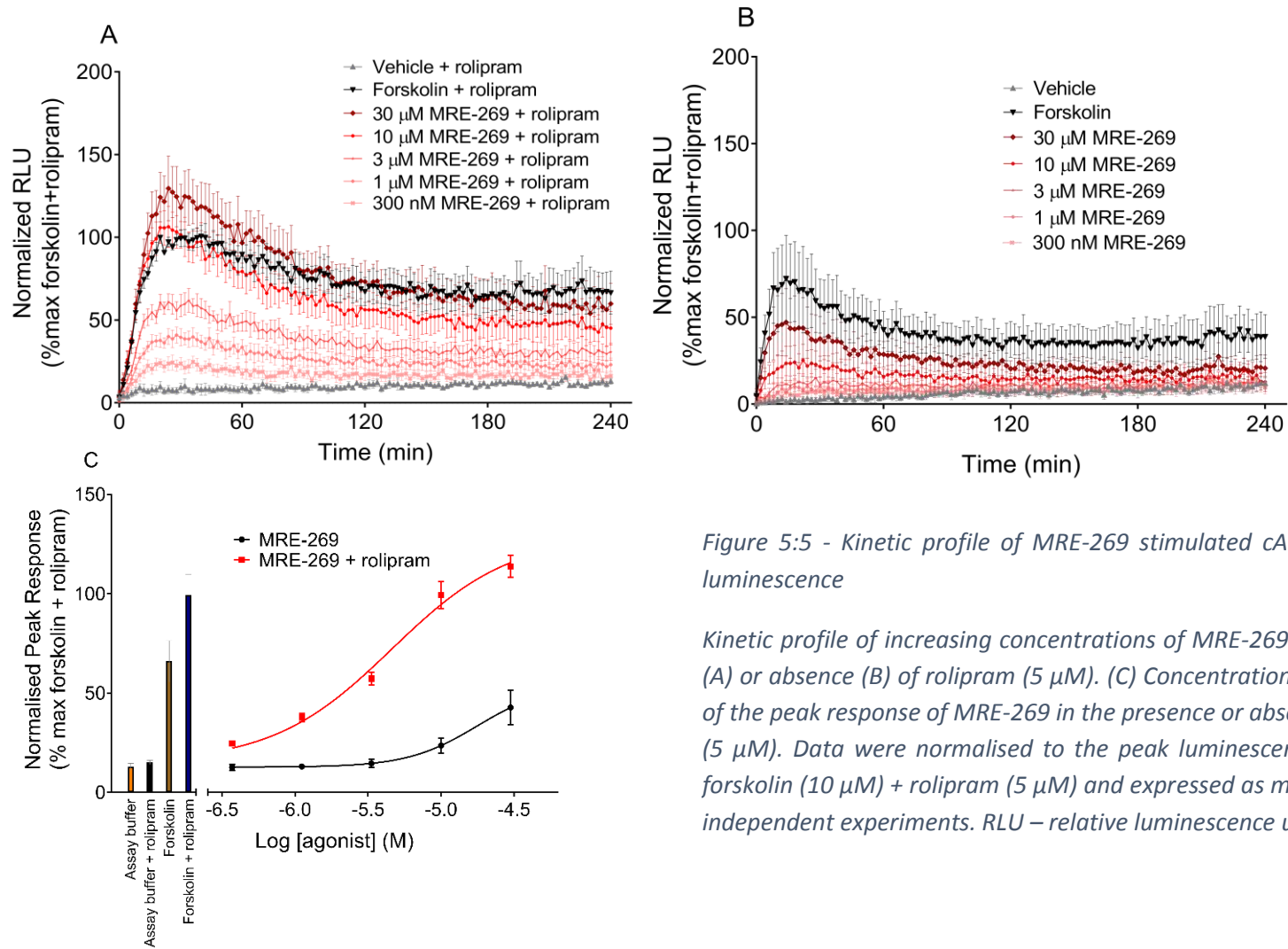


Figure 5:5 - Kinetic profile of MRE-269 stimulated cAMP GloSensor™ luminescence

Kinetic profile of increasing concentrations of MRE-269 in the presence (A) or absence (B) of rolipram (5 μ M). (C) Concentration-response curve of the peak response of MRE-269 in the presence or absence of rolipram (5 μ M). Data were normalised to the peak luminescence obtained by forskolin (10 μ M) + rolipram (5 μ M) and expressed as mean \pm SEM for 4 independent experiments. RLU – relative luminescence units.

Table 5:2 – Rate of cAMP increase and decline for IP receptor agonists GloSensor™ response in HLFs

cAMP elevating agent	Forskolin (10 μM)		Iloprost (3 μM)		Treprostiniil (3 μM)		MRE-269 (30 μM)	
	+ rolipram	- rolipram	+ rolipram	- rolipram	+ rolipram	- rolipram	+ rolipram	- rolipram
Rate of cAMP increase (t_{1/2}, min⁻¹)	8.87 ± 1.33	5.34 ± 1.85	5.52 ± 0.54	2.96 ± 0.42	4.97 ± 0.61	4.21 ± 0.21	12.6 ± 2.04 **	3.23 ± 0.86
Rate of cAMP decline (t_{1/2}, min⁻¹)	33.1 ± 6.57	25.4 ± 3.97	27.2 ± 1.94 ^^	19.9 ± 0.89	30.5 ± 2.02 ^	25.3 ± 5.63	40.5 ± 2.02	45.0 ± 16.6

Rate of increase and decline of cAMP accumulation calculated from forskolin (10 μM), iloprost (3 μM), treprostiniil (3 μM), and MRE-269 (30 μM) in the presence or absence of PDE inhibitor rolipram (5 μM). Data are expressed as mean ± SEM of 4 independent experiments. ** p<0.01, versus rate of cAMP increase for the same compound in the absence of rolipram. Data were analysed by one-way ANOVA with Sidak's multiple comparison test. ^ p<0.05, ^^ p<0.01, versus rate of cAMP decline of IPR agonists in the presence of rolipram. Data were analysed by one-way ANOVA with Tukey's multiple comparison test.

5.2.3 Efficacy of IPR agonists to increase cAMP over time

As MRE-269 was shown to have the greatest efficacy for inhibiting HLF proliferation in comparison to iloprost and treprostinil, it suggests that the large peaks in luminescence signal, and thus cAMP, detected with iloprost and treprostinil in the GloSensor™ assay may not be required for long-term phenotypic changes. Instead, it can be hypothesised that the efficacy of agonists in generating cAMP over time may be important in driving long-term phenotypic changes. We have already suggested that MRE-269 causes less desensitisation of the cAMP pathway, in comparison to iloprost and treprostinil, due to a slower rate of decline of the GloSensor™ signal. To probe the efficacy of IPR agonists in the absence of rolipram to increase cAMP over time, the AUC of the luminescence signal was calculated at different time periods from the time courses in Figure 5:3B; Figure 5:4B; Figure 5:5B.

Calculating the AUC at an early time period (0-30 minutes) and a later time period (150-180 minutes) showed a dramatic loss of efficacy for iloprost, with E_{\max} of $153 \pm 17.5\%$ and $44.0 \pm 4.80\%$ of the forskolin response at the same time period, for early and late time periods, respectively (Figure 5:6A). Potency for iloprost remained similar across the different time periods, with a pEC_{50} of 6.48 ± 0.17 for the early time period and a pEC_{50} of 6.58 ± 0.17 for the later time period. In contrast, responses of treprostinil (Figure 5:6B) and MRE-269 (Figure 5:6C) to increase cAMP levels remained constant between early and late time periods.

To investigate this further cAMP levels were then measured at an even later time period using the GloSensor™ assay. HLFs were stimulated with a range of concentrations of IPR agonists for 22 hours prior to the addition of the GloSensor™ reagent. Luminescence signal was then monitored for 2 hours, and the AUC was

determined at a time period corresponding to 23-24 hours after initial addition of IPR agonists (Figure 5:7). Iloprost had little efficacy in cAMP accumulation at 24 hours, whereas MRE-269 was most efficacious with E_{max} of 140 ± 18.4 % of maximal forskolin response, which is a reversal of agonist efficacy over time. In addition, treprostinil was had high efficacy, with E_{max} of 88.2 ± 8.66 % of maximal forskolin response. From this data it would be predicted that MRE-269 would have greater efficacy in inhibiting HLF proliferation whereas iloprost will be less efficacious – which was observed in Figure 3:7A and Figure 4:3C. Measuring cAMP at 24 hours has greater correlation with phenotypic changes, thus is key to measure when investigating novel targets for IPF.

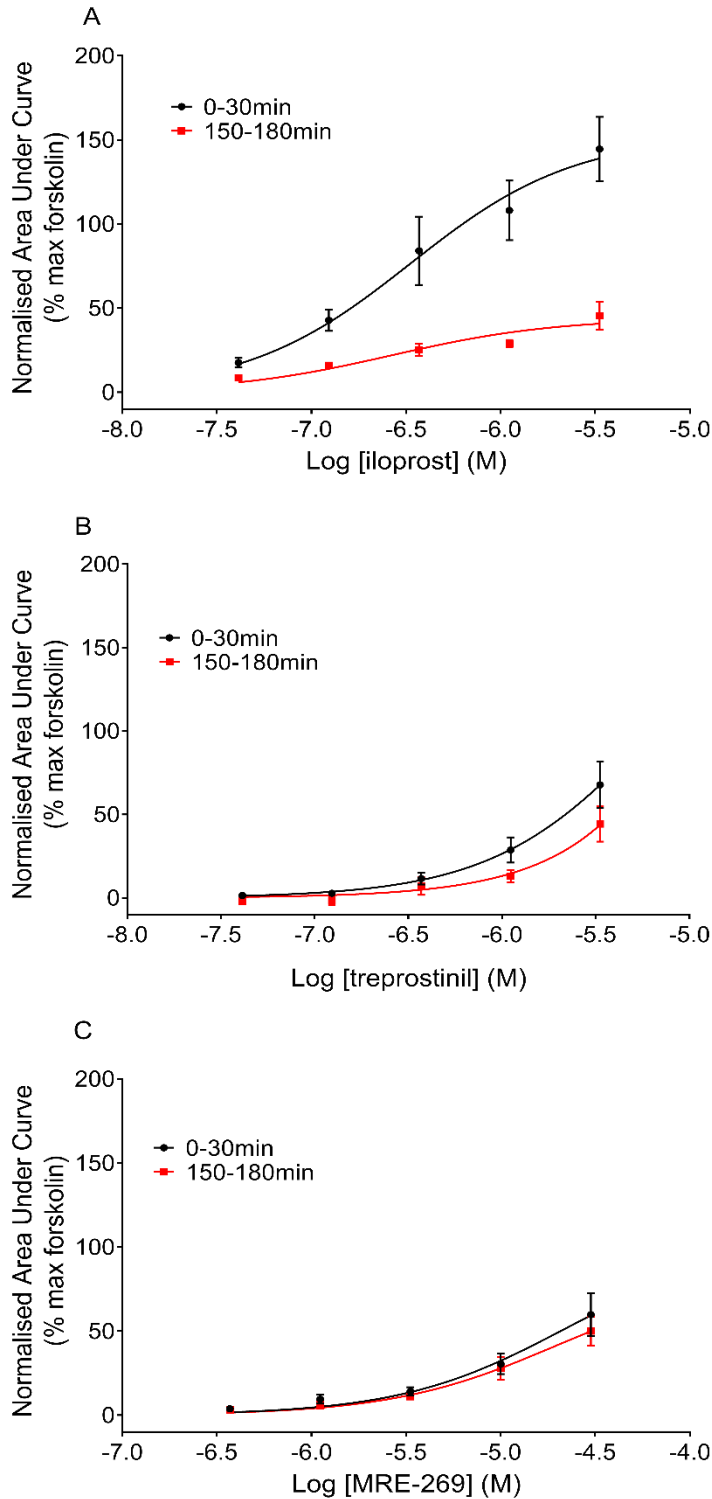


Figure 5:6 - Efficacy of cAMP accumulation over time

Concentration-response curves for cAMP accumulation after stimulation of HLFs with iloprost (A), treprostinil (B), and MRE-269 (C) at an early time period (0-30min) and late time period (150-180min) measured using GloSensor™ luminescence. Data were normalised to the AUC obtained by forskolin (10 μ M) and expressed as mean \pm SEM for 4 independent experiments. Max, maximum.

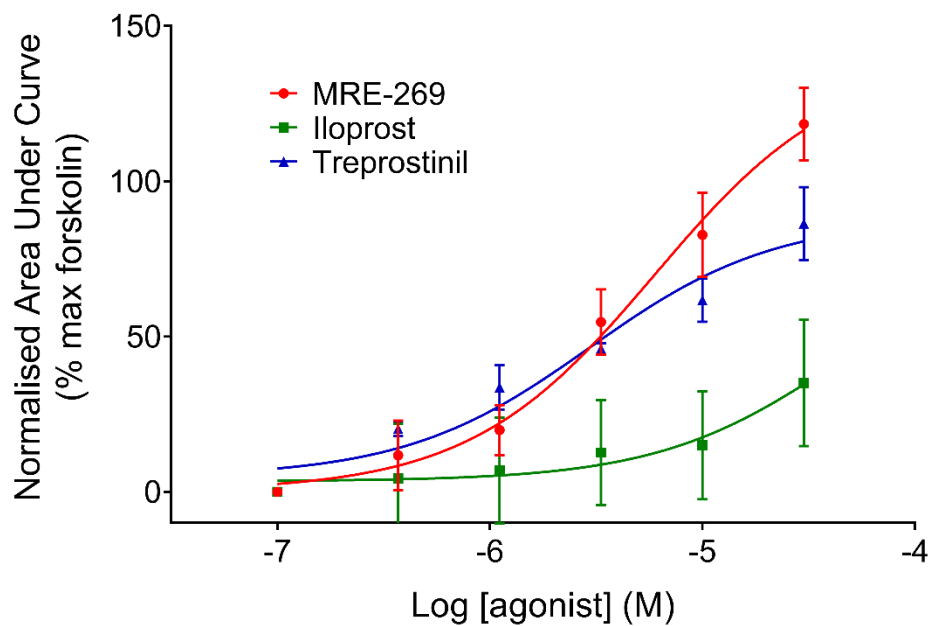


Figure 5:7 - Efficacy of cAMP accumulation at 24 hours in HLFs

Concentration-response curves of cAMP accumulation after stimulation of HLFs with iloprost, treprostinil, and MRE-269 at 24 hours measured using GloSensor™ luminescence. AUC was calculated over a 23-24 hour time period. Data were normalised to the AUC obtained by forskolin (10 μM) and expressed as mean ± SEM for 5 independent experiments. Max – maximum.

5.3 Discussion

In this chapter the importance of measuring cAMP at more phenotypically relevant time periods was established. Although MRE-269 had a low efficacy at early time points where it appears partial relative to iloprost, at later time points it had a greater efficacy than iloprost. Measuring cAMP at 24 hours resulted in the complete abolishment of cAMP signalling from iloprost, which could start to explain its lack of efficacy in inhibiting the long-term phenotypic changes in HLFs, such as proliferation and differentiation. This highlights the need to consider the temporal aspect of signalling when identifying novel therapeutics for chronic diseases such as IPF. A potentially complicating issue to address is the stability of these compounds over time. Studies investigating the stability of treprostinil, iloprost, and MRE-269 in aqueous solutions have shown they are stable for numerous days (Celia et al, 2015; Phares et al, 2003), although their stability in cell culture remains to be determined.

Using targeted FRET biosensors in conjunction with a perfusion system allowed a greater insight into the duration of action of cAMP signalling after removal of agonists. MRE-269 was shown to signal for a longer duration in the cytoplasm when signalling at the plasma membrane had already terminated. This indicates sustained cAMP signalling in the cytoplasm potentially due to signalling from internal pools of receptor, however whether they are internalised from the plasma membrane or a distinct pool activated independently from the plasma membrane receptor pool is unknown. With a large amount of recent evidence suggesting that internalised receptors are capable of continued signalling and contributing to the total cellular signalling (Calebiro et al, 2009; Irannejad et al, 2017; Irannejad et al, 2013), it could be hypothesised that MRE-269 is able to signal from intracellular compartments after receptor internalisation.

A recent study has shown that MRE-269 is a partial agonist for β -arrestin recruitment and receptor internalisation in comparison to iloprost and treprostinil (Gatfield et al, 2015). However, in this study CHO cells over expressing human IPR were utilised, and MRE-269 was identified as a full agonist for cAMP accumulation, instead of a partial agonist as observed in HLFs. Efficacy of an agonist measured by a downstream biochemical responses depends on variable factors in the target cell, such as receptor number. Many compounds that are partial agonists in tissues expressing low levels of receptors are full agonists in over-expression systems due to the high receptor number. In a cell with high receptor numbers, a partial agonist will be able to activate a larger number of receptors, and thus have the ability to generate a full response. Using radiolabelled iloprost to study receptor internalisation in human platelets, Giovanazzi and colleagues demonstrated iloprost causes receptor internalisation (Giovanazzi et al, 1997). Thus further experiments investigating β -arrestin recruitment and IPR internalisation in HLFs with endogenous levels of receptor will be advantageous to determine if receptor internalisation is a factor in the duration of action of MRE-269. Using fluorescently tagged IPR agonists will allow the monitoring of receptor internalisation through imaging of the tagged agonist, however changes to the pharmacology of the tagged agonists will need to be investigated. Furthermore, receptor internalisation may not include the internalisation of agonist, thus internalisation will not be visualised if this was the case. The tagging of receptors with fluorescent proteins whilst retaining endogenous expression levels is possible through CRISPR/Cas9 genome engineering, although it is notoriously difficult in low-passage primary human cells. Knocking out individual genes in primary HLFs using CRISPR/Cas9 technology has been demonstrated to identify genes important in driving the fibrotic response, thus further development of this methodology in HLFs could be promising (Martufi et al, 2019).

Even if MRE-269 is revealed to cause low receptor internalisation in HLFs, it could still remain possible for the longer duration of action observed after removal of agonists to be due to internal receptor signalling. Lipophilicity of agonists has been identified as a contributing factor towards the duration of signalling. It has been shown that highly lipophilic agonists can passively diffuse across the plasma membrane, bypassing the plasma membrane pool of receptors, to activate a Golgi-localised pool of β_1 adrenoceptors (Irannejad et al, 2017). Furthermore, the high lipophilicity of many LABAs has been shown to correlate to their duration of action, although this is thought to be a result of the insertion of agonists into the membrane (Anderson et al, 1994), as signalling from internalised receptors has not yet definitely demonstrated a role in duration of action. MRE-269 is more lipophilic in comparison to iloprost and treprostinil [calculated log P of MRE-269 5.3; treprostinil 4.14; iloprost 3.19; from Chemistry Development Kit; CDK (Willighagen et al, 2017)]. Thus further studies investigating the ability of IPR agonists to diffuse across cellular membranes and activate discrete pools of receptors may provide greater insight into duration of IPR signalling. Utilising fluorescently tagged IPR agonists will allow the monitoring of agonist diffusion across cellular membranes. Furthermore, the generation of nanobodies that can detect activated IPR will be beneficial in probing the activation of receptors at different intracellular locations.

One risk of long-term exposure of a GPCR agonist is desensitization of the response, most commonly via receptor phosphorylation and internalization. It has been demonstrated that the degree of agonist-induced desensitisation is related to agonist efficacy (Clark et al, 1999). For example, the high efficacy β_2 adrenoceptor agonist formoterol causes more phosphorylation and internalisation of the receptor than low-efficacy agonists such as salmeterol (Bleecker et al, 2006; Hanania et al, 2002; Moore

et al, 2007). If this observation is true for the IPR, it would be predicted that the high efficacy of iloprost and treprostinil in cAMP would lead to desensitisation of the cAMP pathway. Although this is observed with iloprost, cAMP was still detected 24 hours after stimulation with treprostinil. The idea that desensitisation of signalling is related to agonist efficacy has since been questioned, with new data suggesting that high-efficacy agonists do not necessarily cause more functional desensitisation as was once believed (Charlton, 2009; Durringer et al, 2009; Rosethorne et al, 2015). Early studies showing a relationship between agonist efficacy and receptor desensitisation were designed so that receptor occupancy was matched for each agonist, regardless of efficacy (Clark et al, 1999; Moore et al, 2007). However, in the clinic, the dose of agonists is determined based on therapeutic effect, not on receptor occupancy. More recent studies addressed this by comparing the desensitisation profile of agonists at equi-effective concentrations, rather than equal occupancy, thus more closely reflecting the clinical situation, and it is within these studies that the correlation between agonist efficacy and receptor desensitisation has been questioned (Durringer et al, 2009; Rosethorne et al, 2015). Initial studies demonstrated that desensitization of the IPR occurs within minutes after exposure to agonists and is due to agonist-induced receptor phosphorylation (Nilius et al, 2000; Smyth et al, 1996). Desensitisation of the cAMP pathway could be investigated in HLFs using FRET biosensors in conjunction with a perfusion system by re-stimulating the cells with agonist after the initial stimulation and wash out period. Furthermore, the wash-out of agonists and re-stimulation could be performed using the GloSensor™ assay.

The presence of a PDE inhibitor in the GloSensor™ assay should result in a sustained signal due the inhibition of the degradation of cAMP, yet there was still a decline in luminescence signal after the peak response which could indicate that other PDEs, not

inhibited by rolipram, may be degrading cAMP. Nonetheless, the plateau observed after treatment with IPR agonists was lower than that of forskolin, suggesting an additional explanation to the further decline in luminescence signal. The further decrease in luminescence signal could be explained by a proportion of signal decline being due to desensitisation of the cAMP pathway. As the presence of rolipram did not significantly alter the rate of decline in luminescence signal of the GloSensor™ response, it suggests that desensitisation of the cAMP pathway is more likely due to receptor desensitisation rather than PDE activity. Greater receptor desensitisation, and thus cAMP pathway desensitisation may affect the ability of agonists to increase cAMP over longer time courses, when alterations in phenotypic processes are observed.

Another potential explanation to the long duration of cAMP signalling is agonist binding kinetics. It has been proposed that the long receptor residence time - the duration that a compound is bound to its target - for a "super" agonist, C26, of the β_2 adrenoceptor contributed to the increased intrinsic activity over time (Rosethorne et al, 2016). In addition, dopamine D2 receptor ligands with slower dissociation kinetics (aripiprazole and bifeprunox) demonstrated an increase in potency over time in functional assays, which can be attributed to an increase in receptor occupancy over time (Klein Herenbrink et al, 2016). It would be interesting to investigate the binding kinetics of IPR agonists to determine if the slow rate of cAMP accumulation and the sustained cAMP signalling observed with MRE-269 can be attributed to slow binding kinetics. However, the slow kinetic binding and signalling of the "super" agonist C26 appears to be unique, as other high-affinity, LABAs have been shown to rapidly dissociate from the receptor (Sykes & Charlton, 2012).

Utilising both the targeted FRET biosensors and the GloSensor™ assay to monitor cAMP in HLFs is advantageous to help investigate temporal cAMP signalling, due to the ability to measure cAMP kinetics in distinct subcellular compartments as well as over long durations. However, comparing the time taken for cAMP to reach maximal levels when using the different assays showed a large discrepancy, with cAMP levels peaking quicker for the FRET sensors. The delay in the GloSensor™ assay is likely due to the requirement for a conformational change in the luciferase GloSensor™ following cAMP binding and the rate of the subsequent enzyme reaction that produces the luminescent signal. Although this results in the rate of cAMP accumulation measured in the GloSensor™ assay being an underestimation, the benefit of using the GloSensor™ assay over FRET biosensors is the ability to measure cAMP over a longer duration.

In conclusion, this chapter has emphasised the requirement to measure temporal changes in cAMP signalling. The ability of MRE-269 to cause sustained cytoplasmic signalling may be important in driving phenotypic changes in HLFs. The complete reversal in the relative efficacy of IPR agonists to generate cAMP at later time points versus early time points suggests the inhibition of long-term phenotypic changes requires a sustained cAMP signal, rather than an acute large cAMP response. Further studies are required to understand the mechanism behind sustained cAMP signalling with the aim to use this knowledge to develop novel IPF therapeutics.

Chapter 6 – General Discussion

IPF is a chronic, fibrotic lung disease with only a median survival of 3 years from diagnosis. Therapeutics currently available, nintedanib and pirfenidone, have been shown to slow disease progression however they cause multiple side effects that lead to patient non-compliance and a lower quality of life (King et al, 2014; Richeldi et al, 2014). Therefore, the development of efficacious and safe therapeutics for IPF are greatly needed. Numerous studies have highlighted the potential for cAMP as an inhibitor of fibrosis, with agonists that target G_s-coupled GPCRs such as the β_2 adrenoceptor, prostaglandin receptors, and the IPR, inhibiting fibrotic processes including fibroblast proliferation and differentiation (Herrmann et al, 2017; Huang et al, 2007; Lambers et al, 2018). This was confirmed in Chapter 3, where a range of agonists that target G_s-coupled GPCRs to increase cAMP were shown to inhibit fibroblast proliferation and differentiation. However, a disconnect was observed between the efficacy of agonists to generate cAMP and inhibit phenotypic processes in fibroblasts, with acute cAMP responses not being a good predictor for phenotypic outcome.

The observation that the efficacy of an agonist to increase cAMP is not a good predictor for anti-fibrotic processes could suggest that alternative pathways may be involved. Different ligands can induce distinct receptor conformations, and these conformations can lead to specific signals to promote different subset of signalling events, also known as biased signalling (Kenakin, 2012). In addition to activating pathways through G protein signalling, GPCRs have been demonstrated to signal independently of G proteins via β arrestin. β arrestin signalling has been demonstrated to activate the MAPK/ERK pathway by promoting the recruitment of Src to receptors resulting in the phosphorylation of ERK, and the activation of biological responses such as proliferation (Luttrell et al, 1999; Miller et al, 2000). If a ligand is biased towards β

arrestin over the G_s protein signalling pathway it will result in a stronger β arrestin signal, the phosphorylation of ERK, and hence proliferation. In contrast, a ligand biased towards the G_s protein signalling pathway over β arrestin will result in a stronger cAMP signal, the inhibition of phosphorylation of ERK, and hence the inhibition of proliferation. The idea that the disconnect between cAMP accumulation and inhibition of proliferation is a result of agonists activating a different pathway that promotes, rather than inhibits ERK phosphorylation, should be acknowledged, however it can somewhat be discounted as an important factor. In Chapter 3, it was shown that increasing cAMP by directly activating adenylyl cyclase fully inhibited PDGF-driven ERK phosphorylation, and the inhibition of fibroblast proliferation is dependent on the inhibition of ERK phosphorylation. Furthermore, in Chapter 4, all IPR agonists were shown to inhibit PDGF-driven ERK phosphorylation with similar efficacy and potency, suggesting that the β arrestin pathways which promotes ERK phosphorylation is not activated or has little effect on overall ERK signalling in lung fibroblasts. In addition, the effect of IPR agonists alone on ERK activity was examined in fibroblasts, and no significant changes were observed (data not shown). Therefore factors other than the ability of GPRCs to activate pathways that promote ERK phosphorylation, must be driving the disconnect between cAMP levels and inhibition of proliferation. However, to confirm the potentially limited role of IPR β arrestin signalling in fibroblasts, β arrestin based assays could be performed. There are four major in vitro assay technologies available on the market that are capable of measuring ligand-induced β-arrestin recruitment: PathHunter β-arrestin Assay (DiscoverX) (Zhao et al, 2008), Tango GPCR Assay (Thermo Fisher Scientific) (Barnea et al, 2008), LinkLight GPCR/ β-arrestin Signaling Pathway Assay (BioInvenu) (Eishingdrelo et al, 2011), and Transfluor Assay (Molecular Devices) (Oakley et al, 2002). All assays involve the expression of β arrestin fused with another protein or fragment, however, PathHunter, Tango and

LinkLight assays also require expression of the GPCR fused to another peptide or protein moiety, which means the assays could not be performed in lung fibroblasts expressing receptors at endogenous levels. A potential simpler way to investigate to role of β arrestin could be to perform knockdown experiments, such as siRNA, to probe the requirement for arrestin in cellular responses.

Two hypotheses were established to investigate why a disconnect between cAMP accumulation and inhibition of proliferation was observed; (1) the location of cAMP accumulation is important in the inhibition of fibroblast proliferation, (2) temporal regulation of cAMP signalling is important for the inhibition of fibroblast proliferation.

Spatial regulation of cAMP has been demonstrated to be highly important in regulating biological responses in highly organized cardiomyocyte cells (Schleicher & Zaccolo, 2018). Using some of the latest technology to probe cAMP signalling with greater spatial resolution we wanted to investigate if compartmentalisation of cAMP is important in mediating the level of proliferation of fibroblasts. In Chapter 4, compartmentalisation of IPR agonists' cAMP signalling in HLFs was investigated using FRET biosensors targeted to the plasma membrane, cytoplasm, and nucleus. The results showed no difference in the ability of IPR agonists to increase cAMP in either the cytoplasm or plasma membrane, however, differences in cAMP signalling in the nucleus was observed, with iloprost generating a transient cAMP response, whereas MRE-269 and treprostinil generated a sustained cAMP response. Whether nuclear cAMP signalling is important for driving the inhibition of fibroblast proliferation is yet to be determined. Using AC inhibitors it was determined that cAMP is important for inhibiting nuclear ERK activity, but whether or not that cAMP is signalling from the nucleus or other intracellular locations is unknown. To determine which compartment of cAMP plays a role in inhibiting nuclear ERK activity would require the inhibition of

cAMP accumulation in each compartment selectively whilst monitoring nuclear ERK. As far as I am aware it is not possible to block nuclear cAMP accumulation with the current tools available. FRET biosensors have affinity for cAMP, so there is the potential for the nuclear FRET biosensor to attract cAMP to the nucleus, which is another factor to consider. We do not know how cAMP accumulates in the nucleus, whether signalling from the plasma membrane or from internal receptor pools is important, or if cAMP is capable of diffusing to this compartment. Using fluorescently tagging cAMP analogues, such as 8-Fluo-cAMP, will enable the monitoring of cAMP diffusion to different cellular compartments, and comparing the diffusion patterns may enable us to probe if nuclear FRET biosensors attract cAMP from the cytoplasm.

From the work done in this thesis it cannot be determined if spatial regulation of cAMP is important for the regulation of fibroblast proliferation. The study of compartmentalised signalling in cardiomyocytes is well established due to decades worth of research, therefore tools and techniques are more established/optimised for these cells (Schleicher & Zaccolo, 2018). The importance of spatial control will differ for different cell types and physiological processes. Cardiomyocytes need to have very rapid activation/deactivation mechanisms so cAMP may need to be more tightly regulated to achieve this, whereas fibroblast proliferation takes place over many hours therefore tight spatial regulation of cAMP may not be as important. There are a whole host of targeted cAMP sensors available to probe intracellular domains that have not been utilised in this thesis, for example early endosomes (Ismail et al, 2016), Golgi (Godbole et al, 2017), and mitochondria (Di Benedetto et al, 2013), and further experiments optimising and using these sensors may help develop greater understanding of cAMP signalling in HLFs. FRET biosensors have a high affinity for cAMP, thus allowing the detection of even the smallest quantities of cAMP. However,

this limits their dynamic range, and the FRET biosensors used in this thesis were saturated due to large concentrations of cAMP after stimulating the IPR and directly activating ACs with forskolin. Numerous FRET sensors have been designed to measure cAMP signalling with greater resolution, however FRET sensors should be optimised/ designed around the cellular system for which they will be used in. “Fourth generation” cAMP FRET biosensors have been described to have increased dynamic range, however they were used in only three cell types (Hek293T cells, mouse neuroblastoma N1E-115 cells, and human osteosarcoma U2OS cells), for which the range of cAMP levels are bound to vary in comparison to fibroblasts (Klarenbeek et al, 2015). Adjusting the dynamic range of the biosensors in the compartment and cell of interest will ensure no saturation effects are observed, whilst maintaining sensitivity.

In this thesis it has been demonstrated that investigating the effect of ligands over time may be important when investigating therapeutics for chronic diseases. Using GloSensor™ cAMP technology it is possible to measure cAMP signalling over time in HLFs in response to IPR agonists (Chapter 5). Measuring the efficacy of IPR agonists to increase cAMP at a later time points (24 hours post stimulation with agonist) revealed a greater ability to predict phenotypic outcome, in comparison to measuring efficacy at early time points. This suggests that selecting the right time point for second messenger signalling is important to understand physiological readouts. Measuring second messenger levels after ligand stimulation at acute time points, e.g. 20-30 minutes, should still provide an accurate prediction of efficacy for acute physiological responses, such as vasodilation. However for chronic physiological responses, such as proliferation, measuring second messenger responses at later time points is required to ensure a more accurate prediction. Ultimately, the use of relevant phenotypic readouts, such as proliferation, would be optimal for determining the anti-fibrotic

efficacy of drugs, however the quick high-throughput screening abilities of second messenger assays make them more appealing for the screening of potentially large compound libraries. The need to starve cells in the proliferation assay to ensure all cells are in the resting state prior to stimulation makes the assay time longer (four days overall), whereas measuring cAMP (even at the more physiologically relevant time point of 24 hours) takes only two days.

The results obtained in this thesis highlight the requirement to rewrite the definition of efficacy, as measured estimates of agonist intrinsic efficacy are influenced by the time of measurement. The operational model determines agonist affinity and efficacy estimations directly from functional data. In the operational model efficacy is dependent on the total concentration of receptors and the concentration of agonist-receptor complex required to generate a half maximal response. One of the key assumptions of the operational model is that a dynamic equilibrium between the ligand and receptor has been achieved. In many cellular assays, a number of signalling events are transient and as such, reaching equilibrium can be difficult, even impossible. The shift of IPR agonist efficacy over time in Chapter 5 shows that equilibrium has not been reached and it would not be possible to determine when, or even if, equilibrium can be reached in live cells. In live cells, levels of cAMP overtime are not only dependent on receptor activation, but also receptor and pathway desensitisation that are also activated. Possibly, the only way to achieve equilibrium would be to isolate the GPCR and G protein, therefore measuring agonists' efficacy independent of a cell system. Alternatively, a concept of time needs to be factored into calculating agonist efficacy as a full efficacy reversal of IPR agonists MRE-269 and iloprost at short versus long time points is an astounding outcome.

The duration of action of GPCR signalling is mediated by factors including receptor or pathway desensitisation, and internalised signalling. What is driving the long duration of cAMP signalling of MRE-269 and treprostinil observed in Chapter 5 is unknown. The use of FRET biosensors targeted to the cytoplasm and plasma membrane showed MRE-269 continues to signal in the cytoplasm after signalling at the plasma membrane has terminated, suggesting MRE-269 may continue signal from distinct intracellular locations. The application of nanobodies that mimic G proteins to probe the location of active GPCRs has demonstrated β_2 adrenoceptors stimulated with isoprenaline and internalised in endosome are active and contribute to the overall cAMP response (Irannejad et al, 2013). Numerous tools have been developed over the years to specifically investigate β adrenoceptor signalling, whereas tools are lacking for the IPR, and whether or not a nanobody can be developed to probe activated IPRs is yet to be investigated. Although tools to probe the location of activated IPRs have not yet been developed, a nanobody that detects conformational activation of G_s has been developed (Nb37-GFP) and used to probe the location of β_2 adrenoceptor G_s signalling (Irannejad et al, 2013). Expression of Nb37-GFP in HLFs, along with the staining of cellular compartments of interest, could be used to investigate IPR activated G_s signalling at different cellular locations.

As receptor/pathway desensitisation and internalisation can have an effect on the duration of signalling, future studies investigating the effect of different agonists on the internalisation/desensitisation of the IPR could provide additional information on what makes an agonist able to signal for longer durations. To investigate the desensitisation of the IPR in HLFs, cells could be pre-treated with agonists and then washed prior to stimulation with the same agonist again. If the efficacy of the agonists to increase cAMP is lower after pre-stimulation in comparison to no pre-stimulation it

could be suggested that the cAMP pathway is desensitised. To probe if the desensitisation of the cAMP pathway is due to internalisation of the IPR, fluorescently labelled agonists could be utilised or tagged receptors, however no fluorescently tagged-IPR agonists are currently available and expression of a tagged receptor can result in alterations of signalling in the cell.

Lipophilicity is a key physiochemical parameter effecting membrane permeability, and hence drug absorption and distribution. The cell membrane consists of a phospholipid bilayer made up of phospholipid molecules. Each phospholipid molecule has a polar hydrophilic head, made up of a negatively charged phosphate group, and a non-polar hydrophobic tail, made up of fatty acid chains. Lipophilic molecules can traverse the lipid membrane however hydrophilic molecules will be repelled by the hydrophobic region. MRE-269 is more lipophilic in comparison to treprostinil and iloprost, the sustained cAMP signalling observed with MRE-269 could be due to its ability to internalise with the receptor due to its high lipophilicity. Cell membranes not only act as barriers, but also allow hydrophobic molecules to accumulate within their hydrocarbon core. A constant exchange of drug molecules between the membrane and the surrounding aqueous medium may allow the plasma membrane to act as a reservoir and prolong the exposure of the targets to a sufficiently high concentration of drug. A “diffusion microkinetic” model has been established based on the plasma membranes ability to act as a ligand reservoir and to offer a link between the long-lasting relaxation of ASM cells in response to lipophilic β_2 adrenoceptor agonists, such as formoterol and salmeterol (Anderson, 1993; Anderson et al, 1994). According to the model, the plasma membrane acts as a reservoir for formoterol where it leaks out into the aqueous medium to interact with the β_2 adrenoceptor. The model has also been used to explain long-lasting effects of salmeterol, although with a slightly different

mechanism to that of formoterol. Lipophilic salmeterol has been proposed to accumulate in the membrane and diffuse laterally within the plane of the membrane to reach the active site of the receptor (Szczuka et al, 2009). It would be interesting to investigate if the “diffusion microkinetic” model can be used to link the long-lasting effect of MRE-269 to increase cAMP. Experiments can be performed using the GloSensor™ cAMP assay as well as the proliferation assay to study the effect of agonist washout on duration of cAMP signalling and the efficacy of the inhibition of proliferation. In addition, it would be interesting to observe if addition of IPR antagonists can inhibit the long-lasting cAMP signalling, and if signalling is recovered after antagonist removal.

If prolonged signalling is an important factor for an effective anti-fibrotic agent, other compound properties, in addition to lipophilicity, can be adjusted to enhance its ability to signal for a sustained period of time. Ion trapping is a term used to describe the presence of a high concentration of drug in the membrane due to its pKa (the pH at which half of the drug is ionized) and the difference of pH across the cell membrane. As mentioned previously, the plasma membrane has a negatively charged polar surface with a hydrophobic core. Non-ionised/uncharged molecules are more lipid soluble and can readily diffuse across the cell membrane, whereas ionised/charged molecules are repelled by the polar membrane. Cells have a more acidic pH inside than outside, creating a pH gradient which can affect the distribution of drugs. Basic drugs outside the cell will be in a non-ionised state and can cross the cell membrane. Inside the cell it will become charged due to gaining a hydrogen ion because of the lower pH, and becomes unable to cross back, resulting in high intracellular concentrations of drug. In contrast, acidic drugs outside the cell will be in an ionised state, therefore cannot cross the cell membrane and are trapped in the extracellular environment.

Throughout this thesis human lung fibroblasts were used as a relevant cell type for identifying potential therapeutics for IPF. The next steps from single cell cultures could be to use more complex and pathophysiological relevant systems. Cell-cell contact between epithelial cells and fibroblasts appears to be important in signalling cascades and critical for wound repair (Selman & Pardo, 2004). Using co-culture systems, such as the one utilised by Prasad and colleagues (Prasad et al, 2014), the effect of cAMP elevating agents on both fibroblasts and epithelial cells fibrotic activity could be monitored. Fibroblasts and alveolar epithelial cells secrete their own growth factors, and TGF β secretion from epithelial cells drive fibroblast phenotype (Selman & Pardo, 2004), therefore coculturing cells together results in a more relevant model for IPF. However, the use of A549 cells rather than primary alveolar epithelial cells is an obvious limitation of this model, as procuring and maintaining primary human alveolar epithelial cells in their physiological state *ex vivo* is difficult (Prasad et al, 2014). Another more pathophysiological relevant system is the use of precision cut lung slices. Slices can be cultured from explanted human lung, diseased human lung, and animal models of disease. They contain all cell types found in the tissue of interest as well as accurately reflecting any changes to the underlying extracellular matrix associated with the disease. (Liu et al, 2019). Furthermore, precision cut lung slices have been developed from transgenic mice expressing targeted cAMP FRET biosensors (Schmidt et al, 2016). This allows the monitoring of cAMP with high spatial and temporal resolution in more complex and physiologically relevant model. However, a limitation with this is signalling in cells derived from mice will vary in comparison to cells derived from humans. Additional challenges associated with the use of precision cut lung slices include maintaining the slices *ex vivo*. During the culture period some changes in slice function, including the loss certain cell populations, will occur resulting in the need to use slices within a short time frame (Liu et al, 2019). Although the use

of precision cut lung slices has limitations, the ability to get close to a patient situation could better translate between laboratory models and the clinic.

These results highlighted a problem in the current drug discovery process, as acute second messenger responses are usually used to predict the efficacy of agonists to inhibit chronic phenotypic responses. In conclusion, to correctly identify potential therapeutics for chronic diseases like IPF the use of the correct cell type, with the correct readout, and the correct time points needs to be established. For IPF drugs targeting the cAMP pathway to inhibit fibrotic processes, compound properties that I recommend include high lipophilicity and/or a weak base at physiological pH to prolong duration of action. This would also require IPF drugs to be stable for long periods of time in the lung. Furthermore, compounds will need to be selective to G_s-coupled GPCRs to ensure no off-target effects and also not activate other pathways that can result in pro-fibrotic responses.

Chapter 7 – References

References

- Adachi, M., Fukuda, M. & Nishida, E. (1999) Two co-existing mechanisms for nuclear import of MAP kinase: passive diffusion of a monomer and active transport of a dimer. *Embo j*, 18(19), 5347-58.
- Adams, S. R., Harootunian, A. T., Buechler, Y. J., Taylor, S. S. & Tsien, R. Y. (1991) Fluorescence ratio imaging of cyclic AMP in single cells. *Nature*, 349(6311), 694-7.
- Adams, T. N., Eiswirth, C., Newton, C. A. & Battaile, J. T. (2016) Pirfenidone for Idiopathic Pulmonary Fibrosis. *Am J Respir Crit Care Med*, 194(3), 374-6.
- Agarwal, S. K. (2014) Integrins and cadherins as therapeutic targets in fibrosis. *Front Pharmacol*, 5, 131.
- Agarwal, S. R., Gratwohl, J., Cozad, M., Yang, P. C., Clancy, C. E. & Harvey, R. D. (2018) Compartmentalized cAMP Signaling Associated With Lipid Raft and Non-raft Membrane Domains in Adult Ventricular Myocytes. *Front Pharmacol*, 9, 332.
- Agarwal, S. R., MacDougall, D. A., Tyser, R., Pugh, S. D., Calaghan, S. C. & Harvey, R. D. (2011) Effects of cholesterol depletion on compartmentalized cAMP responses in adult cardiac myocytes. *J Mol Cell Cardiol*, 50(3), 500-9.
- Agarwal, S. R., Miyashiro, K., Latt, H., Ostrom, R. S. & Harvey, R. D. (2017) Compartmentalized cAMP responses to prostaglandin EP2 receptor activation in human airway smooth muscle cells. *Br J Pharmacol*, 174(16), 2784-2796.
- Ahn, S., Shenoy, S. K., Wei, H. & Lefkowitz, R. J. (2004) Differential kinetic and spatial patterns of beta-arrestin and G protein-mediated ERK activation by the angiotensin II receptor. *J Biol Chem*, 279(34), 35518-25.

Albera, C., Costabel, U., Fagan, E. A., Glassberg, M. K., Gorina, E., Lancaster, L., Lederer, D. J., Nathan, S. D., Spirig, D. & Swigris, J. J. (2016) Efficacy of pirfenidone in patients with idiopathic pulmonary fibrosis with more preserved lung function. *Eur Respir J*, 48(3), 843-51.

Alexander, S. P., Davenport, A. P., Kelly, E., Marrion, N., Peters, J. A., Benson, H. E., Faccenda, E., Pawson, A. J., Sharman, J. L., Southan, C. & Davies, J. A. (2015) The Concise Guide to PHARMACOLOGY 2015/16: G protein-coupled receptors. *Br J Pharmacol*, 172(24), 5744-869.

Alexander, S. P., Mathie, A. & Peters, J. A. (2011) Guide to Receptors and Channels (GRAC), 5th edition. *Br J Pharmacol*, 164 Suppl 1, S1-324.

Ali, F. Y., Egan, K., FitzGerald, G. A., Desvergne, B., Wahli, W., Bishop-Bailey, D., Warner, T. D. & Mitchell, J. A. (2006) Role of prostacyclin versus peroxisome proliferator-activated receptor beta receptors in prostacyclin sensing by lung fibroblasts. *Am J Respir Cell Mol Biol*, 34(2), 242-6.

Allen, J. A., Yu, J. Z., Dave, R. H., Bhatnagar, A., Roth, B. L. & Rasenick, M. M. (2009) Caveolin-1 and lipid microdomains regulate Gs trafficking and attenuate Gs/adenylyl cyclase signaling. *Mol Pharmacol*, 76(5), 1082-93.

Allen, J. T. & Spiteri, M. A. (2002) Growth factors in idiopathic pulmonary fibrosis: relative roles. *Respir Res*, 3, 13.

Allen, R. J., Porte, J., Braybrooke, R., Flores, C., Fingerlin, T. E., Oldham, J. M., Guillen-Guio, B., Ma, S. F., Okamoto, T., John, A. E., Obeidat, M., Yang, I. V., Henry, A., Hubbard, R. B., Navaratnam, V., Saini, G., Thompson, N., Booth, H. L., Hart, S. P., Hill, M. R., Hirani, N., Maher, T. M., McNulty, R. J., Millar, A. B., Molyneaux, P. L., Parfrey, H., Rassel, D. M., Whyte, M. K. B., Fahy, W. A., Marshall, R. P., Oballa, E., Bosse, Y., Nickle, D. C., Sin, D. D., Timens, W., Shrine, N., Sayers, I., Hall, I. P., Noth, I., Schwartz, D. A.,

Tobin, M. D., Wain, L. V. & Jenkins, R. G. (2017) Genetic variants associated with susceptibility to idiopathic pulmonary fibrosis in people of European ancestry: a genome-wide association study. *Lancet Respir Med*, 5(11), 869-880.

Anderson, G. P. (1993) Formoterol: pharmacology, molecular basis of agonism, and mechanism of long duration of a highly potent and selective beta 2-adrenoceptor agonist bronchodilator. *Life Sci*, 52(26), 2145-60.

Anderson, G. P., Linden, A. & Rabe, K. F. (1994) Why are long-acting beta-adrenoceptor agonists long-acting? *Eur Respir J*, 7(3), 569-78.

Andrae, J., Gallini, R. & Betsholtz, C. (2008) Role of platelet-derived growth factors in physiology and medicine. *Genes Dev*, 22(10), 1276-312.

Antoniades, H. N., Bravo, M. A., Avila, R. E., Galanopoulos, T., Neville-Golden, J., Maxwell, M. & Selman, M. (1990) Platelet-derived growth factor in idiopathic pulmonary fibrosis. *J Clin Invest*, 86(4), 1055-64.

Antoniou, K. M., Hansell, D. M., Rubens, M. B., Marten, K., Desai, S. R., Siafakas, N. M., Nicholson, A. G., du Bois, R. M. & Wells, A. U. (2008) Idiopathic pulmonary fibrosis: outcome in relation to smoking status. *Am J Respir Crit Care Med*, 177(2), 190-4.

Armanios, M. Y., Chen, J. J., Cogan, J. D., Alder, J. K., Ingersoll, R. G., Markin, C., Lawson, W. E., Xie, M., Vulto, I., Phillips, J. A., 3rd, Lansdorp, P. M., Greider, C. W. & Loyd, J. E. (2007) Telomerase mutations in families with idiopathic pulmonary fibrosis. *N Engl J Med*, 356(13), 1317-26.

Asaki, T., Kuwano, K., Morrison, K., Gatfield, J., Hamamoto, T. & Clozel, M. (2015) Selexipag: An Oral and Selective IP Prostacyclin Receptor Agonist for the Treatment of Pulmonary Arterial Hypertension. *J Med Chem*, 58(18), 7128-37.

Attramadal, H., Arriza, J. L., Aoki, C., Dawson, T. M., Codina, J., Kwatra, M. M., Snyder, S. H., Caron, M. G. & Lefkowitz, R. J. (1992) Beta-arrestin2, a novel member of the arrestin/beta-arrestin gene family. *J Biol Chem*, 267(25), 17882-90.

Bacskai, B. J., Hochner, B., Mahaut-Smith, M., Adams, S. R., Kaang, B. K., Kandel, E. R. & Tsien, R. Y. (1993) Spatially resolved dynamics of cAMP and protein kinase A subunits in *Aplysia* sensory neurons. *Science*, 260(5105), 222-6.

Baker, J. G., Hall, I. P. & Hill, S. J. (2004) Temporal characteristics of cAMP response element-mediated gene transcription: requirement for sustained cAMP production. *Mol Pharmacol*, 65(4), 986-98.

Balmano, K. & Cook, S. J. (1999) Sustained MAP kinase activation is required for the expression of cyclin D1, p21Cip1 and a subset of AP-1 proteins in CCL39 cells. *Oncogene*, 18(20), 3085-97.

Barnea, G., Strapps, W., Herrada, G., Berman, Y., Ong, J., Kloss, B., Axel, R. & Lee, K. J. (2008) The genetic design of signaling cascades to record receptor activation. *Proc Natl Acad Sci U S A*, 105(1), 64-9.

Barrett, S. D., Bridges, A. J., Dudley, D. T., Saltiel, A. R., Fergus, J. H., Flamme, C. M., Delaney, A. M., Kaufman, M., LePage, S., Leopold, W. R., Przybranowski, S. A., Sebolt-Leopold, J., Van Becelaere, K., Doherty, A. M., Kennedy, R. M., Marston, D., Howard, W. A., Jr., Smith, Y., Warmus, J. S. & Tecle, H. (2008) The discovery of the benzhydroxamate MEK inhibitors CI-1040 and PD 0325901. *Bioorg Med Chem Lett*, 18(24), 6501-4.

Bellou, V., Belbasis, L., Konstantinidis, A. & Evangelou, E. (2017) Tobacco smoking and risk for idiopathic pulmonary fibrosis: a prospective cohort study in UK Biobank. *European Respiratory Journal*, 50(suppl 61), PA4887.

- Bender, A. T. & Beavo, J. A. (2006) Cyclic nucleotide phosphodiesterases: molecular regulation to clinical use. *Pharmacol Rev*, 58(3), 488-520.
- Benovic, J. L. & von Zastrow, M. (2014) Editorial overview: Cell regulation: The ins and outs of G protein-coupled receptors. *Curr Opin Cell Biol*, 27, v-vi.
- Berti, D. A. & Seger, R. (2017) The Nuclear Translocation of ERK. *Methods Mol Biol*, 1487, 175-194.
- Bethani, I., Skanland, S. S., Dikic, I. & Acker-Palmer, A. (2010) Spatial organization of transmembrane receptor signalling. *Embo j*, 29(16), 2677-88.
- Beyer, C. & Distler, J. H. (2013) Tyrosine kinase signaling in fibrotic disorders: Translation of basic research to human disease. *Biochim Biophys Acta*, 1832(7), 897-904.
- Binkowski, B., Fan, F. & Wood, K. (2009) Engineered luciferases for molecular sensing in living cells. *Curr Opin Biotechnol*, 20(1), 14-8.
- Birrell, M. A., Bonvini, S. J., Wortley, M. A., Buckley, J., Yew-Booth, L., Maher, S. A., Dale, N., Dubuis, E. D. & Belvisi, M. G. (2015) The role of adenylyl cyclase isoform 6 in beta-adrenoceptor signalling in murine airways. *Br J Pharmacol*, 172(1), 131-41.
- Bjarnadottir, T. K., Fredriksson, R., Hoglund, P. J., Gloriam, D. E., Lagerstrom, M. C. & Schioth, H. B. (2004) The human and mouse repertoire of the adhesion family of G-protein-coupled receptors. *Genomics*, 84(1), 23-33.
- Bjarnadottir, T. K., Fredriksson, R. & Schioth, H. B. (2005) The gene repertoire and the common evolutionary history of glutamate, pheromone (V2R), taste(1) and other related G protein-coupled receptors. *Gene*, 362, 70-84.

Bjarnadottir, T. K., Gloriam, D. E., Hellstrand, S. H., Kristiansson, H., Fredriksson, R. & Schioth, H. B. (2006) Comprehensive repertoire and phylogenetic analysis of the G protein-coupled receptors in human and mouse. *Genomics*, 88(3), 263-73.

Black, J. B., Premont, R. T. & Daaka, Y. (2016) Feedback regulation of G protein-coupled receptor signaling by GRKs and arrestins. *Semin Cell Dev Biol*, 50, 95-104.

Bleecker, E. R., Yancey, S. W., Baitinger, L. A., Edwards, L. D., Klotsman, M., Anderson, W. H. & Dorinsky, P. M. (2006) Salmeterol response is not affected by beta2-adrenergic receptor genotype in subjects with persistent asthma. *J Allergy Clin Immunol*, 118(4), 809-16.

Bogard, A. S., Adris, P. & Ostrom, R. S. (2012) Adenylyl cyclase 2 selectively couples to E prostanoid type 2 receptors, whereas adenylyl cyclase 3 is not receptor-regulated in airway smooth muscle. *J Pharmacol Exp Ther*, 342(2), 586-95.

Bonner, J. C. (2004) Regulation of PDGF and its receptors in fibrotic diseases. *Cytokine Growth Factor Rev*, 15(4), 255-73.

Borner, S., Schwede, F., Schlipp, A., Berisha, F., Calebiro, D., Lohse, M. J. & Nikolaev, V. O. (2011) FRET measurements of intracellular cAMP concentrations and cAMP analog permeability in intact cells. *Nat Protoc*, 6(4), 427-38.

Borok, Z., Gillissen, A., Buhl, R., Hoyt, R. F., Hubbard, R. C., Ozaki, T., Rennard, S. I. & Crystal, R. G. (1991) Augmentation of functional prostaglandin E levels on the respiratory epithelial surface by aerosol administration of prostaglandin E. *Am Rev Respir Dis*, 144(5), 1080-4.

Bozyk, P. D. & Moore, B. B. (2011) Prostaglandin E2 and the pathogenesis of pulmonary fibrosis. *Am J Respir Cell Mol Biol*, 45(3), 445-52.

Breckler, M., Berthouze, M., Laurent, A. C., Crozatier, B., Morel, E. & Lezoualc'h, F. (2011) Rap-linked cAMP signaling Epac proteins: compartmentation, functioning and disease implications. *Cell Signal*, 23(8), 1257-66.

Brostrom, C. O., Corbin, J. D., King, C. A. & Krebs, E. G. (1971) Interaction of the subunits of adenosine 3':5'-cyclic monophosphate-dependent protein kinase of muscle. *Proc Natl Acad Sci U S A*, 68(10), 2444-7.

Brunet, A., Roux, D., Lenormand, P., Dowd, S., Keyse, S. & Pouyssegur, J. (1999) Nuclear translocation of p42/p44 mitogen-activated protein kinase is required for growth factor-induced gene expression and cell cycle entry. *Embo j*, 18(3), 664-74.

Brunner, D., Frank, J., Appl, H., Schoffl, H., Pfaller, W. & Gstraunthaler, G. (2010) Serum-free cell culture: the serum-free media interactive online database. *Altex*, 27(1), 53-62.

Brunton, L. L., Hayes, J. S. & Mayer, S. E. (1981) Functional compartmentation of cyclic AMP and protein kinase in heart. *Adv Cyclic Nucleotide Res*, 14, 391-7.

Budhiraja, R., Tuder, R. M. & Hassoun, P. M. (2004) Endothelial dysfunction in pulmonary hypertension. *Circulation*, 109(2), 159-65.

Buonomo, R., Giacco, F., Vasaturo, A., Caserta, S., Guido, S., Pagliara, V., Garbi, C., Mansueto, G., Cassese, A., Perruolo, G., Oriente, F., Miele, C., Beguinot, F. & Formisano, P. (2012) PED/PEA-15 controls fibroblast motility and wound closure by ERK1/2-dependent mechanisms. *J Cell Physiol*, 227(5), 2106-16.

Calebiro, D., Nikolaev, V. O., Gagliani, M. C., de Filippis, T., Dees, C., Tacchetti, C., Persani, L. & Lohse, M. J. (2009) Persistent cAMP-signals triggered by internalized G-protein-coupled receptors. *PLoS Biol*, 7(8), e1000172.

Casar, B. & Crespo, P. (2016) ERK Signals: Scaffolding Scaffolds? *Front Cell Dev Biol*, 4, 49.

Castranova, V., Rabovsky, J., Tucker, J. H. & Miles, P. R. (1988) The alveolar type II epithelial cell: a multifunctional pneumocyte. *Toxicol Appl Pharmacol*, 93(3), 472-83.

Caughey, G. E., Cleland, L. G., Penglis, P. S., Gamble, J. R. & James, M. J. (2001) Roles of cyclooxygenase (COX)-1 and COX-2 in prostanoid production by human endothelial cells: selective up-regulation of prostacyclin synthesis by COX-2. *J Immunol*, 167(5), 2831-8.

Celia, C., Locatelli, M., Cilurzo, F., Cosco, D., Gentile, E., Scalise, D., Carafa, M., Ventura, C. A., Fleury, M., Tisserand, C., Barbacane, R. C., Fresta, M., Di Marzio, L. & Paolino, D. (2015) Long Term Stability Evaluation of Prostacyclin Released from Biomedical Device through Turbiscan Lab Expert. *Med Chem*, 11(4), 391-9.

Celli, B. R. & MacNee, W. (2004) Standards for the diagnosis and treatment of patients with COPD: a summary of the ATS/ERS position paper. *Eur Respir J*, 23(6), 932-46.

Charlton, S. J. (2009) Agonist efficacy and receptor desensitization: from partial truths to a fuller picture. *Br J Pharmacol*, 158(1), 165-8.

Chaudhary, N. I., Roth, G. J., Hilberg, F., Muller-Quernheim, J., Prasse, A., Zissel, G., Schnapp, A. & Park, J. E. (2007) Inhibition of PDGF, VEGF and FGF signalling attenuates fibrosis. *Eur Respir J*, 29(5), 976-85.

Cheng, X., Ji, Z., Tsalkova, T. & Mei, F. (2008) Epac and PKA: a tale of two intracellular cAMP receptors. *Acta Biochim Biophys Sin (Shanghai)*, 40(7), 651-62.

Cherezov, V., Rosenbaum, D. M., Hanson, M. A., Rasmussen, S. G., Thian, F. S., Kobilka, T. S., Choi, H. J., Kuhn, P., Weis, W. I., Kobilka, B. K. & Stevens, R. C. (2007) High-

resolution crystal structure of an engineered human beta2-adrenergic G protein-coupled receptor. *Science*, 318(5854), 1258-65.

Choi, J. W., Herr, D. R., Noguchi, K., Yung, Y. C., Lee, C. W., Mutoh, T., Lin, M. E., Teo, S. T., Park, K. E., Mosley, A. N. & Chun, J. (2010) LPA receptors: subtypes and biological actions. *Annu Rev Pharmacol Toxicol*, 50, 157-86.

Civitelli, R., Bacskai, B. J., Mahaut-Smith, M. P., Adams, S. R., Avioli, L. V. & Tsien, R. Y. (1994) Single-cell analysis of cyclic AMP response to parathyroid hormone in osteoblastic cells. *J Bone Miner Res*, 9(9), 1407-17.

Clark, R. B., Knoll, B. J. & Barber, R. (1999) Partial agonists and G protein-coupled receptor desensitization. *Trends Pharmacol Sci*, 20(7), 279-86.

Conte, E., Gili, E., Fagone, E., Fruciano, M., Iemmolo, M. & Vancheri, C. (2014) Effect of pirfenidone on proliferation, TGF-beta-induced myofibroblast differentiation and fibrogenic activity of primary human lung fibroblasts. *Eur J Pharm Sci*, 58, 13-9.

Cook, S. J. & McCormick, F. (1993) Inhibition by cAMP of Ras-dependent activation of Raf. *Science*, 262(5136), 1069-72.

Cooper, D. M. & Tabbasum, V. G. (2014) Adenylate cyclase-centred microdomains. *Biochem J*, 462(2), 199-213.

Corbin, J. D., Sugden, P. H., Lincoln, T. M. & Keely, S. L. (1977) Compartmentalization of adenosine 3':5'-monophosphate and adenosine 3':5'-monophosphate-dependent protein kinase in heart tissue. *J Biol Chem*, 252(11), 3854-61.

Corboz, M. R., Zhang, J., LaSala, D., DiPetrillo, K., Li, Z., Malinin, V., Brower, J., Kuehl, P. J., Barrett, T. E., Perkins, W. R. & Chapman, R. W. (2018) Therapeutic administration of inhaled INS1009, a treprostinil prodrug formulation, inhibits bleomycin-induced pulmonary fibrosis in rats. *Pulm Pharmacol Ther*, 49, 95-103.

Cortijo, J., Iranzo, A., Milara, X., Mata, M., Cerda-Nicolas, M., Ruiz-Sauri, A., Tenor, H., Hatzelmann, A. & Morcillo, E. J. (2009) Roflumilast, a phosphodiesterase 4 inhibitor, alleviates bleomycin-induced lung injury. *Br J Pharmacol*, 156(3), 534-44.

Costa, M., Marchi, M., Cardarelli, F., Roy, A., Beltram, F., Maffei, L. & Ratto, G. M. (2006) Dynamic regulation of ERK2 nuclear translocation and mobility in living cells. *J Cell Sci*, 119(Pt 23), 4952-63.

Coward, W. R., Watts, K., Feghali-Bostwick, C. A., Knox, A. & Pang, L. (2009) Defective histone acetylation is responsible for the diminished expression of cyclooxygenase 2 in idiopathic pulmonary fibrosis. *Mol Cell Biol*, 29(15), 4325-39.

Crestani, B., Huggins, J. T., Kaye, M., Costabel, U., Glaspole, I., Ogura, T., Song, J. W., Stansen, W., Quaresma, M., Stowasser, S. & Kreuter, M. (2019) Long-term safety and tolerability of nintedanib in patients with idiopathic pulmonary fibrosis: results from the open-label extension study, INPULSIS-ON. *Lancet Respir Med*, 7(1), 60-68.

Cruz-Gervis, R., Stecenko, A. A., Dworski, R., Lane, K. B., Loyd, J. E., Pierson, R., King, G. & Brigham, K. L. (2002) Altered prostanoid production by fibroblasts cultured from the lungs of human subjects with idiopathic pulmonary fibrosis. *Respir Res*, 3, 17.

Currie, K. P. (2010) G protein modulation of CaV2 voltage-gated calcium channels. *Channels (Austin)*, 4(6), 497-509.

Davare, M. A., Avdonin, V., Hall, D. D., Peden, E. M., Burette, A., Weinberg, R. J., Horne, M. C., Hoshi, T. & Hell, J. W. (2001) A beta2 adrenergic receptor signaling complex assembled with the Ca²⁺ channel Cav1.2. *Science*, 293(5527), 98-101.

de Rooij, J., Zwartkruis, F. J., Verheijen, M. H., Cool, R. H., Nijman, S. M., Wittinghofer, A. & Bos, J. L. (1998) Epac is a Rap1 guanine-nucleotide-exchange factor directly activated by cyclic AMP. *Nature*, 396(6710), 474-7.

Deak, M., Clifton, A. D., Lucocq, L. M. & Alessi, D. R. (1998) Mitogen- and stress-activated protein kinase-1 (MSK1) is directly activated by MAPK and SAPK2/p38, and may mediate activation of CREB. *Embo j*, 17(15), 4426-41.

Dell'Acqua, M. L., Faux, M. C., Thorburn, J., Thorburn, A. & Scott, J. D. (1998) Membrane-targeting sequences on AKAP79 bind phosphatidylinositol-4, 5-bisphosphate. *Embo j*, 17(8), 2246-60.

Dema, A., Perets, E., Schulz, M. S., Deak, V. A. & Klussmann, E. (2015) Pharmacological targeting of AKAP-directed compartmentalized cAMP signalling. *Cell Signal*, 27(12), 2474-87.

Desmouliere, A., Geinoz, A., Gabbiani, F. & Gabbiani, G. (1993) Transforming growth factor-beta 1 induces alpha-smooth muscle actin expression in granulation tissue myofibroblasts and in quiescent and growing cultured fibroblasts. *J Cell Biol*, 122(1), 103-11.

Dessauer, C. W., Watts, V. J., Ostrom, R. S., Conti, M., Dove, S. & Seifert, R. (2017) International Union of Basic and Clinical Pharmacology. Cl. Structures and Small Molecule Modulators of Mammalian Adenylyl Cyclases. *Pharmacol Rev*, 69(2), 93-139.

Dhillon, A. S., Pollock, C., Steen, H., Shaw, P. E., Mischak, H. & Kolch, W. (2002) Cyclic AMP-dependent kinase regulates Raf-1 kinase mainly by phosphorylation of serine 259. *Mol Cell Biol*, 22(10), 3237-46.

Di Benedetto, G., Scalzotto, E., Mongillo, M. & Pozzan, T. (2013) Mitochondrial Ca²⁺(+) uptake induces cyclic AMP generation in the matrix and modulates organelle ATP levels. *Cell Metab*, 17(6), 965-75.

Diaz de Leon, A., Cronkhite, J. T., Katzenstein, A. L., Godwin, J. D., Raghu, G., Glazer, C. S., Rosenblatt, R. L., Girod, C. E., Garrity, E. R., Xing, C. & Garcia, C. K. (2010) Telomere lengths, pulmonary fibrosis and telomerase (TERT) mutations. *PLoS One*, 5(5), e10680.

DiPilato, L. M., Cheng, X. & Zhang, J. (2004) Fluorescent indicators of cAMP and Epac activation reveal differential dynamics of cAMP signaling within discrete subcellular compartments. *Proc Natl Acad Sci U S A*, 101(47), 16513-8.

Diviani, D., Langeberg, L. K., Doxsey, S. J. & Scott, J. D. (2000) Pericentrin anchors protein kinase A at the centrosome through a newly identified RII-binding domain. *Curr Biol*, 10(7), 417-20.

Diviani, D., Soderling, J. & Scott, J. D. (2001) AKAP-Lbc anchors protein kinase A and nucleates G α 12-selective Rho-mediated stress fiber formation. *J Biol Chem*, 276(47), 44247-57.

Dobrowolski, S., Harter, M. & Stacey, D. W. (1994) Cellular ras activity is required for passage through multiple points of the G₀/G₁ phase in BALB/c 3T3 cells. *Mol Cell Biol*, 14(8), 5441-9.

Downes, G. B. & Gautam, N. (1999) The G protein subunit gene families. *Genomics*, 62(3), 544-52.

Dror, R. O., Mildorf, T. J., Hilger, D., Manglik, A., Borhani, D. W., Arlow, D. H., Philippsen, A., Villanueva, N., Yang, Z., Lerch, M. T., Hubbell, W. L., Kobilka, B. K., Sunahara, R. K. & Shaw, D. E. (2015) SIGNAL TRANSDUCTION. Structural basis for nucleotide exchange in heterotrimeric G proteins. *Science*, 348(6241), 1361-5.

Dumaz, N., Light, Y. & Marais, R. (2002) Cyclic AMP blocks cell growth through Raf-1-dependent and Raf-1-independent mechanisms. *Mol Cell Biol*, 22(11), 3717-28.

Dumaz, N. & Marais, R. (2003) Protein kinase A blocks Raf-1 activity by stimulating 14-3-3 binding and blocking Raf-1 interaction with Ras. *J Biol Chem*, 278(32), 29819-23.

Dunkern, T. R., Feurstein, D., Rossi, G. A., Sabatini, F. & Hatzelmann, A. (2007) Inhibition of TGF-beta induced lung fibroblast to myofibroblast conversion by phosphodiesterase inhibiting drugs and activators of soluble guanylyl cyclase. *Eur J Pharmacol*, 572(1), 12-22.

Duringer, C., Grundstrom, G., Gurcan, E., Dainty, I. A., Lawson, M., Korn, S. H., Jerre, A., Hakansson, H. F., Wieslander, E., Fredriksson, K., Skold, C. M., Lofdahl, M., Lofdahl, C. G., Nicholls, D. J. & Silberstein, D. S. (2009) Agonist-specific patterns of beta 2-adrenoceptor responses in human airway cells during prolonged exposure. *Br J Pharmacol*, 158(1), 169-79.

Ebisuya, M., Kondoh, K. & Nishida, E. (2005) The duration, magnitude and compartmentalization of ERK MAP kinase activity: mechanisms for providing signaling specificity. *J Cell Sci*, 118(Pt 14), 2997-3002.

Eckle, T., Grenz, A., Laucher, S. & Eltzschig, H. K. (2008) A2B adenosine receptor signaling attenuates acute lung injury by enhancing alveolar fluid clearance in mice. *J Clin Invest*, 118(10), 3301-15.

Eichel, K., Jullie, D. & von Zastrow, M. (2016) beta-Arrestin drives MAP kinase signalling from clathrin-coated structures after GPCR dissociation. *Nat Cell Biol*, 18(3), 303-10.

Eishingdrelo, H., Cai, J., Weissensee, P., Sharma, P., Tocci, M. J. & Wright, P. S. (2011) A cell-based protein-protein interaction method using a permuted luciferase reporter. *Curr Chem Genomics*, 5, 122-8.

Ek, B. & Heldin, C. H. (1982) Characterization of a tyrosine-specific kinase activity in human fibroblast membranes stimulated by platelet-derived growth factor. *J Biol Chem*, 257(17), 10486-92.

Esposito, G., Jaiswal, B. S., Xie, F., Krajnc-Franken, M. A., Robben, T. J., Strik, A. M., Kuil, C., Philipson, R. L., van Duin, M., Conti, M. & Gossen, J. A. (2004) Mice deficient for soluble adenylyl cyclase are infertile because of a severe sperm-motility defect. *Proc Natl Acad Sci U S A*, 101(9), 2993-8.

Fabbri, L. M., Calverley, P. M., Izquierdo-Alonso, J. L., Bundschuh, D. S., Brose, M., Martinez, F. J. & Rabe, K. F. (2009) Roflumilast in moderate-to-severe chronic obstructive pulmonary disease treated with longacting bronchodilators: two randomised clinical trials. *Lancet*, 374(9691), 695-703.

Falcetti, E., Flavell, D. M., Staels, B., Tinker, A., Haworth, S. G. & Clapp, L. H. (2007) IP receptor-dependent activation of PPARgamma by stable prostacyclin analogues. *Biochem Biophys Res Commun*, 360(4), 821-7.

Falcetti, E., Hall, S. M., Phillips, P. G., Patel, J., Morrell, N. W., Haworth, S. G. & Clapp, L. H. (2010) Smooth muscle proliferation and role of the prostacyclin (IP) receptor in idiopathic pulmonary arterial hypertension. *Am J Respir Crit Care Med*, 182(9), 1161-70.

Fan, F., Binkowski, B. F., Butler, B. L., Stecha, P. F., Lewis, M. K. & Wood, K. V. (2008) Novel genetically encoded biosensors using firefly luciferase. *ACS Chem Biol*, 3(6), 346-51.

Farkas, L., Farkas, D., Ask, K., Moller, A., Gauldie, J., Margetts, P., Inman, M. & Kolb, M. (2009) VEGF ameliorates pulmonary hypertension through inhibition of endothelial apoptosis in experimental lung fibrosis in rats. *J Clin Invest*, 119(5), 1298-311.

Farkas, L., Gauldie, J., Voelkel, N. F. & Kolb, M. (2011) Pulmonary hypertension and idiopathic pulmonary fibrosis: a tale of angiogenesis, apoptosis, and growth factors. *Am J Respir Cell Mol Biol*, 45(1), 1-15.

Fehrenbach, H. (2001) Alveolar epithelial type II cell: defender of the alveolus revisited. *Respir Res*, 2(1), 33-46.

Fernandez, I. E. & Eickelberg, O. (2012) The impact of TGF-beta on lung fibrosis: from targeting to biomarkers. *Proc Am Thorac Soc*, 9(3), 111-6.

Ferrandon, S., Feinstein, T. N., Castro, M., Wang, B., Bouley, R., Potts, J. T., Gardella, T. J. & Vilardaga, J. P. (2009) Sustained cyclic AMP production by parathyroid hormone receptor endocytosis. *Nat Chem Biol*, 5(10), 734-42.

Fingerlin, T. E., Murphy, E., Zhang, W., Peljto, A. L., Brown, K. K., Steele, M. P., Loyd, J. E., Cosgrove, G. P., Lynch, D., Groshong, S., Collard, H. R., Wolters, P. J., Bradford, W. Z., Kossen, K., Seiwert, S. D., du Bois, R. M., Garcia, C. K., Devine, M. S., Gudmundsson, G., Isaksson, H. J., Kaminski, N., Zhang, Y., Gibson, K. F., Lancaster, L. H., Cogan, J. D., Mason, W. R., Maher, T. M., Molyneaux, P. L., Wells, A. U., Moffatt, M. F., Selman, M., Pardo, A., Kim, D. S., Crapo, J. D., Make, B. J., Regan, E. A., Walek, D. S., Daniel, J. J., Kamatani, Y., Zelenika, D., Smith, K., McKean, D., Pedersen, B. S., Talbert, J., Kidd, R. N., Markin, C. R., Beckman, K. B., Lathrop, M., Schwarz, M. I. & Schwartz, D. A. (2013) Genome-wide association study identifies multiple susceptibility loci for pulmonary fibrosis. *Nat Genet*, 45(6), 613-20.

Fisch, A., Tobusch, K., Veit, K., Meyer, J. & Darius, H. (1997) Prostacyclin receptor desensitization is a reversible phenomenon in human platelets. *Circulation*, 96(3), 756-60.

Fitzgerald, M. F. & Fox, J. C. (2007) Emerging trends in the therapy of COPD: bronchodilators as mono- and combination therapies. *Drug Discov Today*, 12(11-12), 472-8.

Formstecher, E., Ramos, J. W., Fauquet, M., Calderwood, D. A., Hsieh, J. C., Canton, B., Nguyen, X. T., Barnier, J. V., Camonis, J., Ginsberg, M. H. & Chneiweiss, H. (2001) PEA-15 mediates cytoplasmic sequestration of ERK MAP kinase. *Dev Cell*, 1(2), 239-50.

Fredriksson, L., Li, H. & Eriksson, U. (2004) The PDGF family: four gene products form five dimeric isoforms. *Cytokine Growth Factor Rev*, 15(4), 197-204.

Fredriksson, R., Lagerstrom, M. C., Lundin, L. G. & Schioth, H. B. (2003) The G-protein-coupled receptors in the human genome form five main families. Phylogenetic analysis, paralogon groups, and fingerprints. *Mol Pharmacol*, 63(6), 1256-72.

Fritz, R. D., Letzelter, M., Reimann, A., Martin, K., Fusco, L., Ritsma, L., Ponsioen, B., Fluri, E., Schulte-Merker, S., van Rheenen, J. & Pertz, O. (2013) A versatile toolkit to produce sensitive FRET biosensors to visualize signaling in time and space. *Sci Signal*, 6(285), rs12.

Fukuda, M., Gotoh, Y. & Nishida, E. (1997) Interaction of MAP kinase with MAP kinase kinase: its possible role in the control of nucleocytoplasmic transport of MAP kinase. *Embo j*, 16(8), 1901-8.

Fukuhara, S., Sakurai, A., Sano, H., Yamagishi, A., Somekawa, S., Takakura, N., Saito, Y., Kangawa, K. & Mochizuki, N. (2005) Cyclic AMP potentiates vascular endothelial cadherin-mediated cell-cell contact to enhance endothelial barrier function through an Epac-Rap1 signaling pathway. *Mol Cell Biol*, 25(1), 136-46.

Garrison, G., Huang, S. K., Okunishi, K., Scott, J. P., Kumar Penke, L. R., Scruggs, A. M. & Peters-Golden, M. (2013) Reversal of myofibroblast differentiation by prostaglandin E(2). *Am J Respir Cell Mol Biol*, 48(5), 550-8.

Gatfield, J., Menyhart, K., Morrison, K. & Nayler, O. (2015) The non-prostanoid prostacyclin receptor agonist act-333679, the active metabolite of selexipag, is characterized by low beta-arrestin recruitment and receptor internalization activity. *Journal of the American College of Cardiology*, 65(10).

Gatfield, J., Menyhart, K., Wanner, D., Gnerre, C., Monnier, L., Morrison, K., Hess, P., Iglarz, M., Clozel, M. & Nayler, O. (2017) Selexipag Active Metabolite ACT-333679 Displays Strong Anticontractile and Antiremodeling Effects but Low beta-Arrestin Recruitment and Desensitization Potential. *J Pharmacol Exp Ther*, 362(1), 186-199.

Georges, P. C., Hui, J. J., Gombos, Z., McCormick, M. E., Wang, A. Y., Uemura, M., Mick, R., Janmey, P. A., Furth, E. E. & Wells, R. G. (2007) Increased stiffness of the rat liver precedes matrix deposition: implications for fibrosis. *Am J Physiol Gastrointest Liver Physiol*, 293(6), G1147-54.

Gerits, N., Kostenko, S., Shiryaev, A., Johannessen, M. & Moens, U. (2008) Relations between the mitogen-activated protein kinase and the cAMP-dependent protein kinase pathways: comradeship and hostility. *Cell Signal*, 20(9), 1592-607.

Giaid, A., Yanagisawa, M., Langleben, D., Michel, R. P., Levy, R., Shennib, H., Kimura, S., Masaki, T., Duguid, W. P. & Stewart, D. J. (1993) Expression of endothelin-1 in the lungs of patients with pulmonary hypertension. *N Engl J Med*, 328(24), 1732-9.

Giovanazzi, S., Accomazzo, M. R., Letari, O., Oliva, D. & Nicosia, S. (1997) Internalization and down-regulation of the prostacyclin receptor in human platelets. *Biochem J*, 325 (Pt 1), 71-7.

- Glading, A., Koziol, J. A., Krueger, J. & Ginsberg, M. H. (2007) PEA-15 inhibits tumor cell invasion by binding to extracellular signal-regulated kinase 1/2. *Cancer Res*, 67(4), 1536-44.
- Gloerich, M. & Bos, J. L. (2010) Epac: defining a new mechanism for cAMP action. *Annu Rev Pharmacol Toxicol*, 50, 355-75.
- Godbole, A., Lyga, S., Lohse, M. J. & Calebiro, D. (2017) Internalized TSH receptors en route to the TGN induce local Gs-protein signaling and gene transcription. *Nat Commun*, 8(1), 443.
- Gorissen, S. H., Hristova, M., Habibovic, A., Sipse, L. M., Spiess, P. C., Janssen-Heininger, Y. M. & van der Vliet, A. (2013) Dual oxidase-1 is required for airway epithelial cell migration and bronchiolar reepithelialization after injury. *Am J Respir Cell Mol Biol*, 48(3), 337-45.
- Graves, L. M., Bornfeldt, K. E., Raines, E. W., Potts, B. C., Macdonald, S. G., Ross, R. & Krebs, E. G. (1993) Protein kinase A antagonizes platelet-derived growth factor-induced signaling by mitogen-activated protein kinase in human arterial smooth muscle cells. *Proc Natl Acad Sci U S A*, 90(21), 10300-4.
- Groot-Kormelink, P. J., Fawcett, L., Wright, P. D., Gosling, M. & Kent, T. C. (2012) Quantitative GPCR and ion channel transcriptomics in primary alveolar macrophages and macrophage surrogates. *BMC Immunol*, 13, 57.
- Gryglewski, R. J. (2008) Prostacyclin among prostanoids. *Pharmacol Rep*, 60(1), 3-11.
- Gryglewski, R. J., Korbut, R. & Ocetkiewicz, A. (1978) Generation of prostacyclin by lungs in vivo and its release into the arterial circulation. *Nature*, 273(5665), 765-7.

- Gurujeyalakshmi, G., Hollinger, M. A. & Giri, S. N. (1999) Pirfenidone inhibits PDGF isoforms in bleomycin hamster model of lung fibrosis at the translational level. *Am J Physiol*, 276(2), L311-8.
- Halls, M. L., Poole, D. P., Ellisdon, A. M., Nowell, C. J. & Canals, M. (2015) Detection and Quantification of Intracellular Signaling Using FRET-Based Biosensors and High Content Imaging. *Methods Mol Biol*, 1335, 131-61.
- Halls, M. L., Yeatman, H. R., Nowell, C. J., Thompson, G. L., Gondin, A. B., Civciristov, S., Bunnett, N. W., Lambert, N. A., Poole, D. P. & Canals, M. (2016) Plasma membrane localization of the mu-opioid receptor controls spatiotemporal signaling. *Sci Signal*, 9(414), ra16.
- Hanania, N. A., Sharafkhaneh, A., Barber, R. & Dickey, B. F. (2002) Beta-agonist intrinsic efficacy: measurement and clinical significance. *Am J Respir Crit Care Med*, 165(10), 1353-8.
- Harrison, R. K. (2016) Phase II and phase III failures: 2013-2015. *Nat Rev Drug Discov*, 15(12), 817-818.
- Harvey, C. D., Ehrhardt, A. G., Cellurale, C., Zhong, H., Yasuda, R., Davis, R. J. & Svoboda, K. (2008) A genetically encoded fluorescent sensor of ERK activity. *Proc Natl Acad Sci U S A*, 105(49), 19264-9.
- Hashimoto, N., Jin, H., Liu, T., Chensue, S. W. & Phan, S. H. (2004) Bone marrow-derived progenitor cells in pulmonary fibrosis. *J Clin Invest*, 113(2), 243-52.
- Hata, A. & Chen, Y. G. (2016) TGF-beta Signaling from Receptors to Smads. *Cold Spring Harb Perspect Biol*, 8(9).

Hauser, A. S., Attwood, M. M., Rask-Andersen, M., Schioth, H. B. & Gloriam, D. E. (2017) Trends in GPCR drug discovery: new agents, targets and indications. *Nat Rev Drug Discov*, 16(12), 829-842.

Hayes, J. S., Brunton, L. L., Brown, J. H., Reese, J. B. & Mayer, S. E. (1979) Hormonally specific expression of cardiac protein kinase activity. *Proc Natl Acad Sci U S A*, 76(4), 1570-4.

Hayes, J. S., Brunton, L. L. & Mayer, S. E. (1980) Selective activation of particulate cAMP-dependent protein kinase by isoproterenol and prostaglandin E1. *J Biol Chem*, 255(11), 5113-9.

Heldin, C. H., Ostman, A. & Ronnstrand, L. (1998) Signal transduction via platelet-derived growth factor receptors. *Biochim Biophys Acta*, 1378(1), F79-113.

Herrmann, F. E., Wollin, L., Wirth, J., Gantner, F., Lammle, B. & Wex, E. (2017) Olodaterol shows anti-fibrotic efficacy in in vitro and in vivo models of pulmonary fibrosis. *Br J Pharmacol*, 174(21), 3848-3864.

Hess, K. C., Jones, B. H., Marquez, B., Chen, Y., Ord, T. S., Kamenetsky, M., Miyamoto, C., Zippin, J. H., Kopf, G. S., Suarez, S. S., Levin, L. R., Williams, C. J., Buck, J. & Moss, S. B. (2005) The "soluble" adenylyl cyclase in sperm mediates multiple signaling events required for fertilization. *Dev Cell*, 9(2), 249-59.

Hetzel, M., Bachem, M., Anders, D., Trischler, G. & Faehling, M. (2005) Different effects of growth factors on proliferation and matrix production of normal and fibrotic human lung fibroblasts. *Lung*, 183(4), 225-37.

Hilberg, F., Roth, G. J., Krssak, M., Kautschitsch, S., Sommergruber, W., Tontsch-Grunt, U., Garin-Chesa, P., Bader, G., Zoephel, A., Quant, J., Heckel, A. & Rettig, W. J. (2008)

BIBF 1120: triple angiokinase inhibitor with sustained receptor blockade and good antitumor efficacy. *Cancer Res*, 68(12), 4774-82.

Hinz, S., Lacher, S. K., Seibt, B. F. & Muller, C. E. (2014) BAY60-6583 acts as a partial agonist at adenosine A2B receptors. *J Pharmacol Exp Ther*, 349(3), 427-36.

Hoegl, S., Brodsky, K. S., Blackburn, M. R., Karmouty-Quintana, H., Zwissler, B. & Eltzschig, H. K. (2015) Alveolar Epithelial A2B Adenosine Receptors in Pulmonary Protection during Acute Lung Injury. *J Immunol*, 195(4), 1815-24.

Hostettler, K. E., Zhong, J., Papakonstantinou, E., Karakiulakis, G., Tamm, M., Seidel, P., Sun, Q., Mandal, J., Lardinois, D., Lambers, C. & Roth, M. (2014) Anti-fibrotic effects of nintedanib in lung fibroblasts derived from patients with idiopathic pulmonary fibrosis. *Respir Res*, 15, 157.

Houslay, M. D. & Milligan, G. (1997) Tailoring cAMP-signalling responses through isoform multiplicity. *Trends Biochem Sci*, 22(6), 217-24.

Huang, L. J., Wang, L., Ma, Y., Durick, K., Perkins, G., Deerinck, T. J., Ellisman, M. H. & Taylor, S. S. (1999) NH₂-Terminal targeting motifs direct dual specificity A-kinase-anchoring protein 1 (D-AKAP1) to either mitochondria or endoplasmic reticulum. *J Cell Biol*, 145(5), 951-9.

Huang, S., Wettlaufer, S. H., Hogaboam, C., Aronoff, D. M. & Peters-Golden, M. (2007) Prostaglandin E₂ inhibits collagen expression and proliferation in patient-derived normal lung fibroblasts via E prostanoid 2 receptor and cAMP signaling. *Am J Physiol Lung Cell Mol Physiol*, 292(2), L405-13.

Huang, S. K., Fisher, A. S., Scruggs, A. M., White, E. S., Hogaboam, C. M., Richardson, B. C. & Peters-Golden, M. (2010) Hypermethylation of PTGER2 confers prostaglandin

E2 resistance in fibrotic fibroblasts from humans and mice. *Am J Pathol*, 177(5), 2245-55.

Huang, S. K., Wettlaufer, S. H., Chung, J. & Peters-Golden, M. (2008a) Prostaglandin E2 inhibits specific lung fibroblast functions via selective actions of PKA and Epac-1. *Am J Respir Cell Mol Biol*, 39(4), 482-9.

Huang, S. K., Wettlaufer, S. H., Hogaboam, C. M., Flaherty, K. R., Martinez, F. J., Myers, J. L., Colby, T. V., Travis, W. D., Toews, G. B. & Peters-Golden, M. (2008b) Variable prostaglandin E2 resistance in fibroblasts from patients with usual interstitial pneumonia. *Am J Respir Crit Care Med*, 177(1), 66-74.

Hulme, J. T., Lin, T. W., Westenbroek, R. E., Scheuer, T. & Catterall, W. A. (2003) Beta-adrenergic regulation requires direct anchoring of PKA to cardiac CaV1.2 channels via a leucine zipper interaction with A kinase-anchoring protein 15. *Proc Natl Acad Sci U S A*, 100(22), 13093-8.

Humbert, M. & Ghofrani, H. A. (2016) The molecular targets of approved treatments for pulmonary arterial hypertension. *Thorax*, 71(1), 73-83.

Humbert, M., Morrell, N. W., Archer, S. L., Stenmark, K. R., MacLean, M. R., Lang, I. M., Christman, B. W., Weir, E. K., Eickelberg, O., Voelkel, N. F. & Rabinovitch, M. (2004) Cellular and molecular pathobiology of pulmonary arterial hypertension. *J Am Coll Cardiol*, 43(12 Suppl S), 13s-24s.

Hynes, R. O. & Naba, A. (2012) Overview of the matrisome--an inventory of extracellular matrix constituents and functions. *Cold Spring Harb Perspect Biol*, 4(1), a004903.

Inomata, M., Nishioka, Y. & Azuma, A. (2015) Nintedanib: evidence for its therapeutic potential in idiopathic pulmonary fibrosis. *Core Evid*, 10, 89-98.

Irannejad, R., Pessino, V., Mika, D., Huang, B., Wedegaertner, P. B., Conti, M. & von Zastrow, M. (2017) Functional selectivity of GPCR-directed drug action through location bias. *Nat Chem Biol*, 13(7), 799-806.

Irannejad, R., Tomshine, J. C., Tomshine, J. R., Chevalier, M., Mahoney, J. P., Steyaert, J., Rasmussen, S. G., Sunahara, R. K., El-Samad, H., Huang, B. & von Zastrow, M. (2013) Conformational biosensors reveal GPCR signalling from endosomes. *Nature*, 495(7442), 534-8.

Irannejad, R., Tsvetanova, N. G., Lobingier, B. T. & von Zastrow, M. (2015) Effects of endocytosis on receptor-mediated signaling. *Curr Opin Cell Biol*, 35, 137-43.

Ismail, S., Gherardi, M. J., Froese, A., Zanoun, M., Gigoux, V., Clerc, P., Gaits-Iacovoni, F., Steyaert, J., Nikolaev, V. O. & Fourmy, D. (2016) Internalized Receptor for Glucose-dependent Insulinotropic Peptide stimulates adenylyl cyclase on early endosomes. *Biochem Pharmacol*, 120, 33-45.

Iwami, G., Kawabe, J., Ebina, T., Cannon, P. J., Homcy, C. J. & Ishikawa, Y. (1995) Regulation of adenylyl cyclase by protein kinase A. *J Biol Chem*, 270(21), 12481-4.

Iyer, S. N., Gurujeyalakshmi, G. & Giri, S. N. (1999) Effects of pirfenidone on transforming growth factor-beta gene expression at the transcriptional level in bleomycin hamster model of lung fibrosis. *J Pharmacol Exp Ther*, 291(1), 367-73.

Iyer, S. N., Hyde, D. M. & Giri, S. N. (2000) Anti-inflammatory effect of pirfenidone in the bleomycin-hamster model of lung inflammation. *Inflammation*, 24(5), 477-91.

Jacobson, K., Mouritsen, O. G. & Anderson, R. G. (2007) Lipid rafts: at a crossroad between cell biology and physics. *Nat Cell Biol*, 9(1), 7-14.

Jensen, D. D., Lieu, T., Halls, M. L., Veldhuis, N. A., Imlach, W. L., Mai, Q. N., Poole, D. P., Quach, T., Aurelio, L., Conner, J., Herenbrink, C. K., Barlow, N., Simpson, J. S.,

Scanlon, M. J., Graham, B., McCluskey, A., Robinson, P. J., Escriou, V., Nassini, R., Materazzi, S., Geppetti, P., Hicks, G. A., Christie, M. J., Porter, C. J. H., Canals, M. & Bunnett, N. W. (2017) Neurokinin 1 receptor signaling in endosomes mediates sustained nociception and is a viable therapeutic target for prolonged pain relief. *Sci Transl Med*, 9(392).

Johnstone, T. B., Agarwal, S. R., Harvey, R. D. & Ostrom, R. S. (2018) cAMP Signaling Compartmentation: Adenylyl Cyclases as Anchors of Dynamic Signaling Complexes. *Mol Pharmacol*, 93(4), 270-276.

Kam, Y., Chow, K. B. & Wise, H. (2001) Factors affecting prostacyclin receptor agonist efficacy in different cell types. *Cell Signal*, 13(11), 841-7.

Kamio, K., Liu, X., Sugiura, H., Togo, S., Kobayashi, T., Kawasaki, S., Wang, X., Mao, L., Ahn, Y., Hogaboam, C., Toews, M. L. & Rennard, S. I. (2007) Prostacyclin analogs inhibit fibroblast contraction of collagen gels through the cAMP-PKA pathway. *Am J Respir Cell Mol Biol*, 37(1), 113-20.

Kaneko, M. & Takahashi, T. (2004) Presynaptic mechanism underlying cAMP-dependent synaptic potentiation. *J Neurosci*, 24(22), 5202-8.

Kang, D. S., Tian, X. & Benovic, J. L. (2013) beta-Arrestins and G protein-coupled receptor trafficking. *Methods Enzymol*, 521, 91-108.

Kardash, E., Bandemer, J. & Raz, E. (2011) Imaging protein activity in live embryos using fluorescence resonance energy transfer biosensors. *Nat Protoc*, 6(12), 1835-46.

Katzenstein, A. L. & Myers, J. L. (1998) Idiopathic pulmonary fibrosis: clinical relevance of pathologic classification. *Am J Respir Crit Care Med*, 157(4 Pt 1), 1301-15.

Kawasaki, H., Springett, G. M., Mochizuki, N., Toki, S., Nakaya, M., Matsuda, M., Housman, D. E. & Graybiel, A. M. (1998) A family of cAMP-binding proteins that directly activate Rap1. *Science*, 282(5397), 2275-9.

Kenakin, T. & Williams, M. (2014) Defining and characterizing drug/compound function. *Biochem Pharmacol*, 87(1), 40-63.

Kenakin, T. P. (2012) Biased signalling and allosteric machines: new vistas and challenges for drug discovery. *Br J Pharmacol*, 165(6), 1659-1669.

Keogh, B. A. & Crystal, R. G. (1982) Alveolitis: the key to the interstitial lung disorders. *Thorax*, 37(1), 1-10.

Khalil, N., O'Connor, R. N., Flanders, K. C. & Unruh, H. (1996) TGF-beta 1, but not TGF-beta 2 or TGF-beta 3, is differentially present in epithelial cells of advanced pulmonary fibrosis: an immunohistochemical study. *Am J Respir Cell Mol Biol*, 14(2), 131-8.

Khalil, N., O'Connor, R. N., Unruh, H. W., Warren, P. W., Flanders, K. C., Kemp, A., Berezney, O. H. & Greenberg, A. H. (1991) Increased production and immunohistochemical localization of transforming growth factor-beta in idiopathic pulmonary fibrosis. *Am J Respir Cell Mol Biol*, 5(2), 155-62.

Khan, S. M., Sleno, R., Gora, S., Zylbergold, P., Laverdure, J. P., Labbe, J. C., Miller, G. J. & Hebert, T. E. (2013) The expanding roles of Gbetagamma subunits in G protein-coupled receptor signaling and drug action. *Pharmacol Rev*, 65(2), 545-77.

Kheradmand, F., Folkesson, H. G., Shum, L., Derynk, R., Pytela, R. & Matthay, M. A. (1994) Transforming growth factor-alpha enhances alveolar epithelial cell repair in a new in vitro model. *Am J Physiol*, 267(6 Pt 1), L728-38.

Khokhlatchev, A. V., Canagarajah, B., Wilsbacher, J., Robinson, M., Atkinson, M., Goldsmith, E. & Cobb, M. H. (1998) Phosphorylation of the MAP kinase ERK2 promotes its homodimerization and nuclear translocation. *Cell*, 93(4), 605-15.

Kim, E. S. & Keating, G. M. (2015) Pirfenidone: a review of its use in idiopathic pulmonary fibrosis. *Drugs*, 75(2), 219-30.

Kim, K. K., Kugler, M. C., Wolters, P. J., Robillard, L., Galvez, M. G., Brumwell, A. N., Sheppard, D. & Chapman, H. A. (2006) Alveolar epithelial cell mesenchymal transition develops in vivo during pulmonary fibrosis and is regulated by the extracellular matrix. *Proc Natl Acad Sci U S A*, 103(35), 13180-5.

King, T. E., Jr., Bradford, W. Z., Castro-Bernardini, S., Fagan, E. A., Glaspole, I., Glassberg, M. K., Gorina, E., Hopkins, P. M., Kardatzke, D., Lancaster, L., Lederer, D. J., Nathan, S. D., Pereira, C. A., Sahn, S. A., Sussman, R., Swigris, J. J. & Noble, P. W. (2014) A phase 3 trial of pirfenidone in patients with idiopathic pulmonary fibrosis. *N Engl J Med*, 370(22), 2083-92.

Kisseleva, T., Cong, M., Paik, Y., Scholten, D., Jiang, C., Benner, C., Iwaisako, K., Moore-Morris, T., Scott, B., Tsukamoto, H., Evans, S. M., Dillmann, W., Glass, C. K. & Brenner, D. A. (2012) Myofibroblasts revert to an inactive phenotype during regression of liver fibrosis. *Proc Natl Acad Sci U S A*, 109(24), 9448-53.

Klarenbeek, J., Goedhart, J., van Batenburg, A., Groenewald, D. & Jalink, K. (2015) Fourth-generation epac-based FRET sensors for cAMP feature exceptional brightness, photostability and dynamic range: characterization of dedicated sensors for FLIM, for ratiometry and with high affinity. *PLoS One*, 10(4), e0122513.

Klein Herenbrink, C., Sykes, D. A., Donthamsetti, P., Canals, M., Coudrat, T., Shonberg, J., Scammells, P. J., Capuano, B., Sexton, P. M., Charlton, S. J., Javitch, J. A.,

- Christopoulos, A. & Lane, J. R. (2016) The role of kinetic context in apparent biased agonism at GPCRs. *Nat Commun*, 7, 10842.
- Klinger, J. R. (2016) Group III Pulmonary Hypertension: Pulmonary Hypertension Associated with Lung Disease: Epidemiology, Pathophysiology, and Treatments. *Cardiol Clin*, 34(3), 413-33.
- Knudsen, L. & Ochs, M. (2018) The micromechanics of lung alveoli: structure and function of surfactant and tissue components. *Histochem Cell Biol*, 150(6), 661-676.
- Kohler, N. & Lipton, A. (1974) Platelets as a source of fibroblast growth-promoting activity. *Exp Cell Res*, 87(2), 297-301.
- Kohyama, T., Liu, X., Kim, H. J., Kobayashi, T., Ertl, R. F., Wen, F. Q., Takizawa, H. & Rennard, S. I. (2002) Prostacyclin analogs inhibit fibroblast migration. *Am J Physiol Lung Cell Mol Physiol*, 283(2), L428-32.
- Kolb, M., Richeldi, L., Behr, J., Maher, T. M., Tang, W., Stowasser, S., Hallmann, C. & du Bois, R. M. (2017) Nintedanib in patients with idiopathic pulmonary fibrosis and preserved lung volume. *Thorax*, 72(4), 340-346.
- Kolodsick, J. E., Peters-Golden, M., Larios, J., Toews, G. B., Thannickal, V. J. & Moore, B. B. (2003) Prostaglandin E2 inhibits fibroblast to myofibroblast transition via E. prostanoid receptor 2 signaling and cyclic adenosine monophosphate elevation. *Am J Respir Cell Mol Biol*, 29(5), 537-44.
- Kolosionek, E., Savai, R., Ghofrani, H. A., Weissmann, N., Guenther, A., Grimminger, F., Seeger, W., Banat, G. A., Schermuly, R. T. & Pullamsetti, S. S. (2009) Expression and activity of phosphodiesterase isoforms during epithelial mesenchymal transition: the role of phosphodiesterase 4. *Mol Biol Cell*, 20(22), 4751-65.

Komolov, K. E. & Benovic, J. L. (2018) G protein-coupled receptor kinases: Past, present and future. *Cell Signal*, 41, 17-24.

Kothapalli, D., Stewart, S. A., Smyth, E. M., Azonobi, I., Pure, E. & Assoian, R. K. (2003) Prostacyclin receptor activation inhibits proliferation of aortic smooth muscle cells by regulating cAMP response element-binding protein- and pocket protein-dependent cyclin a gene expression. *Mol Pharmacol*, 64(2), 249-58.

Krizhanovsky, V., Yon, M., Dickins, R. A., Hearn, S., Simon, J., Miething, C., Yee, H., Zender, L. & Lowe, S. W. (2008) Senescence of activated stellate cells limits liver fibrosis. *Cell*, 134(4), 657-67.

Lambers, C., Roth, M., Jaksch, P., Murakozy, G., Tamm, M., Klepetko, W., Ghanim, B. & Zhao, F. (2018) Treprostinil inhibits proliferation and extracellular matrix deposition by fibroblasts through cAMP activation. *Sci Rep*, 8(1), 1087.

Lamyel, F., Warnken-Uhlich, M., Seemann, W. K., Mohr, K., Kostenis, E., Ahmedat, A. S., Smit, M., Gosens, R., Meurs, H., Miller-Larsson, A. & Racke, K. (2011) The beta2-subtype of adrenoceptors mediates inhibition of pro-fibrotic events in human lung fibroblasts. *Naunyn Schmiedebergs Arch Pharmacol*, 384(2), 133-45.

Larsson-Callerfelt, A. K., Hallgren, O., Andersson-Sjoland, A., Thiman, L., Bjorklund, J., Kron, J., Nihlberg, K., Bjermer, L., Lofdahl, C. G. & Westergren-Thorsson, G. (2013) Defective alterations in the collagen network to prostacyclin in COPD lung fibroblasts. *Respir Res*, 14, 21.

Lasky, J. A. & Brody, A. R. (2000) Interstitial fibrosis and growth factors. *Environ Health Perspect*, 108 Suppl 4, 751-62.

Lee, S. M., Booe, J. M. & Pioszak, A. A. (2015) Structural insights into ligand recognition and selectivity for classes A, B, and C GPCRs. *Eur J Pharmacol*, 763(Pt B), 196-205.

Lemmon, M. A. & Schlessinger, J. (2010) Cell signaling by receptor tyrosine kinases. *Cell*, 141(7), 1117-34.

Li, M., Krishnaveni, M. S., Li, C., Zhou, B., Xing, Y., Banfalvi, A., Li, A., Lombardi, V., Akbari, O., Borok, Z. & Minoo, P. (2011) Epithelium-specific deletion of TGF-beta receptor type II protects mice from bleomycin-induced pulmonary fibrosis. *J Clin Invest*, 121(1), 277-87.

Light, Y., Paterson, H. & Marais, R. (2002) 14-3-3 antagonizes Ras-mediated Raf-1 recruitment to the plasma membrane to maintain signaling fidelity. *Mol Cell Biol*, 22(14), 4984-96.

Liu, C. Y., Jamaledin, A. J., Zhang, H. & Christofi, F. L. (1999) FICRHR/cyclic AMP signaling in myenteric ganglia and calbindin-D28 intrinsic primary afferent neurons involves adenylyl cyclases I, III and IV. *Brain Res*, 826(2), 253-69.

Liu, G., Betts, C., Cunoosamy, D. M., Aberg, P. M., Hornberg, J. J., Sivars, K. B. & Cohen, T. S. (2019) Use of precision cut lung slices as a translational model for the study of lung biology. *Respir Res*, 20(1), 162.

Liu, X., Li, F., Sun, S. Q., Thangavel, M., Kaminsky, J., Balazs, L. & Ostrom, R. S. (2010) Fibroblast-specific expression of AC6 enhances beta-adrenergic and prostacyclin signaling and blunts bleomycin-induced pulmonary fibrosis. *Am J Physiol Lung Cell Mol Physiol*, 298(6), L819-29.

Liu, X., Ostrom, R. S. & Insel, P. A. (2004) cAMP-elevating agents and adenylyl cyclase overexpression promote an antifibrotic phenotype in pulmonary fibroblasts. *Am J Physiol Cell Physiol*, 286(5), C1089-99.

Liu, X., Thangavel, M., Sun, S. Q., Kaminsky, J., Mahautmr, P., Stitham, J., Hwa, J. & Ostrom, R. S. (2008) Adenylyl cyclase type 6 overexpression selectively enhances beta-

adrenergic and prostacyclin receptor-mediated inhibition of cardiac fibroblast function because of colocalization in lipid rafts. *Naunyn Schmiedebergs Arch Pharmacol*, 377(4-6), 359-69.

Lohse, M. J., Benovic, J. L., Codina, J., Caron, M. G. & Lefkowitz, R. J. (1990) beta-Arrestin: a protein that regulates beta-adrenergic receptor function. *Science*, 248(4962), 1547-50.

Lovgren, A. K., Kovacs, J. J., Xie, T., Potts, E. N., Li, Y., Foster, W. M., Liang, J., Meltzer, E. B., Jiang, D., Lefkowitz, R. J. & Noble, P. W. (2011) beta-arrestin deficiency protects against pulmonary fibrosis in mice and prevents fibroblast invasion of extracellular matrix. *Sci Transl Med*, 3(74), 74ra23.

Lu, P., Zhang, C. H., Lifshitz, L. M. & ZhuGe, R. (2017) Extraoral bitter taste receptors in health and disease. *J Gen Physiol*, 149(2), 181-197.

Luttrell, L. M., Ferguson, S. S., Daaka, Y., Miller, W. E., Maudsley, S., Della Rocca, G. J., Lin, F., Kawakatsu, H., Owada, K., Luttrell, D. K., Caron, M. G. & Lefkowitz, R. J. (1999) Beta-arrestin-dependent formation of beta2 adrenergic receptor-Src protein kinase complexes. *Science*, 283(5402), 655-61.

Luttrell, L. M. & Lefkowitz, R. J. (2002) The role of beta-arrestins in the termination and transduction of G-protein-coupled receptor signals. *J Cell Sci*, 115(Pt 3), 455-65.

Macdonald, G. (2008) Harrison's Internal Medicine, 17th edition. - by A. S. Fauci, D. L. Kasper, D. L. Longo, E. Braunwald, S. L. Hauser, J. L. Jameson and J. Loscalzo. *Internal Medicine Journal*, 38(12), 932-932.

Madala, S. K., Schmidt, S., Davidson, C., Ikegami, M., Wert, S. & Hardie, W. D. (2012) MEK-ERK pathway modulation ameliorates pulmonary fibrosis associated with epidermal growth factor receptor activation. *Am J Respir Cell Mol Biol*, 46(3), 380-8.

Manitsopoulos, N., Kotanidou, A., Magkou, C., Ninou, I., Tian, X., Aidinis, V., Schermuly, R. & Orfanos, S. (2015) Treprostinil administration attenuates bleomycin-induced lung fibrosis in mice. *European Respiratory Journal*, 46(suppl 59), PA3837.

Markovic, T., Jakopin, Z., Dolenc, M. S. & Mlinaric-Rascan, I. (2017) Structural features of subtype-selective EP receptor modulators. *Drug Discov Today*, 22(1), 57-71.

Martinez, F. J., Calverley, P. M., Goehring, U. M., Brose, M., Fabbri, L. M. & Rabe, K. F. (2015) Effect of roflumilast on exacerbations in patients with severe chronic obstructive pulmonary disease uncontrolled by combination therapy (REACT): a multicentre randomised controlled trial. *Lancet*, 385(9971), 857-66.

Martinez, F. J., Rabe, K. F., Sethi, S., Pizzichini, E., McIvor, A., Anzueto, A., Alagappan, V. K., Siddiqui, S., Rekeda, L., Miller, C. J., Zetterstrand, S., Reisner, C. & Rennard, S. I. (2016) Effect of Roflumilast and Inhaled Corticosteroid/Long-Acting beta2-Agonist on Chronic Obstructive Pulmonary Disease Exacerbations (RE(2)SPOND). A Randomized Clinical Trial. *Am J Respir Crit Care Med*, 194(5), 559-67.

Martufi, M., Good, R. B., Rapiteanu, R., Schmidt, T., Patili, E., Tvermosegaard, K., New, M., Nanthakumar, C. B., Betts, J., Blanchard, A. D. & Maratou, K. (2019) Single-Step, High-Efficiency CRISPR-Cas9 Genome Editing in Primary Human Disease-Derived Fibroblasts. *Crispr j*, 2, 31-40.

McCrea, K. E. & Hill, S. J. (1996) Comparison of duration of agonist action at beta 1- and beta 2- adrenoceptors in C6 glioma cells: evidence that the long duration of action of salmeterol is specific to the beta 2-adrenoceptor. *Mol Pharmacol*, 49(5), 927-37.

Meyer, K. C. & Decker, C. A. (2017) Role of pirfenidone in the management of pulmonary fibrosis. *Ther Clin Risk Manag*, 13, 427-437.

Midgett, C., Stitham, J., Martin, K. & Hwa, J. (2011) Prostacyclin receptor regulation--from transcription to trafficking. *Curr Mol Med*, 11(7), 517-28.

Milara, J., Morcillo, E., Monleon, D., Tenor, H. & Cortijo, J. (2015) Roflumilast Prevents the Metabolic Effects of Bleomycin-Induced Fibrosis in a Murine Model. *PLoS One*, 10(7), e0133453.

Milara, J., Peiro, T., Serrano, A., Guijarro, R., Zaragoza, C., Tenor, H. & Cortijo, J. (2014) Roflumilast N-oxide inhibits bronchial epithelial to mesenchymal transition induced by cigarette smoke in smokers with COPD. *Pulm Pharmacol Ther*, 28(2), 138-48.

Miller, W. E., Maudsley, S., Ahn, S., Khan, K. D., Luttrell, L. M. & Lefkowitz, R. J. (2000) beta-arrestin1 interacts with the catalytic domain of the tyrosine kinase c-SRC. Role of beta-arrestin1-dependent targeting of c-SRC in receptor endocytosis. *J Biol Chem*, 275(15), 11312-9.

Molyneaux, P. L. & Maher, T. M. (2013) The role of infection in the pathogenesis of idiopathic pulmonary fibrosis. *Eur Respir Rev*, 22(129), 376-81.

Mongillo, M., Tocchetti, C. G., Terrin, A., Lissandron, V., Cheung, Y. F., Dostmann, W. R., Pozzan, T., Kass, D. A., Paolocci, N., Houslay, M. D. & Zaccolo, M. (2006) Compartmentalized phosphodiesterase-2 activity blunts beta-adrenergic cardiac inotropy via an NO/cGMP-dependent pathway. *Circ Res*, 98(2), 226-34.

Moodley, Y. P., Caterina, P., Scaffidi, A. K., Misso, N. L., Papadimitriou, J. M., McAnulty, R. J., Laurent, G. J., Thompson, P. J. & Knight, D. A. (2004) Comparison of the morphological and biochemical changes in normal human lung fibroblasts and fibroblasts derived from lungs of patients with idiopathic pulmonary fibrosis during FasL-induced apoptosis. *J Pathol*, 202(4), 486-95.

Moore, B. B., Ballinger, M. N., White, E. S., Green, M. E., Herrygers, A. B., Wilke, C. A., Toews, G. B. & Peters-Golden, M. (2005) Bleomycin-induced E prostanoïd receptor changes alter fibroblast responses to prostaglandin E2. *J Immunol*, 174(9), 5644-9.

Moore, R. H., Millman, E. E., Godines, V., Hanania, N. A., Tran, T. M., Peng, H., Dickey, B. F., Knoll, B. J. & Clark, R. B. (2007) Salmeterol stimulation dissociates beta2-adrenergic receptor phosphorylation and internalization. *Am J Respir Cell Mol Biol*, 36(2), 254-61.

Mor, A. & Philips, M. R. (2006) Compartmentalized Ras/MAPK signaling. *Annu Rev Immunol*, 24, 771-800.

Mulder, K. M. (2000) Role of Ras and Mapks in TGFbeta signaling. *Cytokine Growth Factor Rev*, 11(1-2), 23-35.

Muller, J., Ory, S., Copeland, T., Piwnica-Worms, H. & Morrison, D. K. (2001) C-TAK1 regulates Ras signaling by phosphorylating the MAPK scaffold, KSR1. *Mol Cell*, 8(5), 983-93.

Mullershausen, F., Zecri, F., Cetin, C., Billich, A., Guerini, D. & Seuwen, K. (2009) Persistent signaling induced by FTY720-phosphate is mediated by internalized S1P1 receptors. *Nat Chem Biol*, 5(6), 428-34.

Murphy, L. O., MacKeigan, J. P. & Blenis, J. (2004) A network of immediate early gene products propagates subtle differences in mitogen-activated protein kinase signal amplitude and duration. *Mol Cell Biol*, 24(1), 144-53.

Murphy, L. O., Smith, S., Chen, R. H., Fingar, D. C. & Blenis, J. (2002) Molecular interpretation of ERK signal duration by immediate early gene products. *Nat Cell Biol*, 4(8), 556-64.

Myerburg, M. M., Latoche, J. D., McKenna, E. E., Stabile, L. P., Siegfried, J. S., Feghali-Bostwick, C. A. & Pilewski, J. M. (2007) Hepatocyte growth factor and other fibroblast secretions modulate the phenotype of human bronchial epithelial cells. *Am J Physiol Lung Cell Mol Physiol*, 292(6), L1352-60.

Nathan, S. D., Noble, P. W. & Tuder, R. M. (2007) Idiopathic pulmonary fibrosis and pulmonary hypertension: connecting the dots. *Am J Respir Crit Care Med*, 175(9), 875-80.

National Asthma Education and Prevention Program (2007) Expert Panel Report 3 (EPR-3): Guidelines for the Diagnosis and Management of Asthma-Summary Report 2007. *J Allergy Clin Immunol*, 120(5 Suppl), S94-138.

National Institute for Health and Care Excellence (2017) *Roflumilast for treating chronic obstructive pulmonary disease*, 2017. Available online: <https://www.nice.org.uk/guidance/ta461> [Accessed].

Navaratnam, V., Fleming, K. M., West, J., Smith, C. J., Jenkins, R. G., Fogarty, A. & Hubbard, R. B. (2011) The rising incidence of idiopathic pulmonary fibrosis in the U.K. *Thorax*, 66(6), 462-7.

Neves, S. R., Ram, P. T. & Iyengar, R. (2002) G protein pathways. *Science*, 296(5573), 1636-9.

Niimura, M., Miki, T., Shibasaki, T., Fujimoto, W., Iwanaga, T. & Seino, S. (2009) Critical role of the N-terminal cyclic AMP-binding domain of Epac2 in its subcellular localization and function. *J Cell Physiol*, 219(3), 652-8.

Nikam, V. S., Wecker, G., Schermuly, R., Rapp, U., Szelepusa, K., Seeger, W. & Voswinckel, R. (2011) Treprostinil inhibits the adhesion and differentiation of fibrocytes via the cyclic adenosine monophosphate-dependent and Ras-proximate

protein-dependent inactivation of extracellular regulated kinase. *Am J Respir Cell Mol Biol*, 45(4), 692-703.

Nikolaev, V. O., Bunemann, M., Hein, L., Hannawacker, A. & Lohse, M. J. (2004) Novel single chain cAMP sensors for receptor-induced signal propagation. *J Biol Chem*, 279(36), 37215-8.

Nilius, S. M., Hasse, A., Kuger, P., Schror, K. & Meyer-Kirchrath, J. (2000) Agonist-induced long-term desensitization of the human prostacyclin receptor. *FEBS Lett*, 484(3), 211-6.

Nishioka, Y., Azuma, M., Kishi, M. & Aono, Y. (2013) Targeting platelet-derived growth factor as a therapeutic approach in pulmonary fibrosis. *J Med Invest*, 60(3-4), 175-83.

Noble, P. W., Albera, C., Bradford, W. Z., Costabel, U., Glassberg, M. K., Kardatzke, D., King, T. E., Jr., Lancaster, L., Sahn, S. A., Swarcberg, J., Valeyre, D. & du Bois, R. M. (2011) Pirfenidone in patients with idiopathic pulmonary fibrosis (CAPACITY): two randomised trials. *Lancet*, 377(9779), 1760-9.

Oakley, R. H., Hudson, C. C., Cruickshank, R. D., Meyers, D. M., Payne, R. E., Jr., Rhem, S. M. & Loomis, C. R. (2002) The cellular distribution of fluorescently labeled arrestins provides a robust, sensitive, and universal assay for screening G protein-coupled receptors. *Assay Drug Dev Technol*, 1(1 Pt 1), 21-30.

Oberholte, R., Ratzliff, J., Baecker, P. A., Daniels, D. V., Zuppan, P., Jarnagin, K. & Shelton, E. R. (1997) Multiple splice variants of phosphodiesterase PDE4C cloned from human lung and testis. *Biochim Biophys Acta*, 1353(3), 287-97.

Oh, P. & Schnitzer, J. E. (2001) Segregation of heterotrimeric G proteins in cell surface microdomains. G(q) binds caveolin to concentrate in caveolae, whereas G(i) and G(s) target lipid rafts by default. *Mol Biol Cell*, 12(3), 685-98.

- Oku, H., Shimizu, T., Kawabata, T., Nagira, M., Hikita, I., Ueyama, A., Matsushima, S., Torii, M. & Arimura, A. (2008) Antifibrotic action of pirfenidone and prednisolone: different effects on pulmonary cytokines and growth factors in bleomycin-induced murine pulmonary fibrosis. *Eur J Pharmacol*, 590(1-3), 400-8.
- Oldham, W. M. & Hamm, H. E. (2008) Heterotrimeric G protein activation by G-protein-coupled receptors. *Nat Rev Mol Cell Biol*, 9(1), 60-71.
- Olschewski, H., Rose, F., Schermuly, R., Ghofrani, H. A., Enke, B., Olschewski, A. & Seeger, W. (2004) Prostacyclin and its analogues in the treatment of pulmonary hypertension. *Pharmacol Ther*, 102(2), 139-53.
- Ostrom, R. S. & Insel, P. A. (2004) The evolving role of lipid rafts and caveolae in G protein-coupled receptor signaling: implications for molecular pharmacology. *Br J Pharmacol*, 143(2), 235-45.
- Ostrom, R. S., Violin, J. D., Coleman, S. & Insel, P. A. (2000) Selective enhancement of beta-adrenergic receptor signaling by overexpression of adenylyl cyclase type 6: colocalization of receptor and adenylyl cyclase in caveolae of cardiac myocytes. *Mol Pharmacol*, 57(5), 1075-9.
- Ozawa, Y., Suda, T., Naito, T., Enomoto, N., Hashimoto, D., Fujisawa, T., Nakamura, Y., Inui, N., Nakamura, H. & Chida, K. (2009) Cumulative incidence of and predictive factors for lung cancer in IPF. *Respirology*, 14(5), 723-8.
- Pan, L. H., Yamauchi, K., Uzuki, M., Nakanishi, T., Takigawa, M., Inoue, H. & Sawai, T. (2001) Type II alveolar epithelial cells and interstitial fibroblasts express connective tissue growth factor in IPF. *Eur Respir J*, 17(6), 1220-7.

Peng, F., Dhillon, N. K., Yao, H., Zhu, X., Williams, R. & Buch, S. (2008) Mechanisms of platelet-derived growth factor-mediated neuroprotection--implications in HIV dementia. *Eur J Neurosci*, 28(7), 1255-64.

Phares, K. R., Weiser, W. E., Miller, S. P., Myers, M. A. & Wade, M. (2003) Stability and preservative effectiveness of treprostinil sodium after dilution in common intravenous diluents. *Am J Health Syst Pharm*, 60(9), 916-22.

Ponsioen, B., Zhao, J., Riedl, J., Zwartkruis, F., van der Krogt, G., Zaccolo, M., Moolenaar, W. H., Bos, J. L. & Jalink, K. (2004) Detecting cAMP-induced Epac activation by fluorescence resonance energy transfer: Epac as a novel cAMP indicator. *EMBO Rep*, 5(12), 1176-80.

Prasad, S., Hogaboam, C. M. & Jarai, G. (2014) Deficient repair response of IPF fibroblasts in a co-culture model of epithelial injury and repair. *Fibrogenesis Tissue Repair*, 7, 7.

Ragaller, M. & Richter, T. (2010) Acute lung injury and acute respiratory distress syndrome. *J Emerg Trauma Shock*, 3(1), 43-51.

Raghu, G., Anstrom, K. J., King, T. E., Jr., Lasky, J. A. & Martinez, F. J. (2012) Prednisone, azathioprine, and N-acetylcysteine for pulmonary fibrosis. *N Engl J Med*, 366(21), 1968-77.

Raghu, G., Collard, H. R., Egan, J. J., Martinez, F. J., Behr, J., Brown, K. K., Colby, T. V., Cordier, J. F., Flaherty, K. R., Lasky, J. A., Lynch, D. A., Ryu, J. H., Swigris, J. J., Wells, A. U., Ancochea, J., Bouros, D., Carvalho, C., Costabel, U., Ebina, M., Hansell, D. M., Johkoh, T., Kim, D. S., King, T. E., Jr., Kondoh, Y., Myers, J., Muller, N. L., Nicholson, A. G., Richeldi, L., Selman, M., Dudden, R. F., Griss, B. S., Protzko, S. L. & Schunemann, H. J. (2011) An official ATS/ERS/JRS/ALAT statement: idiopathic pulmonary fibrosis:

evidence-based guidelines for diagnosis and management. *Am J Respir Crit Care Med*, 183(6), 788-824.

Raghu, G., Freudenberger, T. D., Yang, S., Curtis, J. R., Spada, C., Hayes, J., Sillery, J. K., Pope, C. E., 2nd & Pellegrini, C. A. (2006) High prevalence of abnormal acid gastro-oesophageal reflux in idiopathic pulmonary fibrosis. *Eur Respir J*, 27(1), 136-42.

Rajakulendran, T., Sahmi, M., Lefrancois, M., Sicheri, F. & Therrien, M. (2009) A dimerization-dependent mechanism drives RAF catalytic activation. *Nature*, 461(7263), 542-5.

Reddel, H. K., Bateman, E. D., Becker, A., Boulet, L. P., Cruz, A. A., Drazen, J. M., Haahtela, T., Hurd, S. S., Inoue, H., de Jongste, J. C., Lemanske, R. F., Jr., Levy, M. L., O'Byrne, P. M., Paggiaro, P., Pedersen, S. E., Pizzichini, E., Soto-Quiroz, M., Szeffler, S. J., Wong, G. W. & FitzGerald, J. M. (2015) A summary of the new GINA strategy: a roadmap to asthma control. *Eur Respir J*, 46(3), 622-39.

Reszka, A. A., Seger, R., Diltz, C. D., Krebs, E. G. & Fischer, E. H. (1995) Association of mitogen-activated protein kinase with the microtubule cytoskeleton. *Proc Natl Acad Sci U S A*, 92(19), 8881-5.

Richeldi, L., Costabel, U., Selman, M., Kim, D. S., Hansell, D. M., Nicholson, A. G., Brown, K. K., Flaherty, K. R., Noble, P. W., Raghu, G., Brun, M., Gupta, A., Juhel, N., Kluglich, M. & du Bois, R. M. (2011) Efficacy of a tyrosine kinase inhibitor in idiopathic pulmonary fibrosis. *N Engl J Med*, 365(12), 1079-87.

Richeldi, L., Davies, H. R., Ferrara, G. & Franco, F. (2003) Corticosteroids for idiopathic pulmonary fibrosis. *Cochrane Database Syst Rev*(3), Cd002880.

Richeldi, L., du Bois, R. M., Raghu, G., Azuma, A., Brown, K. K., Costabel, U., Cottin, V., Flaherty, K. R., Hansell, D. M., Inoue, Y., Kim, D. S., Kolb, M., Nicholson, A. G., Noble, P.

W., Selman, M., Taniguchi, H., Brun, M., Le Maulf, F., Girard, M., Stowasser, S., Schlenker-Herceg, R., Disse, B. & Collard, H. R. (2014) Efficacy and safety of nintedanib in idiopathic pulmonary fibrosis. *N Engl J Med*, 370(22), 2071-82.

Rivera-Lebron, B. N., Forfia, P. R., Kreider, M., Lee, J. C., Holmes, J. H. & Kawut, S. M. (2013) Echocardiographic and hemodynamic predictors of mortality in idiopathic pulmonary fibrosis. *Chest*, 144(2), 564-570.

Roberts, M. J., Broome, R. E., Kent, T. C., Charlton, S. J. & Rosethorne, E. M. (2018) The inhibition of human lung fibroblast proliferation and differentiation by Gs-coupled receptors is not predicted by the magnitude of cAMP response. *Respir Res*, 19(1), 56.

Rosethorne, E. M., Bradley, M. E., Gherbi, K., Sykes, D. A., Sattikar, A., Wright, J. D., Renard, E., Trifilieff, A., Fairhurst, R. A. & Charlton, S. J. (2016) Long Receptor Residence Time of C26 Contributes to Super Agonist Activity at the Human beta2 Adrenoceptor. *Mol Pharmacol*, 89(4), 467-75.

Rosethorne, E. M., Bradley, M. E., Kent, T. C. & Charlton, S. J. (2015) Functional desensitization of the beta 2 adrenoceptor is not dependent on agonist efficacy. *Pharmacol Res Perspect*, 3(1), e00101.

Rosethorne, E. M., Nahorski, S. R. & Challiss, R. A. (2008) Regulation of cyclic AMP response-element binding-protein (CREB) by Gq/11-protein-coupled receptors in human SH-SY5Y neuroblastoma cells. *Biochem Pharmacol*, 75(4), 942-55.

Ross, R., Glomset, J., Kariya, B. & Harker, L. (1974) A platelet-dependent serum factor that stimulates the proliferation of arterial smooth muscle cells in vitro. *Proc Natl Acad Sci U S A*, 71(4), 1207-10.

- Roy, S. G., Nozaki, Y. & Phan, S. H. (2001) Regulation of alpha-smooth muscle actin gene expression in myofibroblast differentiation from rat lung fibroblasts. *Int J Biochem Cell Biol*, 33(7), 723-34.
- Rubinfeld, H., Hanoch, T. & Seger, R. (1999) Identification of a cytoplasmic-retention sequence in ERK2. *J Biol Chem*, 274(43), 30349-52.
- Sadana, R. & Dessauer, C. W. (2009) Physiological roles for G protein-regulated adenylyl cyclase isoforms: insights from knockout and overexpression studies. *Neurosignals*, 17(1), 5-22.
- Sakaba, T. & Neher, E. (2003) Direct modulation of synaptic vesicle priming by GABA(B) receptor activation at a glutamatergic synapse. *Nature*, 424(6950), 775-8.
- Sakai, N. & Tager, A. M. (2013) Fibrosis of two: Epithelial cell-fibroblast interactions in pulmonary fibrosis. *Biochim Biophys Acta*, 1832(7), 911-21.
- Salton, F., Volpe, M. C. & Confalonieri, M. (2019) Epithelial(-)Mesenchymal Transition in the Pathogenesis of Idiopathic Pulmonary Fibrosis. *Medicina (Kaunas)*, 55(4).
- Santos, R., Ursu, O., Gaulton, A., Bento, A. P., Donadi, R. S., Bologa, C. G., Karlsson, A., Al-Lazikani, B., Hersey, A., Oprea, T. I. & Overington, J. P. (2017) A comprehensive map of molecular drug targets. *Nat Rev Drug Discov*, 16(1), 19-34.
- Savarino, E., Carbone, R., Marabotto, E., Furnari, M., Sconfienza, L., Ghio, M., Zentilin, P. & Savarino, V. (2013) Gastro-oesophageal reflux and gastric aspiration in idiopathic pulmonary fibrosis patients. *Eur Respir J*, 42(5), 1322-31.
- Schaeffer, H. J., Catling, A. D., Eblen, S. T., Collier, L. S., Krauss, A. & Weber, M. J. (1998) MP1: a MEK binding partner that enhances enzymatic activation of the MAP kinase cascade. *Science*, 281(5383), 1668-71.

- Schaeffer, H. J. & Weber, M. J. (1999) Mitogen-activated protein kinases: specific messages from ubiquitous messengers. *Mol Cell Biol*, 19(4), 2435-44.
- Schleicher, K. & Zaccolo, M. (2018) Using cAMP Sensors to Study Cardiac Nanodomains. *J Cardiovasc Dev Dis*, 5(1).
- Schmidt, M., Evellin, S., Weernink, P. A., von Dorp, F., Rehmann, H., Lomasney, J. W. & Jakobs, K. H. (2001) A new phospholipase-C-calcium signalling pathway mediated by cyclic AMP and a Rap GTPase. *Nat Cell Biol*, 3(11), 1020-4.
- Schmidt, M., Zuo, H., Poppinga, W. J. & Nikolaev, V. (2016) Monitoring local pulmonary cAMP levels: Combining precision cut lung slice (PCLS) and fluorescence resonance energy transfer (FRET) technologies in mice. *European Respiratory Journal*, 48(suppl 60), PA5055.
- Schmitt, J. M. & Stork, P. J. (2001) Cyclic AMP-mediated inhibition of cell growth requires the small G protein Rap1. *Mol Cell Biol*, 21(11), 3671-83.
- Schwartz, T. W., Frimurer, T. M., Holst, B., Rosenkilde, M. M. & Elling, C. E. (2006) Molecular mechanism of 7TM receptor activation--a global toggle switch model. *Annu Rev Pharmacol Toxicol*, 46, 481-519.
- Selige, J., Hatzelmann, A. & Dunkern, T. (2011) The differential impact of PDE4 subtypes in human lung fibroblasts on cytokine-induced proliferation and myofibroblast conversion. *J Cell Physiol*, 226(8), 1970-80.
- Selman, M., King, T. E. & Pardo, A. (2001) Idiopathic pulmonary fibrosis: prevailing and evolving hypotheses about its pathogenesis and implications for therapy. *Ann Intern Med*, 134(2), 136-51.

Selman, M. & Pardo, A. (2004) Idiopathic pulmonary fibrosis: misunderstandings between epithelial cells and fibroblasts? *Sarcoidosis Vasc Diffuse Lung Dis*, 21(3), 165-72.

Selman, M. & Pardo, A. (2006) Role of epithelial cells in idiopathic pulmonary fibrosis: from innocent targets to serial killers. *Proc Am Thorac Soc*, 3(4), 364-72.

Seoane, J. & Gomis, R. R. (2017) TGF-beta Family Signaling in Tumor Suppression and Cancer Progression. *Cold Spring Harb Perspect Biol*, 9(12).

Shakur, Y., Takeda, K., Kenan, Y., Yu, Z. X., Rena, G., Brandt, D., Houslay, M. D., Degerman, E., Ferrans, V. J. & Manganiello, V. C. (2000) Membrane localization of cyclic nucleotide phosphodiesterase 3 (PDE3). Two N-terminal domains are required for the efficient targeting to, and association of, PDE3 with endoplasmic reticulum. *J Biol Chem*, 275(49), 38749-61.

Shayo, C., Legnazzi, B. L., Monczor, F., Fernandez, N., Riveiro, M. E., Baldi, A. & Davio, C. (2004) The time-course of cyclic AMP signaling is critical for leukemia U-937 cell differentiation. *Biochem Biophys Res Commun*, 314(3), 798-804.

Sidovar, M. F., Kozlowski, P., Lee, J. W., Collins, M. A., He, Y. & Graves, L. M. (2000) Phosphorylation of serine 43 is not required for inhibition of c-Raf kinase by the cAMP-dependent protein kinase. *J Biol Chem*, 275(37), 28688-94.

Sieber, P., Schafer, A., Lieberherr, R., Le Goff, F., Stritt, M., Welford, R. W. D., Gatfield, J., Peter, O., Nayler, O. & Luthi, U. (2018) Novel high-throughput myofibroblast assays identify agonists with therapeutic potential in pulmonary fibrosis that act via EP2 and EP4 receptors. *PLoS One*, 13(11), e0207872.

- Sin, D. D., McAlister, F. A., Man, S. F. & Anthonisen, N. R. (2003) Contemporary management of chronic obstructive pulmonary disease: scientific review. *Jama*, 290(17), 2301-12.
- Singer, S. J. & Nicolson, G. L. (1972) The fluid mosaic model of the structure of cell membranes. *Science*, 175(4023), 720-31.
- Sitbon, O., Channick, R., Chin, K. M., Frey, A., Gaine, S., Galie, N., Ghofrani, H. A., Hoeper, M. M., Lang, I. M., Preiss, R., Rubin, L. J., Di Scala, L., Tapson, V., Adzerikho, I., Liu, J., Moiseeva, O., Zeng, X., Simonneau, G. & McLaughlin, V. V. (2015) Selexipag for the Treatment of Pulmonary Arterial Hypertension. *N Engl J Med*, 373(26), 2522-33.
- Smith, J. S. & Rajagopal, S. (2016) The beta-Arrestins: Multifunctional Regulators of G Protein-coupled Receptors. *J Biol Chem*, 291(17), 8969-77.
- Smyth, E. M., Li, W. H. & FitzGerald, G. A. (1998) Phosphorylation of the prostacyclin receptor during homologous desensitization. A critical role for protein kinase c. *J Biol Chem*, 273(36), 23258-66.
- Smyth, E. M., Nestor, P. V. & FitzGerald, G. A. (1996) Agonist-dependent phosphorylation of an epitope-tagged human prostacyclin receptor. *J Biol Chem*, 271(52), 33698-704.
- Stork, P. J. & Schmitt, J. M. (2002) Crosstalk between cAMP and MAP kinase signaling in the regulation of cell proliferation. *Trends Cell Biol*, 12(6), 258-66.
- Sun, C. X., Zhong, H., Mohsenin, A., Morschl, E., Chunn, J. L., Molina, J. G., Belardinelli, L., Zeng, D. & Blackburn, M. R. (2006) Role of A2B adenosine receptor signaling in adenosine-dependent pulmonary inflammation and injury. *J Clin Invest*, 116(8), 2173-2182.

- Sun, Y., Liu, W. Z., Liu, T., Feng, X., Yang, N. & Zhou, H. F. (2015) Signaling pathway of MAPK/ERK in cell proliferation, differentiation, migration, senescence and apoptosis. *J Recept Signal Transduct Res*, 35(6), 600-4.
- Sunahara, R. K. & Taussig, R. (2002) Isoforms of mammalian adenylyl cyclase: multiplicities of signaling. *Mol Interv*, 2(3), 168-84.
- Sykes, D. A. & Charlton, S. J. (2012) Slow receptor dissociation is not a key factor in the duration of action of inhaled long-acting beta2-adrenoceptor agonists. *Br J Pharmacol*, 165(8), 2672-83.
- Szczuka, A., Wennerberg, M., Packeu, A. & Vauquelin, G. (2009) Molecular mechanisms for the persistent bronchodilatory effect of the beta 2-adrenoceptor agonist salmeterol. *Br J Pharmacol*, 158(1), 183-94.
- Tager, A. M., LaCamera, P., Shea, B. S., Campanella, G. S., Selman, M., Zhao, Z., Polosukhin, V., Wain, J., Karimi-Shah, B. A., Kim, N. D., Hart, W. K., Pardo, A., Blackwell, T. S., Xu, Y., Chun, J. & Luster, A. D. (2008) The lysophosphatidic acid receptor LPA1 links pulmonary fibrosis to lung injury by mediating fibroblast recruitment and vascular leak. *Nat Med*, 14(1), 45-54.
- Tanjore, H., Lawson, W. E. & Blackwell, T. S. (2013) Endoplasmic reticulum stress as a pro-fibrotic stimulus. *Biochim Biophys Acta*, 1832(7), 940-7.
- Teoh, C. M., Tan, S. S. & Tran, T. (2015) Integrins as Therapeutic Targets for Respiratory Diseases. *Curr Mol Med*, 15(8), 714-34.
- Thomas, P. E., Peters-Golden, M., White, E. S., Thannickal, V. J. & Moore, B. B. (2007) PGE(2) inhibition of TGF-beta1-induced myofibroblast differentiation is Smad-independent but involves cell shape and adhesion-dependent signaling. *Am J Physiol Lung Cell Mol Physiol*, 293(2), L417-28.

Togo, S., Liu, X., Wang, X., Sugiura, H., Kamio, K., Kawasaki, S., Kobayashi, T., Ertl, R. F., Ahn, Y., Holz, O., Magnussen, H., Fredriksson, K., Skold, C. M. & Rennard, S. I. (2009) PDE4 inhibitors roflumilast and rolipram augment PGE2 inhibition of TGF- β 1-stimulated fibroblasts. *Am J Physiol Lung Cell Mol Physiol*, 296(6), L959-69.

Trakada, G. & Spiropoulos, K. (2001) Arterial endothelin-1 in interstitial lung disease patients with pulmonary hypertension. *Monaldi Arch Chest Dis*, 56(5), 379-83.

Tresguerres, M., Levin, L. R. & Buck, J. (2011) Intracellular cAMP signaling by soluble adenylyl cyclase. *Kidney Int*, 79(12), 1277-88.

Tsvetanova, N. G. & von Zastrow, M. (2014) Spatial encoding of cyclic AMP signaling specificity by GPCR endocytosis. *Nat Chem Biol*, 10(12), 1061-5.

Uhal, B. D., Joshi, I., Hughes, W. F., Ramos, C., Pardo, A. & Selman, M. (1998) Alveolar epithelial cell death adjacent to underlying myofibroblasts in advanced fibrotic human lung. *Am J Physiol*, 275(6), L1192-9.

Verde, I., Pahlke, G., Salanova, M., Zhang, G., Wang, S., Coletti, D., Onuffer, J., Jin, S. L. & Conti, M. (2001) Myomegalin is a novel protein of the golgi/centrosome that interacts with a cyclic nucleotide phosphodiesterase. *J Biol Chem*, 276(14), 11189-98.

Vestbo, J., Hurd, S. S., Agusti, A. G., Jones, P. W., Vogelmeier, C., Anzueto, A., Barnes, P. J., Fabbri, L. M., Martinez, F. J., Nishimura, M., Stockley, R. A., Sin, D. D. & Rodriguez-Roisin, R. (2013) Global strategy for the diagnosis, management, and prevention of chronic obstructive pulmonary disease: GOLD executive summary. *Am J Respir Crit Care Med*, 187(4), 347-65.

Voelkel, N. F., Gomez-Arroyo, J., Abbate, A., Bogaard, H. J. & Nicolls, M. R. (2012) Pathobiology of pulmonary arterial hypertension and right ventricular failure. *Eur Respir J*, 40(6), 1555-65.

- Vossler, M. R., Yao, H., York, R. D., Pan, M. G., Rim, C. S. & Stork, P. J. (1997) cAMP activates MAP kinase and Elk-1 through a B-Raf- and Rap1-dependent pathway. *Cell*, 89(1), 73-82.
- Vouret-Craviari, V., Van Obberghen-Schilling, E., Scimeca, J. C., Van Obberghen, E. & Pouyssegur, J. (1993) Differential activation of p44mapk (ERK1) by alpha-thrombin and thrombin-receptor peptide agonist. *Biochem J*, 289 (Pt 1), 209-14.
- Wachten, S., Masada, N., Ayling, L. J., Ciruela, A., Nikolaev, V. O., Lohse, M. J. & Cooper, D. M. (2010) Distinct pools of cAMP centre on different isoforms of adenylyl cyclase in pituitary-derived GH3B6 cells. *J Cell Sci*, 123(Pt 1), 95-106.
- Walsh, D. A., Perkins, J. P. & Krebs, E. G. (1968) An adenosine 3',5'-monophosphate-dependant protein kinase from rabbit skeletal muscle. *J Biol Chem*, 243(13), 3763-5.
- Walsh, J., Absher, M. & Kelley, J. (1993) Variable expression of platelet-derived growth factor family proteins in acute lung injury. *Am J Respir Cell Mol Biol*, 9(6), 637-44.
- Walters, J. A., Wood-Baker, R. & Walters, E. H. (2005) Long-acting beta2-agonists in asthma: an overview of Cochrane systematic reviews. *Respir Med*, 99(4), 384-95.
- Watanabe, T., Satoh, H., Togoh, M., Taniguchi, S., Hashimoto, Y. & Kurokawa, K. (1996) Positive and negative regulation of cell proliferation through prostaglandin receptors in NIH-3T3 cells. *J Cell Physiol*, 169(2), 401-9.
- Weksler, B. B., Ley, C. W. & Jaffe, E. A. (1978) Stimulation of endothelial cell prostacyclin production by thrombin, trypsin, and the ionophore A 23187. *J Clin Invest*, 62(5), 923-30.
- Wennstrom, S., Hawkins, P., Cooke, F., Hara, K., Yonezawa, K., Kasuga, M., Jackson, T., Claesson-Welsh, L. & Stephens, L. (1994a) Activation of phosphoinositide 3-kinase is required for PDGF-stimulated membrane ruffling. *Curr Biol*, 4(5), 385-93.

Wennstrom, S., Siegbahn, A., Yokote, K., Arvidsson, A. K., Heldin, C. H., Mori, S. & Claesson-Welsh, L. (1994b) Membrane ruffling and chemotaxis transduced by the PDGF beta-receptor require the binding site for phosphatidylinositol 3' kinase. *Oncogene*, 9(2), 651-60.

Westermark, B. & Wasteson, A. (1976) A platelet factor stimulating human normal glial cells. *Exp Cell Res*, 98(1), 170-4.

White, E. S., Atrasz, R. G., Dickie, E. G., Aronoff, D. M., Stambolic, V., Mak, T. W., Moore, B. B. & Peters-Golden, M. (2005) Prostaglandin E(2) inhibits fibroblast migration by E-prostanoid 2 receptor-mediated increase in PTEN activity. *Am J Respir Cell Mol Biol*, 32(2), 135-41.

White, K. E., Ding, Q., Moore, B. B., Peters-Golden, M., Ware, L. B., Matthay, M. A. & Olman, M. A. (2008) Prostaglandin E2 mediates IL-1beta-related fibroblast mitogenic effects in acute lung injury through differential utilization of prostanoid receptors. *J Immunol*, 180(1), 637-46.

Whitehurst, A. W., Wilsbacher, J. L., You, Y., Luby-Phelps, K., Moore, M. S. & Cobb, M. H. (2002) ERK2 enters the nucleus by a carrier-independent mechanism. *Proc Natl Acad Sci U S A*, 99(11), 7496-501.

Williams, M. C. (2003) Alveolar type I cells: molecular phenotype and development. *Annu Rev Physiol*, 65, 669-95.

Willighagen, E. L., Mayfield, J. W., Alvarsson, J., Berg, A., Carlsson, L., Jeliaskova, N., Kuhn, S., Pluskal, T., Rojas-Cherto, M., Spjuth, O., Torrance, G., Evelo, C. T., Guha, R. & Steinbeck, C. (2017) The Chemistry Development Kit (CDK) v2.0: atom typing, depiction, molecular formulas, and substructure searching. *J Cheminform*, 9(1), 33.

- Wollin, L., Maillet, I., Quesniaux, V., Holweg, A. & Ryffel, B. (2014) Antifibrotic and anti-inflammatory activity of the tyrosine kinase inhibitor nintedanib in experimental models of lung fibrosis. *J Pharmacol Exp Ther*, 349(2), 209-20.
- Wong, W. & Scott, J. D. (2004) AKAP signalling complexes: focal points in space and time. *Nat Rev Mol Cell Biol*, 5(12), 959-70.
- WorldHealthOrganization (2013) *Global surveillance, prevention and control of chronic respiratory diseases: a comprehensive approach* Geneva: World Health Organization.
- Wright, C. E., Fraser, S. D., Brindle, K., Morice, A. H., Hart, S. P. & Crooks, M. G. (2017) Inhaled beclomethasone/formoterol in idiopathic pulmonary fibrosis: a randomised controlled exploratory study. *ERJ Open Res*, 3(4).
- Wu, H., Zhang, Y., Xu, Z., Zhang, J., Zhang, X. & Zhao, Z. (1999) [The expression of integrin alpha5beta1 and transforming growth factor-beta in pulmonary fibrosis of rat]. *Zhonghua Bing Li Xue Za Zhi*, 28(6), 427-31.
- Wu, J., Dent, P., Jelinek, T., Wolfman, A., Weber, M. J. & Sturgill, T. W. (1993) Inhibition of the EGF-activated MAP kinase signaling pathway by adenosine 3',5'-monophosphate. *Science*, 262(5136), 1065-9.
- Wynn, T. A. & Ramalingam, T. R. (2012) Mechanisms of fibrosis: therapeutic translation for fibrotic disease. *Nat Med*, 18(7), 1028-40.
- Xu, P. B., Mao, Y. F., Meng, H. B., Tian, Y. P. & Deng, X. M. (2011) STY39, a novel alpha-melanocyte-stimulating hormone analogue, attenuates bleomycin-induced pulmonary inflammation and fibrosis in mice. *Shock*, 35(3), 308-14.
- Yamamoto, T., Ebisuya, M., Ashida, F., Okamoto, K., Yonehara, S. & Nishida, E. (2006) Continuous ERK activation downregulates antiproliferative genes throughout G1 phase to allow cell-cycle progression. *Curr Biol*, 16(12), 1171-82.

Yoshida, K., Kuwano, K., Hagimoto, N., Watanabe, K., Matsuba, T., Fujita, M., Inoshima, I. & Hara, N. (2002) MAP kinase activation and apoptosis in lung tissues from patients with idiopathic pulmonary fibrosis. *J Pathol*, 198(3), 388-96.

Zaccolo, M., De Giorgi, F., Cho, C. Y., Feng, L., Knapp, T., Negulescu, P. A., Taylor, S. S., Tsien, R. Y. & Pozzan, T. (2000) A genetically encoded, fluorescent indicator for cyclic AMP in living cells. *Nat Cell Biol*, 2(1), 25-9.

Zaccolo, M. & Pozzan, T. (2002) Discrete microdomains with high concentration of cAMP in stimulated rat neonatal cardiac myocytes. *Science*, 295(5560), 1711-5.

Zhang, A., Wang, M. H., Dong, Z. & Yang, T. (2006) Prostaglandin E2 is a potent inhibitor of epithelial-to-mesenchymal transition: interaction with hepatocyte growth factor. *Am J Physiol Renal Physiol*, 291(6), F1323-31.

Zhao, X., Jones, A., Olson, K. R., Peng, K., Wehrman, T., Park, A., Mallari, R., Nebalasca, D., Young, S. W. & Xiao, S. H. (2008) A homogeneous enzyme fragment complementation-based beta-arrestin translocation assay for high-throughput screening of G-protein-coupled receptors. *J Biomol Screen*, 13(8), 737-47.

Zhou, Y., Murthy, J. N., Zeng, D., Belardinelli, L. & Blackburn, M. R. (2010) Alterations in adenosine metabolism and signaling in patients with chronic obstructive pulmonary disease and idiopathic pulmonary fibrosis. *PLoS One*, 5(2), e9224.

Zhou, Y., Schneider, D. J., Morschl, E., Song, L., Pedroza, M., Karmouty-Quintana, H., Le, T., Sun, C. X. & Blackburn, M. R. (2011) Distinct roles for the A2B adenosine receptor in acute and chronic stages of bleomycin-induced lung injury. *J Immunol*, 186(2), 1097-106.

Zhu, Y., Liu, Y., Zhou, W., Xiang, R., Jiang, L., Huang, K., Xiao, Y., Guo, Z. & Gao, J. (2010) A prostacyclin analogue, iloprost, protects from bleomycin-induced pulmonary fibrosis in mice. *Respir Res*, 11, 34.

Zisman, D. A., Schwarz, M., Anstrom, K. J., Collard, H. R., Flaherty, K. R. & Hunninghake, G. W. (2010) A controlled trial of sildenafil in advanced idiopathic pulmonary fibrosis. *N Engl J Med*, 363(7), 620-8.

Zmajkovicova, K., Menyhart, K., Bauer, Y., Studer, R., Renault, B., Schnoebelen, M., Bolinger, M., Nayler, O. & Gatfield, J. (2018) The Antifibrotic Activity of Prostacyclin Receptor Agonism is Mediated through Inhibition of YAP/TAZ. *Am J Respir Cell Mol Biol*.